Technische Universität München
TUM School of Life Sciences

Characterization of gut microbial profiles in Inflammatory Bowel Disease patients in response to therapy

Mohamed Adel Abdelhakim Ahmed

Vollständiger Abdruck der von der TUM School of Life Sciences der Technischen Universität München zur Erlangung eines

Doktors der Naturwissenschaften (Dr. rer. nat.)

genehmigten Dissertation.

Vorsitz: Prof. Dr. Corinna Dawid

Prüfer*innen der Dissertation:

1. Prof. Dr. Dirk Haller
2. Prof. Dr. Markus Gerhard

Die Dissertation wurde am 21.02.2023 bei der Technischen Universität München eingereicht und durch die TUM School of Life Sciences am 17.07.2023 angenommen.

To my father, who has influenced and believed in me till his last days, I miss you so much.

October 1950 - December 2022

Abstract

Inflammatory bowel diseases (IBD), predominantly ulcerative colitis (UC), and Crohn's disease (CD), are multifactorial chronic inflammatory conditions that affect the gastrointestinal tract. Gut microbiota alterations have been associated with IBD, but the functional relevance of gut microbial changes in disease pathology is still hampered. Biological therapy with monoclonal antibodies targeting the immune signaling pathways has delivered substantial benefits to IBD patients resulting in improved quality of life, endoscopic healing, and clinical symptoms. We analyzed a prospective study with thirty-five UC, forty-one CD, and six pouchitis (Poc) patients initiating biological therapies (biotherapy cohort) and assessed the longitudinal dynamics of stool and mucosa-associated gut microbiota composition using 16S rRNA amplicon sequencing. In addition, the fecal metabolome was characterized using untargeted metabolomics. Moreover, we studied the microbial profiles of two distinct IBD cohorts (the lifestyle intervention UC cohort and the biotherapy cohort) to identify a shared IBD gut microbial signature between two geographically separate regional cohorts. We investigated the impact of clustering methods, including operational taxonomic units (OTUs) and zero radius OTUs (zOTUs) of 16S rRNA amplicon sequencing on gut microbial analysis in a subset of the biotherapy cohort. To address the functional relevance of gut microbial changes in IBD pathogenesis, we colonized germfree (GF) *Il10*$^{-/-}$ mice, as an IBD-related mouse model, with gut microbiota obtained from IBD patients.

Biological therapy induced remission in up to 60% of IBD patients of the biotherapy cohort over the one-year study duration. Longitudinal gut microbial profiling of mucosal and luminal bacteria showed significant clustering based on individual-specific signatures rather than disease activity status. CD and UC patients showed distinct mucosal and luminal gut microbial communities. Fecal microbiota in CD patients was enriched in *Escherichia coli* and *Bacteroides*, while UC patients had higher levels of *Faecalibacterium* and *Bifidobacterium*. Mucosa-associated bacteria from CD patients with ileal and colonic involvement revealed a clear separation of their microbial profiles based on disease location, and colonic CD patients showed a similar microbial profile to UC patients in contrast to ileal CD patients. IBD patients with active disease showed higher levels of *Klebsiella*, *Fusobacterium*, and *Escherichia coli*. Untargeted metabolomic profiling

identified alterations in fecal fatty and bile acids profiles in CD patients. Higher levels of platelet-activating factor and lactosylceramide were observed in fecal microbial communities derived from inflamed UC patients, while UC patients in remission showed higher levels of bile acids. Integrative microbiome-metabolome analysis of the biotherapy cohort depicted overlapping associations between IBD disease phenotypes. Analysis of the gut microbial composition of two IBD cohorts in two countries showed distinct microbial signatures, highlighting the crucial role of environmental factors in shaping the gut microbiome. Clustering methods (OTUs & zOTUs) of the amplicon sequencing showed similar alpha and beta diversity patterns, but the zOTUs analysis demonstrated better taxonomic resolution. The transfer of the disease activity phenotype of the human donors was not fully recapitulated in the colonized *Il10*$^{-/-}$ mice. Yet, after the microbial colonization, there was a selective expansion of some pathobiont in the inflamed *Il10*$^{-/-}$ mice, suggesting that the disease induction in this mouse model relied on the colonization of specific taxa, which are capable of disease initiation in the absence of the IL-10, and it is independent of the donor disease status.

Zusammenfassung

Chronisch-entzündliche Darmerkrankungen (CED), vor allem Colitis ulcerosa (UC) und Morbus Crohn (CD), sind multifaktorielle chronische Entzündungskrankheiten, die den Magen-Darm-Trakt betreffen. Veränderungen der Darmmikrobiota wurden mit CED in Verbindung gebracht, aber die funktionelle Bedeutung von Veränderungen des Darmmikrobioms für die Krankheitspathologie ist immer noch nicht eindeutig geklärt. Die biologische Therapie mit monoklonalen Antikörpern, die auf die Immunsignalwege abzielen, hat CED-Patienten erhebliche Vorteile gebracht und zu einer Verbesserung der Lebensqualität, der endoskopischen Heilung und der klinischen Symptome geführt. Wir haben eine prospektive Studie mit fünfunddreißig UC-, einundvierzig CD- und sechs Pouchitis-Patienten, bei denen eine biologische Therapie eingeleitet wurde (Biotherapie-Kohorte), analysiert und die Längsschnittdynamik der Zusammensetzung der Stuhl- und Schleimhaut-assoziierten Darmmikrobiota mittels 16S rRNA-Amplikon-Sequenzierung untersucht. Des Weiteren wurde das fäkale Metabolom mittels ungezielter Metabolomik charakterisiert. Darüber hinaus untersuchten wir die mikrobiellen Profile von zwei verschiedenen CED-Kohorten (die UC-Kohorte mit Lebensstilintervention und die Biotherapie-Kohorte), um eine gemeinsame CED-Darmmikrobiota-Signatur zwischen zwei geografisch getrennten regionalen Kohorten zu identifizieren. Wir untersuchten die Auswirkungen von Clustering-Methoden, einschließlich operativer taxonomischer Einheiten (OTUs) und Nullradius-OTUs (zOTUs) der 16S rRNA-Amplikon-Sequenzierung auf die mikrobiologische Analyse des Darms in einer Teilmenge der Biotherapie-Kohorte. Um die funktionelle Bedeutung von Veränderungen des Darmmikrobioms bei der Pathogenese von CED zu untersuchen, haben wir keimfreie *Il10*$^{-/-}$-Mäuse (GF) als CED-verwandtes Mausmodell mit Darmmikrobiota von CED-Patienten kolonisiert.

Die biologische Therapie führte bei bis zu 60 % der IBD-Patienten der Biotherapie-Kohorte während der einjährigen Studiendauer zu einer Remission. Die Längsschnittuntersuchung des Darmmikrobioms von mukosalen und luminalen Bakterien zeigte eine signifikante Clusterbildung, die auf individualspezifischen Signaturen und nicht auf dem Status der

Krankheitsaktivität beruhte. CD- und UC-Patienten wiesen unterschiedliche mukosale und luminale mikrobielle Gemeinschaften im Darm auf. Die fäkale Mikrobiota von CD-Patienten war angereichert mit *Escherichia coli* und *Bacteroides*, während UC-Patienten höhere Werte an *Faecalibacterium* und *Bifidobacterium* aufwiesen. Schleimhautassoziierte Bakterien von CD-Patienten mit Ileus- und Kolonbefall zeigten eine klare Trennung ihrer mikrobiellen Profile je nach Krankheitsort, und CD-Patienten mit Kolonbefall zeigten ein ähnliches mikrobielles Profil wie UC-Patienten, im Gegensatz zu CD-Patienten mit Ileusbefall. IBD-Patienten mit aktiver Erkrankung wiesen höhere Werte von *Klebsiella*, *Fusobacterium* und *Escherichia coli* auf. Die ungezielte metabolomische Profilerstellung ergab Veränderungen im fäkalen Fett- und Gallensäureprofil von CD-Patienten. In fäkalen mikrobiellen Gemeinschaften von entzündeten UC-Patienten wurden höhere Gehalte an plättchenaktivierendem Faktor und Lactosylceramid beobachtet, während UC-Patienten in Remission höhere Gehalte an Gallensäuren aufwiesen. Die integrative Mikrobiom-Metabolom-Analyse der Biotherapie-Kohorte zeigte überlappende Assoziationen zwischen den Phänotypen der CED-Krankheit. Die Analyse der Zusammensetzung des Darmmikrobioms von zwei IBD-Kohorten in zwei Ländern ergab unterschiedliche mikrobielle Signaturen, was die entscheidende Rolle von Umweltfaktoren bei der Gestaltung des Darmmikrobioms unterstreicht. Die Clustering-Methoden (OTUs & zOTUs) der Amplikon-Sequenzierung zeigten ähnliche Alpha- und Beta-Diversitätsmuster, aber die zOTUs-Analyse zeigte eine bessere taxonomische Auflösung. Die Übertragung des Phänotyps der Krankheitsaktivität der menschlichen Spender wurde in den kolonisierten *Il10*$^{-/-}$-Mäusen nicht vollständig rekapituliert. Nach der mikrobiellen Besiedlung kam es jedoch zu einer selektiven Ausbreitung einiger Pathobionten in den entzündeten *Il10*$^{-/-}$-Mäusen, was darauf hindeutet, dass die Krankheitsinduktion in diesem Mausmodell von der Besiedlung spezifischer Taxa abhängt, die in Abwesenheit von IL-10 zur Krankheitsauslösung fähig sind, und dass sie unabhängig vom Krankheitsstatus des Spenders ist.

Table of Contents

1 Introduction

1.1 An overview of gut microbiome

Mammals and other vertebrae are colonized by broad microbial communities composed of archaea, fungi, protozoa, viruses, and predominantly bacteria. These microbes cover all mucosal surfaces in the body, defined as microbiota (Human Microbiome Project, 2012). The terminology of the microbiome field has been evolving, and the key terms used in this work are summarized in the glossary box.

Glossary box:

Gut microbiota encloses the largest microbial community in the body, which stands for the microbes that inhabit the gastrointestinal tract (GIT) (Metwaly et al., 2022b).

The gut microbiome includes the gut microbiota and its "theatre of activity" and is shaped by the host. Theatre of activity, which is prone to change in scale and time, includes microbial structures, mobile genetic elements (phages, viruses, and transposons), metabolites, and the other remaining DNA that exist in the habitat (Berg et al., 2020).

Microbial dysbiosis refers to the loss of the mutualistic relationship between microbial communities, and it was described as bacterial diversity reduction and an increase/decrease in the abundance of disease-associating/mutualistic-associating taxa (Petersen and Round, 2014).

Pathobionts are opportunistic microbes that can lead to diseases under certain conditions, such as alterations in the genetic or environmental factors in the host (Jochum and Stecher, 2020).

1.1.1 Structure and function of gut microbiota

Bacteria are the most dominant microorganisms in the human gut, with an estimated total mass of 0.2 kg ($3.8*10^{13}$) (Sender et al., 2016). The gut microbiome is dominated by two phyla: Bacteroidetes and Firmicutes, and other phyla such as Actinobacteria, Verrucomicrobia, and Proteobacteria represent less than five percent of the total community (Segata et al., 2012). The

gut microbial density and diversity vary in the distinct gut compartments, where the bacterial density and diversity gradually increase toward the distal gut, ranging from $10^{\wedge 1}$ microbial cells/gram of content in the stomach to reaching the highest ($10^{\wedge 12}$ microbial cells/gram of content) in the colon (Sommer and Backhed, 2013). Intestinal microorganisms live in synergy with the host under normal conditions, with a mutual symbiosis between them. For instance, the gut microbiota breaks down several indigestible carbohydrates to produce various short-chain fatty acids (SCFA) and vitamins to support host metabolism, while the GIT presents a nutrient-rich milieu for the microbiota to reside. Further, microbial signals play a central role in establishing gut homeostasis by supporting the development and differentiation of the intestinal epithelium and the mucosal immune system (Gensollen et al., 2016; Sommer and Backhed, 2013). Moreover, it prevents the invasion of opportunistic pathogens. Gut microbiota composition is stable under normal conditions (Lozupone et al., 2012) but shows a strong inter-individual variation (Claesson et al., 2011; Faith et al., 2013; Kurilshikov et al., 2021; Schloissnig et al., 2013; Turnbaugh et al., 2010). Intestinal microbial composition fluctuates with some factors such as diet (Flint et al., 2017; Muegge et al., 2011), medications (Dethlefsen and Relman, 2011; Jakobsson et al., 2010), age (Mariat et al., 2009; Morgan et al., 2012), circadian rhythm (Reitmeier et al., 2020a), suggesting a strong role of environmental factors in shaping the microbiome. Strikingly, host genetics plays a minor role in shaping the gut microbiota, with an overall estimation of the microbiome heritability at 1.9-8.1% (Goodrich et al., 2016; Kurilshikov et al., 2021; Rothschild et al., 2018), highlighting a dominating role of environmental factors in defining gut microbiota composition. Notably, intestinal transit time plays an essential part in shaping the gut microbiota, as stool consistency influenced microbial richness and overall composition in healthy individuals (Falony et al., 2016; Vandeputte et al., 2016). Interestingly, microbial dysbiosis, the loss of the mutualistic relationship between microbial communities, has been associated with several diseases such as IBD (Gevers et al., 2014; Schirmer et al., 2018), type 2 diabetes mellitus (Larsen et al., 2010; Qin et al., 2012), allergy, asthma (Fujimura and Lynch, 2015), type 1 diabetes mellitus (Kostic et al., 2015), autism spectrum disorders (Strati et al., 2017), rheumatoid arthritis (Scher et al., 2013), atherosclerosis (Koeth et al., 2013) and multiple sclerosis (Tremlett et al., 2016), demonstrating the contributing role of gut microbiota in health and disease.

There are two main approaches used to study gut microbiota composition, which include culture-dependent and culture-independent methods. Culture-dependent identification of bacteria relies on culturing bacteria on various growth conditions that were later described as "Culturomics" (Lagier et al., 2018). In brief, culture-based methods are indispensable for understanding microbial functions, but it does not capture the full microbial diversity and is very laborious. Although the rich knowledge we acquired from culturing bacteria studying single microbes, we still could not culture a vast majority of gut microbiota. Moreover, culturing single bacteria provide little/no information on the influence of microbe-microbe interactions and their collective functional roles (Weinstock, 2012). Culture-independent methods involve applying a genomic approach to study the composition of bacterial communities. It can capture the extensive microbial diversity that is not possible via traditional culturing methods. The advancement in technologies such as next-generation sequencing (NGS) allowed a more sophisticated analysis of various complex microbial communities. Culture-independent methods used in gut microbiota research involve targeted 16S ribosomal RNA (rRNA) amplicon sequencing and shotgun metagenomics. The 16S rRNA gene sequencing depends on the dissimilarity of the variable regions in the conserved bacterial ribosomal genes (rRNA), and the shotgun metagenomics catalog all the available genes (Almeida et al., 2020).

1.1.2 Gut Metabolomics – a tool to study the functional relevance of gut microbiota

Gut microbiota interacts with the host in different ways, such as direct production of microbial metabolites of its breakdown of dietary substrates or indirect modulation of host molecules such as bile acids (Lavelle and Sokol, 2020). Metabolomics is a term used to describe the analysis of metabolites (small molecular compounds $\leq$1500 Dalton). Metabolomics can provide a better understanding of the interactions between host metabolism, gut microbiota, and dietary components (Ursell et al., 2014). Metabolomics methodologies fall into two distinct groups; targeted and untargeted metabolomics. Targeted metabolomics analyzes a defined class of metabolites of interest, whereas untargeted metabolomics captures all available metabolites (Zhang et al., 2012a). Targeted methods mandate prior knowledge of the metabolites of interest to validate a pre-identified biomarker or to explore a specific metabolic pathway, but it does not

achieve global metabolic profiling. Although untargeted metabolomics covers all available metabolites, it entails several challenges in metabolite identification and the presence of redundant and background signals (Schrimpe-Rutledge et al., 2016). Recent advancements in analytical technologies, such as gas chromatography and high-performance liquid chromatography (HPLC) for separation coupled with mass spectrometry (MS) or nuclear magnetic resonance (NMR) for metabolites detection have revolutionized the metabolomics field (Zhang et al., 2012a). With technological advancements in metabolomic profiling systems and data analytics platforms, metabolomics is considered a vital asset in understanding the functional relevance of host-microbe interactions.

1.1.3 Gut microbiota crosstalk with intestinal epithelium and the immune system

Gut microbiota, intestinal epithelial cells (IECs), and the mucosal immune system co-evolved building a mutualistic relationship, and effective crosstalk between them supports gut homeostasis. The sampling of luminal antigens to the immune system is processed via various cell types and mechanisms (Peterson and Artis, 2014). For example, in the small intestine under normal conditions, Microfold cells (M cells) (Mabbott et al., 2013), Goblet cells (GC) (McDole et al., 2012), and dendritic cells (DCs) (Rescigno et al., 2001) mediate the antigen sampling to the immune system. Then it directs either a tolerogenic or inflammatory (anti-pathogenic) immune response to the sampled antigens to maintain intestinal homeostasis. IECs express a variety of pattern recognition receptors (PRRs), which sense microbial-associated molecular patterns (MAMPs) and damage-associated molecular patterns (DAMPs) (Boyapati et al., 2016; Burgueno and Abreu, 2020). In addition, IECs activate host defense signaling pathways (Boyapati et al., 2016; Burgueno and Abreu, 2020). PRRs include cell surface Toll-like receptors 1-9 (TLRs), cytoplasmic nucleotide-binding and oligomerization domain (NOD)-like receptors (NLRs), and RIG-I-like receptor (RLRs) families (Peterson and Artis, 2014).

Several gnotobiotic and germfree (GF) mouse models demonstrated that specific bacterial strains modulate a particular immune response, suggesting specific gut-microbe immune interactions. For instance, Atarashi and colleagues described a reduction of regulatory T cells (T_{reg}) community in the colon of GF mice compared to SPF counterparts (Atarashi et al., 2011).

Colonization of GF mice with mouse-derived 46 *Clostridium* strains (Atarashi et al., 2011) or mono-association of *Bacteroides fragilis* (Round and Mazmanian, 2010) displayed accumulation of T_{reg} in the gut. Interestingly, microbial metabolites such as SCFA, mainly butyrate, promoted T_{reg} development in mouse models (Furusawa et al., 2013), which indicates a mechanistic insight of host-microbiota interactions. Further, Th17 cells were accumulated in the gut of wild type (WT) mice after mono-colonization with segmented filamentous bacteria (SFB) (Ivanov et al., 2009), or SFB flagellins (Wang et al., 2019), or *Escherichia coli O157* (Atarashi et al., 2015), or a mixture of twenty strains derived from UC patients (Atarashi et al., 2015), suggesting a Th17 response was driven by a microbial adhesion to epithelial cells (such as SFB). Moreover, the mono-association of WT GF mice with a *Klebsiella pneumoniae* strain induced a Th1 response (Atarashi et al., 2017). Further, a consortium of 11 strains was obtained from a healthy human donor, which induced IFNɣ CD8 cells in the gut of colonized mice, and it enhanced the host resistance against *Listeria monocytogenes* infection (Tanoue et al., 2019). Interestingly, complex colonization of gut microbiota obtained from healthy human donors showed an increase of T_{reg}, but colonization of fecal bacteria from IBD patients increased numbers of Th17 and Th2 and reduction in T_{reg} in GF WT mice (Britton et al., 2019). These data collectively reveal selective interaction between gut microbiota components and the host immune system.

1.2 Inflammatory Bowel Diseases

Inflammatory bowel diseases (IBD) are chronic non-infectious inflammatory conditions that affect the GIT, with symptoms developing in a relapsing and remitting manner. IBD comprise two disease subtypes: Crohn's disease (CD) and ulcerative colitis (UC). CD is characterized by patchy transmural inflammation that could affect any part of the gut, but mainly the terminal ileum and colon (Torres et al., 2017) (**Figure 1**). Approximately, 50% of CD patients develop complications over time, such as fistulas, strictures, or abscesses, and often result in surgeries (Thia et al., 2010). In contrast, UC is characterized by inflammation confined to the superficial layer of the mucosa and submucosa of the colon—and patients usually display symptoms of bloody diarrhea (Ungaro et al., 2017). IBD patients display various symptoms, such as abdominal pain, fatigue, chronic diarrhea, and rectal bleeding and have a higher risk to develop colorectal cancer (Axelrad et al.,

2016) as well as extra-intestinal malignancies (Pedersen et al., 2010). IBD patients, with a higher prevalence in CD patients, were reported to show extra-intestinal manifestations such as arthritis (inflammation of the joints), aphthous stomatitis (recurrent ulcers in the oral mucosa), erythema nodosum (an inflammatory condition that affects the fat cells under the skin), ankylosing spondylitis (a form of arthritis that mainly affects the spine), and psoriasis (a chronic inflammatory skin disease) (Vavricka et al., 2011), suggesting shared mechanisms between these diseases. Interestingly, 25% of IBD patients revealed symptoms for one of the extra-intestinal manifestations before the onset of IBD symptoms (Rogler et al., 2021; Vavricka et al., 2015).

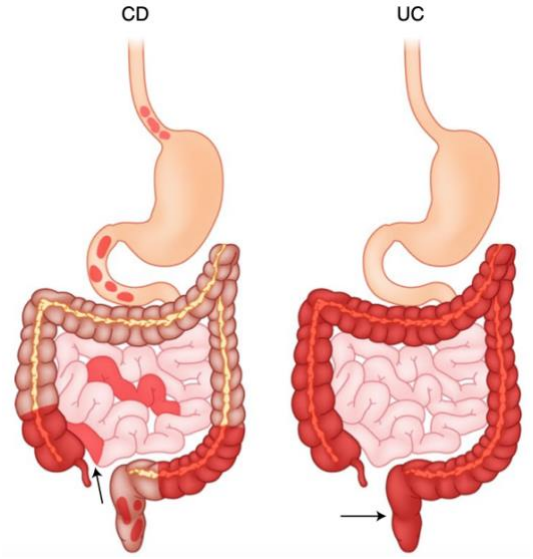

Figure 1 Inflammation localization of CD and UC
Inflammation in UC (right) mainly affects the rectum (arrow) and sometimes the entire colon. Inflammation in CD (left) has a patchy pattern and could affect any part of the alimentary tract but most frequently affects the terminal ileum (arrow). Adapted from (Neurath, 2019).

Although IBD onset occurs at any age, it usually starts in early adulthood (between the second and fourth decade of life, and pediatric IBD patients represent approximately 25% of cases (Peloquin et al., 2016). After diagnosing patients with CD, they are further stratified according to Montreal classification based on their age of onset (A1: <16 years, A2: 17-40 years, and A3: >40 years), disease location (terminal ileum (L1), colon (L2), ileocolonic (L3), and upper GI (L4)) and disease behavior ((B1) without stricture formation & non-penetrating, (B2) structuring, and (B3) penetrating) (Silverberg et al., 2005). UC patients are further stratified by disease extent (E1: proctitis (limited to the rectum), E2: left-sided colitis (limited to a proportion of the colorectum distal to the splenic flexure), and E3: pancolitis (involvement extends proximal to the splenic flexure)) and severity (remission, mild, moderate, and severe) (Silverberg et al., 2005). CD patients

with an ileal phenotype (terminal ileum and ileocolonic involvement) represent around 70% of cases, while 30% of patients show a colonic phenotype (Dulai et al., 2019; Thia et al., 2010). Notably, population-based studies in Europe and Asia demonstrated that proctitis and left-sided colitis represent the majority of UC cases, and pan-colitis is found in a minority of cases (Ng et al., 2013; Portela et al., 2010; Qiu et al., 2019), suggesting a comparable UC disease extent across geographies.

1.3 Epidemiology of IBD

Global IBD incidences have been growing drastically over the years, with an 85.1% increase in total cases numbers from 1990 to 2017, recording 6·8 million patients in 2017 (Collaborators, 2020). However, the global age-standardized prevalence rate rose from 79.5 per 100,000 population in 1990 to only 84.3 cases in 2017 (Collaborators, 2020). IBD is slightly more prevalent in females, with 57% of patients recorded in 2017 (approximately 3.9 million), while males entail 43% of the cases (nearly 3 million) (Collaborators, 2020). Most IBD patients are reported in North America and Western Europe, where more than 2 million North Americans suffer from the disease (Windsor and Kaplan, 2019) and more than 2.5 million in Europe (Ananthakrishnan, 2015; Kaplan, 2015). Intriguingly, there is a sharp rise in IBD incidences in low-income countries, especially the ones that adopted a western lifestyle, such as Eastern Europe (Lakatos et al., 2011), South America (Gasparini et al., 2018), Middle East (Abdulla et al., 2017; Al-Mofarreh and Al-Mofleh, 2013) and in Asia-Pacific (Kaplan and Ng, 2016; Ng et al., 2013). For example, in Hong Kong, the age-adjusted incidence of IBD rose from 0.1/100,000 in 1985 to 3.12/100,000 in 2014 (Ng et al., 2016). Remarkably, there has been a stabilization in the incidence rate (new cases reported) of IBD in North America, Oceania, and Europe but the burden of the disease is still extraordinary, with the prevalence exceeding 0.3% of the total population in these regions (Ng et al., 2018). In contrast, low-income countries such as South America, Africa, and Asia showed a higher incidence rate and lower prevalence (Ng et al., 2018).

IBD has a substantial influence on the psychological, physical, and social life of patients, which affects their productivity and incorporates a massive burden on the healthcare system. For example, IBD was ranked as the fifth most costly GIT condition in the United States in the 2015

annual healthcare expenditures at 7.2 billion USD (Peery et al., 2019). These high costs emerge from a high rate of hospitalizations, surgeries, management of the disease complications, and medical therapies such as biologics.

1.4 IBD Pathogenesis

IBD is a complex disease involving multiple factors; genome, epigenome, gut microbiota, and various environmental triggers, which contribute to the disease's pathogenesis (Renz et al., 2011; Ventham et al., 2013). IBD is best described as mucosal immune dysregulation and defects in the epithelial tissue homeostasis towards commensal gut microbiota in a genetically susceptible host, potentially triggered by environmental factors (Lee and Chang, 2021).

1.4.1 Genetics of IBD

Early twin studies shed light on the role of genetics in the pathogenesis of IBD. For instance, an analysis of a German IBD twin cohort showed a 35% concordance rate for CD monozygotic twins and 16% for UC (Spehlmann et al., 2008). Besides, IBD was described in familial population studies (Bengtson et al., 2009b; Moller et al., 2015) with 12% of IBD patients having a family history, and the risk of the familial CD was more pronounced than UC (Moller et al., 2015). Notably, early onset of IBD in the patients' offspring was observed (Bengtson et al., 2009a) and mutations in *IL10* receptors (Glocker et al., 2009), *TRIM22* (Li et al., 2016), *XIAP* (Zeissig et al., 2015), and *TTC7A* (Jardine et al., 2019) were described in early IBD onset. Furthermore, Ashkenazi Jewish populations show a two to four times higher risk of developing IBD than non-Jewish Europeans (Baumgart and Sandborn, 2012; Ordas et al., 2012; Rivas et al., 2018). Remarkably, Asian and African American descendants have lower IBD prevalence in the United States (Wang et al., 2013). Genome-wide association studies (GWAS) showed that most genetic risk loci are common among patients from different ancestries (Brant et al., 2017; Liu et al., 2015), suggesting a shared pathology across various descendants. Notably, *NOD-2* risk variants are most common in European populations, *TNFSF15* dominates in East Asia (Liu et al., 2015), and African-specific SNPs at *LSAMP* and *ZNF649* were reported in African Americans (Brant et al., 2017). Interestingly, Cleynen and colleagues suggested that IBD is better classified into three separate groups: ileal CD

"iCD"; colonic CD "cCD"; and UC, and cCD is considered an intermediate between iCD and UC, as these three disease subtypes are genetically distinct (Cleynen et al., 2016). For instance, several genetic studies connected *NOD-2* variants with iCD (Cleynen et al., 2013) and HLA-DRB1*01:03 variants with cCD and UC (Goyette et al., 2015).

Genome-wide association studies and subsequent meta-analysis studies have discovered more than 240 susceptible genetic loci implicated in IBD (de Lange et al., 2017). Collectively, 68% of the susceptible loci were associated with CD and UC, but 18% and 14% were specific to CD and UC, respectively (Jostins et al., 2012), suggesting common molecular mechanisms between both phenotypes. These genetic loci involve several pathways such as inflammasome signaling, microbial sensing and clearance (*NOD-2*, *TLR9*, *IL12R, CARD9, RIPK2*, *TNFAIP3*, *LRRK2*, *LACC1*, *NCF4*, and *ATG16L1*), epithelial cell dysfunctionality & barrier disruption (*RNF186*, *C1orf106* & *HNF4A*), aberrant innate and adaptive immune system (HLA locus, *Il23R* & *Il10R*), cell stress pathways such as endoplasmic reticulum (ER) stress, unfolded protein response (UPR), apoptosis, necroptosis and autophagy (*ATG16L1*, *IRGM*, *RIPK1*, *TMEM258* & *KEAP1*) (Graham and Xavier, 2020; Huang et al., 2017; Torok et al., 2009), indicating the multifactorial nature of IBD. Interestingly, around 40% of the reported genetic variants in IBD patients were also implicated in other immune-mediated diseases, such as psoriasis and ankylosing spondylitis (Jostins et al., 2012), suggesting shared pathways among various immune-mediated diseases. Remarkably, treatment with an antibody against IL-12/23 p40 showed efficacy in psoriasis (Papp et al., 2008) and IBD (Sandborn et al., 2012; Sands et al., 2019), highlighting the shared pathways between the two immune-mediated diseases.

1.4.2 Environmental factors in IBD

Although IBD genetics has fundamentally enhanced our understanding of the disease pathogenesis, it only elucidates 13% of the disease susceptibility in CD and 8% for UC (Liu et al., 2015), highlighting the indispensable role of environmental factors in IBD pathogenesis. For instance, a low concordance rate was reported in CD monozygotic twins (Halfvarson, 2011). Besides, not all individuals who carry IBD genetic variants develop IBD (Knights et al., 2013), suggesting an immense influence of additional factors, including environment and gut microbiota,

in enhancing the disease. Interestingly, there was a surge in IBD incidence in first-generation immigrants in Canada compared to their parents, who grew up in low IBD incidence countries (Benchimol et al., 2015), indicating the vital role of early life exposures in triggering IBD.

Epidemiological studies have shown that several environmental factors such as smoking, appendicectomy, cessation of breastfeeding, changes in dietary habits, enteric infections, air pollution, medications, early antibiotics exposure, improved sanitation, and higher socioeconomic status have been linked to increased risk of developing IBD (Abegunde et al., 2016; Ananthakrishnan, 2015; Collaborators, 2020; Kronman et al., 2012), suggesting that some environmental factors are influencing gut microbiota changes. The pioneering work of Strachan has proposed what is known as the "hygiene hypothesis", where he connected the rise of immune-mediated diseases and fewer exposures to microbes in early life (Strachan, 1989, 2000), highlighting the essential role of microbes in training the immune system. In addition, several epidemiological studies have supported the relationship between high urbanization, reduction of infectious diseases, lack of parasitic infestations, and the higher incidence of immune-mediated diseases, including IBD (Bach, 2018; Cheema et al., 2014; Kaplan and Ng, 2016; Rook, 2012; Swinburn et al., 2011). More specifically, changing dietary habits accompanied the rise of IBD in newly industrialized countries such as China, where the incidence of IBD cases was increasing, side-by-side with the country's westernization of diet and culture (Kaplan and Ng, 2016). These changes were characterized by less consumption of plant-based food and increased intake of animal-based products, refined sugar, and processed foods (Kaplan and Ng, 2016). In sum, environmental factors play a pivotal role in IBD pathogenesis and have an indispensable impact on shaping the gut microbiome.

1.4.3 Gut microbial dysbiosis and metabolomic alterations in IBD

1.4.3.1 Gut microbial dysbiosis in IBD

Gut microbial dysbiosis has been associated with IBD development and progression, supported by compiling evidence from clinical observations and animal models (Ahmed et al., 2021; Lee and Chang, 2021; Sartor and Wu, 2017; Schirmer et al., 2019). An earlier study of fecal stream diversion in a group of CD patients with active disease showed remission during the study

duration of six months, which provided the first clinical evidence to support the role of gut microbiota in disease reactivation (Rutgeerts et al., 1991). Remarkably, fecal stream restoration in the neo-terminal ileum triggered a postoperative recurrence of CD (D'Haens et al., 1998; Rutgeerts et al., 1991). Further, most IBD animal models are disease free under germfree housing conditions, and selective colonization of pathobionts re-establish disease activity (Ahmed et al., 2021), highlighting the fundamental role of gut microbiota in IBD pathogenesis. In addition, antibiotic treatment success for a subset of CD patients underlines the role of gut microbiota in IBD pathogenesis (Nitzan et al., 2016). Moreover, serological markers against gut microbial components are associated with IBD patients (Chen et al., 2020), providing further evidence of the gut microbiome's role in IBD pathogenesis. Several antibodies against microbial antigens, such as *Saccharomyces cerevisiae* antibodies (ASCA), outer membrane porin C (anti-OmpC), *Pseudomonas fluorescence* I2 component, and Cbir1 flagellin, were increased in IBD patients (Ferrante et al., 2007; Targan et al., 2005). Interestingly, antimicrobial antibodies correlate with the complicated CD phenotype and are currently used for diagnosis and prognosis purposes (Choung et al., 2016), even though their exact mechanism to IBD pathogenesis is not clearly understood.

The advancement of high-throughput sequencing technologies enabled the identification of distinct gut microbial profiles linked to IBD disease phenotypes (Yilmaz et al., 2019), specific geographical regions (Rehman et al., 2016), and response to therapy (Ananthakrishnan et al., 2017; Lewis et al., 2015; Metwaly et al., 2020; Schwerd et al., 2016). Microbial dysbiosis was reported in CD patients in several studies characterized by bacterial richness reduction in addition to an expansion of specific taxa such as *Enterobacteriaceae*, *Fusobacteriaceae*, *Veillonellaceae*, and *Pasteurellacaea* and reduction of *Clostridiales* and *Bacteroidales* (Darfeuille-Michaud et al., 2004; Frank et al., 2007; Gevers et al., 2014; Pascal et al., 2017; Strauss et al., 2011; Willing et al., 2010). Gevers and colleagues analyzed mucosal-associated and fecal samples in a multi-center trial of 447 newly diagnosed pediatric CD patients and 221 controls (Gevers et al., 2014). The newly diagnosed CD patients showed an increased abundance of *Enterobacteriaceae*, *Veillonellaceae*, *Pasteurellacaea*, and *Fusobacteriaceae*, and decreased levels of Bacteroidales, Clostridiales, Erysipelotrichales, and *Bifidobacteriaceae*. Interestingly, CD patients, who had

antibiotics, amplified the microbial dysbiosis (Gevers et al., 2014). In addition, analyzing fecal samples of 234 IBD patients and 38 healthy controls showed a significant reduction of alpha diversity in IBD patients compared to healthy controls (Sokol et al., 2017). IBD patients showed increased levels of *Streptococcus anginosus* and *Ruminococcus gnavus* in iCD patients as well as an increase of *Aggregatibacter segnis* and *Actinobacillus* in IBD patients during flares compared to patients in remission. Several taxa, such as *Ruminococcus*, *Coprococcus*, *Blautia*, *Eubacterium*, and *Dorea*, were reduced in abundance in IBD patients (Sokol et al., 2017). Further, analysis of 2045 IBD and non-IBD stool samples from 4 countries (Germany, the UK, Spain, and Belgium) has revealed a specific gut microbial signature of CD patients, characterized by a decrease in the relative abundance of *Faecalibacterium prausnitzii,* unknown *Christensenellaceae*, *Collinsella*, *Methanobrevibacter*, *Anaerostipes*, and unknown *Peptostreptococcaceae* and an increase in the relative abundance of *Escherichia* and *Fusobacterium* (Pascal et al., 2017). Furthermore, three Dutch study cohorts performed a metagenomic sequencing analysis on 355 IBD patients, 412 irritable bowel syndrome (IBS) patients, and 1025 healthy individuals, revealing a similar pattern of increased abundance of *Escherichia coli* and *Bacteroidetes fragilis* in CD patients and reduced abundance of *Roseburia intestinalis* and *Faecalibacterium prausnitzii* (Vich Vila et al., 2018). Swidsinski and colleagues showed a rise in the density of microbial-binding to mucosa in IBD patients correlating with the disease severity in non-inflamed and inflamed regions of the colon (Swidsinski et al., 2002). These findings suggest that the localization of bacteria interferes with immune homeostasis. Moreover, microbial biofilms, derived from bacteria such as *Bacteroides fragilis,* were two-time higher in IBD patients in the ileal and colonic mucosa when compared to healthy controls (Swidsinski et al., 2005). Although the convenience and non-invasive nature of collecting stool samples, several studies highlighted the importance of analyzing the mucosa-associated microbiota. Regional microbial profiles in the mucosa add spatial information and play a critical role in the host interactions, while the stool microbiota represents the entire GIT and mostly resembles the descending colon (Gevers et al., 2014; Lavelle et al., 2015; Yasuda et al., 2015). For instance, Gevers and colleagues revealed that mucosa-associated microbiota demonstrated microbial dysbiosis in CD patients and a better disease classification compared to luminal microbiota (Gevers et al., 2014). Besides bacterial dysbiosis, IBD patients showed fungal

microbiota dysbiosis characterized by alterations in community diversity and composition, suggesting a potential role of fungi in IBD pathogenesis (Sokol et al., 2017).

Notably, large GWAS highlighted the association between host genetics and shaping the gut microbial compartment in several cohorts (Turpin et al., 2016; Wang et al., 2016). Intriguingly, host genotype and gut microbial data from different IBD cohorts showed that patients with *NOD-2* genetic variants were associated with an increased relative abundance of *Enterobacteriaceae* (Knights et al., 2014) and a reduction of *Faecalibacterium prausnitzii* and *Rosuburia* relative abundances (Aschard et al., 2019). *NOD-2*$^{-/-}$ knockout mice showed a dysbiotic microbiota that when transferred to germfree WT mice worsened the severity of chemically-induced colitis (Couturier-Maillard et al., 2013), suggesting a selective role of *NOD-2* in shaping the gut microbiota composition. Gut microbial profiles differed in CD patients, who were homozygous for the *ATG16L1* risk allele (ATG16L1-T300A), characterized by a surge in *Fusobacteriaceae* levels in inflamed ileal mucosa (Sadaghian Sadabad et al., 2015). However, patients homozygous for the *ATG16L1* protective allele (ATG16L1-T300) had higher levels of *Lachnospiraceae* and reduced numbers of *Enterobacteriaceae* and *Bacteroidaceae* (Sadaghian Sadabad et al., 2015). Taken together, these data propose that some IBD genetic variants are influenced by gut microbiota, and therapeutics that target the gut microbiota could overcome gene-induced disease susceptibility.

Several studies reported different gut microbial profiles between colonic and ileal CD phenotypes (Halfvarson et al., 2017; Naftali et al., 2016; Willing et al., 2010). CD patients with an ileal phenotype were characterized by more adherent invasive *Escherichia coli* (AIEC) (Baumgart et al., 2007; Darfeuille-Michaud et al., 2004; Lapaquette et al., 2010), and *Faecalibacterium* was diminished (Sokol et al., 2008). However, colonic CD showed higher levels of *Faecalibacterium*, unidentified *Ruminococceae*, and *Clostridiales* (Naftali et al., 2016), suggesting a difference between the ileal and colonic CD on the microbiome level. Gut microbiota composition shifted based on the disease activity in CD patients (Kolho et al., 2015; Metwaly et al., 2020). Analyzing 133 fecal samples from 29 CD patients undergoing hematopoietic stem cell transplantation (HSCT) during a 5-year follow-up showed distinct microbial signatures for active and inactive

diseases (Metwaly et al., 2020). There were significant differences in microbial diversity profiles (alpha and beta diversities) between active and inactive CD patients. CD patients with the active disease showed higher levels of pathobionts, such as *Fusobacterium*, *Enterococcus*, *Haemophilus*, *Campylobacter*, and *Megasphaera*, while *Oscillibacter*, *Roseburia*, and *Christensenellaceae* were enriched in inactive CD patients (Metwaly et al., 2020). In contrast, other studies revealed that disease activity does not influence the microbiome composition (Galazzo et al., 2019; Halfvarson et al., 2017; Ohman et al., 2021). Treatments such as antibiotics, biologics, and enteral nutrition, which are prescribed to induce remission in CD patients, showed associations with microbial profile changes (Gevers et al., 2014; Lewis et al., 2015; Schwerd et al., 2016; Wu et al., 2011), highlighting the heterogenicity of gut microbial profiles in IBD patients. These data highlight the fundamental role of gut microbial dysbiosis in IBD pathogenesis and emphasize the importance of sub-stratification of patients (iCD & cCD or responder & non-responder or disease severity) along with their gut microbial description to reveal better insights into various disease phenotypes and pave the way toward better therapeutic interventions. Taken together, although the rich data collected from the various gut microbiome studies, our current understanding of its contribution to IBD pathogenesis remains limited. It is due to the high inter-individual variations in disease evolution, the heterogeneous microbial community structure in individuals, and the limited understanding of the mechanisms of microbe-host interactions and their signaling pathways.

1.4.3.2 Gut metabolome in IBD

Fecal metabolite analysis is considered a reliable tool to discriminate between healthy individuals and IBD patients (De Preter et al., 2015; Franzosa et al., 2019; Santoru et al., 2017), IBD disease subtypes (Kolho et al., 2017; Marchesi et al., 2007) and disease activity (De Preter et al., 2015). Alterations of several fecal metabolites of IBD patients were described, such as SCFA (Bjerrum et al., 2015; Lloyd-Price et al., 2019), medium-chain fatty acids (De Preter et al., 2015; Franzosa et al., 2019), bile acids (Franzosa et al., 2019; Jacobs et al., 2016; Lloyd-Price et al., 2019) and tryptophan metabolites (Nikolaus et al., 2017). **Table 1** summarizes various studies that showed altered fecal metabolites in IBD patients. For instance, in an Italian IBD cohort (82 UC, 50

CD, and 51 healthy controls), the gut metabolome showed a significant difference between IBD phenotypes (CD and UC) and healthy controls, but the metabolite patterns did not show significant differences between IBD phenotypes (CD vs UC). In addition, it did not show significant differences in the gut metabolome based on therapy, diet, or disease localization (Santoru et al., 2017). Recently, some studies have integrated gut metabolomes with gut microbiota datasets showing robust associations between disease-associating microbiota and metabolites (Franzosa et al., 2019; Jacobs et al., 2016; Lloyd-Price et al., 2019), suggesting that multi-omics technologies will play a crucial role in understanding the complex microbe-host interactions. For instance, gut metabolome and microbiota analysis revealed a positive correlation between the abundance of *Ruminococcus gnavus* and docosapentaenoic (polyunsaturated long-chain fatty acid), and a negative correlation between *Ruminococcus gnavus* and caprylic acid (medium chain fatty acid) (Franzosa et al., 2019). Interestingly, integrative microbiome-metabolome analysis from CD patients showed better separation based on disease activity compared to metabolome or microbiome analysis separately (Metwaly et al., 2020). Taken together, metabolomics and multi-omics approaches are fundamental tools to understand the functional relevance of gut microbial dysbiosis in IBD and are crucial resources for discovering new therapeutics.

Table 1 Alterations of the fecal metabolome of IBD patients

Subjects	Method	Altered metabolites in IBD patients	Reference
32 UC and 23 healthy controls	Targeted metabolomics	▪ Lower levels of secondary bile acids (deoxycholic acid, lithocholic acid, taurolithocholate, glycolithocholic acid, and glycodeoxycholic acid in UC patients than in healthy control ▪ Higher levels of primary bile acids (cholic acid, taurocholic acid, taurochenodeoxycholate, and glycochenodeoxycholate) in UC patients than in the healthy control group	(Yang et al., 2021)
29 newly diagnosed pediatric CD and 20 healthy children	Targeted metabolomics	▪ Reduced levels of SCFAs (butyric acid, acetic acid, and propanol acid) and bile acids (deoxycholic acid, hyodeoxycholic acid, lithocholic acid) in newly diagnosed CD patients than in healthy children ▪ Higher levels of L-leucine and L-norleucine (amino acids) and succinic acid and methylmalonic acid (organic acids) in newly diagnosed CD patients than in healthy children	(Wang et al., 2021)
27 pediatric IBD and 38 healthy children	Untargeted metabolomics	▪ Higher levels of primary bile acids (cholate and chenodeoxycholate) in pediatric IBD than in healthy control ▪ Higher levels of ceramide (sphingomyelin breakdown metabolite), Sphingomyelin (sphingolipids), cadaverine (a polyamine produced by lysine decarboxylation), Cadaverine, and several amino acids (tryptophan, leucine, valine, glutamine, and glycine) in IBD patients than healthy controls ▪ Lower levels of the secondary bile acids (deoxycholic acid and lithocholic acid) in IBD patients than in healthy controls	(Bushman et al., 2020)
43 newly diagnosed pediatric CD and 31	Untargeted and targeted (amino acids	▪ Higher levels of amino acids (alanine, tryptophan, tyrosine, valine, isoleucine, leucine, phenylalanine), primary bile acids, and microbial	(Diederen et al., 2020)

healthy controls	and bile acids) metabolomics	metabolites (cadaverine, lactate, propionate, putrescine, trimethylamine) in CD patients compared to healthy controls	
68 CD, 53 UC, and 34 healthy controls	Untargeted metabolomics	▪ Higher levels of bile acids (cholate and chenodeoxycholate) and sphingolipids (ceramide and sphingomyelin) in IBD patients compared to healthy controls ▪ Lower levels of secondary bile acids (lithocholate and deoxycholate) in CD patients ▪ Lower levels of long-chain fatty acids, SCFA (butyrate and propionate) triterpenoids, phenylbenzodioxanes, triacylglycerols, and cholesterols were reported in IBD patients compared to healthy control	(Franzosa et al., 2019)
67 CD, 38 UC and 27 healthy controls	Untargeted metabolomics	▪ Decreased levels of SCFA (Butyrate, Propionate, Valerate/isovalerate) and secondary bile acids (lithocholate and deoxycholate) in IBD patients ▪ Increased levels of primary bile acid cholate and its glycine and taurine conjugates (glycocholate and taurocholate), acylcarnitine, and free arachidonate in IBD patients to healthy control	(Lloyd-Price et al., 2019)
25 IBD and 14 controls	Targeted metabolomics	▪ High levels of primary bile acids (cholate) in IBD patients compared to the healthy controls. ▪ Low level of secondary bile acids (deoxycholate and lithocholate) in IBD patients than in healthy control group	(Das et al., 2019)
7 new-onset CD cases, and 11 controls	Untargeted metabolomics	▪ Lower levels of Tyrosine and Ornithine isomer in pediatric CD patients compared to the healthy control group ▪ Higher levels of Octadecenoylsphingenine, Arachidonic acid, Docosatetraenoic acid, Eicosatrienoic acid, SM (d18:1/24:1), C20 sphingenine in pediatric CD patients compared to healthy control	(Alghamdi et al., 2018)

82 UC, 50 CD, and 51 healthy controls	Untargeted metabolomics	▪ Higher levels of alanine, beta-alanine, phenylacetic acid, 4-hydroxyphenylacetic acid, glyceric acid, phenylethylamine, putrescine, and cadaverine were reported in CD patients compared to healthy control ▪ Lower levels of nicotinic acid, pantothenic acid, 3-methyladipic acid, 5β-coprostanol, 3-hydroxybutyric acid, and hydrocinnamic acid in CD patients compared to healthy control ▪ Higher levels of glucose, cadaverine, hydroxyphenylacetic acid, trimethylamine-N-oxide (TMAO), tyramine, 5-aminovaleric acid, and phenylalanine in UC patients than the healthy controls ▪ Lower levels of linoleic acid, 3-hydroxybutyric acid, nicotinic acid, 3-methyladipic acid, pyroglutamic acid, pantothenic acid, 5β-coprostanol, hydrocinnamic acid, tricarballylic acid, and sebacic acid in UC patients than in healthy controls	(Santoru et al., 2017)
67 CD, 35 UC, and 37 healthy controls	Targeted metabolomics	▪ Lower levels of tryptophan and indole-3-acetic acid in IBD patients compared to healthy control ▪ Increased levels of kynurenine in the fecal samples of IBD patients	(Lamas et al., 2016)
83 CD, 68 UC, 13 with pouchitis, and 40 healthy controls	Untargeted metabolomics	▪ Decreased levels of medium chain fatty acids (pentanoate, hexanoate, heptanoate, octanoate, and nonanoate) and some typical protein fermentation metabolites in IBD patients than healthy control	(De Preter et al., 2015)
26 CD, 10 UC, and 54 healthy controls	Untargeted metabolomics	▪ Increased levels of amino acid derivatives (phenylethylamine and N-acetylcadaverine) and bile acids (cholic acid, 7-ketodeoxycholic acid, chenodeoxycholic acid sulfate, and 3-sulfodeoxycholic acid), taurine, and tryptophan in pediatric IBD patients compared to healthy controls. ▪ Decreased levels of a glutamate derivative (acetyl-glutamic acid), a heme degradation product (stercobilin), and a product of steroid catabolism (boldione) in pediatric IBD patients compared to healthy controls.	(Jacobs et al., 2016)

1.4.4 The role of host factors in IBD pathogenesis

The host epithelium in the small and large intestine is equipped with various cell types pursuing various functions to establish homeostasis between the luminal content, containing loads of antigens from food and microorganisms, and the mucosal immune system (**Figure 2**). Disruption of epithelial homeostasis, loss of barrier function, and aberrant immune activity are suggested to contribute to IBD pathogenesis.

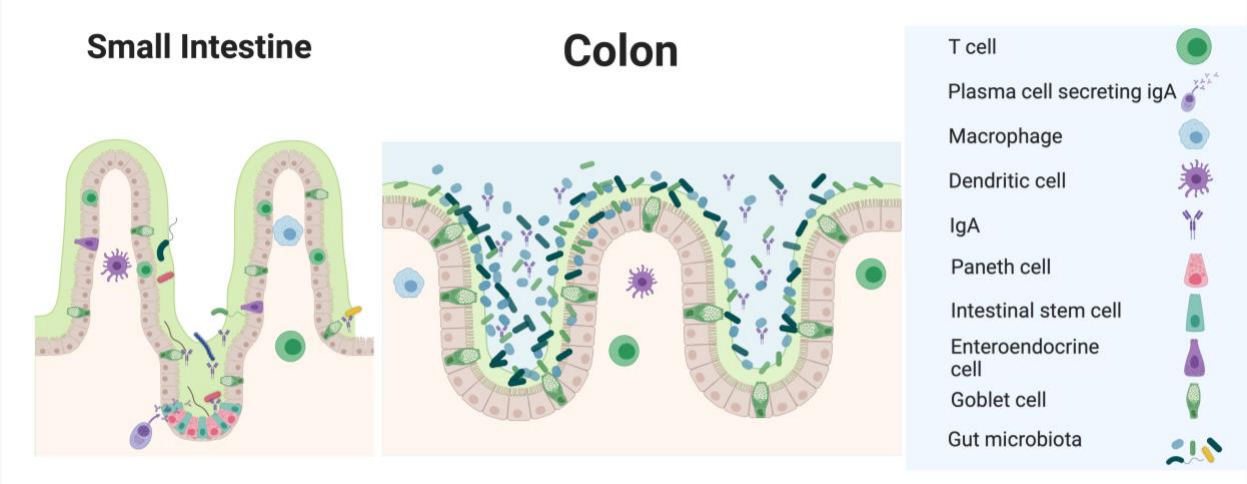

Figure 2 The intestinal epithelium in the small intestine (left) and colon (right)
IECs separate the host immune cells from the microbial environment. IECs are formed from various cell types pursuing diverse functions, where most of its cells are enterocytes. Paneth cells produce antimicrobial peptides (AMP) that support controlling the microbial load in the small intestine. Goblet cells produce mucus, which acts as a physical barrier to microbiota and food antigens from direct contact with IECs. Enteroendocrine cells are specialized cells that produce several hormones that support digestion and metabolism. Secretory IgA (sIgA) is produced by plasma cells and translocated to the lumen. The illustration was created using BioRender.com.

1.4.4.1 Dysfunctional intestinal epithelium in IBD

Intestinal stem cells (ISCs), which reside in the crypt base, are responsible for the regeneration and replenishing of all cells in the epithelium (Barker, 2014; van der Flier and Clevers, 2009). In a recent study, dysfunction of ISCs was reported in CD patients and an IBD mouse model (Khaloian et al., 2020). Enterocytes form the physical barrier of the epithelium via its intercellular tight junction proteins including claudins and occludins (Assimakopoulos et al., 2011). Tight junctions (TJ) and epithelial barrier function were impaired in UC (Heller et al., 2005) and CD patients with active disease (Zeissig et al., 2007). Interestingly, barrier dysfunction predicted the relapse in IBD patients (Kiesslich et al., 2012), suggesting that barrier dysregulation precedes active disease phenotype. Paneth cell (PC) dysfunction has been associated with iCD

(Haberman et al., 2019; Khaloian et al., 2020; Perminow et al., 2010; Thachil et al., 2012; Wehkamp et al., 2005). Moreover, it was reported in various studies that Paneth cell aberrations are associated with microbial dysbiosis in iCD patients (Liu et al., 2016; Zhang et al., 2012b) and iCD mouse models (Schaubeck et al., 2016), indicating complex interactions between PC, the gut microbiome and iCD. Goblet cells—the most abundant epithelial cells from the secretory lineage— reside throughout the GIT, with an increase in cell numbers toward the large intestine, where the majority of bacteria inhabit (Hansson and Johansson, 2010). Mucin 2 (MUC2), which is produced mainly by GC, was reduced in UC patients even in non-inflamed colonic regions (van der Post et al., 2019), and goblet cell numbers were reduced in CD and UC patients (Gersemann et al., 2009), emphasizing the crucial role of goblet cells in IBD pathogenesis. Intriguingly, an increase of mucolytic bacteria such as *Ruminococcus gnavus* and *Ruminococcus torques* was reported in IBD patients with a subsequent surge in mucosa-associated bacteria (Png et al., 2010), suggesting that microbial proteases influence the mucus layer (Johansson et al., 2011).

1.4.4.2 Aberrant immune system in IBD

Disturbed immune homeostasis is a hallmark feature among IBD phenotypes. The success of various biologics, which target cytokines and leukocyte trafficking pathways, highlights the fundamental role of the immune system in IBD (de Souza and Fiocchi, 2016).

Aberrant innate immune cells were reported in IBD patients, including DCs (Hart et al., 2005; Middel et al., 2006), neutrophils (Zhou and Liu, 2017), monocytes (Koch et al., 2010), and macrophages (Kamada et al., 2008), in addition to the innate lymphoid cells (ILCs) (Bernink et al., 2013; Geremia et al., 2011). Aberrant T helper (Th) responses were reported in IBD patients (de Souza and Fiocchi, 2016). CD patients are associated with Th1/Th17 response, which is characterized by high secretion of interferon-gamma (IFNɣ), TNF, IL-1ß, IL-6, IL-22, and IL-17, among other cytokines in the intestinal mucosa (Annunziato et al., 2007; Brand et al., 2006; Eastaff-Leung et al., 2010), while UC patients are associated with Th2 immune response, characterized by higher IL-4, IL-5, and IL-13 cytokines (Ungaro et al., 2017), and more recently Th9 immune response via IL-9 signaling (Gerlach et al., 2014). Moreover, IBD patients exhibit

reduced Treg cell numbers in the peripheral circulation and an increase in Th17 (Eastaff-Leung et al., 2010).

IBD patients showed enrichment of a specific subset of IgA^+ plasma cells (Cupi et al., 2014) and IgG^+ plasma cells (Uo et al., 2013) in the intestinal mucosa, suggesting diverse roles of plasma cells in IBD. IgA and IgG antibodies coated to specific gut microbiota members were reported in the human gut (Fadlallah et al., 2019; Palm et al., 2014). Interestingly, colonization of germfree mice with the enriched IgA^+ bacterial community, which originated from human donors, increased susceptibility to colitis (Palm et al., 2014), and revealed diet-dependent enteropathy (Kau et al., 2015), suggesting a distinct function of IgA-coated bacterial community on influencing the host phenotype. Notably, the specificity of intestinal immunoglobulins towards luminal microbiota and other antigens is largely unknown (Pabst and Slack, 2020). Recent data from Oliver Pabst's group showed that IgA-coated microbiota is a defining property of healthy and IBD patients (Kabbert et al., 2020). Remarkably, the anatomical location of microbes influences their chances of being IgA-bound. For instance, a higher abundance of IgA-coated bacteria in the small intestine than in the large intestine was reported (Bunker et al., 2015). Segmented filamentous bacteria (SFB) and *Mucispirillum*, bacteria that inhabit the small intestine, were described to be bound to IgA (Bunker et al., 2015; Lecuyer et al., 2014). Although higher levels of SFB were reported in the ileal mucosa of UC patients compared to a healthy control group (Finotti et al., 2017), we could not detect SFB in three independent IBD cohorts (412 mucosal samples) (Metwaly et al., 2022a).

1.5 Treatment options for IBD—Current and emerging therapies

There are currently several options to manage IBD patients, and the treatment choice depends on the disease severity and the response to the previous therapy (Dignass et al., 2010; Harbord et al., 2017). Management of IBD patients includes several therapeutic agents, nutritional-therapy, surgery, and emerging therapeutics such as stem cell transplantation and gut microbiota-derived remedies. Therapeutic agents comprise various classes, such as corticosteroids, anti-inflammatory agents such as mesalamine, immunosuppressants such as thiopurines and methotrexate, antibiotics, and biological therapy (Torres et al., 2017; Ungaro et

al., 2017). Biological therapy includes the use of monoclonal antibodies targeting cytokines and integrins involved in inflammatory and leucocyte trafficking pathways, such as TNF (Colombel et al., 2010; Rutgeerts et al., 2005), IL-12/23 p40 (Feagan et al., 2016; Sands et al., 2019), $\alpha_4\beta_7$ integrins (Feagan et al., 2013; Sandborn et al., 2013). Although biologics are considered one of the most effective therapies to induce and sustain remission, up to 40% of patients do not respond to it (Roda et al., 2016), indicating the need for better treatment options for these subsets of patients. Remarkably, one of the most effective methods to treat pediatric CD patients is the administration of exclusive enteral nutrition (EEN), which induces remission characterized by mucosal healing, improved bone health, and nutritional enhancement and is recommended to be the first line of therapy in Europe for pediatric CD (Day and Lopez, 2015; Grover et al., 2014; Ruemmele et al., 2014). In brief, EEN is a liquid-based diet provided either in an elemental, semi-elemental, or polymeric formula, given to patients to be their only source of energy for some weeks.

Stem cell-based therapies are one of the emerging therapies to treat IBD, where mesenchymal stem cells (MSCs) and hematopoietic stem cells (HSCs) have been trialed on IBD patients (Cassinotti et al., 2021). For instance, autologous HSCs transplantation led to significant improvements in endoscopic healing and clinical disease activity for 40 refractory CD patients after one year, but some serious adverse events were reported (Lindsay et al., 2017). Allogenic MSCs derived from bone marrow (Forbes et al., 2014) and adipose tissues (Panes et al., 2018) resulted in significant improvements in clinical and endoscopic disease activities of CD patients, who were refractory to biologic therapy, and with complex perianal fistulas, respectively. Although the promising positive results of stem cell-based therapy, the field is still in its infancy, and more efforts are needed to address its safety (Qiu et al., 2017). Furthermore, newly promising small molecule medications that block sphingosine-1 phosphate and the Janus kinases (JAK) show promising results in clinical studies and recent approval (Pagnini et al., 2019).

Several strategies have been developed to correct microbial dysbiosis as a therapeutic target or adjunct to other IBD therapy. It includes using live microbe/microbial consortium, or complex ecosystem as medications, prebiotics administration, or small molecules that target a

specific member of gut microbiota or its metabolite (Plichta et al., 2019). Probiotics or selected microbial consortia reveal the potential in manipulating gut-microbe host interactions (Atarashi et al., 2013; Lawley et al., 2012). For instance, in a randomized placebo-controlled trial, supplementation of VSL#3 probiotics beside 5-ASA and or immunosuppressants in relapsing UC patients improved disease status in those patients compared to its control (Tursi et al., 2010). Fecal microbial transplantation (FMT), the infusion of fecal suspension of a healthy donor(s) into patients with dysbiosis, was explored in some dysbiosis-associated diseases. FMT showed great success in treating *Clostridium difficile* infection and is more effective than antibiotic treatment (Quraishi et al., 2017; van Nood et al., 2013). FMT showed to be effective in inducing remission in nearly 30% of UC patients in three randomized controlled trials (Costello et al., 2019; Moayyedi et al., 2015; Paramsothy et al., 2017a), while FMT did not show a significant difference in inducing clinical and endoscopic remission for UC patients in one randomized controlled trial (Rossen et al., 2015). The discrepancy in the results of these studies can be attributed to the differences in the donor selection criteria, preparation protocol of FMT (frozen or fresh samples, aerobic or anaerobic conditions, etc.), administration route (nasoduodenal tube, enema, colonoscopy, or multiple methods), and the frequency of administration. There were only a few prospective uncontrolled studies that investigated the impact of FMT on CD patients, and the results were mixed (Cui et al., 2015; Suskind et al., 2015; Vaughn et al., 2016). More recently, the first randomized controlled trial evaluated FMT in maintaining clinical remission for CD patients (Sokol et al., 2020). In brief, FMT resulted in a significant decrease in Crohn's Disease Endoscopic Index of Severity (CDEIS) and C-reactive protein (CRP) levels after six weeks of the trial compared to the control sham group. In addition, the steroid-free clinical remission for the FMT group was 87.5% and 50.0% at 10 and 24 weeks, compared to 44.4% and 33.3% in the sham control group (Sokol et al., 2020). These data suggest a potential role of FMT in IBD management, but the long-term durability and safety remain unclear (Paramsothy et al., 2017b). Further, genetically engineered gut bacteria as an anti-inflammatory drug delivery cargo to the inflammation site was proposed (Vandenbroucke et al., 2010). Targeted depletion of certain pathobionts using phages (Nale et al., 2018) acts as a probable approach for specific modulation of certain gut microbes. Additionally, blocking the pathobiont binding to the epithelium was described, such as antagonists of the

fimbrial adhesion protein (FimH), used by the *adherent-invasive Escherichia coli* (Sivignon et al., 2017). Taken together, gut microbiota modulation is considered a vital target in IBD management, but safety and identifying triggers of IBD flare remain a hurdle for microbiota-based therapeutics development.

Finally, the complexity of IBD pathobiology and the high variability of disease course, in addition to the heterogeneous response to treatments, have directed physicians and scientists toward a personalized approach to IBD management. Personalized medicine looks for accurate biomarkers to match the right treatment for the right patient (Noor et al., 2020). There is a growing interest in IBD biomarkers identification, which could predict prognosis, disease outcome, and response to treatment. These biomarkers include genetic, microbial, clinical, transcriptomic, and proteomic, which could be used separately or combined, known as the multi-omics approach. For instance, microbiome composition was used to predict the response to therapies in IBD patients (Ananthakrishnan et al., 2017; Shaw et al., 2016), and the multi-omics approach predicted the endoscopic response in CD patients (Verstockt et al., 2019). Currently, markers, such as CRP or fecal calprotectin are considered reliable disease activity markers (Noor et al., 2020).

1.6 Mouse models in IBD

More than 74 genetically engineered mouse models, and over 790 genetically engineered mouse models that influence the susceptibility to chemically-induced colitis, were developed for studying IBD pathogenesis, preclinical evaluation of various drug candidates, and identification of diagnostic biomarkers (Bamias et al., 2017; Mizoguchi et al., 2016), indicating the multifactorial nature of IBD. These mouse models are further classified based on the location of the inflammation (ileitis, colitis, enterocolitis, and systemic), or based on the method used (chemical-induced, genetic engineered, spontaneous, or adoptive cell transfer), or based on the inflammation type (acute or chronic), or based on the pathway involved (epithelial cells and barrier dysfunctionality, innate or adaptive immunity) (Cominelli et al., 2017; Mizoguchi et al., 2020). Notably, several IBD mouse models were developed to study various pathways involved in epithelial dysregulation, such as ER stress, UPR, mitochondrial dysfunction, autophagy, necrosis,

and necroptosis. These mouse models include *TNF*$^{\Delta ARE}$ (Kontoyiannis et al., 1999), *Caspase8*$^{\Delta IEC}$ (Gunther et al., 2011), *Xbp1*$^{IEC\text{-}KO}$ (Kaser et al., 2008), *Atg16l1*$^{IEC\text{-}KO}$ (Adolph et al., 2013), *FADD*$^{IEC\text{-}KO}$ (Welz et al., 2011), *NEMO*$^{IEC\text{-}KO}$ (Vlantis et al., 2016), *Phb1*$^{\Delta PC}$ (Jackson et al., 2020) and *Xiap*$^{-/-}$ (Gopalakrishnan et al., 2019), suggesting different mechanisms involved in IBD pathogenesis. In addition, mouse models that lack PRRs such as *TLR2*$^{-/-}$, *TLR4*$^{-/-}$, *TLR9*$^{-/-}$ or Myd88$^{-/-}$, a TLR adaptor protein, and *NOD2*$^{-/-}$ increased colitis susceptibility in epithelial injury models (Maloy and Powrie, 2011; Umiker et al., 2019). Furthermore, TLR associated microbial dysbiosis was reported in several mouse models (Chassaing et al., 2014; Lu et al., 2018), suggesting a complex interplay between the gut microbiota, PRRs, and IBD. Remarkably, *Il10*$^{-/-}$ mice did not develop colitis when it was backcrossed to *Myd88*$^{-/-}$ (Rakoff-Nahoum et al., 2006), indicating that TLRs contribute to dysbiosis and IBD. Intriguingly, several IBD mouse models, such as *Il10*$^{-/-}$, *TNF*$^{\Delta ARE}$, *Xbp1*$^{IEC\text{-}KO}$, *Il2*$^{-/-}$, *T-bet*$^{-/-}$ *RAG2*$^{-/-}$ (TRUC), *TCR-alpha*$^{-/-}$, *TM-IEC C1galt1*$^{-/-}$ and T cell transfer in a SCID model, are disease-free or reduced disease activity under germfree conditions (Ahmed et al., 2021; Hildner et al., 2018; Hormannsperger et al., 2015), suggesting the fundamental role of microbiota in IBD.

1.6.1 Gnotobiotic mouse models—elegant way for dissecting the functional role of microbiota

Colonization of GF animals with a single microbe, selection of a defined number of bacteria (minimal consortia), or a complex microbial environment (SPF-housed or FMT) is considered a vital tool to dissect the functional role of gut microbiota in host responses (Rogala et al., 2020). In this section, gnotobiotic models are discussed in detail with a focus on the *Il10*$^{-/-}$ mouse model as a well-established IBD mouse model. *Il10*$^{-/-}$ mouse model is one of the extensively used models in studying IBD pathogenesis and treatment response in preclinical studies (Keubler et al., 2015; Mizoguchi et al., 2020). *Il10*$^{-/-}$ mice develop spontaneous colitis under SPF conditions, described histologically as patchy transmural inflammation with inflammatory cell infiltrates in the lamina propria and submucosa, coupled with mucin reduction, epithelial hyperplasia, crypt abscess, and thickening of the intestinal wall (Keubler et al., 2015). Some factors influence colitis severity in *Il10*$^{-/-}$, such as genetic background and microbial colonization (Rogala et al., 2020). Colitis development in this model is mediated by aberrant Th1/Th17 response to bacterial antigens characterized by substantial secretion of proinflammatory cytokines, such as IL-12, IL-17, IL-6, and

IFNɣ (Berg et al., 1996; Yen et al., 2006). Several microbial colonization experiments were conducted in *Il10*$^{-/-}$ mice implementing various strategies are summarized in **Table 2**. For instance, mono-association studies in *Il10*$^{-/-}$ mice with *Enterococcus faecalis* or *Escherichia coli* induced colitis in this model, but mono-colonization of various strains of *Lactobacillus* did not develop inflammation (Balish and Warner, 2002; Kim et al., 2005), suggesting selective host-microbiome interactions. Although mono-association studies are a vital tool to study the causative effect of individual gut microbiota components, it neglects microbe-microbe interactions and their overall influence on gut microbiota and host. Therefore, several defined minimum microbial consortia were developed to better study the influence of specific bacterial species in the context of a microbial community. These minimal consortia mimic the multifaceted nature of gut microbiota but with reduced complexity. Schaedler and colleagues developed the first minimal consortium termed "Schaedler-defined flora" (Schaedler et al., 1965). Schaedler-defined flora was later refined to "altered Schaedler flora" (ASF), which contained eight bacterial strains. (Orcutt et al., 1987). More recently, Brugiroux and colleagues have developed a defined microbial consortium that includes 12 bacterial isolates called Oligo-Mouse-Microbiota (Oligo-MM), which provided partial colonization resistance against *Salmonella enterica serovar Typhimurium*, and a complete resistance was achieved after the addition of three facultative anaerobes bacteria to the consortium (Brugiroux et al., 2016). Murine norovirus (MNV) worsened colitis severity in *Il10*$^{-/-}$ mice colonized with ASF consortium, but not with Oligo-MM consortium (Bolsega et al., 2019). Interestingly, co-colonization of SFB with ASF in the same model abolished MNV-induced colitis (Bolsega et al., 2019), suggesting a crucial role of bacterial composition on virus-induced colitis and a potential protective role of SFB in this model. Additionally, a simplified human microbiota consortium (SIHUMI), a consortium of seven well-characterized bacterial species derived from human IBD patients, was stable in mice after colonization (Wohlgemuth et al., 2011). Indeed, colonization of GF *Il10*$^{-/-}$ with SIHUMI induced inflammation in the colon characterized by Th1 and Th17 immune response, and the intensity of inflammation was dependent on the host genotype background (129S6/SvEv or C57BL/6) and independent of luminal bacterial concentration (Eun et al., 2014). Lengfelder and colleagues revealed that the mutant *E. faecalis* strain (Δeut) exacerbates colitis in *Il10*$^{-/-}$ mice when added to SIHUMI colonized mice compared to WT *E.*

faecalis plus SIHUMI (Lengfelder et al., 2019), suggesting a protective function of eut in the complex bacterial community. Interestingly, mono-colonization of *E. faecalis* (Δeut) showed no influence on the colitogenic activity in *Il10*$^{-/-}$ mice compared to WT *E. faecalis* (Lengfelder et al., 2019). Mice colonization with a complex microbial community derived from human donors has emerged to address microbiome functional relevance (Faith et al., 2010). For example, colonization of GF *Il10*$^{-/-}$ mice with microbiota obtained from CD patients caused colitis, but gut microbiota derived from healthy individuals or UC patients failed to induce colitis (Nagao-Kitamoto et al., 2016). Further, colonization of GF *Il10*$^{-/-}$ mice with gut microbiota, obtained from CD patients with active disease, induced inflammation in the cecum, in contrast to gut microbiota derived from CD patients in remission (Metwaly et al., 2020). Noteworthy, not all gut microbiota components were successfully transferred from the human donors to the recipient ex-germfree mice (Metwaly et al., 2020; Nagao-Kitamoto et al., 2016), suggesting that other factors such as diet, host factors, and other environmental factors influence gut microbiota composition. In another spontaneous IBD mouse model, SAMP1/YitFc, colonization of GF SAMP1/YitFc with microbiota obtained from healthy and IBD patients in remission showed a high level of engraftment with 95% on the genus level (Basson et al., 2020). Interestingly, fecal transfer from IBD patients, who were in remission, showed variable disease activity (pro-inflammatory, neutral, and anti-inflammatory) in the SAMP1/YitFc recipients (Basson et al., 2020). Further, gut microbiota obtained from IBD patients exacerbated colitis severity upon the transfer of naïve T cells into *Rag1*$^{-/-}$ (Britton et al., 2019). Collectively, gnotobiotic animal models are an invaluable tool to disentangle the functional role of gut microbiota components in influencing host phenotype. However, it has some ecological and evolutionary limitations (Arrieta et al., 2016).

In summary, gut microbial dysbiosis has been associated with IBD, but the exact mechanism of its role in the disease pathogenesis is still largely unknown. Identifying microbiome signatures in IBD patients and their changes throughout the disease course, coupled with a mechanistic understanding of the microbe-host interactions, will enhance our disease understanding and the development of targeted therapies.

Table 2 Microbial colonization summary in Il10$^{-/-}$ mice

	Experiment	Phenotype	Reference(s)
Mono-colonization experiments	Mono-colonization with ***E. faecalis***	Colitis	(Balish and Warner, 2002; Kim et al., 2005; Kim et al., 2007; Steck et al., 2011)
	Mono-colonization with ***E. Coli* NC101**	Colitis	(Kim et al., 2005; Kim et al., 2007; Schmitz et al., 2019)
	Dual colonization of ***E. faecalis* and *E. coli***	Aggressive pancolitis and duodenal inflammation	(Kim et al., 2007)
	Mono-colonization with ***Bifidobacterium animalis***	duodenal inflammation and mild colitis	(Moran et al., 2009)
	Mono-colonization with **various strains of Lactobacillus (*Lactobacillus casei*, *L. reuteri*, *L. acidophilus*), *Bifidobacterium* species., *Lactococcus lactis*, or a *Bacillus* species**	No inflammation	(Balish and Warner, 2002)
	Mono-colonization with **MNV**	No Colitis	(Basic et al., 2014)
Minimal consortia colonization experiments	**SIHUMI consortium**	Colitis	(Eun et al., 2014)
	SIHUMI consortium lacking E. faecalis	Enhanced inflammation	(Lengfelder et al., 2019)
	ASF consortium	No colitis/mild inflammation	(Bolsega et al., 2019)
	ASF consortium + MNV	Moderate colitis	(Bolsega et al., 2019)
	ASF consortium + MNV +SFB	No Colitis	(Bolsega et al., 2019)
	Oligo-MM consortium	No colitis/mild inflammation	(Bolsega et al., 2019)
	Oligo-MM consortium +MNV	No colitis/mild inflammation	(Bolsega et al., 2019)
Complex gut microbiota colonization obtained from human donors	**Complex gut microbiota from CD patients**	Colitis	(Nagao-Kitamoto et al., 2016)
	Complex gut microbiota from CD patients (active disease status)	Typhlitis	(Metwaly et al., 2020)
	Complex gut microbiota from UC patients, and healthy donors	No Colitis	(Nagao-Kitamoto et al., 2016)

2 Aim of the dissertation

IBD is a devastating chronic disease that affects millions of people worldwide, and there is no cure for the disease yet. A dysregulated immune system, gut microbial dysbiosis, defects in the epithelial tissue homeostasis, and genetic predisposition are among the main features of IBD pathogenesis. Although the enormous research efforts to dissect the role of gut microbiota in IBD pathogenesis, functional evidence to the role of disease-conditioned gut microbiomes as the underlying cause of chronic inflammation is largely unclear. The advancements of multi-omics technologies such as NGS, its integrative analysis, and the growing computational power have resulted in a better understanding of various disease pathogenesis, including IBD. Modulation of gut microbiota is considered a promising therapeutic target in IBD management, but safety and identifying triggers of IBD flare remain a hurdle for developing microbiota-based therapeutics.

In this work, we investigated the gut microbial dynamics in IBD patients throughout the study period (one year), after the initiation of biological therapy, aiming for identifying a gut microbial disease signature linked to disease phenotype, disease location, response to treatment, and disease activity, with a potential application as gut microbial biomarkers. Further, we analyzed microbial profiles of two IBD cohorts (biotherapy cohort and lifestyle intervention UC cohort) to identify IBD gut microbial signature among different IBD cohorts. In addition, we explored the fecal metabolome profiles of IBD patients in the biotherapy cohort and performed a multi-omics (microbiome-metabolome) integrative analysis to understand the molecular mechanisms of IBD pathogenesis. In addition, we compared two clustering methods for the downstream analysis of the 16S rRNA amplicon analysis of the gut microbiota composition in a subset of the biotherapy cohort to assess their impact on the bacterial profiling outcome.

Colonization of GF *Il10*$^{-/-}$ mice with gut microbiota obtained from IBD patients was used as an IBD gnotobiotic mouse model to address the functional relevance of gut microbiota in causing disease phenotype and studying the microbe-host interactions in controlled settings. The gut microbial transfer efficiency was evaluated for the human-derived gut microbiota in gnotobiotic experiments.

3 Materials and Methods

3.1 Human study cohorts- cohort description

3.1.1 Biotherapy cohort

This longitudinal study involved 82 IBD patients (41 CD, 35 UC & 6 pouchitis), where patients were followed for one year after the initiation of therapy (**Figure 3**). IBD patients were recruited for the observational clinical trial in Paris (Hospital San Louis, Prof. Dr. Matthieu Allez and Dr. Lionel Le-Bouhris) with the registration number NCT: 02693340. The initial recruitment period for the study was from February 2016 to March 2018. In brief, CD or UC patients with active disease at baseline (W0) were included aged 18 or more, who were diagnosed according to defined criteria (ECCO recommendations). Patients signed consent before undertaking procedures related to the study. Then initiation of an anti-tumor necrosis factor therapy (Infliximab, Golimumab, Adalimumab) or newly approved biological therapy (Ustekinumab, Vedolizumab) was provided in connection with the management of digestive disease, and the patients were followed up during the year. Stool and intestinal mucosal biopsies samples were collected at baseline (W0), 14 weeks (W14), and 52 weeks (W52) after biological therapy initiation, and the blood samples were collected at W0, W6, W14, W30, and W52 (**Figure 3**). Clinical response to the biological therapies and gut microbial variations have been the focus of the study outcomes. Pregnant or lactating patients were excluded from the study. Disease activity of UC patients was assessed during baseline and overtime using the Mayo score (Paine, 2014) and the Ulcerative Colitis Endoscopic Index of Severity (UCEIS) (Travis et al., 2013) to accurately assess the endoscopic severity of the UC phenotype. Disease activity of the CD patients was evaluated at baseline and throughout the study duration by the Harvey-Bradshaw Index (HBI) (Harvey and Bradshaw, 1980) and the Crohn's Disease Endoscopic Index of Severity (CDEIS) (Mary and Modigliani, 1989) for mucosal assessment of disease severity. Patients' details at baseline (inclusion time) are listed in **Table 3**. A clinical response for CD patients was defined when HBI decrease four points compared to baseline and overall less than eight. The clinical response for UC patients was achieved when the Mayo score is less than two, no rectal bleeding, and no item in the scheme scored more than one. C-reactive protein (CRP) level in plasma was used as a biomarker for disease activity during the

study duration (Henriksen et al., 2008). Stool samples were collected from patients at home or in the clinic using a stool collection kit 24 hours preceding the study visit. Patients were informed to store the stool samples in the home freezer till shipping to the study site, where it was kept on ice in a cooling bag during transportation. Upon arrival at the study site, sterile 20% glycerol-containing phosphate-buffered saline (PBS) was added to the samples, then homogenized via vortexing. Then, samples were transferred to the biobank and stored at -80°C till further use in metagenomic sequencing and metabolomics analysis, as well as colonization of germfree mice. Cryopreservation in glycerol was applied to maintain higher bacterial viability for applications in mice colonization experiments.

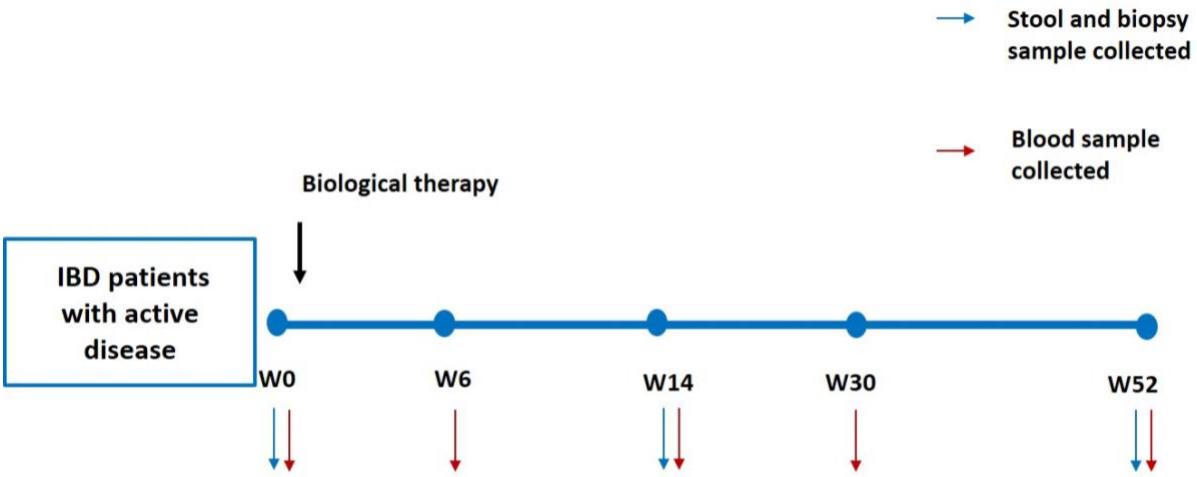

Figure 3 The biotherapy study timeline

Table 3 shows IBD patients (biotherapy cohort) characteristics at inclusion time

Disease phenotype	CD (41)	UC (35)	Poc (6)	NA
Gender (male/female)	(17/24)	(23/12)	(3/3)	0
HBI score (0 - >16)	9 ± 6.5	NA	-	2
Crohn's Disease Endoscopic Index of Severity (CDEIS) (0 - 44)	13.9 ± 9.1	NA	-	4
CRP	21 ± 19.6	NA	-	4
Mayo score (0 - 12)	-	7.5 ± 2.3	-	1
Ulcerative Colitis Endoscopic Index of Severity (UCEIS) (0 - 8)	-	4.8 ± 1.5	-	1
CRP	-	10.1 ± 20.8	-	3
Tobacco status				
Active smoker	9	2	0	-

Non-smoker	19	19	3	-
Ex-smoker	9	11	3	-
NA	4	3	0	-
Corticosteroids				
Currently having Corticosteroids	10	8	1	-
Never had Corticosteroids	4	4	0	-
Stopped having Corticosteroids	24	22	5	-
NA	3	1	0	-
Biologics treatment				
1: INFLIXIMAB	9	11	0	-
2: ADALIMUMAB	13	4	0	-
3: GOLIMUMAB	0	9	0	-
4: USTEKINUMAB	12	0	6	-
5: VEDOLIZUMAB	5	10	0	-
NA	2	1	0	-
Montreal Classification				
Terminal-Ileum	5	NA	NA	-
Colonic	18	NA	NA	-
Ileocolonic	17	NA	NA	-

3.1.2 Ulcerative colitis lifestyle intervention cohort

An independent cohort of ninety-seven UC patients was compared to the biotherapy cohort to study the microbial profiles of different IBD cohorts. This cohort is part of a registered clinical trial on clinicaltrials.gov (ID: NCT02721823) that was conducted at the Kliniken Essen-Mitte in Germany from 2016 to 2019 and is described in detail (Langhorst et al., 2020). Patients with chronically active colitis, infectious disease, severe psychological illness, severe somatic disease (diabetes mellitus or oncological diseases), or pregnancy were excluded. Although the clinical study involved longitudinal sampling, patients at baseline (on clinical remission) only were included in our analysis to reduce any bias from the intervention. Patients received a stool collection kit to collect stool specimens. Stool samples were then frozen at −80°C till further use in 16S amplicon sequencing.

3.2 Metagenomic DNA extraction from fecal samples

The detailed procedures for bacterial metagenomic DNA isolation from the frozen mice content and human stool samples were performed as mentioned in the Structured Transparent Accessible Reproducible (STAR) protocol (Reitmeier et al., 2020b). In brief, 500mg of autoclaved 0.1mm silica beads (Roth), 600µL DNA stabilizing solution (Stratec Biomedical, Germany) were added to the fecal aliquots in a 2-ml screw-cap polypropylene microcentrifuge tube and kept on ice. Then, 500µL of 5% N-lauroyl sarcosine – 0.1M phosphate buffer (pH 8.0) and 250µL of 4M guanidine thiocyanate – 0.1 M Tris (pH 7.5) were added. Fecal suspensions were vortexed and incubated for 1 hour at 70°C with constant shaking. Mechanical microbial cell lysis using a FastPrep®-24 bead beater (MP Biomedicals) fitted with a 24 × 2mL cooling adaptor three times each for 40 seconds at 6.5 m/s speed. A total of 15mg of Polyvinylpolypyrrolidone (PVPP, Sigma Aldrich) was added as polyphenol adsorbent followed by centrifugation of the suspension at 15000×g for 3 minutes at 4°C. The supernatant was then transferred to a new 2mL tube and centrifuged at 15000×g for 3 minutes at 4°C. Then, RNAse (10 mg/ml) was added to the supernatant and incubated for 30 minutes at 37°C with continuous shaking to eliminate bacterial RNA. Metagenomic DNA was purified using the NucleoSpin® columns (silica membrane-based columns) (Macherey Nagel) following the manufacturer's guidelines. Genomic DNA concentrations and purity were measured using the NanoDrop® Spectrophotometer ND-1000 (ThermoFisher Scientific, USA), and samples were used for immediate library preparation or kept at -20°C as 35µl aliquots for longer storage. After the genomic DNA extraction, all pipetting steps were performed using a robotized liquid handler to maximize reproducibility.

3.3 Metagenomic DNA extraction from tissue biopsies (mucosa-associated bacteria)

Bacterial metagenomic DNA was extracted using the NucleoSpin® Tissue kit (Macherey-Nagel). Patients' tissue biopsies were resuspended in 180µL sterile-filtered lysis buffer (2 mM EDTA, 1% Triton X-100 & 20 mM Tris/HCl) (pH 8) and 20mg/mL lysozyme, freshly prepared before use, were added. Then, biopsies suspensions were incubated in a shaker for 30 minutes at 37°C with 950 rpm. Proteinase K (10mg/mL) was supplemented to the suspension and vortexed vigorously, followed by incubation for 1-3 hours at 56°C with 950 rpm till complete tissue lysis.

Afterward, purification was performed by the NucleoSpin® Tissue kit following the manufacturer's recommendations.

3.4 High-throughput 16S ribosomal RNA (rRNA) gene amplicon sequencing

Following the genomic DNA extraction, bacterial DNA was further diluted in PCR-grade water and used as a template for PCR that was performed in duplicates. The V3/V4 regions of the 16S rRNA genes were amplified (25 cycles for fecal samples & 15x15 cycles for biopsies) using the bacteria-specific primers 341F and 785R (Klindworth et al., 2013), followed by a two-step procedure to limit amplification bias (Berry et al., 2011). PCR-product concentration was measured using fluorometry and was adjusted to 2nM concentration before pooling. Amplicon purification was conducted by the AMPure XP system (Beckman-Coulter, MA, USA). Amplicon sequencing was performed with pooled samples in paired-end modus (2×250 bp) using a MiSeq system (Illumina, CA, USA) according to the manufacturer's guidelines and 25% (v/v) PhiX standard library. Two samples were used as a positive control (a mock community (ZymoBIOMICS, No. D6300), and negative controls (PCR control without DNA template and a DNA extraction control of DNA stabilizer) to control artifacts among sequencing runs.

3.5 Bioinformatic analysis of the 16S rRNA gene amplicon sequencing

Raw sequencing data were pre-processed using the IMNGS pipeline (Lagkouvardos et al., 2016) according to the UPARSE approach for Operational Taxonomic Units (OTUs) analysis (Edgar, 2013) and to the UNOISE2 approach for Zero-radius operational taxonomic unit (zOTUs) analysis (Edgar, 2016). In brief, sequences were demultiplexed, trimmed to the first base with a quality score of <3, and then paired. Sequences with <300 and >600 nucleotides plus paired reads with an expected error of >3 were eliminated from the analysis. The remaining reads were further trimmed by five nucleotides on each end to avoid GC bias and non-random base composition. In addition, Chimera presence was examined using UCHIME (Edgar et al., 2011). The clustering of sequences for generating OTUs was performed at 97% sequence similarity and 100% similarity for zOTUs. zOTUs and OTUs with a relative abundance of less than 0.25% across all samples were removed to exclude spurious zOTUs and OTUs (Reitmeier et al., 2021). Taxonomic annotation of

OTUs was assigned at an 80% confidence level using the RDP classifier (Wang et al., 2007) and compared to the SILVA ribosomal RNA gene database project (Quast et al., 2013). The taxonomic annotations of zOTUs were generated using the SILVA ribosomal RNA gene database project (Quast et al., 2013). Precise identification of some sequences of interest of the OTUs and zOTUs was achieved using the EzBioCloud database (Yoon et al., 2017). Downstream analysis was done by R-package Rhea (Lagkouvardos et al., 2017). Rarefaction curves were used to evaluate the sequencing depth and to exclude samples with low read count. Absolute read counts were normalized by minimum sum counts. The description of taxonomic composition is based on relative abundances. Alpha-diversity analysis, the variation within one sample, was depicted by either richness (number of OTUs and zOTUs) or Shannon effective (an exponential function of Shannon index/bacterial diversity index). Alpha-diversity calculation involved a denoising threshold of 0.5 read counts per OTU/zOTU to eliminate low abundant OTUs/zOTUs. Beta-diversity analysis, the similarities between samples, was calculated based on generalized UniFrac distances (using GUniFrac v1.1. distances). For the beta diversity analysis, the significance between the groups was calculated using a permutational multivariate analysis of variances (PERMANOVA) (adonis function of the vegan R-package 570v.2.5-6), and p-values were corrected for multiple testing following Benjamini-Hochberg. For visual illustrations of beta-diversity, projections of each sample in a two-dimensional space were used, such as multidimensional scaling (MDS) (Lagkouvardos et al., 2017) and dendrogram using EvolView (Subramanian et al., 2019). The linear discriminant analysis effect size (LEfSe) was conducted on the microbial relative abundance data using http://huttenhower.sph.harvard.edu/lefse/ (Segata et al., 2011). Taxa with Kruskal-Wallis p-value <5% and LDA score with at least ×100-fold change (log10 fold change of 2) were considered significant.

3.6 Bacterial function prediction

Prediction of the bacterial metagenomic functions from the 16S rRNA gene analysis was performed using the Phylogenetic Investigation of Communities by Reconstruction of Unobserved States tool (PICRUSt2) (Douglas et al., 2020). The results of the PICRUSt2 were then explored and

visualized using the LEfSe analyses (Segata et al., 2011) to identify the microbial pathways that were significantly different between groups.

3.7 Machine learning method

The 10-fold cross-validated random forest models with 500 trees were performed to validate microbial signatures in different subsets of the biotherapy cohort. For each iteration, a receiver operating characteristic curve (ROC curves) with the area under the curve (AUC) values were generated. Random forest analysis was performed using the 16S amplicon analysis tool Namco (https://exbio.wzw.tum.de/namco/) (Dietrich et al., 2022), which was developed by Dr. Markus List group, Technical University Munich Chair of Experimental Bioinformatics.

3.8 Untargeted metabolomics

Untargeted metabolomics measurement and data analysis was performed in collaboration with the BayBioMS (Bayerisches Zentrum für Biomolekulare MassenSpektrometrie) at the Technical University of Munich. The untargeted analysis was accomplished using a Nexera UHPLC system (Shimadzu) coupled to a Q-TOF mass spectrometer (TripleTOF 6600, AB Sciex). Patients' frozen stool samples (2mL per sample) were placed on 15mL Precellys® lysis tubes. Separation of the fecal samples was performed using a HILIC UPLC BEH Amide 2.1x100, 1.7 µm analytic column (Waters Corp.) with 400µL/min flow rate and a reversed-phase Kinetex XB-C18, 2.1x100, 1.7µm analytic column (Phenomenex). The mobile phase for the HILIC separation was 5mM ammonium acetate in water (eluent A) and 5 mM ammonium acetate in acetonitrile/water (95/5, v/v) (eluent B). The gradient profile was 100% B from 0 to 1.5 minutes, 60% B at 8 minutes and 20% B at 10 minutes to 11.5 minutes, and 100% B at 12 to 15 minutes. The mobile phase for the reversed-phase separation was 0.1% formic acid (eluent A) and 0.1% formic acid in acetonitrile (eluent B) with a 300µL/minute flow rate. The gradient profile was 0.2% B from 0 to 0.5 min to 100% B at 10 minutes which was hold for 3.25 minutes, afterwards, the column was equilibrated to starting conditions. A volume of 5µL per sample was injected for both chromatographic methods. The autosampler was cooled to 10°C and the column oven heated to 40°C. Every tenth run a quality control (QC) sample which was pooled from all samples was injected. The fecal samples were

measured in a randomized order. The samples have been measured in Information Dependent Acquisition (IDA) mode. MS settings in the positive mode were as follows: Gas 1 55, Gas 2 65, Curtain gas 35, Temperature 500°C, Ion Spray Voltage 5500, de-clustering potential 80. The mass range of the TOF MS and MS/MS scans were 50 - 2000 *m/z* and the collision energy was ramped from 15 - 55 V. MS settings in the negative mode were as follows: Gas 1 55, Gas 2 65, Cur 35, Temperature 500°C, Ion Spray Voltage -4500, de-clustering potential -80. The mass range of the TOF MS and MS/MS scans was 50 - 2000 m/z and the collision energy was ramped from -15 - -55 V.

3.9 Metabolomics data analysis

The raw data was converted to an mzXML file using proteomeWizard (using centroid mode) (Morgulis et al., 2008). Then the mzXML files were processed using the R/Bioconductor package "xcms" (Smith et al., 2006). In detail, peak picking was performed using the "matchedFilter" algorithm. The peaks identified by less than three data points of intensity >1000 were excluded. The retention time correction was performed based on the peak groups presented in more than half of all samples. Finally, peaks from the same and different samples were grouped into features (potential metabolites) using the peak density algorithm, which groups peaks based on the distance of peaks on the mass-charge-ratio (m/z) and retention time (RT) dimension. As a result, the xcms process results in a feature table where the rows are features, characterized by m/z and RT, and columns are samples. To annotate the features with known metabolites, the features' m/z, MS/MS fragments, and retention time are compared to the in-house standard metabolite library, consisting of 123 metabolites. Additionally, the features were compared to metabolites recorded in the public databases, including HMDB4.0 (Wishart et al., 2018) and MSDIAL (Tsugawa et al., 2015), to have a more comprehensive annotation. The principal component analysis was used to describe the general pattern in the data. The student t-test was used to perform pairwise differential expression between the different groups. The resulted p-values were corrected using Benjamini-Hochberg methods to control the false discovery rate (FDR). The data were visualized and explored using the in-house data exploration tool "xcmsViewer" (unpublished tool). All analyses were performed using R (version 3.6.3).

3.10 Microbial and metabolomic data integration and analysis

Multi-omics data integration of gut microbiota and untargeted metabolomics from the stool samples of the biotherapy cohort was performed in collaboration with the LipiTUM - Computational Systems Medicine on Lipids and Metabolism at the Technical University of Munich. In brief, prior to data integration, log-transformed metabolite data was scaled (feature-wise) to have a mean of 0 and unit variance. Besides, 16S count data was centered log-ratio transformed with a pseudo-count added for numerical stability.

3.10.1 Multi-omics factor analysis (MOFA)

Multi-omics factor analysis (MOFA) (Argelaguet et al., 2020; Argelaguet et al., 2018) is an unsupervised framework designed to integrate heterogeneous multimodal data measured on the same set of samples with missing values allowed. Similar to the well Principal Component Analysis (PCA), MOFA uncovers the major direction of variation in the data. For this purpose, each matrix data is decomposed into a weight matrix and a set of latent factors shared across all data sets. The weight matrix indicates the influence of each variable on any given factor, while the position of each sample on any factor is represented by the latent factor matrix. Both the weight matrices and latent factor matrix are inferred using (Bayesian) variational inference. For running MOFA, the mofapy2 python package (version 0.5.8) and the MOFA2 R package (version 1.0.1) (for downstream analysis) were used together with custom visualization tools. The analysis was run without internal correction for specific covariates, but factors with the highest variance were checked for highly correlating covariates.

3.10.2 Data Integration Analysis for Biomarker discovery using Latent variable approaches for Omics studies (DIABLO)

Data Integration Analysis for Biomarker discovery using Latent variable approaches for Omics studies (DIABLO) (Singh et al., 2019) was used as a supervised analysis framework. DIABLO generalizes (sparse) Partial Least-Squares Discriminant Analysis (PLS-DA) for the integration of multiple datasets measured on the same samples. Analogous to a regular PLS-DA, it can be used to find the most discriminative features separating sample groups by considering feature

coefficients. For DIABLO analyses, the mixOmics R package (version 6.14.0) (Rohart et al., 2017) was used along with custom scripts for robust performance estimation. All data were analyzed using R version 4.0.4 and python version 3.8.5.

3.11 Gnotobiotic mouse studies

Germfree *Il10*$^{-/-}$ and WT (129S6/SvEv) mice (each experiment had 4-6 mice per group) were colonized with gut microbiota derived from two CD patients of the biotherapy cohort to study the effects of different complex microbiota in IBD pathogenesis. Paired fecal samples from two CD donors, which were collected 14 and 52 weeks after the initiation of the biotherapy medication, were used to colonize GF mice (WT and *Il10*$^{-/-}$*).* Microbial inoculation in GF mice was done for three consecutive days at the age of 8 weeks for four weeks, as illustrated in **Figure 4**. In total, 21 GF WT control and 24 GF *Il10*$^{-/-}$ mice were used in the four colonization experiments. Mice were sacrificed at 12 weeks of age using CO2.

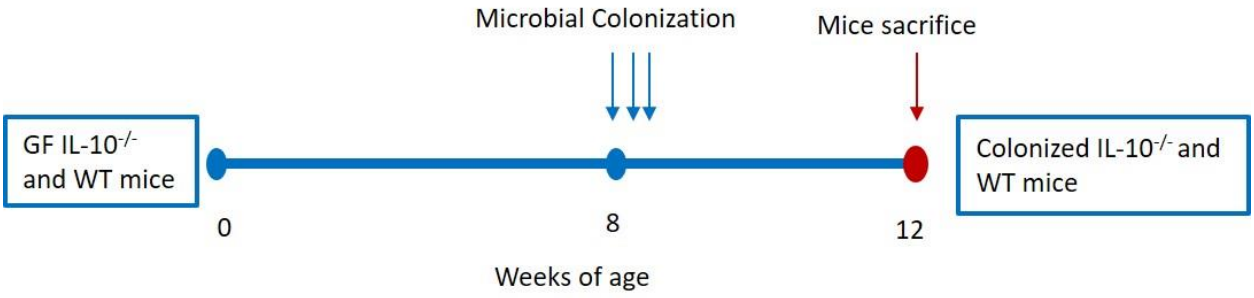

Figure 4 The experimental setup of the gnotobiotic mice experiments

3.11.1 Ethical statements and housing conditions

Gnotobiotic mice experiments were approved by the committee on animal health and care of the local government with the approval number (55.2-1-54-2532-133-2014). Mice experiments were conducted at the germfree core facility Mikrobiom/Gnotobiologie of the Technical University Munich, ZIEL – institute for food & health (school of life sciences Weihenstephan). Mice were housed in gnotobiotic isolators (plastic films) with controlled HEPA-filtered air at 22±1°C with a 12-hour dark/light cycle. Before experiments, littermates were pooled and randomly allocated to treatment groups, with a maximum of five mice per cage (floor area ~540 cm^2). Mice were housed separately in cages according to their genotype and gender, whereas mice with the

same genotype and gender were housed together. Group-specific isolators were assigned to mice colonized with the same microbiota. Mice were fed autoclaved chow diet (V1124-300, Ssniff, Soest, Germany) and water ad libitum. To ensure the germfree status of mice before experiments, cultivation of feces in Wilkins-Chalgren Anaerobe (WCA) (OXOID, UK) and by Gram staining of fecal suspensions were performed.

3.11.2 Stool sample processing for germfree mice colonization

Four stool samples from two CD donors, including two time-points from each donor (W14 and W52), were used for the colonization experiments. In brief, the frozen stool samples (containing glycerol 20%) were preprocessed in an ultraviolet sterilized biosafety hood and pulverized using sterile mortar and pestle, while submerged in liquid nitrogen to ensure higher microbial viability as described previously (Ridaura et al., 2013). Individual autoclaved sets (1 mortar and 1 pestle per sample) were used to prevent samples' cross-contamination. Aliquots of 400mg of the pulverized stool samples were collected from each sample and stored at -80°C till further use.

3.11.3 Colonization of GF mice with human-derived gut microbiota

On the days of colonization of GF mice, the frozen stool aliquots were prepared under anaerobic conditions using the anaerobic chamber. In brief, 400mg of the frozen pulverized stool aliquot was diluted in 2mL reduced PBS (PBS supplemented with 0.05% L-cysteine-HCl) in an anaerobic chamber (Whitley Hypoxystation H85, Meintrup DWS Laborgeräte GmbH) with 75% N_2, 20% CO_2, and 5% H_2 at 37°C. Then, it was vortexed for 5 minutes, and the stool suspension was settled by gravity for 5 minutes to exclude the residual particulate matter. The clear supernatant was transferred into a Hungate tube (VWR International), gassed with N_2, and then transferred to the gnotobiotic facility. Each GF recipient mouse (WT and *Il10*$^{-/-}$) received 100µL of the human-derived gut microbial suspension by oral gavage using a 20 Gauge gavage needle (Fine Science Tools) for three consecutive days.

3.11.4 Histological assessment (tissue processing and H&E staining)

For the histological evaluation, cecal and colon swiss-roll tissues were collected from mice immediately after sacrifice, and it was dissected from the adjacent tissues. Then, they were fixed in formalin 4% for 24 hours. The tissues were then dehydrated (Leica TP1020, **Table 4**) and embedded in melted paraffin (McCormick; Leica EG1150C). Tissues were cut into 5µm tissue sections (Leica RM2255), mounted on SuperFrost® microscope slides (VWR), and dried overnight. The tissue sections were then deparaffinized, rehydrated, and stained with hematoxylin and eosin (H&E) (MEDITE) in an automated manner (Leica ST5020, **Table 5**). The slides were mounted with a mounting media DPX new (Merck) and covered with a glass slide (VWR). Histological images were acquired using a digital microscope M8 (PreciPoint GmbH). Histopathological scoring of H&E-stained tissue sections was evaluated blindly by an independent pathologist of the Comparative Experimental Pathology department (Dr. med. vet. Katja Steiger) at the Technical University of Munich. Signs of inflammation were assessed by the mononuclear cell infiltration, mucosal architecture distortion, and epithelial damage resulting in a score spanning from 0 (not inflamed) to 13 (highly inflamed) (manuscript in preparation).

Table 4 describes the tissue processing steps (dehydration and paraffin)

Step	Reagent	Duration (minutes)	Step	Reagent	Duration (minutes)
1	Ethanol 70%	60	**7**	Ethanol 100%	60
2	Ethanol 70%	60	**8**	Ethanol 100%	60
3	Ethanol 80%	60	**9**	Xylene	60
4	Ethanol 96%	60	**10**	Xylene	60
5	Ethanol 96%	60	**11**	Paraffin	60
6	Ethanol 100%	60	**12**	Paraffin	60

Table 5 Deparaffinization, rehydration and H&E staining steps

Deparaffinization and Rehydration		
Step	**Reagent**	**Duration (minutes)**
1	Xylene	5
2	Xylene	5
3	Ethanol 100%	5
4	Ethanol 100%	5
5	Ethanol 96%	2
6	Ethanol 96%	2

7	Ethanol 70%	2
8	Ethanol 70%	2
H&E staining		
9	Distal water	0.5
10	Hematoxylin	2
11	Running distal water	0.25
12	Scotts solution	0.5
13	Distal water	0.5
14	Ethanol 96%	0.5
15	Eosin	2
16	Ethanol 96%	0.5
17	Ethanol 96%	0.5
18	Ethanol 100%	0.5
19	Ethanol 100%	0.5
20	Xylene	1.5
21	Xylene	1.5

3.11.5 Gene expression analysis

Tissue sections from the cecum and proximal colon (sites of inflammation) were immediately collected after mice euthanization and stored in RNAlater (Sigma Aldrich) at -80°C. RNA was isolated from whole intestinal tissues using the NucleoSpin® RNA Kit (Macherey Nagel), followed by cDNA generation and qRT-PCR. In brief, tissue samples were thawed on ice and mixed with 500µl RA1 buffer (Macherey Nagel) supplemented with 10mM DTT (Sigma Aldrich) in a 2mL tube containing ceramic beads. Mechanical cell lysis was done using a FastPrep®-24 bead beater (MP Biomedicals) one time for 40 seconds at 6.5 m/s speed. Then, RNA was isolated and purified from whole intestinal tissues using the NucleoSpin® RNA Kit (Macherey Nagel) as per the manufacturer's instructions. RNA quantity and purity were measured by a NanoDrop® ND-1000 spectrophotometer (Thermo Fisher Scientific).

3.11.6 Reverse transcription and gene expression analysis via qPCR

Complementary DNA (cDNA) was synthesized from 500ng RNA using the Moloney murine leukemia virus (MMLV) Point Mutant Synthesis System (Promega) and random hexamers. Quantification was performed by LightCycler 480 Universal Probe Library System (UPL, Roche)

with a two-step program: 95°C for 3 min, 40 cycles of 95°C for 5 seconds, and 60°C for 10 seconds. The reactions were in 10µl volumes containing 1µl of cDNA template, 1x PCR master mix (Agilent), 400nM of each primer, and 200nM of the probe. Primers (Sigma Aldrich) and corresponding UPL probes (Roche) are listed in **Table 6**. The relative expression of gene expression was calculated using the $2^{-\Delta\Delta Ct}$ method (Livak and Schmittgen, 2001) and normalized for the expression of the housekeeping gene GAPDH.

Table 6 highlights primers used for gene expression analyses of mice experiments

Gene name	Primer sequences; (5' – 3'); left; right	UPL probe
GAPDH	tccactcatggcaaattcaa; tttgatgttagtggggtctcg	#9
TNF	tgcctatgtctcagcctcttc; gaggccatttgggaacttct	#49

3.11.7 Bacterial enumeration of fecal samples

Bacterial cultivation on WCA was performed on the collected fecal pellets of mice to determine the microbial count. In brief, bacterial enumeration was performed through serial dilutions of fecal suspension in reduced PBS and homogenized by vortexing. Serial dilutions were then plated on WCA plates at 37°C under anaerobic conditions (Whitley Hypoxystation H85, Meintrup DWS Laborgeräte GmbH). Then, the colonies were counted two days after cultivation, and the colony forming unit (CFU) per gram of feces/content was calculated.

3.11.8 IgA coated bacterial quantification

Semi-quantification of IgA-coated bacteria from mice fecal pellets was performed using flow cytometry. In brief, frozen fecal pellets were placed in FastPrep Lysing Matrix D tubes containing ceramic beads, which contained 1 ml PBS (0.1µm sterile filtered) and incubated on ice for one hour. Fecal pellets were well-homogenized using a vortex for a few minutes and then centrifuged at 50g for 15 minutes at 4°C to remove large particles. Fecal supernatants were removed and washed with 1mL of the staining buffer (0.1µm sterile-filtered PBS containing 3% fetal bovine serum) and then centrifuged for 5 minutes at 8000g and 4°C. Fecal pellets were resuspended in 1mL staining buffer and centrifuged at 8000g for 10 minutes at 4°C. Microbial concentration was measured using OD_{600} via NanoDrop® Spectrophotometer ND-1000 (ThermoFisher Scientific,

USA), and then an OD_{600} of 0.13-0.14 were standardized for samples. Microbial cells were transferred to a V-bottom 96 microtiter plate then stained with mouse anti-goat IgA antibody (SouthernBiotech) (1:200) and incubated for 30 minutes. Then, cells were stained with nucleic acid dye Syto9 (Invitrogen) (1:1000) for 10 minutes and washed once at 3500rpm for 10 minutes at 4°C. Cells were analyzed using an LSRII system (BD Biosciences). The data output was analyzed using FlowJo software. The percentage of IgA-coated bacteria was calculated by dividing the IgA-positive community by the whole bacterial community (Syto9 positive). Gating was performed based on NOD/SCID mice that lack IgA-secreting plasma cells and GF samples as a negative control.

3.12 Statistical analysis

Statistical analyses were performed using GraphPad Prism (version 9.0.1, GraphPad Software for Mac, San Diego, California USA, www.graphpad.com) unless otherwise stated. For comparison between two groups, Student's two-tailed unpaired t-test, and for comparison between more than two groups, one-way ANOVA followed by pairwise comparison testing (Bonferroni posthoc test). $P \leq 0.05$ was considered significant; *, $p \leq 0.01$; **, $p \leq 0.001$; ***, $p \leq 0.0001$; ****. For microbiota data analysis, which is characterized by non-parametric data distribution, comparison between two groups, the Mann Whitney U test was used, and comparison between more than two groups, one-way ANOVA followed by multiple comparison testing (Dunn test). Over time changes were performed by the non-parametrical Friedman test and adjusted for multiple testing.

4 Results

4.1 Characterization of the biotherapy cohort

4.1.1 Phenotypic characterization of the biotherapy cohort

The biotherapy cohort comprised 41 CD, 35 UC, and 6 pouchitis patients initiating biological therapy, and patients were followed up for one year. The 16S rRNA amplicon sequencing was conducted on fecal (n = 142) and mucosa-associated (n= 167) samples to evaluate the longitudinal gut microbial composition variations in IBD patients. Further, untargeted metabolomics analysis of the stool samples (n = 145) was performed to study the fecal-associated metabolomic signatures in IBD patients. Integrative microbiome-metabolome analysis of the stool-derived gut microbial and metabolomic data was conducted to get further insights on IBD pathogenesis. All IBD patients in the biotherapy cohort showed active disease phenotype at baseline (W0), and administration of the biological therapies induced clinical and endoscopic remission in up to 60% of patients assessed by reduction of CRP, HBI and Mayo scores, CDEIS, and UCEIS (**Table 7**).

Table 7 The phenotypic characteristics of the biotherapy cohort during the study time

CD patients			
	W0	**W14**	**W52**
HBI score (number of patients)	9 ± 6.5 (n= 39)	5.1 ± 5.9 (n= 30)	3.5 ± 6 (n= 17)
CDEIS (number of patients)	13.9 ± 9.1 (n = 37)	9.8 ± 10.4 (n= 26)	5.6 ± 5.2 (n= 18)
CRP (number of patients)	21.2 ± 19.6 (n= 37)	12.1 ± 19.2 (n= 25)	7.1 ± 5.2 (n= 7)
Active CD patients	41	16	9
Inactive CD patients	-	16	17
Missing disease activity data	-	9	15
UC Patients			
	W0	**W14**	**W52**
Mayo score (number of patients)	7.5 ± 2.3 (n=33)	4.3 ± 3.4 (n=27)	1.6 ± 1.3 (n=8)

UCEIS (number of patients)	4.8 ± 1.5 (n =34)	3.2 ± 2.5 (n=28)	1.5 ± 1.3 (n=8)
CRP (number of patients)	10.1 ± 20.8 (n= 32)	4.7 ± 6 (n=20)	2.1 ± 1.7 (n=7)
Active UC patients	35	17	6
Inactive UC patients	-	14	16
Missing disease activity data	-	4	13
pouchitis patients			
	W0	**W14**	**W52**
CRP	16.5 ± 16.5 (n =6)	8.2 ± 7.6 (n =3)	2.7 ± 3.1 (n =3)
Active pouchitis patients	6	3	4
Inactive pouchitis patients	-	2	
Missing disease activity data	-	1	2

4.1.2 Characterization of the stool gut microbial profiles of the biotherapy cohort

Stool samples (n =142) were collected from 65 IBD patients at three time points (W0, W14, and W52) after the initiation of biological therapy to characterize the gut microbial profiles of IBD patients over time and identify disease phenotype associated taxa **(Table S1**). Further, we investigated the effect of disease activity in shaping the gut microbial composition of IBD patients. The remission (inactive disease status) for CD patients was defined when HBI decreases four points compared to baseline and overall less than eight. The remission (inactive disease status) for UC patients was achieved when the Mayo score is less than two, no rectal bleeding, and no item in the scheme scored more than one.

4.1.2.1 Longitudinal analysis of gut microbial profiles reveals a strong individualized microbial signature of IBD patients

To assess the microbial profile variation over time, 66 stool samples of 22 IBD patients were analyzed at baseline (W0), 14 and 52 weeks after biological therapy initiation (**Figure 5**). The 22 patients comprise 10 CD (5 iCD & 5 cCD), 2 pouchitis, and 10 UC. Unsupervised beta diversity analysis showed that 41% of stool samples (derived from 9 patients) had a distinct personalized cluster throughout the year, where the three stool samples derived from the same patient

clustered together, suggesting a strong personal microbial signature regardless of disease activity state and the biotherapy medication (**Figure 5**). Moreover, in 31% of stool samples (derived from 7 patients) 2 out of the 3 samples formed a uniform cluster. Further, alpha diversity measures, such as richness and Shannon effective, showed a stable individualized profile during the three time-points with no significant changes over the year, regardless of the disease activity status (**Figure 6**). These data demonstrate that the biotherapy medication did not influence the gut microbial composition assessed by the insignificant difference of their microbial diversity (richness and Shannon effective measures) of W14 and W52 compared to baseline (**Figure 6**) and beta diversity analysis (**Figure 7**).

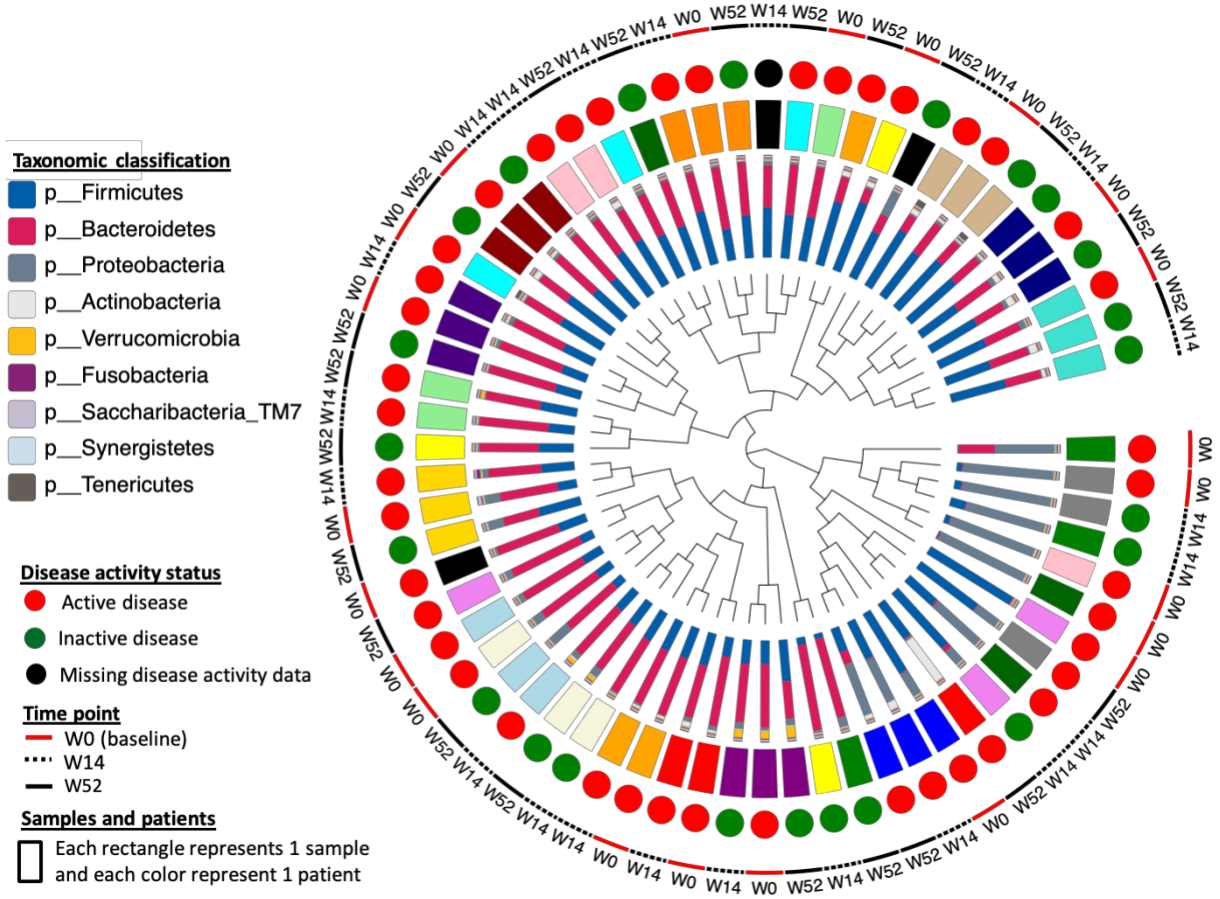

Figure 5 Beta-diversity analysis of longitudinal fecal samples collected over one year from 22 IBD patients of the biotherapy cohort

The dendrogram describes microbial profile similarities based on generalized UniFrac distances between 66 samples. The individual microbial composition on the phylum level is depicted as a stacked bar plot around the dendrogram. Each rectangle, outer of the stacked bar plot, represents one sample, and each patient is represented by one color of the rectangle. Circles, outer of the rectangles, depict the disease activity of the patients (red: active disease, green: inactive disease & black: missing disease activity data). Finally, bars in the outer part of the figure represent the sample time points (bold red line: baseline sample (W0), dotted black line: W14, and bold black line: W52).

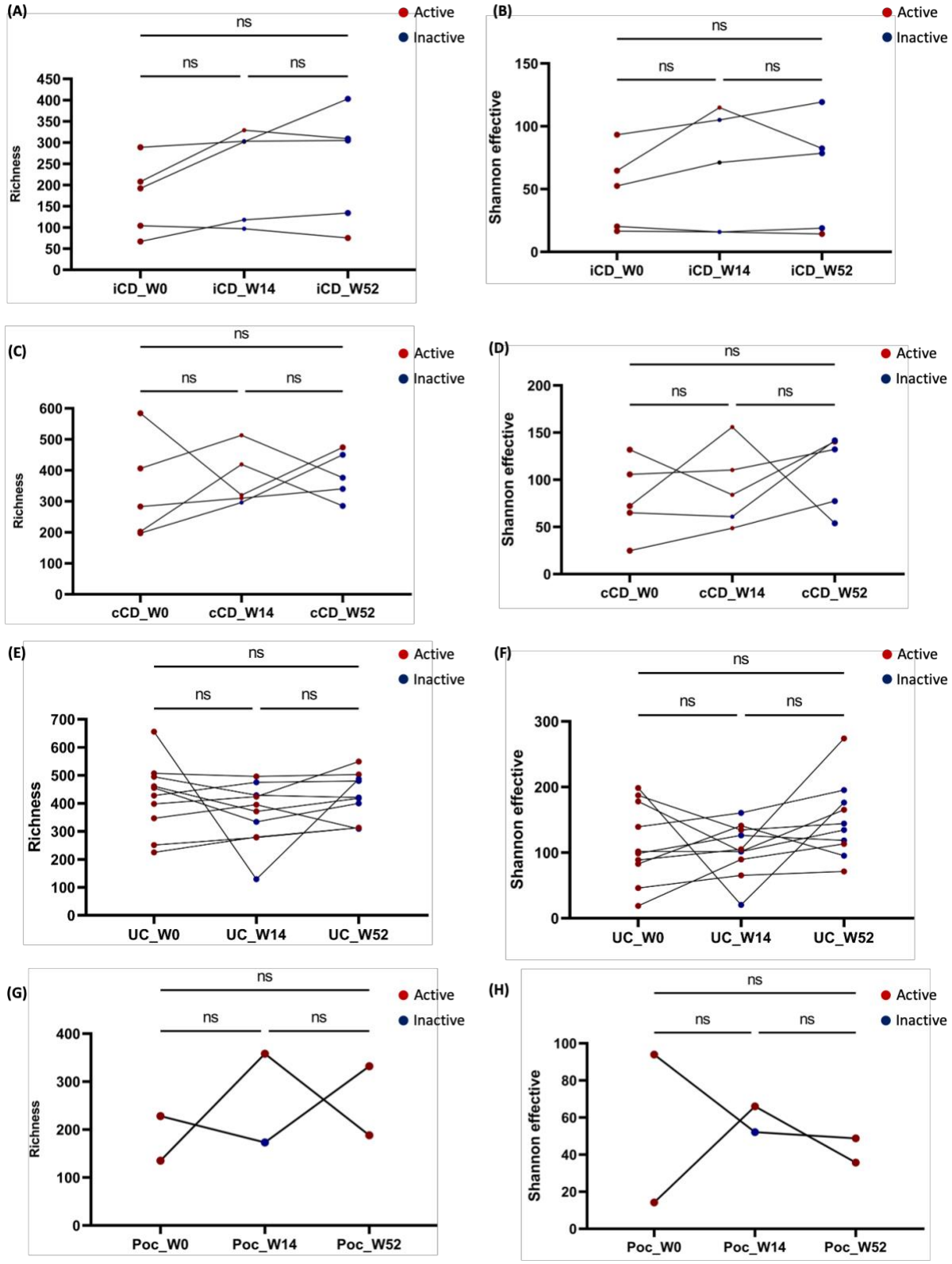

Figure 6 Alpha diversity analysis of longitudinal fecal samples collected over one year from 22 IBD patients (biotherapy cohort) *The microbial community richness (**A**, **C**, **E** & **G**) for iCD, cCD, UC, and pouchitis patients respectively at baseline (W0), 14 and 52 weeks. The Shannon effective analysis (**B**, **D**, **F** & **H**) for iCD, cCD, UC, and pouchitis patients respectively at baseline (W0), 14 and 52 weeks. The circle color depicts the disease activity (red: active disease & blue: inactive disease).*

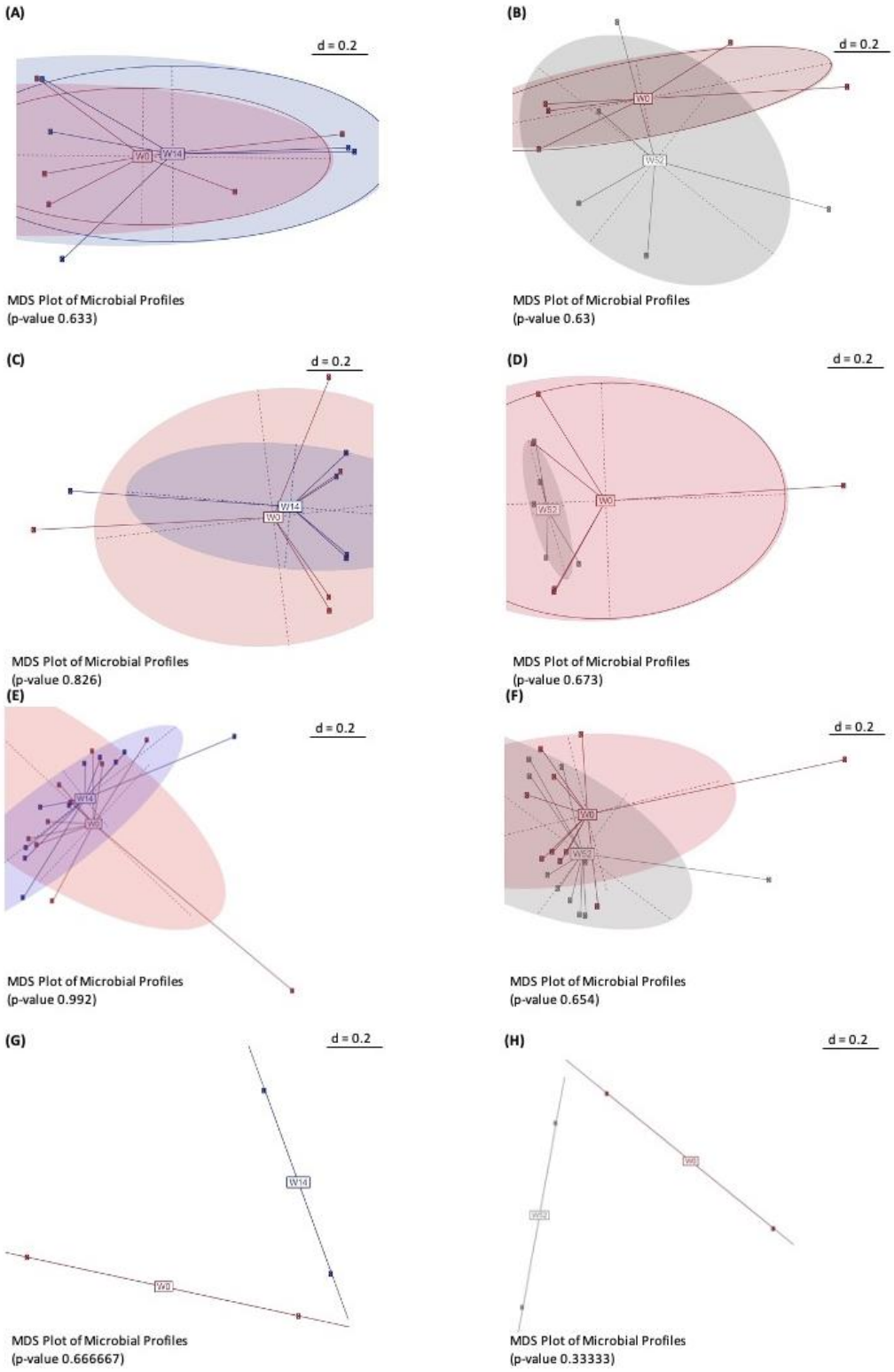

Figure 7 Beta-diversity analysis of longitudinal stool samples collected over one year from 22 IBD patients
*MDS plots show the microbial profiles of paired samples of iCD patients of baseline (W0) to W14 (**A**) and baseline (W0) and W52 (**B**). MDS plots show the microbial profiles of paired samples of cCD patients of baseline (W0) to W14 (**C**) and baseline (W0) and W52 (**D**). MDS plots show the microbial profiles of paired samples of UC patients of baseline (W0) to W14 (**E**) and baseline (W0) and W52 (**F**). MDS plots show the microbial profiles of paired samples of pouchitis patients of baseline (W0) to W14 (**G**) and baseline (W0) and W52 (**H**).*

4.1.2.2 Distinct gut microbial communities between CD and UC patients

Our data show a significant difference in the microbial profiles of CD (n = 67) and UC patients (n = 65) assessed by alpha and beta diversity measures (**Figure 8**). Alpha diversity measures, such as richness and Shannon effective, were significantly higher in UC patients when compared to CD patients (**Figure 8A** & **Figure 8B**). Further, beta diversity analysis revealed a significant separation (p-value = 0.001) of the gut microbial profiles of CD and UC patients (**Figure 8C**). The key differentiating taxa, on the genus and zOTUs levels, between CD and UC patients were depicted using LEfSe analyses (**Figure 8D** & **Figure 8E**). The fecal microbiota of CD patients was enriched in *Escherichia coli* and *Bacteroidetes*, while UC patients showed a higher relative abundance of *Faecalibacterium* and *Bifidobacterium*. Although the overall higher enrichment of *Bacteroidetes* genus in CD patients compared to UC patients depicted at genus level LEfSe analysis, there was an enrichment of zOTU 4018 (in zOTUs LEfSe analysis) in UC patients, which corresponds to *Bacteroidetes*. PICRUSt analysis, which was used to predict the functions of the microbial communities of CD and UC patients, revealed differences in various pathways between the groups (**Figure 9**). Fatty acids biosynthesis pathways were enriched in CD patients, while several amino biosynthesis pathways and glycogen biosynthesis were enriched in UC patients. Stratification of CD patients according to Montreal's classification to ileal (iCD), ileocolonic, and colonic CD (cCD) did not show specific microbial signatures between these phenotypes (**Figure 10** & **Figure 11**). A random forest classifier (machine-learning method) validated the microbial separation between CD (n = 67) and UC (n = 67) patients with an area under the curve (AUC) = 0.86 (**Figure 12A**). The receiver operating curve (ROC) is a probability curve, and the AUC represents the model accuracy, where an AUC of 1 indicates a perfect model and 0 implies model failure. Besides, it showed that *Bifidobacterium* and *Faecalibacterium* were among the most important features (bacterial taxa) in this model (**Figure 12B**). These data suggest that the microbial profiles of IBD patients could classify the disease phenotype (CD or UC) of the patients with 86% accuracy. Disease activity did not show a distinct microbial signature in IBD patients on the alpha and beta-diversity levels (**Figure 13** &**Figure 14**). There was no significant difference in microbial richness and Shannon effective between CD and UC patients when stratified based on disease activity status (**Figure 13**). Beta diversity analysis showed no significant difference

between active (n = 42) and inactive (n = 22) CD patients, but there was a significant difference between UC patients with active (n = 42) and inactive (n = 22) (**Figure 14A** & **Figure 14B**). Remarkably, LEfSe analysis revealed a selective enrichment of potential pathobionts in IBD patients with active disease status such as *Escherichia coli*, *Klebsiella*, and unknown *Clostridiales* (**Figure 14C** & **Figure 14D**).

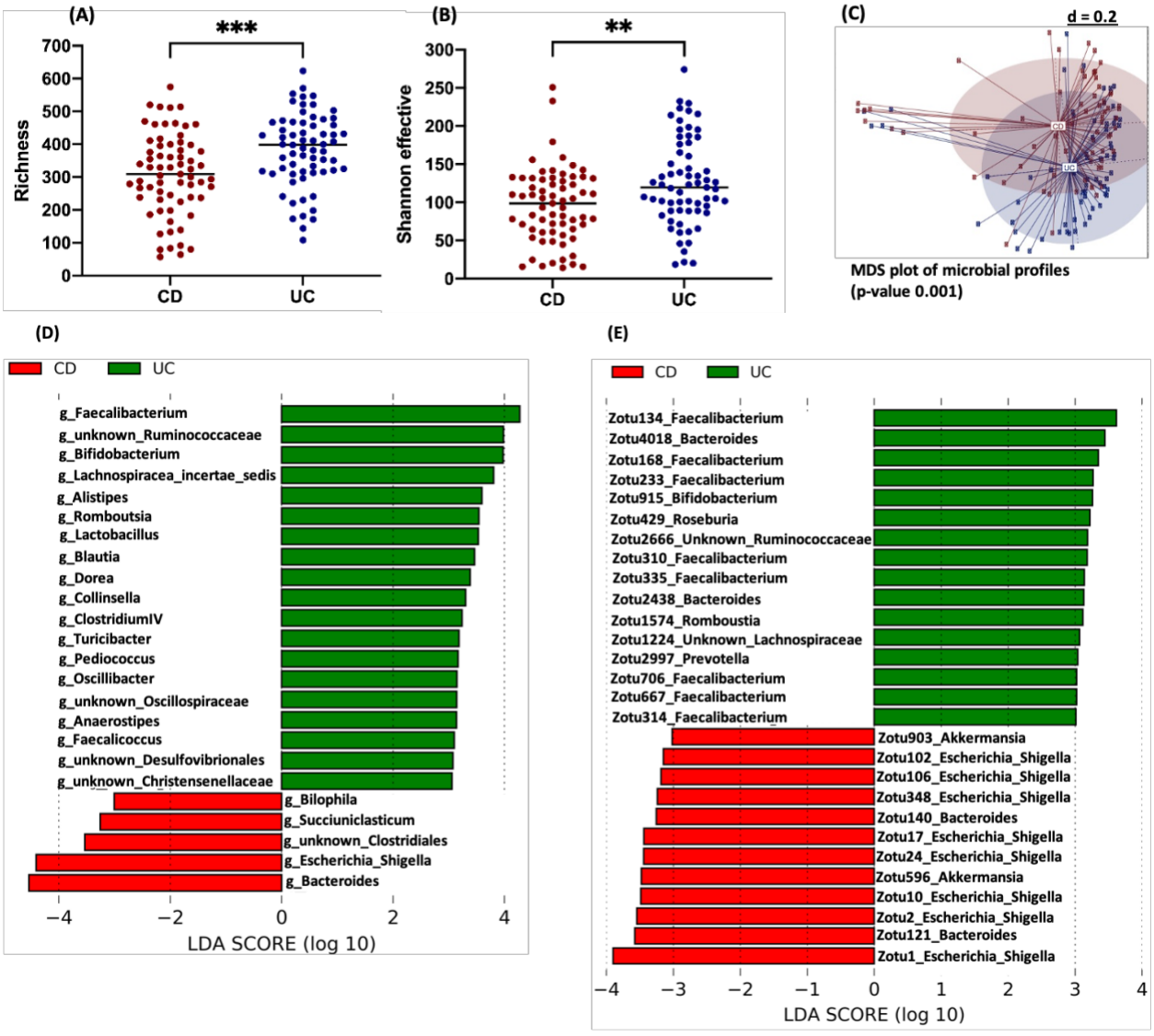

Figure 8 Distinguished gut microbial profiles of CD and UC patients

*Alpha diversity measures for CD and UC patients: microbial community richness **(A)**, Shannon effective **(B)**. MDS plot shows the microbial profiles of CD and UC patients **(C)**. LEfSe analysis highlights the most differentiating genus **(D)** and zOTUs **(E)** of CD and UC patients. For alpha diversity measures, the Mann-Whitney test was used. P ≤0.05 was considered significant; *, p ≤0.01; **, p ≤0.001; ***, p ≤0.0001; ****.*

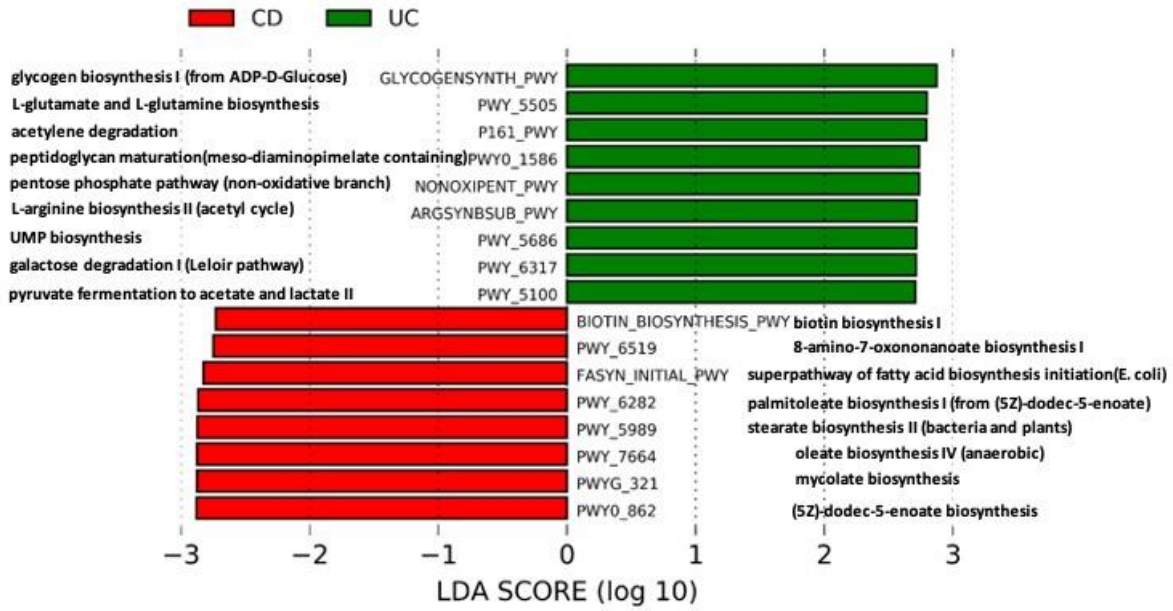

Figure 9 Functional pathways analysis of the gut microbiome that is differentially enriched in CD and UC patients
LEfSe supervised analysis depicting the functional pathways of the predicted microbiota in CD and UC patients.

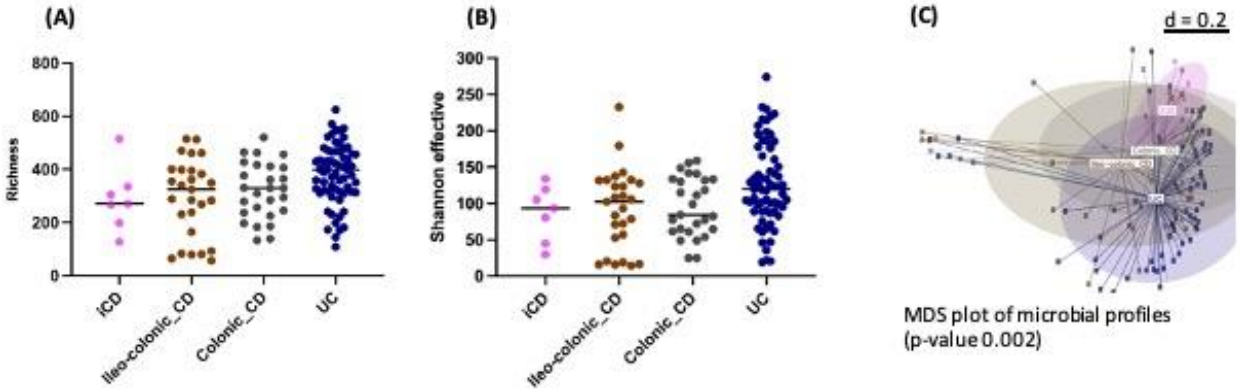

Figure 10 Microbial profiles of IBD patients from the biotherapy cohort stratified according to Montreal classification
*Microbial community richness (**A**), Shannon effective (**B**), and an MDS plot (**C**) describes the microbial variation between iCD, cCD, Ileo colonic CD, and UC patients.*

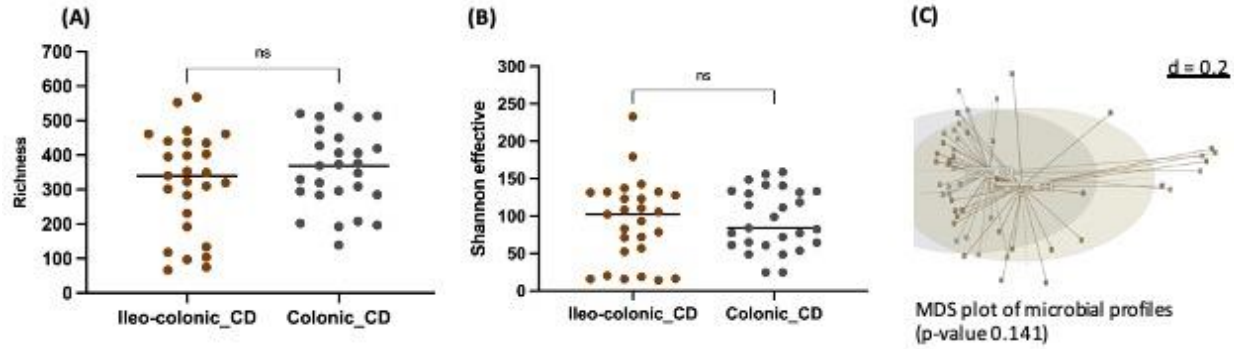

Figure 11 Microbial profiles of ileo-colonic CD and colonic CD patients from the biotherapy cohort
*Microbial community richness (A), Shannon effective (B), and an MDS plot (C) describes the microbial variation between Ileo colonic CD, and colonic CD patients. For alpha diversity measures, Mann-Whitney test was used. P ≤ 0.05 was considered significant; *, p ≤ 0.01; **, p ≤ 0.001; ***, p ≤ 0.0001; ****.*

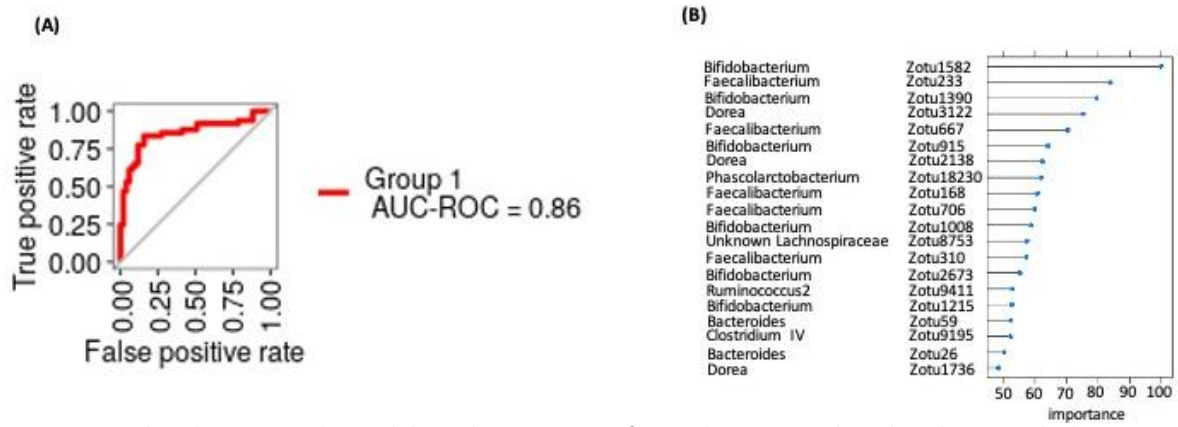

Figure 12 Machine learning analysis validates the separation of CD and UC patients based on their microbial composition
*ROC curve with AUC = 0.86 highlighting the prediction capability of CD and UC patients based on their fecal microbial profiles (**A**). The key differentiating bacterial taxa that describe the random forest model (**B**).*

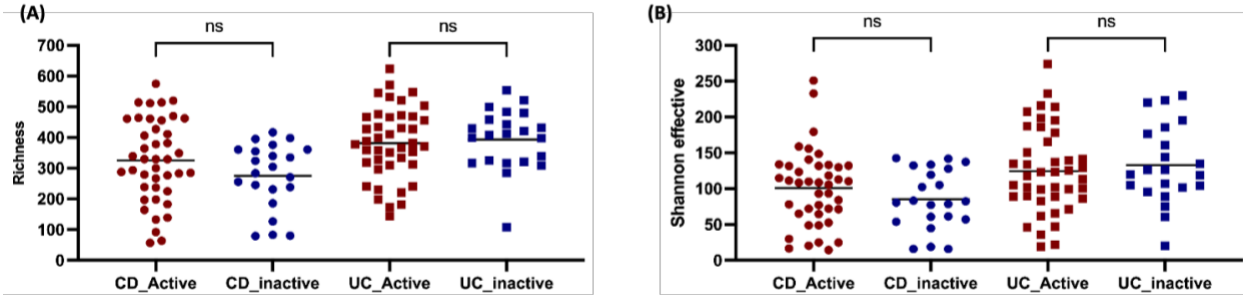

Figure 13 Alpha diversity analysis of CD and UC patients did not show significant differences based on disease activity status
*microbial community richness (**A**), Shannon effective (**B**). The Mann-Whitney test was used. P ≤0.05 was considered significant; *, p ≤0.01; **, p ≤0.001; ***, p ≤0.0001; ****.*

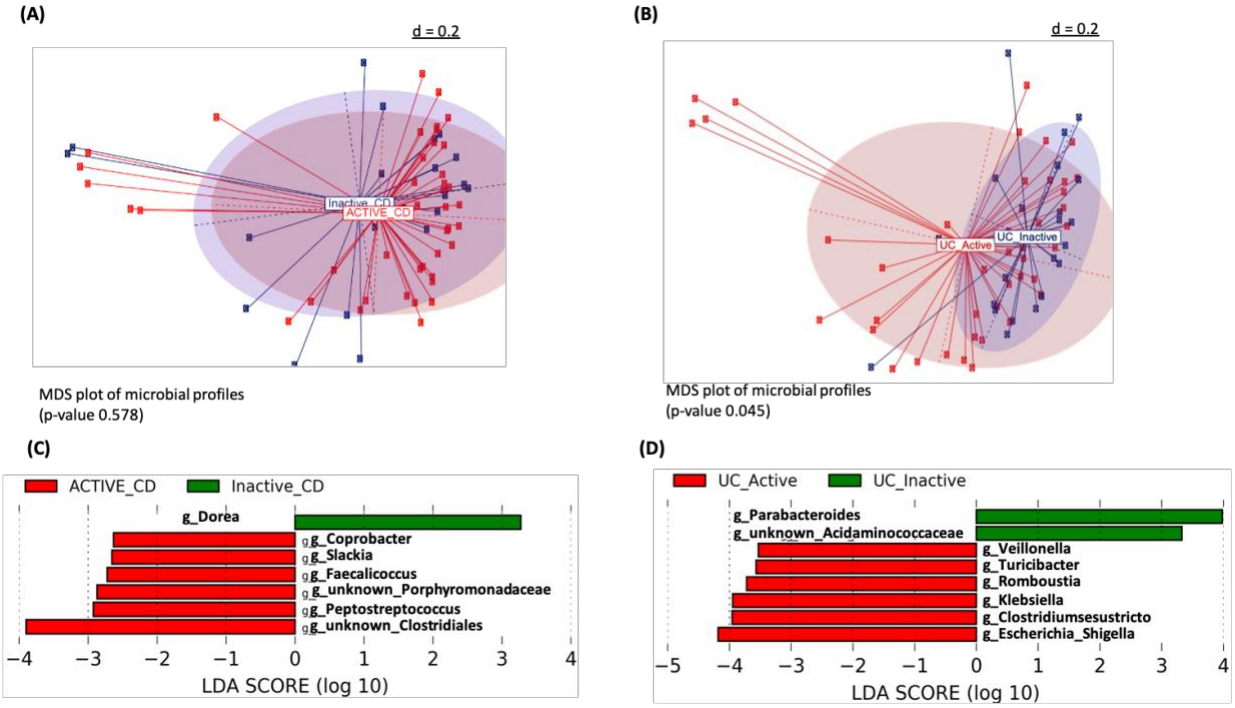

Figure 14 Characterization of the microbial profiles of IBD patients based on disease activity
*MDS plot shows the microbial profiles of CD patients with active disease and inactive disease (**A**) and UC patients with active disease and inactive disease(**B**). LEfSe analysis highlights the most differentiating genus of CD patients with active and inactive disease status (**C**) and active and inactive UC patients (**D**).*

4.1.2.3 Characterization of the microbial profiles of CD, UC, and pouchitis patients

The microbial profiles of CD (n = 67), UC (n = 65), and pouchitis (n = 10) patients were evaluated via alpha and beta diversity measures. Our results showed that pouchitis patients had the lowest microbial diversity, assessed by the richness and Shannon effective, followed by CD patients and UC patients (**Figure 15A** & **Figure 15B**). Unsupervised beta diversity analysis visualized by a phylogram depicted the heterogeneous microbial profiles of the different IBD phenotypes (**Figure 15C**).

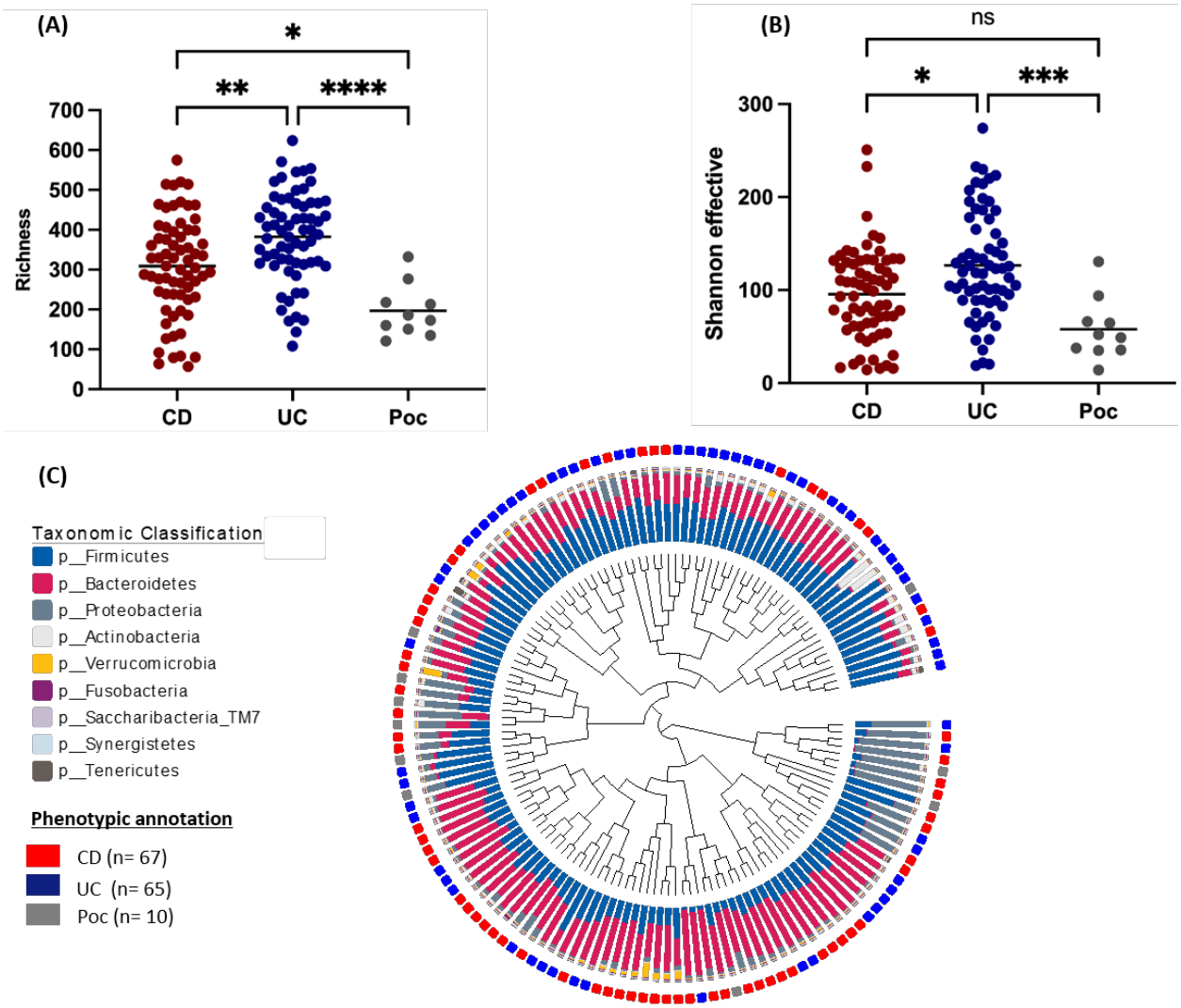

Figure 15 Microbial profiles characterization of CD, UC, and pouchitis patients
*Alpha diversity measures for CD, UC, and pouchitis patients: microbial community richness (**A**), Shannon effective (**B**). The dendrogram describes microbial profile similarities based on generalized UniFrac distances between CD, UC, and pouchitis patients (**C**). The individual microbial composition on the phylum level is represented as a stacked bar plot around the dendrogram. Each rectangle, outer of the stacked bar plot, represents one sample, and each color depicts the disease phenotype (red: CD, blue: UC, and grey: pouchitis). For alpha diversity measures, one-way ANOVA followed by multiple comparison testing (Dunn test) was used. P ≤0.05 was considered significant; *, p ≤0.01; **, p ≤0.001; ***, p ≤0.0001; ****.*

4.1.3 Characterization of mucosa-associated gut microbial profiles of the biotherapy cohort

The mucosa-associated samples (n =167) were collected from 39 CD, 32 UC, and 6 pouchitis patients at three time points (W0, W14, and W52) to characterize the mucosa-associated gut microbial profiles of IBD patients over time and identify disease-associated taxa (**Table S2**), in an analysis similar the fecal bacteria. Moreover, we investigated the effect of disease activity in shaping the gut microbial composition of IBD patients. Labeling disease activity status (active & inactive) in this analysis was dependent on the endoscopic evaluation of the samples. CD patients were further stratified to ileal (iCD) and colonic (cCD) in this analysis based on the location of the most affected part during the endoscopic assessment.

4.1.3.1 Mucosal biopsy analysis reveals that colonic CD patients show a similar microbial profile to UC patients

The mucosa-associated gut microbiota of 72 UC and 64 CD patients' samples of the biotherapy cohort were evaluated. The mucosa-associated microbiota showed significant differences between CD and UC patients (**Figure 16**). UC patients showed a higher microbial richness and Shannon effective when compared to CD patients, and a significant difference in the overall microbial communities, beta-diversity analysis, between the groups. LEfSe analysis of the mucosa-associated gut microbiota unveils similar findings of the stool analysis with enrichment of *Escherichia coli* in CD patients and *Faecalibacterium* and *Bifidobacterium* in UC patients. However, the mucosa-associated analysis revealed particular taxa that differentiate the groups that were not identified in the stool analysis, such as *Roseburia* and *Ruminococcus* enrichment in UC and *Ruminoccous_g5* enrichment in CD patients (**Figure 16**). A machine-learning analysis classified CD and UC patients based on their mucosa-associated microbial profiles with AUC = 0.86. It revealed that *Coprococcus* and *Bacteroides* were among the key important bacteria in this model (**Figure 17**). The analysis of the mucosa-associated microbial profiles of CD, UC, and pouchitis patients revealed a similar pattern of the stool analysis, where pouchitis patients had the least microbial diversity (**Figure 18**). Our data show that CD patients with colonic involvement have more similar microbial profiles to UC patients than CD patients with an ileal phenotype. Alpha diversity analysis, assessed by microbial community richness and

Shannon effective, revealed that iCD microbial communities are characterized by the lowest bacterial diversity, followed by cCD, and the highest alpha diversity measures were observed for UC patients (**Figure 19A** & **Figure 19B**). Further, an unsupervised assessment of the gut microbiota showed that cCD microbial profiles are closer to UC than iCD (**Figure 19C**).

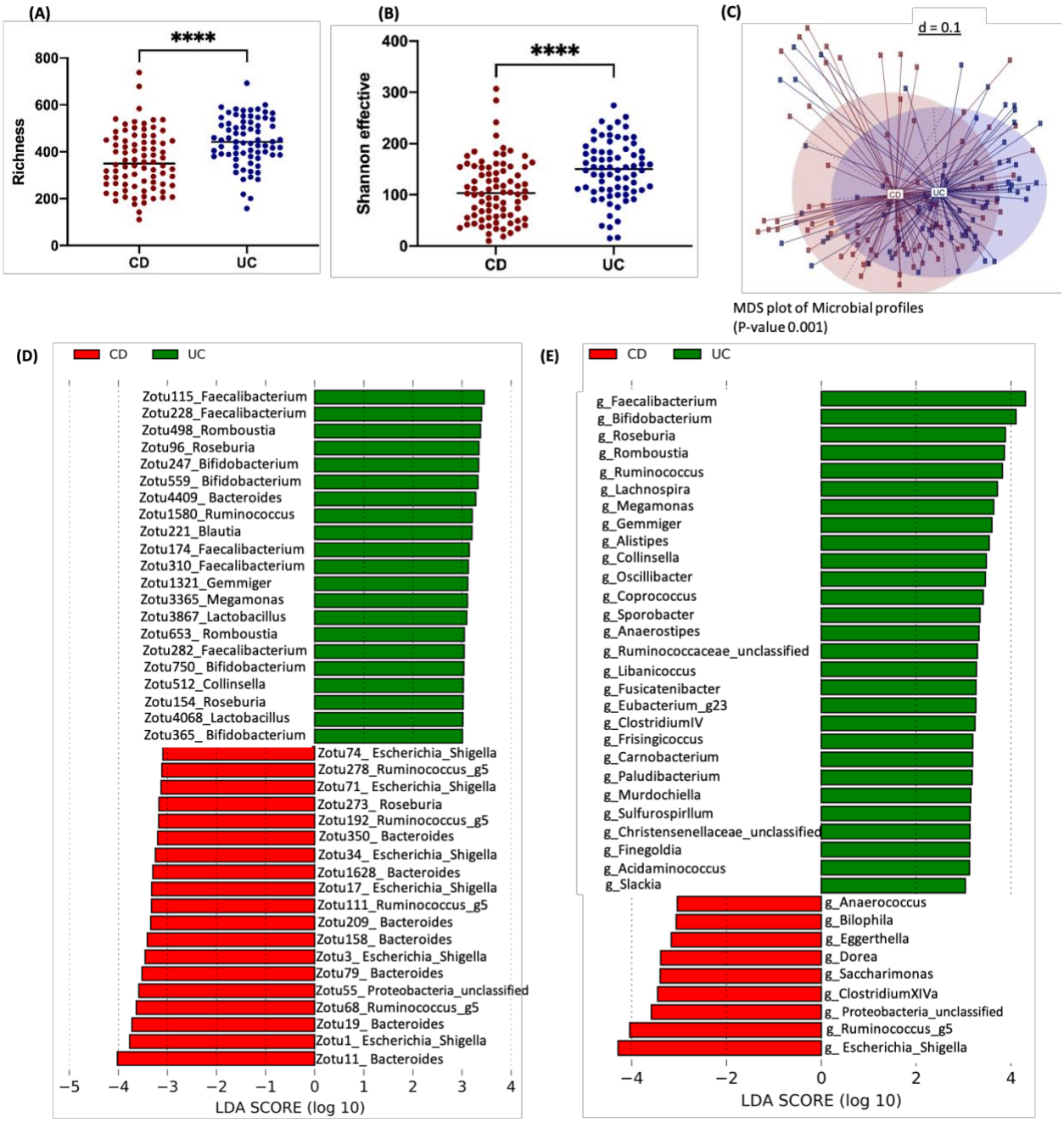

Figure 16 Distinct mucosa-associated gut microbial signature between CD and UC patients

*The microbial community richness (A), Shannon effective (B) between CD and UC patients' samples. MDS plot shows the microbial profiles of CD and UC patients (C). LEfSe analysis depicts the most differentiating zOTUs (D) and genus (E) of CD and UC patients based on mucosa-associated gut microbial analysis. For alpha diversity measures, the Mann-Whitney test was used. P ≤ 0.05 was considered significant; *, p ≤ 0.01; **, p ≤ 0.001; ***, p ≤ 0.0001; ****.*

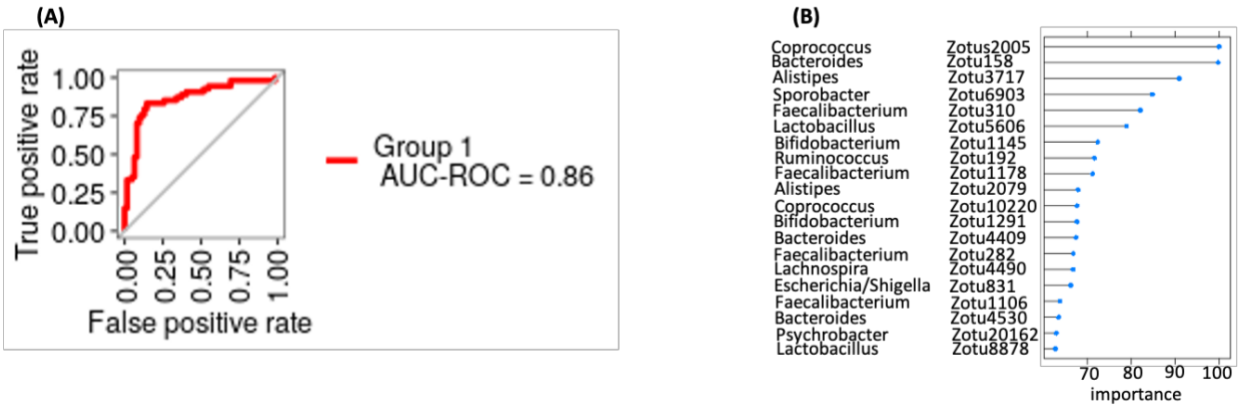

Figure 17 Random Forest analysis validates the separation of CD and UC patients based on their mucosa-associated microbiota
*ROC curve with AUC = 0.86 highlighting the prediction capability of CD and UC patients based on their biopsy-associated microbial profiles (**A**). The key differentiating bacterial taxa that describe the random forest model (**B**).*

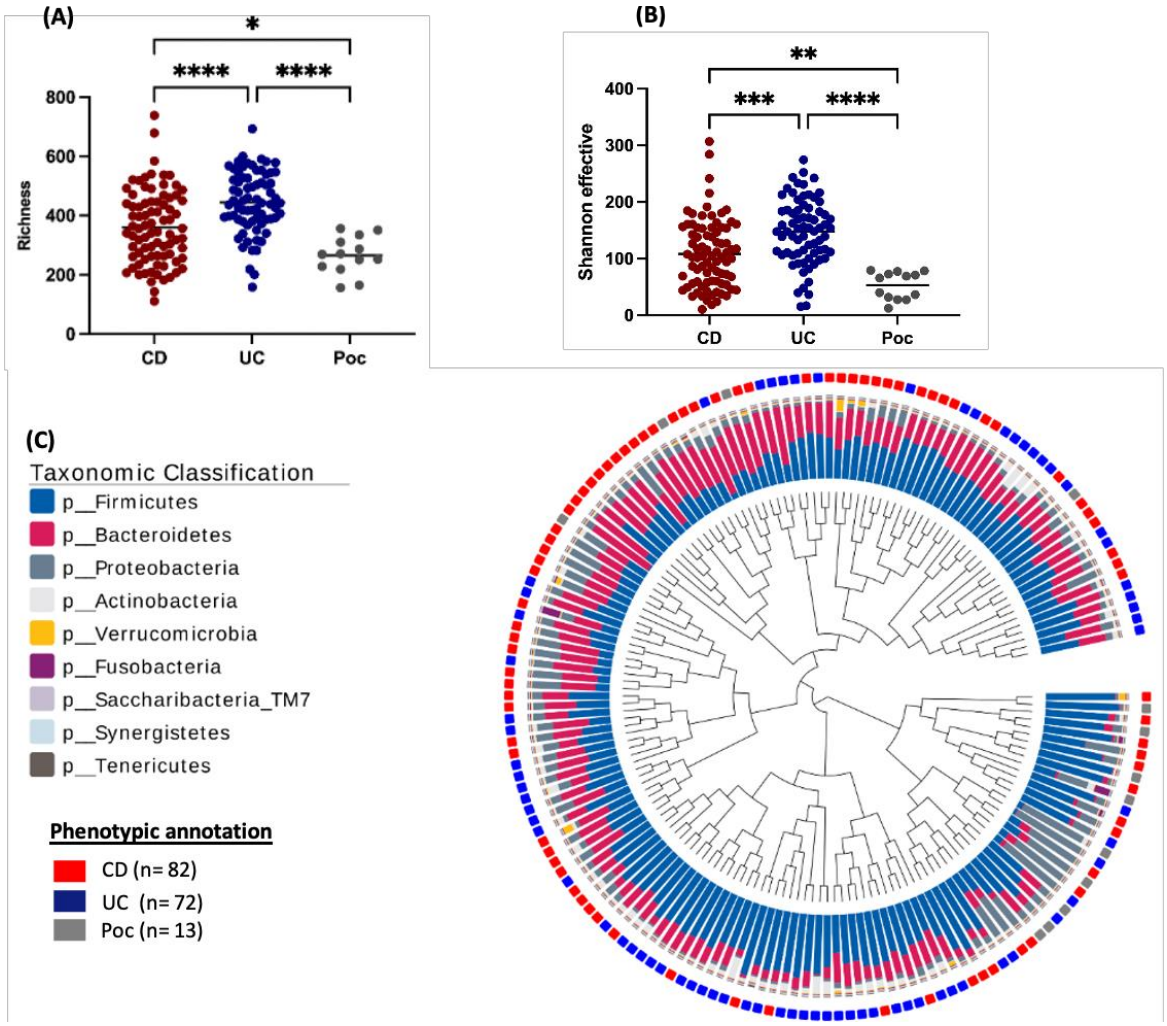

Figure 18 Characterization of the mucosa-associated microbial profiles of CD, UC, and pouchitis patients
*The microbial community richness (**A**), Shannon effective (**B**) of CD, UC, and pouchitis patients. The dendrogram describes microbial profile similarities based on generalized UniFrac distances between CD, UC, and pouchitis patients (**C**). The individual microbial composition on the phylum level is represented as a stacked bar plot around the dendrogram. Each rectangle, outer of the stacked bar plot, represents one sample, and each color depicts disease phenotype (red: CD, blue: UC, and grey: pouchitis). For alpha diversity measures, one-way ANOVA followed by multiple comparison testing (Dunn test) was used. $P \leq 0.05$ was considered significant; *, $p \leq 0.01$; **, $p \leq 0.001$; ***, $p \leq 0.0001$; ****.*

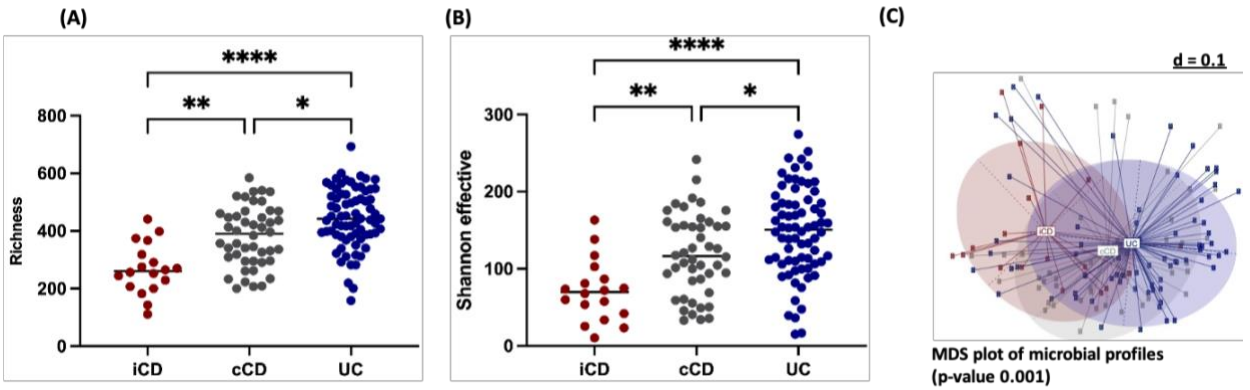

Figure 19 Mucosa-associated microbial profiles analysis shows that colonic CD patients are close to UC than iCD patients
*Microbial community richness (**A**), Shannon effective (**B**). MDS plot shows the microbial profiles of iCD, cCD, and UC patients (**C**). For alpha diversity measures, one-way ANOVA followed by multiple comparison testing (Dunn test) was used. P ≤ 0.05 was considered significant; *, p ≤0.01; **, p ≤0.001; ***, p ≤0.0001; ****.*

Further, gut microbial composition assessment of CD patients with ileal and colonic inflammatory phenotypes revealed a significant difference in their mucosal bacterial community profiles on the alpha and beta diversity measures (**Figure 20**). The key differentiating taxa between iCD and cCD patients were evaluated using LEfSe analyses (**Figure 20**). Our data showed enrichment of *Escherichia coli* and *Veillonella* in iCD patients. On the contrary, cCD patients had higher levels of *Faecalibacterium* and *Roseburia*, among other bacteria.

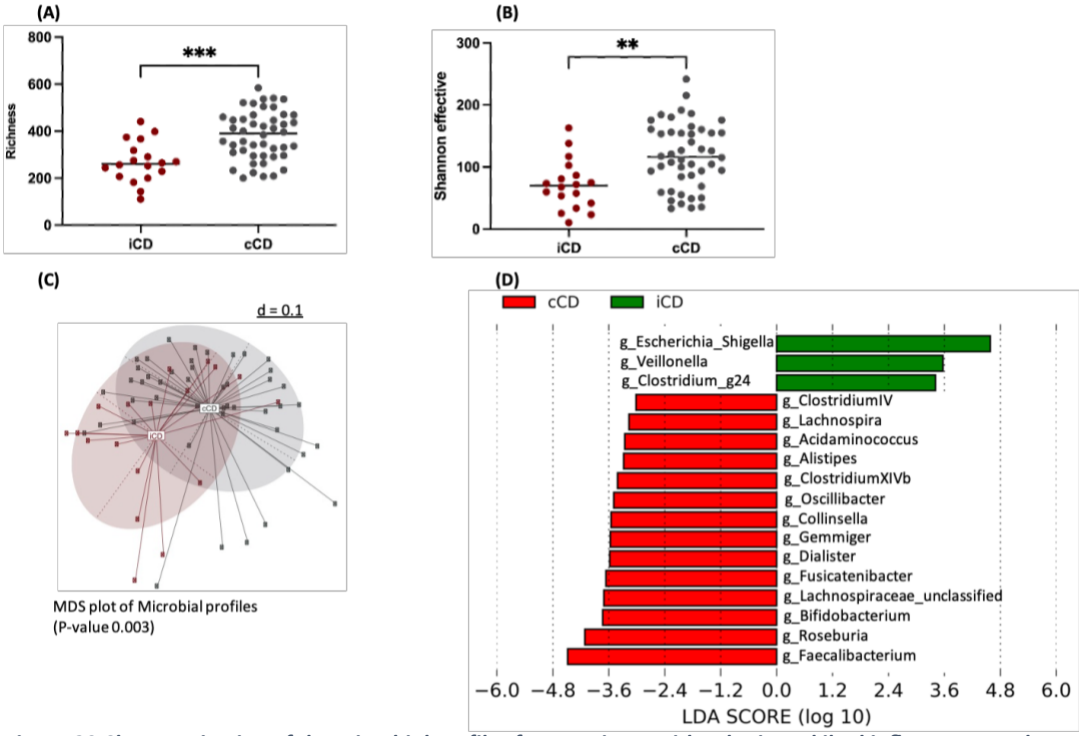

Figure 20 Characterization of the microbial profiles from patients with colonic and ileal inflammatory phenotypes
*Microbial community richness (**A**), Shannon effective (**B**) of iCD and cCD patients. MDS plot illustrates the significant difference in the microbial profiles of iCD, and cCD patients (**C**). LEfSe analysis depicts the most differentiating genus of iCD and cCD patients (**D**). For alpha diversity measures, the Mann-Whitney test was used. P ≤0.05 was considered significant; *, p ≤0.01; **, p ≤0.001; ***, p ≤0.0001; ****.*

4.1.3.2 *Characterization of the mucosa-associated microbiota for IBD patients based on the disease activity*

To evaluate the influence of the disease activity on gut microbial changes, we grouped CD patients, based on their endoscopic assessment, into active and inactive disease. We further stratified CD patients according to disease location to iCD and cCD. We did not include the UC patients in this analysis due to the biased sample distribution of active (n = 64) and inactive (n = 6). Our results show no unique disease-associated gut microbial signature explains disease activity in iCD assessed by insignificant differences at the alpha and beta diversity measures (**Figure 21**).

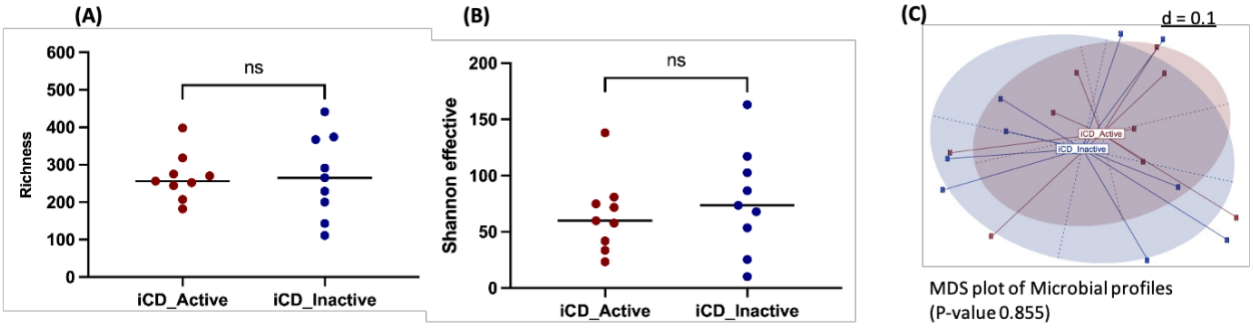

Figure 21 No distinct mucosa-associated gut microbial signature differentiates active and inactive ileal CD patients
*The microbial community richness (**A**), Shannon effective (**B**) between active (n = 9) and inactive CD patients (n = 9) with ileal involvement. MDS plot shows the microbial profiles of active (n = 9) and inactive ileal CD patients (n = 9) (**C**). For alpha diversity measures, the Mann-Whitney test was used. P ≤0.05 was considered significant; *, p ≤0.01; **, p ≤0.001; ***, p ≤0.0001; ****.*

Although colonic CD patients did not show a significant difference in microbial richness and Shannon effective between active (n = 33) and inactive disease status (n = 11), unsupervised beta diversity analysis revealed a significant difference between the groups (**Figure 22**). Remarkably, the mucosa-associated bacterial community of colonic CD patients with an active disease phenotype showed enrichment of *Fusobacterium* and *Bacteroidetes*, while patients with an inactive disease phenotype showed expansion of *Blautia* and *Clostridium* (**Figure 22**).

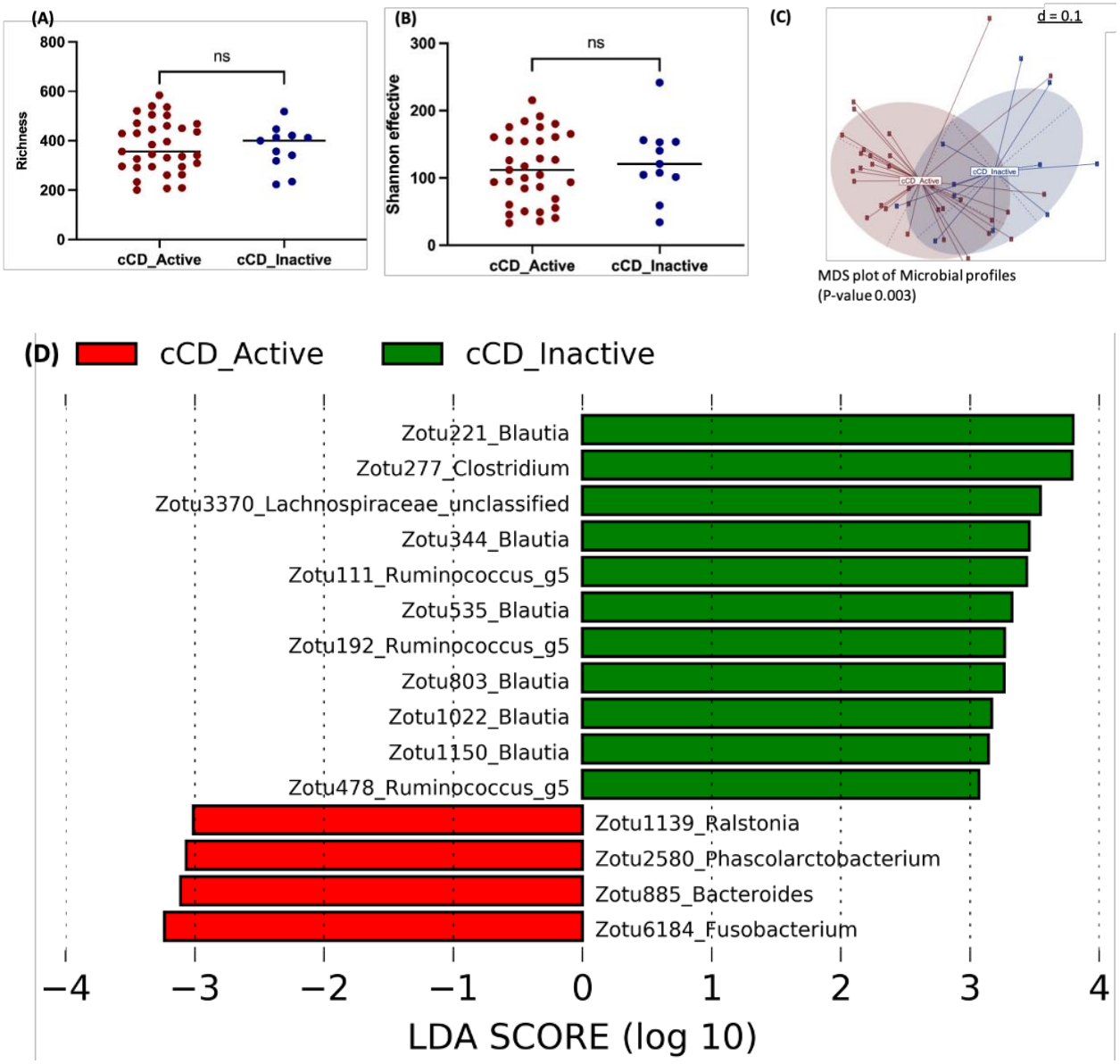

Figure 22 The mucosa-associated gut microbial signature between active and inactive colonic CD patients

*The microbial community richness (**A**), Shannon effective (**B**) between active and inactive colonic CD patients' samples. MDS plot shows the microbial profiles of active and inactive colonic CD patients(**C**). LEfSe analysis describes the most differentiating zOTUs of active and inactive colonic CD patients based on mucosa-associated gut microbial analysis (**D**). For alpha diversity measures, the Mann-Whitney test was used. P ≤0.05 was considered significant; *, p ≤0.01; **, p ≤0.001; ***, p ≤0.0001; ****.*

4.1.3.3 Longitudinal mucosa-associated gut microbial signature of IBD patients

To evaluate the microbial profile fluctuations over time, 84 mucosa-associated samples were collected from 28 IBD patients at baseline (W0), 14 and 52 weeks after introducing the biological therapy. These 28 patients include 10 CD (4 iCD & 6 cCD), 3 pouchitis, and 15 UC patients. Alpha diversity analysis, assessed by microbial community richness and Shannon effective, did not show significant changes throughout the year regardless of biotherapy

medications and the disease activity status (**Figure 23**), suggesting a strong personal microbial community structure on the mucosal level with no substantial effects of biotherapy medications and disease activity status.

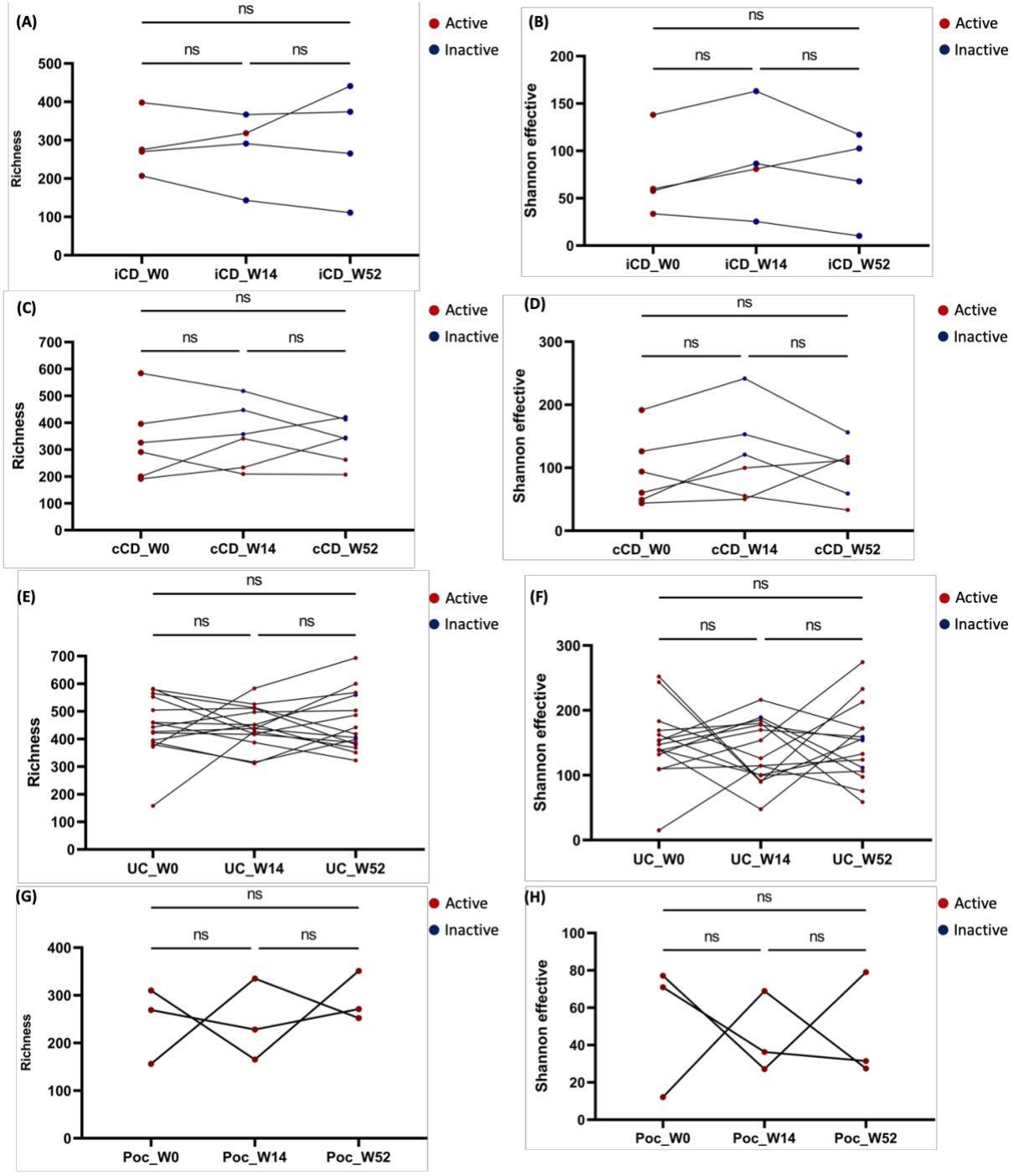

Figure 23 Alpha diversity analysis of longitudinal gut microbial mucosa-associated samples from 28 IBD patients.
*The microbial community richness (**A**, **C**, **E** & **G**) for iCD, cCD, UC, and pouchitis patients respectively at baseline (W0), 14 and 52 weeks. The Shannon effective analysis (**B**, **D**, **F** & **H**) for iCD, cCD, UC, and pouchitis patients respectively at baseline (W0), 14 and 52 weeks. The circle color depicts the disease activity (red: active disease & blue: inactive disease).*

The beta diversity analysis of the mucosa-associated microbial profiles showed fewer individualized signatures over the three-time points compared to the stool sample analysis (**Figure 24**). Only 18% of patients (5 patients) clustered together over time, showing an individualized signature, and 39% of patients (11 patients) showed a cluster of two-time points (**Figure 24**). There was no specific clustering based on the disease activity phenotype.

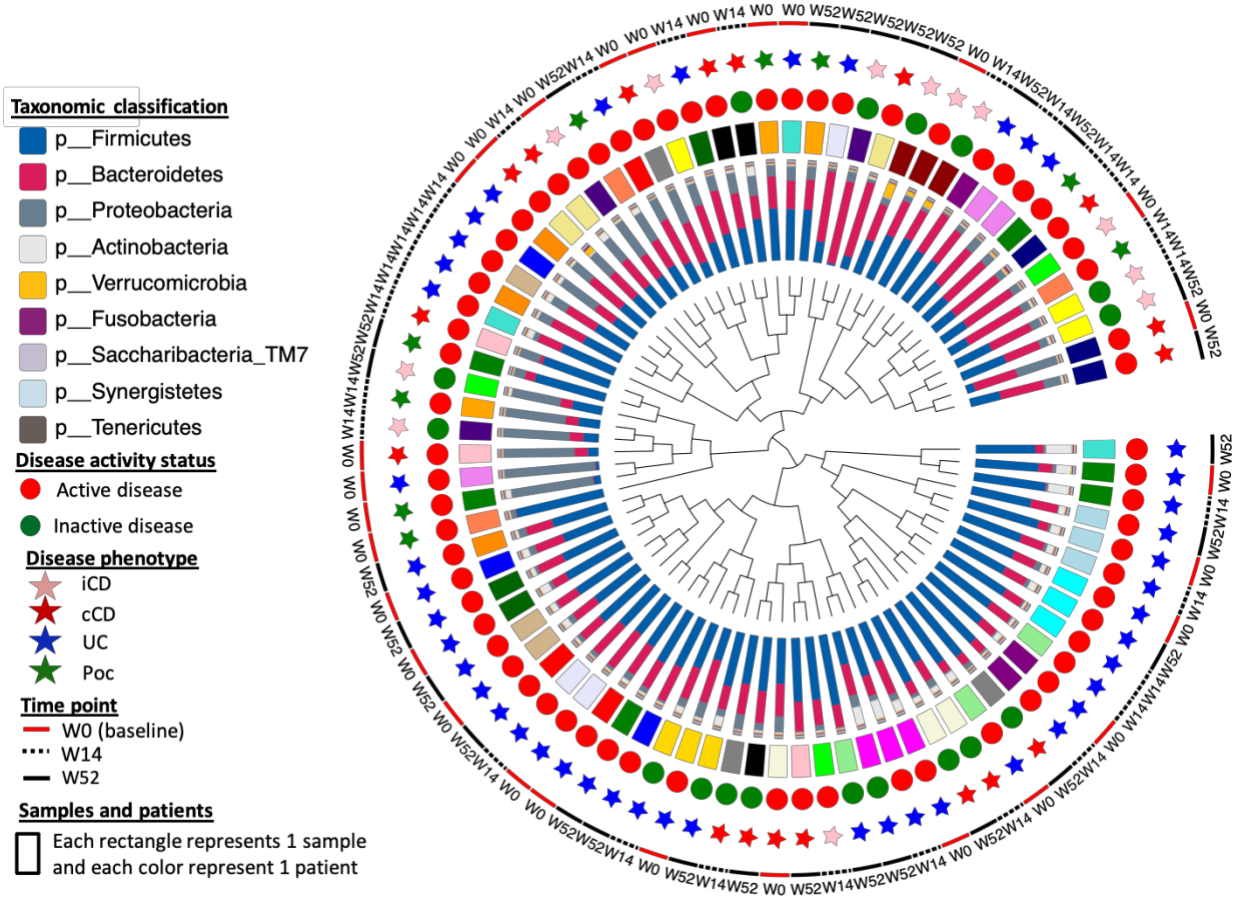

Figure 24 Beta-diversity analysis of longitudinal gut microbial mucosa-associated samples collected from 28 IBD patients
The dendrogram describes microbial profile similarities based on generalized UniFrac distances between the 84 samples. The individual microbial composition on the phylum level is visualized as a stacked bar plot around the dendrogram. Each rectangle, outer of the stacked bar plot, represents one sample, and each patient is represented by one color of the rectangle. Circles, outer of the rectangles, depict the disease activity of the patients (red: active disease & green: inactive disease). Stars, outer of the circles, describe different disease phenotypes (pink: ileal CD, red: colonic CD, blue: UC & pouchitis: green). Finally, bars in the outer part of the figure represent the sample time points (bold red line: baseline (W0), dotted black line: W14, and bold black line: W52).

4.1.4 Characterization of the fecal metabolomic profiles of the biotherapy cohort

To evaluate the metabolomic signatures linked to different IBD phenotypes and disease activity, untargeted metabolomics of stool samples was conducted using a UHPLC system coupled to a Q-TOF mass spectrometer. Two modes of measurement were used to cover a wide array of metabolites. It included hydrophilic interaction liquid chromatography (Hilic) and reverse phase

(RP) liquid chromatography in both positive and negative electrospray ionization modes for Hilic and RP modes. Principal Component Analysis (PCA) was used to analyze the variation between samples. Assessment of the most significantly differential metabolites between the groups is visualized by volcano plots, where the X-axis represents the mean difference of the metabolite of interest between the groups and the Y-axis represents the log False Discovery Rate (FDR). Annotation of the metabolites was performed based on internal references and public databases including HMDB4.0 and MSDIAL.

4.1.4.1 Characterization of the fecal metabolomic profiles of CD and UC patients

Untargeted metabolomics analysis of 66 UC and 67 CD patients' stool samples of the biotherapy cohort were evaluated using four modes of measurement (Hilic negative, Hilic positive, RP negative, and RP positive). PCA plots show the fecal metabolomic profiles of CD and UC patients, where the Hilic modes showed the best separation (**Figure 25A** & **Figure 25C**). Volcano plots depicted the most differentiating metabolites between the groups, where the Hilic negative mode had the highest number of significantly differential metabolites (**Figure 25B** & **Figure 25D**). To analyze the metabolomic profiles of the volcano plots, 0.3 mean difference and 1.5 log FDR was used as a significant threshold for metabolites annotation (**Table S3**). CD patients showed higher levels of different fatty acids and bile acids, such as hyodeoxycholic acid, lithochol-11-enic acid, and eicosenoic acid (**Table S3**). UC patients had higher levels of some medicinal metabolites such as acetaminophen and N-acetyl-5-aminosalicylic acid and dietary metabolites such as 1,7-Dimethyluric acid (**Table S3**).

4.1.4.2 Characterization of fecal metabolomic profiles of IBD patients based on disease activity

To assess the effect of disease activity on the metabolomic profile of IBD patients, we grouped CD and UC patients based on their disease activity into active and inactive disease phenotypes. The metabolomic profiles of active (n= 43) and inactive (n= 22) UC patients samples showed separation between the groups, especially in the Hilic modes (**Figure 26**). There was a significant enrichment of some metabolites in UC patients with active disease phenotype, such as platelet-activating factor and lactosylceramide (**Table S4**). Inactive UC patients showed higher levels of some bile acids, such as lithocholenic acid, hyodeoxycholic acid, and

STD_chenodeoxycholic acid (**Table S4**). There was not a profound difference in the fecal metabolomic profiles between active and inactive CD patients (**Figures S1 Metabolomic profiles of active and inactive cCD patients& S2**).

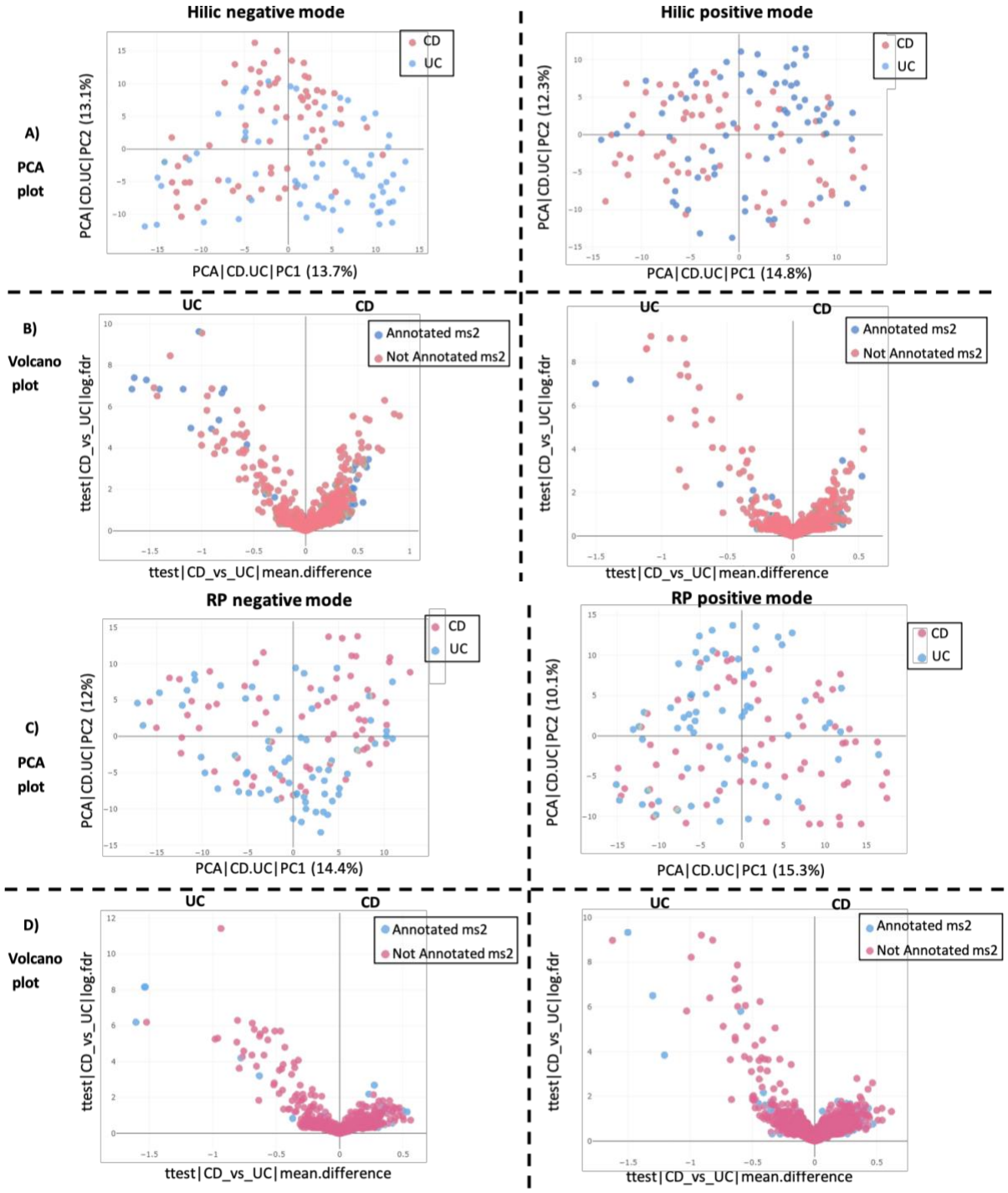

Figure 25 Altered fecal metabolomic profiles of CD and UC patients

*Principal Component Analysis (PCA) shows the variation between CD and UC patients' samples in the four measurement modes (**A:** Hilic negative & Hilic positive **& C:** RP negative & RP positive). Volcano plots highlighting the key differentiating metabolites between CD and UC patients in the four different measurements (**B:** Hilic negative & Hilic positive **& D:** RP negative & RP positive).*

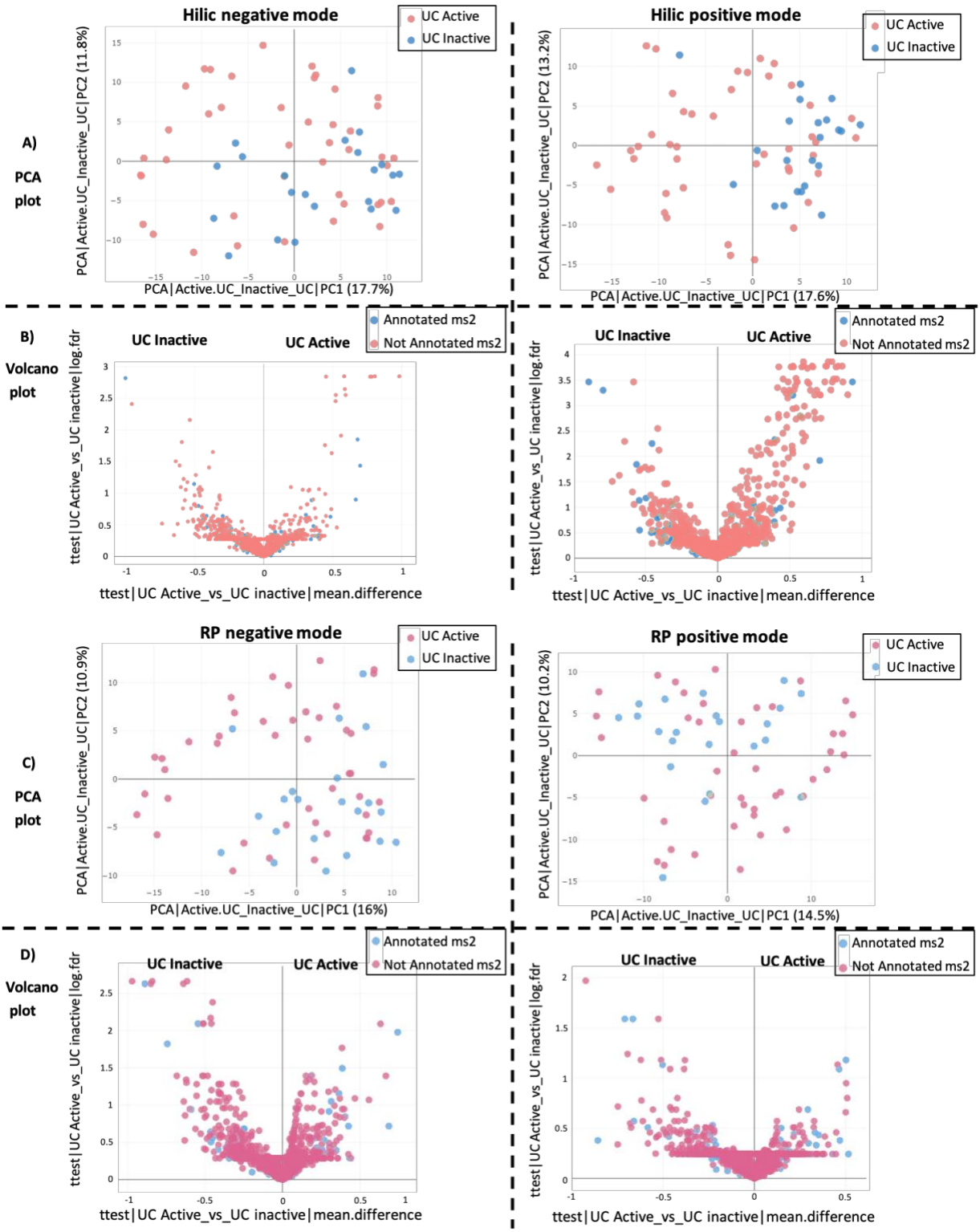

Figure 26 Altered fecal metabolomic profiles of active and inactive UC patients

*Principal Component Analysis (PCA) shows the variation between active and inactive UC patients in the four measurement modes (**A:** Hilic negative & Hilic positive **& C:** RP negative & RP positive). Volcano plots highlighting the key differentiating metabolites between active and inactive UC patients in the four different measurements (**B:** Hilic negative & Hilic positive **& D:** RP negative & RP positive).*

4.1.5 Fecal microbiome-metabolome integrative analyses of the biotherapy cohort

The integration of the fecal gut microbiota (16S rRNA amplicon sequencing) and untargeted metabolomics data of the biotherapy cohort was conducted. In brief, stool samples of 137 IBD patients of the biotherapy cohort were used in the integrative microbiome and metabolome analysis to further investigate the complex biological processes in IBD pathogenesis and predict the disease activity outcome.

Applying unsupervised multi-omics data integration analysis (MOFA) on the microbial and metabolomics datasets (n = 137) of the biotherapy cohort did not show a distinct separation between either CD and UC patients' samples or their disease activity phenotypes (**Figure 27A**). To evaluate the potential of microbiome-metabolome integrative analysis in classifying the response to therapy at W52, a supervised machine learning analysis was used (DIABLO) on the baseline samples that were labeled according to the W52 disease activity phenotype. DIABLO analysis managed to separate the active and inactive IBD disease phenotypes based on the microbial and metabolomic integrative datasets at baseline (**Figure 27B**). The key differentiating bacteria in this model were *Streptococcus*, *Acidaminococcus*, and *Fusicatenibacter*. The key differentiating metabolites in this model included lithocholic acid (bile acid) and Trehalose-6-Phosphate (**Table S5**). Although the well-articulated separation in the PLS-DA model, further validation of the results needed to be conducted.

The possibility of using microbiome-metabolome integrative analysis on classifying the response to therapy and the disease phenotypes was assessed using the supervised machine learning analysis (DIABLO) on all samples. The supervised PLS-DA analysis revealed a minor separation of IBD patients based on the disease activity phenotypes (**Figure 27C**). The key differentiating metabolites in this model included lactosylceramide (**Table S6**), and there was no significant gut microbiota competent in this model. PLS-DA analysis showed better separation of IBD patients based on IBD disease phenotypes (**Figure 27D**). *Escherichia coli* was the main microbial differentiator, while N-acetyl-5-aminosalicylic acid (mesalazine's metabolite) and acetaminophen (drug) were among the differentiator metabolites in this model (**Table S7**).

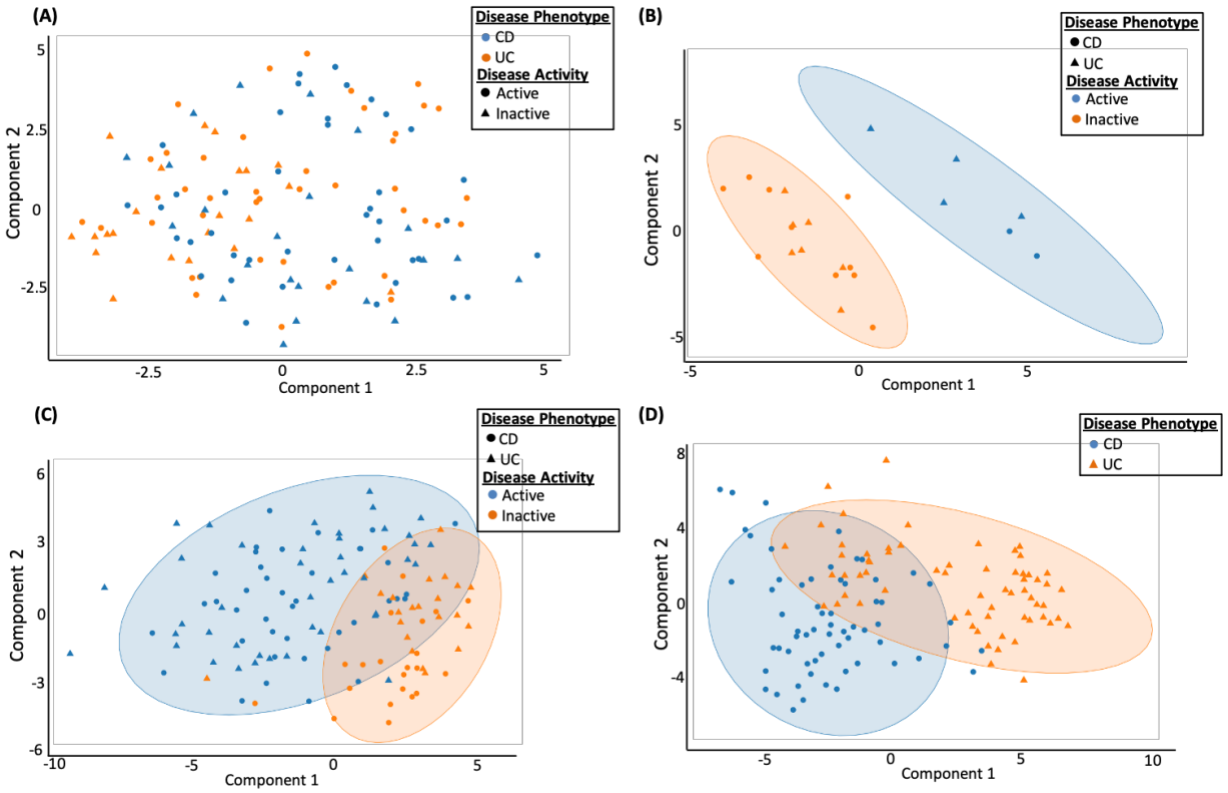

Figure 27 Fecal microbiome-metabolome integrative analysis of the biotherapy cohort

*Unsupervised PCA plot highlights the variance between CD and UC patients (CD: blue color and UC: orange color) and the disease activity phenotypes (Active: circles and Inactive: triangles) (**A**). PLS-DA plot of integrated omics datasets from IBD patients at baseline that was labeled based on their disease activity status at W52 (**B**). PLS-DA plot of integrated omics datasets from all IBD patients' samples that were labeled based on their disease activity (**C**) and disease phenotype (**D**).*

4.2 Comparison between different gut microbial analyses (OTUs and zOTUs) in a subset of the biotherapy cohort

To assess two downstream bioinformatics clustering methods of 16S rRNA amplicon analysis, we compared OTUs and zOTUs analyses of fecal samples collected from CD and UC patients of the biotherapy cohort (**Figure 28**). In brief, an OTU is generated by clustering sequences that have a 97% similarity threshold, but a zOTU is created for 100% identical sequences, which provides higher specificity/resolution of bacterial identification. Both analyses showed a similar trend reflected by an increase in alpha diversity measures for UC patients compared to CD patients, but zOTUs analysis almost tripled in richness and Shannon effective values (**Figure 28**). For instance, the richness values in the OTUs analysis ranged from 20-229, and the zOTUs analysis ranged from 57 to 624. Further, there was a significant separation of the

microbial profiles of the two patient groups for both analyses, evaluated by beta-diversity analysis (**Figure 28**).

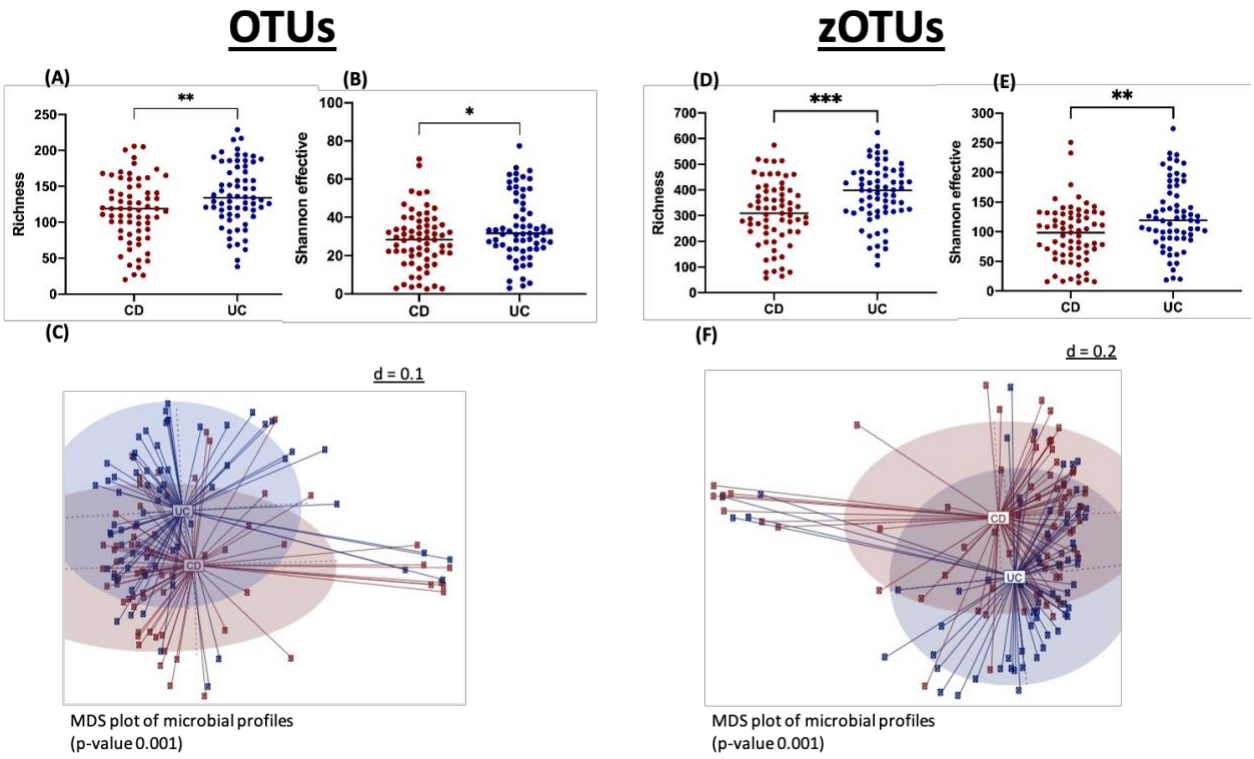

Figure 28 The microbial profiles of CD and UC patients of the biotherapy cohort show similarities in OTUs and zOTUs analyses
*The microbial community richness (**A**), Shannon effective (**B**) for the OTUs analysis of CD and UC patients. The microbial community richness (**D**), Shannon effective (**E**) for the zOTUs analysis of CD and UC patients. MDS plot shows the microbial profiles of CD and UC patients for the OTUs analysis (**C**) and the zOTUs analysis (**F**). For alpha diversity measures, the Mann-Whitney test was used. P ≤ 0.05 was considered significant; *, p ≤ 0.01; **, p ≤ 0.001; ***, p ≤ 0.0001; ****.*

LEfSe analysis was conducted on OTUs and zOTUs datasets to compare the key differentiating microbial components for CD and UC patients of the biotherapy cohort (**Figure 29**). LEfSe analysis showed a similar trend of enriched *Escherichia coli* in CD patients with two OTUs detected and eight zOTUs (**Figure 29**). UC patients were enriched in *Faecalibacterium* with two OTUs and eight zOTUs. Interestingly, there were two zOTUs of *Akkermansia* enriched in CD patients, but it was not detected at the OTUs level analysis (**Figure 29**). An OTU of the *Ruminococcus gnavus* group was enriched in CD patients, which was not observed in the zOTUs analysis (**Figure 29**). These data suggest a comparable result of both analysis methods, in terms of statistical significance, at the alpha and beta diversity levels. However, taxonomic resolution analysis showed differences in the top differentiator taxa in both methods. These data highlight

the challenges in choosing a gut microbial analysis method, and careful interpretation of gut microbial analysis is needed.

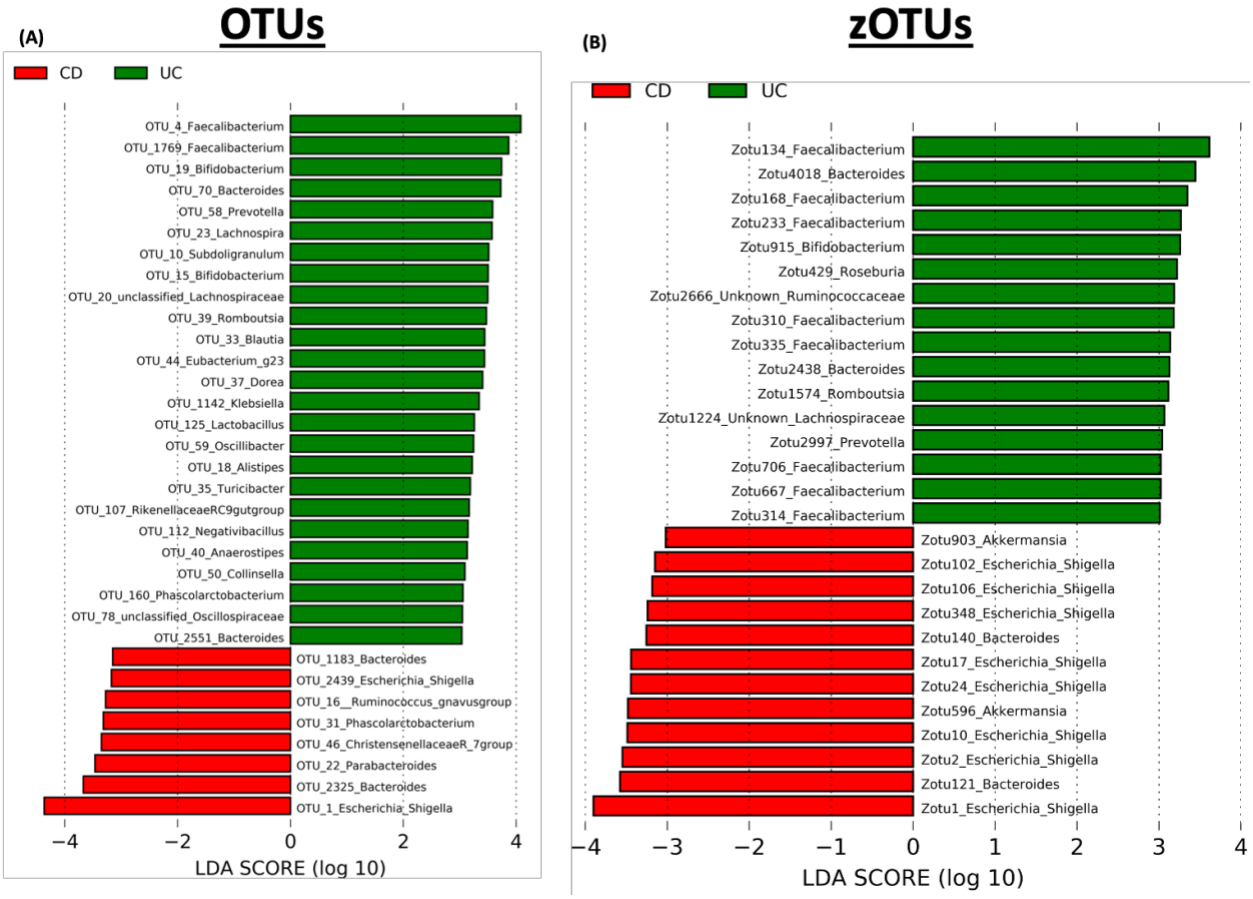

Figure 29 The key differentiating taxa between CD and UC patients of the biotherapy cohort based on OTUs and zOTUs analyses
*LEfSe analysis highlights the most differentiating OTUs (**A**) and zOTUs (**B**) of CD and UC patients of the biotherapy cohort.*

4.3 Characterization of gut microbiota profiles of two IBD cohorts to assess the existence of common disease-associated taxa across different cohorts

A comparison of the microbial profiles of two IBD cohorts (biotherapy cohort and ulcerative colitis lifestyle intervention cohort) was conducted to address the characteristics of microbial profiles in different IBD cohorts. The analysis includes the biotherapy cohort (CD (n =67) & UC (n =65)), which was described earlier, and the ulcerative colitis patients (n =84) of the lifestyle intervention cohort (UC cohort 2). The microbial community richness showed the least diversity in CD patients of the biotherapy cohort, with significant differences from the UC patients of both cohorts (**Figure 30**). Shannon effective, a measure of alpha diversity, showed a similar trend of increased Shannon effective diversity in UC patients of both cohorts (**Figure 30**). Unsupervised

beta diversity analysis visualized by a phylogram showed the heterogeneous microbial profiles of CD and the UC patients of the two cohorts (**Figure 30**).

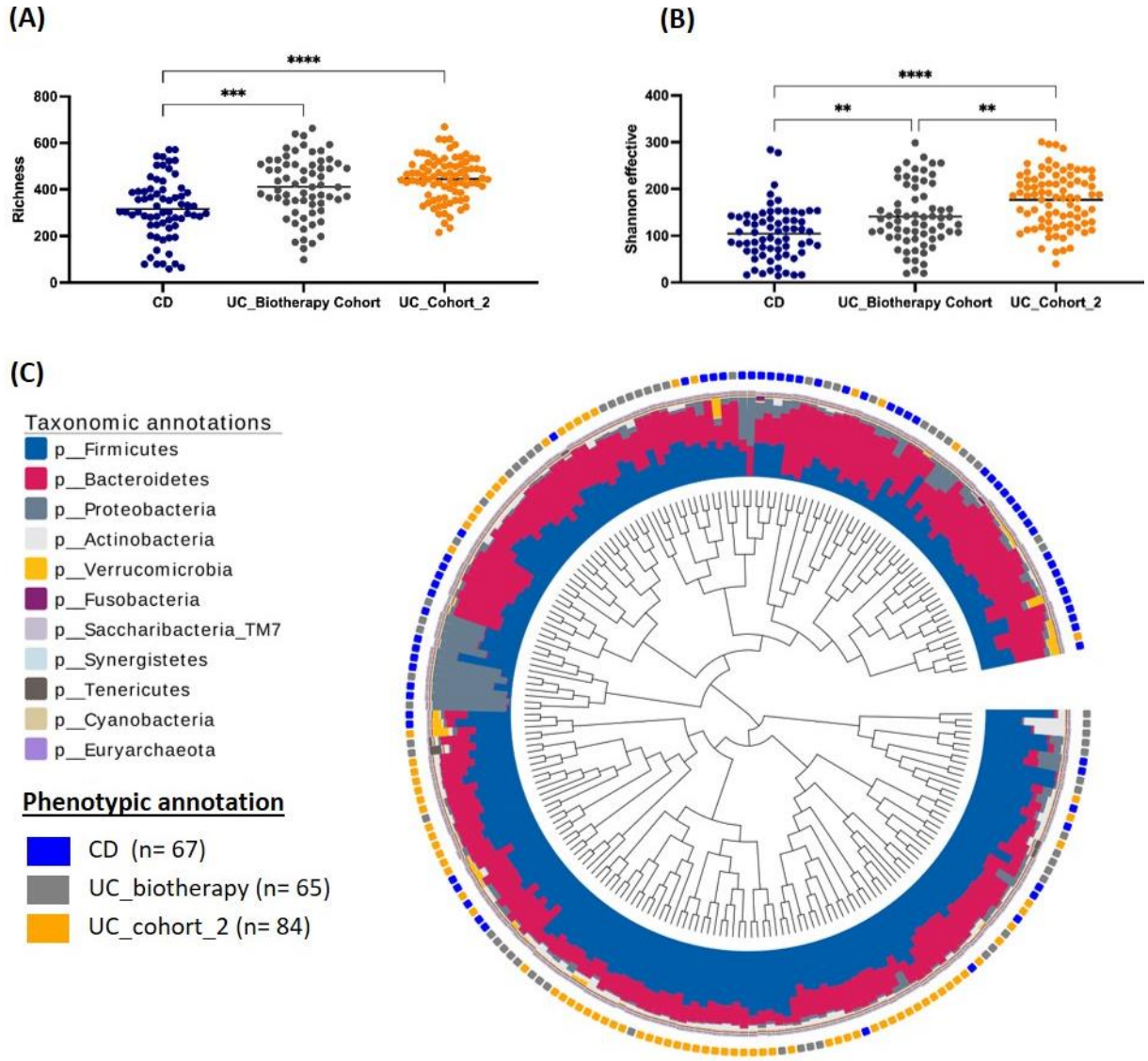

Figure 30 Gut microbial profiles characterization of IBD patients from different cohorts
*The microbial community richness (**A**), Shannon effective (**B**) of CD, UC (biotherapy cohort), and UC cohort_2 patients' samples. The dendrogram depicts microbial profile similarities based on generalized UniFrac distances between CD, UC (biotherapy cohort), and UC (cohort 2) patients (**C**). The individual microbial composition on the phylum level is shown as a stacked bar plot around the dendrogram. Each rectangle, outer of the stacked bar plot, represents one sample, and each color represents disease phenotype (blue: CD, grey: UC biotherapy cohort, and yellow: UC cohort 2). For alpha diversity measures, one-way ANOVA followed by multiple comparison testing (Dunn test) was used. P ≤0.05 was considered significant; *, p ≤0.01; **, p ≤0.001; ***, p ≤0.0001; ****.*

4.3.1 Characterization of the gut microbial profiles of UC patients from the biotherapy and lifestyle intervention cohorts

To evaluate the microbial profile differences of UC patients from different cohorts, the microbial profiles of the UC biotherapy cohort (n = 65) and UC cohort 2 (n = 84) were analyzed. Alpha diversity analysis showed slightly higher levels of microbial richness (non-significant) and

Shannon effective (significant) in UC cohort 2 (**Figure 31**). Unsupervised beta diversity analysis showed a significant difference in the overall microbial profiles between the two UC cohorts (**Figure 31**). LEfSe analysis highlighted *Escherichia coli* and *Clostridium* are enriched in UC (biotherapy cohort), and *Blautia* and *Gemmiger* are among the key differentiating taxa for UC cohort 2 (**Figure 31**).

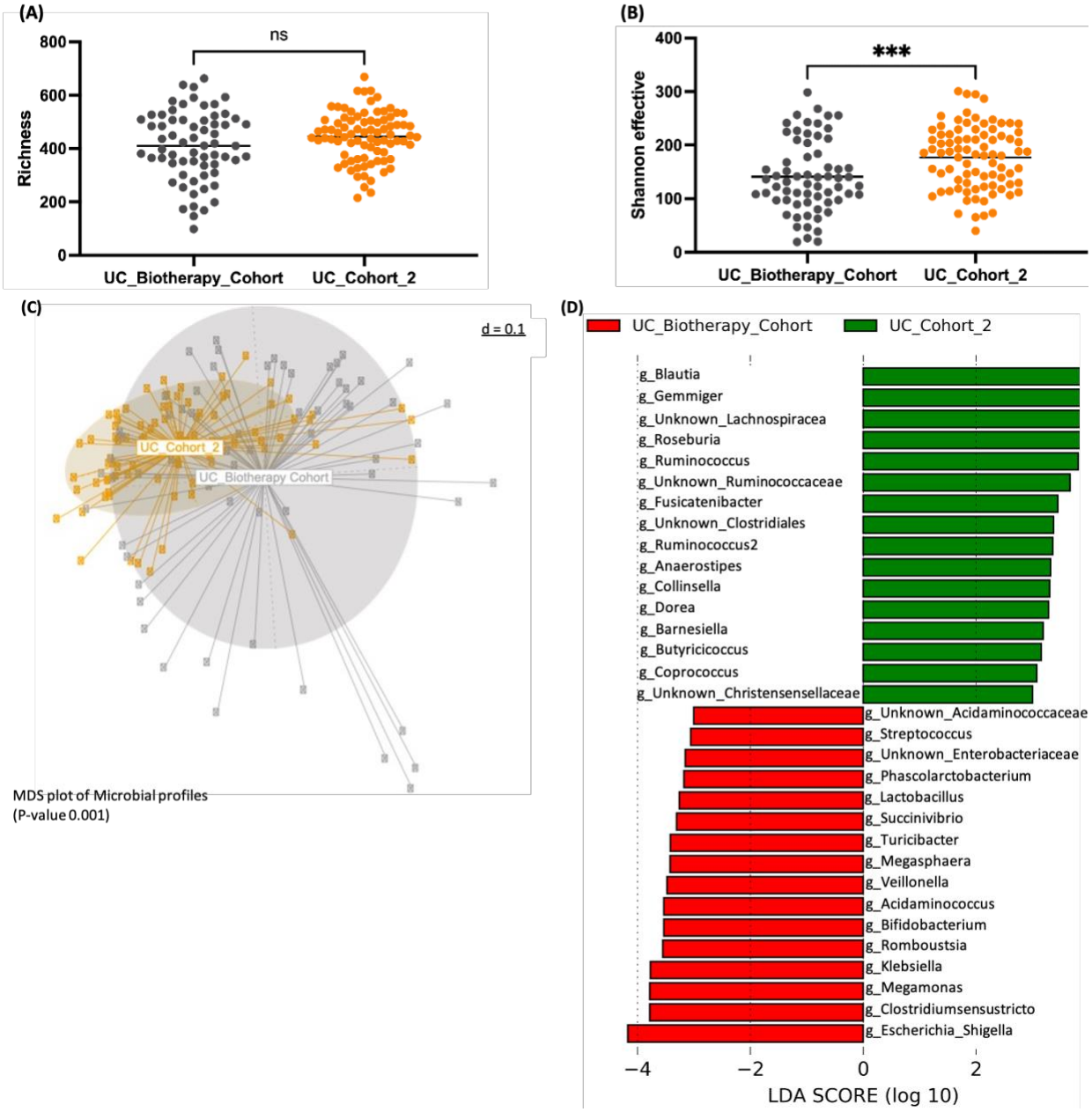

Figure 31 Gut microbial profile characterization of two UC patients' cohorts

*The microbial community richness (**A**), Shannon effective (**B**) between UC (biotherapy cohort) and UC cohort 2. MDS plot shows the microbial profiles of UC (biotherapy cohort) and UC cohort 2 (**C**). LEfSe analysis depicts the most differentiating genus (**D**) of UC (biotherapy cohort) and UC cohort 2. For alpha diversity measures, Mann-Whitney test was used. P ≤0.05 was considered significant; *, p ≤0.01; **, p ≤0.001; ***, p ≤0.0001; ****.*

4.4 Functional characterization of gut-microbiota in driving IBD disease phenotype using a gnotobiotic mouse model

Germfree WT and *Il10*$^{-/-}$ mice were colonized at the age of eight weeks for four weeks with microbiota obtained from two CD patients of the biotherapy cohort. Two paired stool samples from each patient, which were collected 14 and 52 weeks after the study initiation, were used to colonize GF mice, summing up four experiments to address the functional role of the biologics-conditioned gut microbiota. Donors were selected based on their disease phenotype, disease activity, the availability of stool samples over time, and microbial profiling of 16S rRNA amplicon sequencing (**Table 8**). To evaluate the microbe-host interactions in *Il10*$^{-/-}$ gnotobiotic mice, histological assessment of the inflammation, gene expression analysis of inflammatory marker as well as gut microbiota characterization were conducted.

Table 8 The phenotypic characterizations of the CD patients used for colonization experiments

Donors	Disease phenotype	Montreal classification	Disease activity at W14	Disease activity at W52
CD patient 1	CD	Ileocolonic	Active	Inactive
CD patient 2	CD	Ileocolonic	Inactive	Inactive

4.4.1 Transfer of disease-activity phenotype from two paired stool samples of CD patient-1 to recipients' *Il10*$^{-/-}$ mice was successfully recapitulated

Germfree *Il10*$^{-/-}$ mice that received microbiota from CD patient-1 at W14 with clinically active disease were inflamed in the cecum and colon tissues after four weeks of inoculation. Further, *Il10*$^{-/-}$ mice that received microbiota from CD patient-1 at W52 with the clinically inactive disease did not show an inflammatory phenotype (**Figure 32**). WT mice did not show any signs of inflammation in both experiments, confirming the non-infectious role of IBD-derived gut microbiota in driving the disease phenotype in susceptible hosts. Gene expression analysis of whole cecum and colon tissues revealed higher expression levels of TNF, an inflammatory cytokine, in *Il10*$^{-/-}$ mice (**Figure 32**).

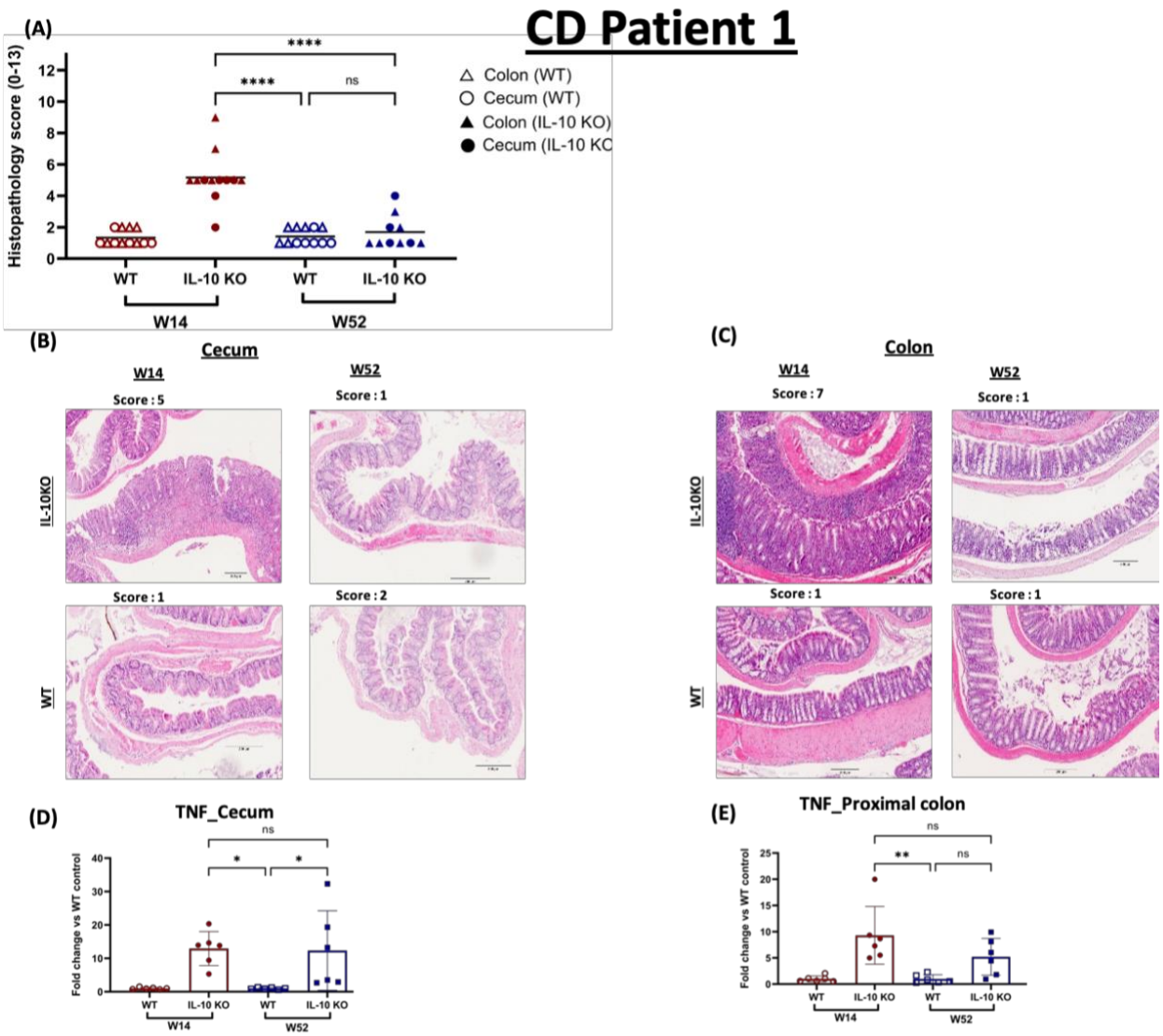

Figure 32 Inflammation assessment of the large intestine of gnotobiotic mice colonized by CD patient-1 gut microbiota
*Histopathological scores of the gnotobiotic mice of the cecum tissues and colon tissues (**A**). Representative H/E staining of the cecum (**B**) and colon (**C**) of colonized mice at 12 weeks of age. Gene expression analysis of TNF in the cecum (**D**) and proximal colon (**E**) of the colonized mice by CD patient-1 gut microbiota. One-way ANOVA followed by Bonferroni posthoc comparisons test was used. *, p≤0.05, **, p≤0.01, ***, p≤0.001, ****, p≤0.0001.*

4.4.1.1 Gut microbial dysbiosis reflects the inflammation phenotype in the gnotobiotic mice colonized by CD patient-1 derived microbiota

Beta diversity analysis of the microbial profiles of *Il10*$^{-/-}$ mice was significantly different from the WT mice that were colonized with gut microbiota derived from CD patient-1 at W14 (**Figure 33**), which reflected the active disease phenotype of the donor in the *Il10*$^{-/-}$ mice. Remarkably, there was no significant difference between the microbial profiles of the *Il10*$^{-/-}$ and WT mice that were colonized with gut microbiota obtained from CD patient-1 at W52 (**Figure 33**),

which mirrored the inactive disease phenotype of the donor in the *Il10*$^{-/-}$ mice. LEfSe analysis revealed the key bacterial genera that dominated the *Il10*$^{-/-}$ mice (the inflammatory phenotype) at W14, such as *Escherichia coli* and *Streptococcus*. *Blautia* and *Anaerotruncus* were more abundant in their respective WT mice (**Figure 33**). There were no specific taxa revealed differences between the WT and *Il10*$^{-/-}$ mice of the W52 experiment using LEfSe analysis. Alpha diversity measures (richness and Shannon effective) did not show significant differences between the different genotypes in both experiments (**Figure 33**). Fecal pellets cultured on WCA showed a higher CFU count in mice at W14 than at W52, but there was almost no difference between the different genotypes (**Figure 33**).

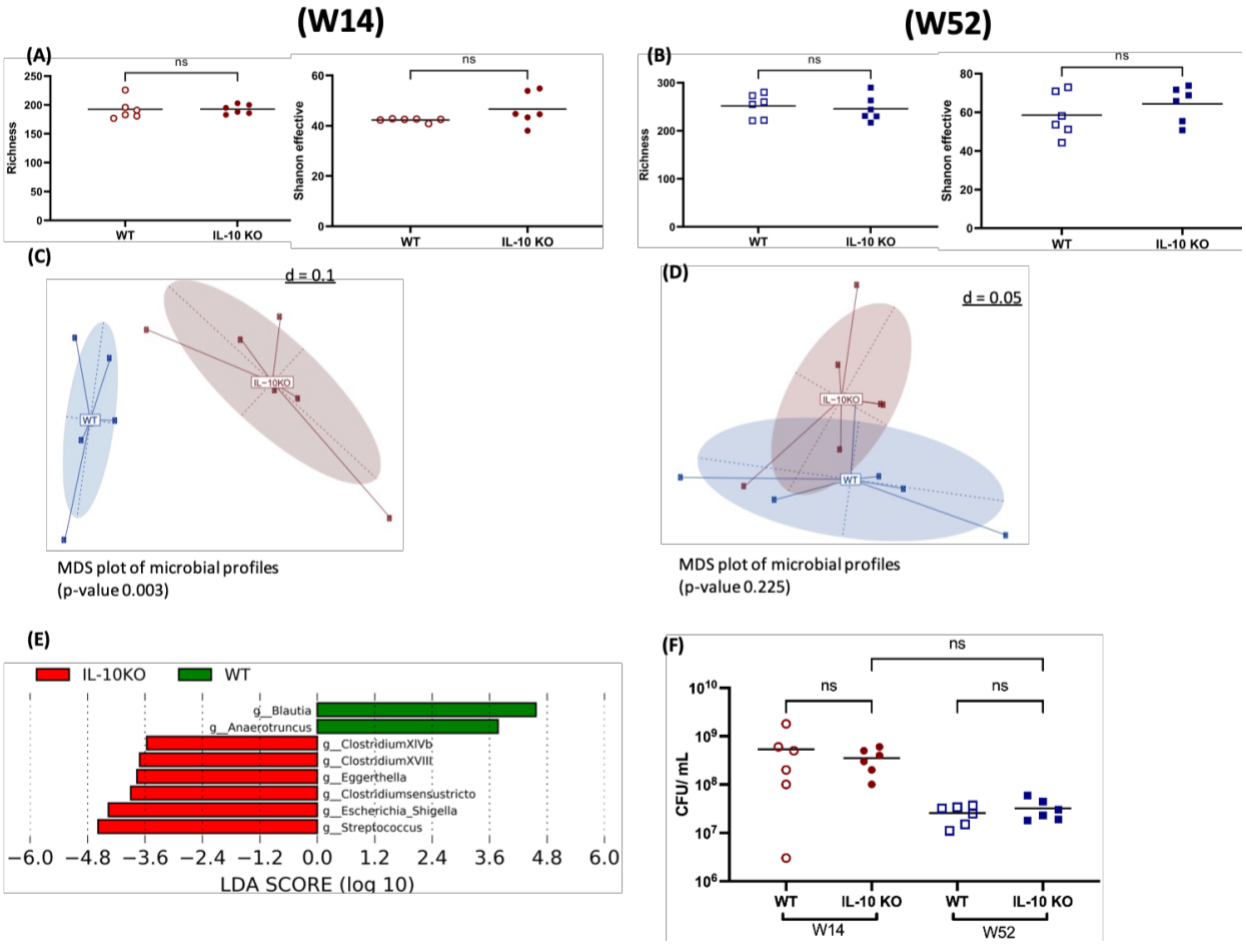

Figure 33 Microbial profiles characterization of mice colonized by CD patient-1 gut microbiota at two time points (W14 &W52) *Alpha diversity analysis (richness and Shannon effective) of Il10*$^{-/-}$ *and WT mice colonized by gut microbiota derived from CD patient-1 at W14 (**A**) and W52 (**B**). MDS plots show the microbial profile differences between Il10*$^{-/-}$ *and WT mice colonized by CD patient-1 microbiota obtained at W14 (**C**) and W52 (**D**). Relative abundance comparison of bacterial genera between Il10*$^{-/-}$ *and WT mice, colonized by gut microbiota obtained from CD patient-1 at W14, using LEfSe analysis between WT and Il10*$^{-/-}$ *(**E**). CFU counts of fecal pellets cultured on WCA for both experiments (**F**). For alpha diversity measures, the Mann-Whitney test was used. P ≤0.05 was considered significant; *, p ≤0.01; **, p ≤0.001; ***, p ≤0.0001; ****.*

4.4.1.2 *Increased percentage of IgA coated bacteria in Il10$^{-/-}$ mice colonized by CD patient-1 derived microbiota*

Semi-quantification analysis of the gut microbiota bound to IgA revealed an increase in the overall percentage of the IgA-bound bacteria in *Il10*$^{-/-}$ mice in both experiments when compared to their WT counterparts (**Figure 34**). Besides, there was a significant increase in the IgA-bound bacteria percent in *Il10*$^{-/-}$ mice to their WT counterparts of the W14 experiment.

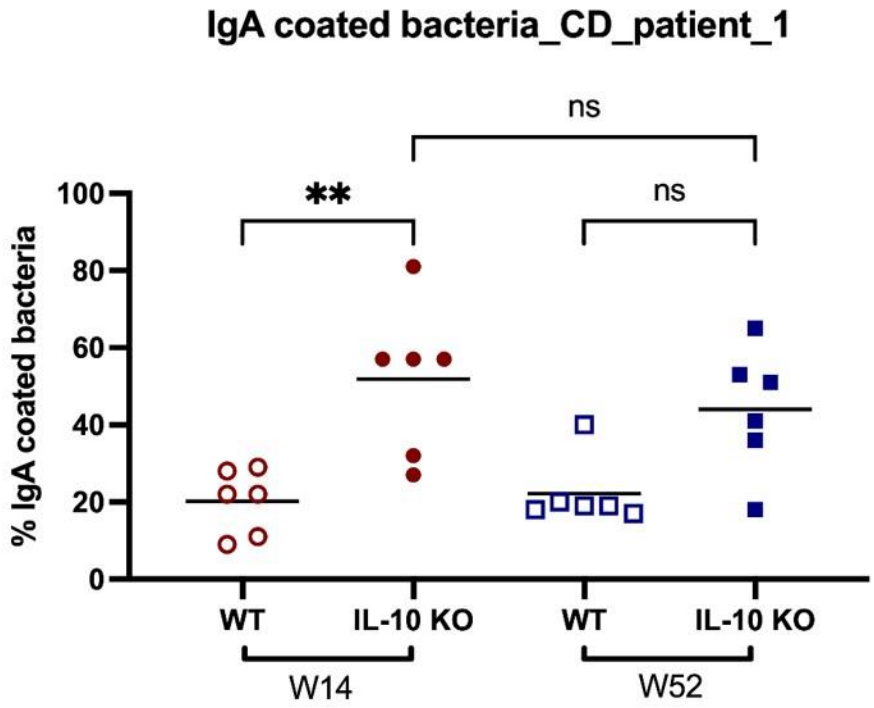

Figure 34 The percentage of IgA-bound bacteria in the gnotobiotic mice colonized by patient CD-1 gut microbiota (W14 & W52)
*One-way ANOVA followed by Bonferroni posthoc comparisons test was used. *, p≤0.05, **, p≤0.01, ***, p≤0.001, ****, p≤0.0001.*

4.4.2 Disease-activity phenotype was not successfully recapitulated from two paired stool samples of CD patient-2 to recipients' *Il10*$^{-/-}$ mice

Germfree *Il10*$^{-/-}$ mice that received microbiota from CD patient-2 at W14 and W52 with clinically inactive disease phenotype at the two timepoints showed inflammation in the cecum and colon tissues after four weeks of colonization (**Figure 35**). Gene expression analysis of whole colon and cecum tissues showed higher expression levels of TNF, an inflammatory cytokine in inflamed *Il10*$^{-/-}$ mice (**Figure 35**).

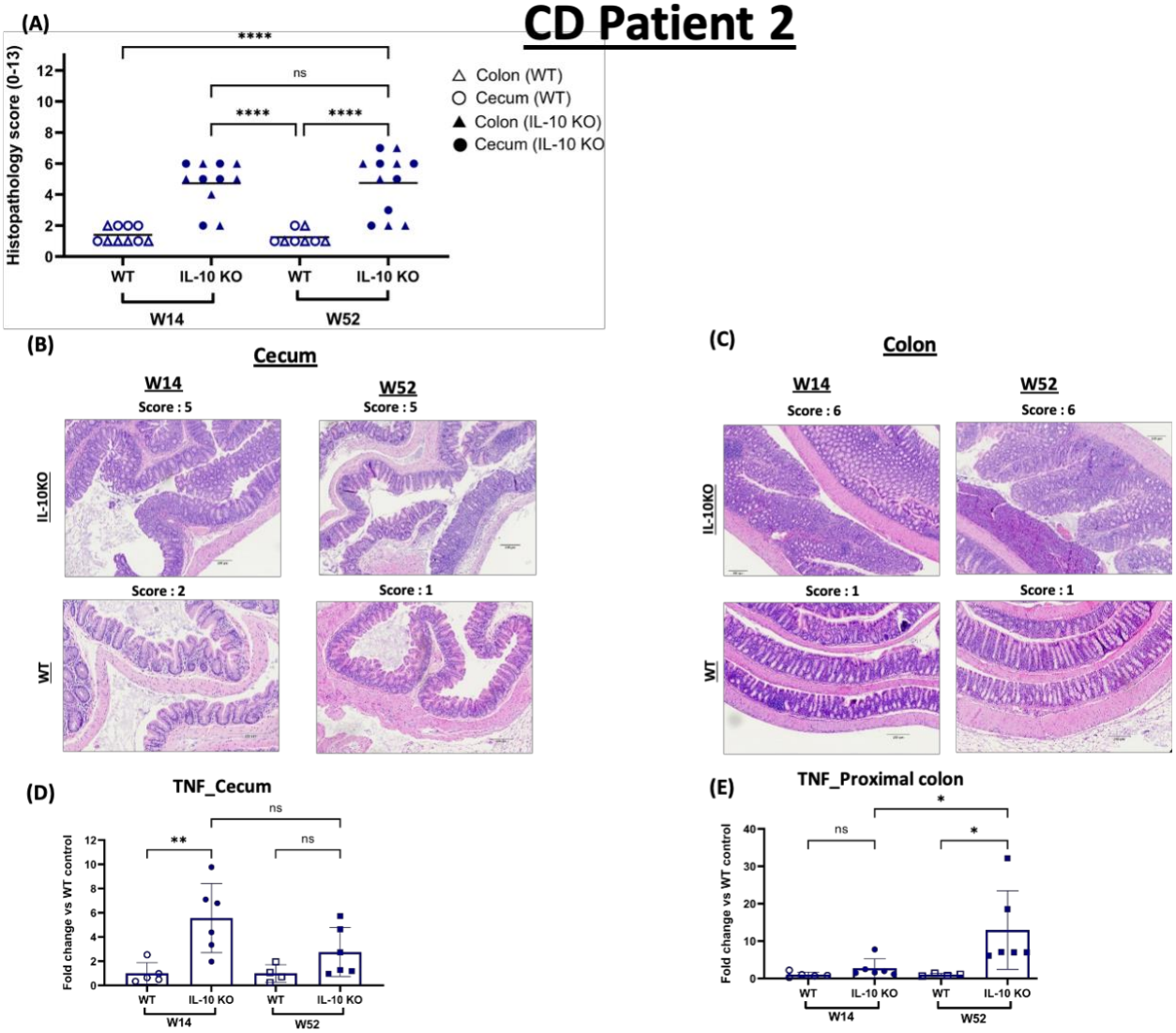

Figure 35 Evaluation of the inflammation in the large intestine of gnotobiotic mice colonized by CD patient-2 gut microbiota
*Histopathological scores of the gnotobiotic mice of the cecum tissues and colon tissues (**A**). Representative H/E staining of the cecum (**B**) and colon (**C**) of colonized mice at 12 weeks of age. Gene expression analysis of TNF in the cecum (**D**) and proximal colon (**E**) of the colonized mice by CD patient-2 gut microbiota. One-way ANOVA followed by Bonferroni posthoc comparisons test was used. *, p≤0.05, **, p≤0.01, ***, p≤0.001, ****, p≤0.0001.*

4.4.2.1 Gut microbial dysbiosis reflects the inflammation phenotype in the gnotobiotic mice colonized by CD patient-2 derived microbiota

The microbial alpha diversity measures (richness and Shannon effective) did not show a similar pattern in both experiments (W14 & W52). *Il10*$^{-/-}$ mice showed reduced richness and Shannon effective when compared with their WT counterparts for the W14 experiment, but the *Il10*$^{-/-}$ mice in the W52 experiment showed higher alpha diversity measures when compared with their WT control (**Figure 36A** & **B**). Fecal pellets cultured on WCA showed a higher CFU count in

Il10$^{-/-}$ mice when compared with their WT counterparts for W14 and W52 (**Figure 36CFigure 37**). Beta diversity analysis of the microbial profiles of *Il10*$^{-/-}$ mice was significantly different from the WT mice that were colonized with gut microbiota-derived from CD patient-2 at W52 (**Figure 37**). However, there was no significant difference (p-value = 0.06) between the microbial profiles of the *Il10*$^{-/-}$ and WT mice that were colonized with gut microbiota obtained from CD patient-2 at W14 (**Figure 37**). LEfSe analysis revealed the key bacterial genera that dominated the *Il10*$^{-/-}$ mice at W14, such as unknown *Enterobacteriaceae* and *Blautia*. *Bifidobacterium* and *Clostridium XIVa* were among the most enriched taxa in their respective WT mice (**Figure 37**). LEfSe analysis highlighted some taxa, such as *Enterococcus* and *Alistipes* to be significantly abundant in *Il10*$^{-/-}$ mice and *Escherichia coli* in their WT control mice of the W52 experiment.

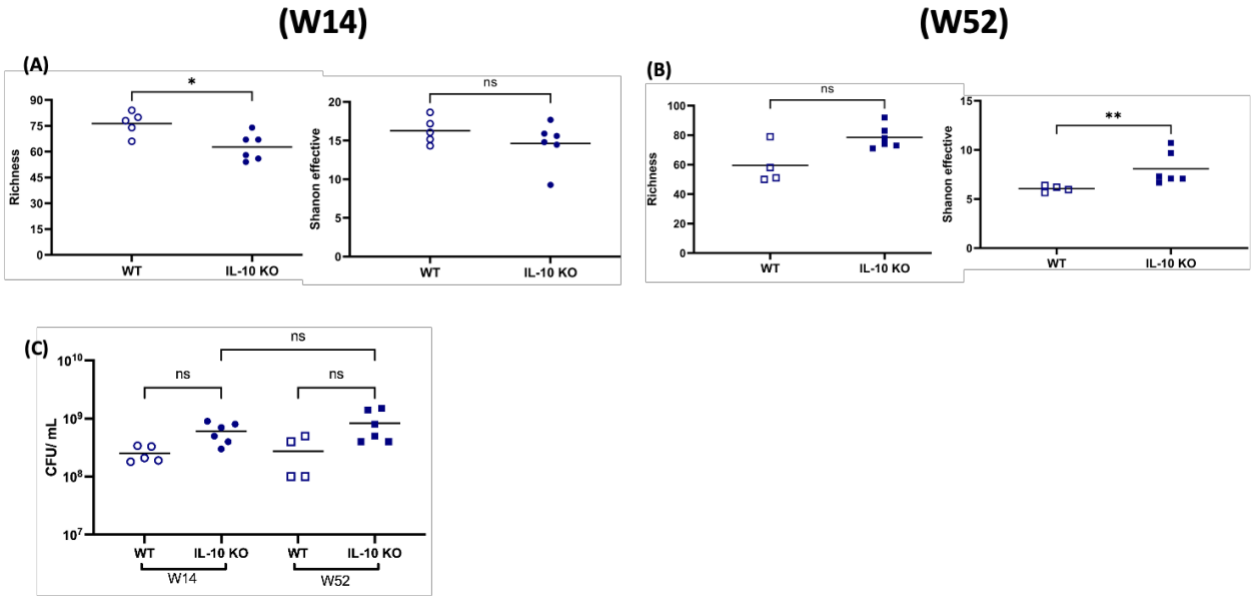

Figure 36 Alpha diversity analysis and colony forming unit counts of mice colonized by CD patient-2 gut microbiota at two time points (W14&W52)

Alpha diversity analysis (richness and Shannon effective) of Il10$^{-/-}$ *and WT mice colonized by gut microbiota derived from CD patient-2 at W14 (**A**) and W52 (**B**). CFU counts of fecal pellets cultured on WCA for both experiments (W14 & W52) (**C**). For CFU counts, one-way ANOVA followed by Bonferroni posthoc comparisons test was used *, p≤ 0.05, **, p≤0.01, ***, p≤0.001, ****, p≤0.0001. The Mann-Whitney test was used for alpha diversity analyses, P ≤ 0.05 was considered significant; *, p ≤ 0.01; **, p ≤ 0.001; ***, p ≤ 0.0001; ****.*

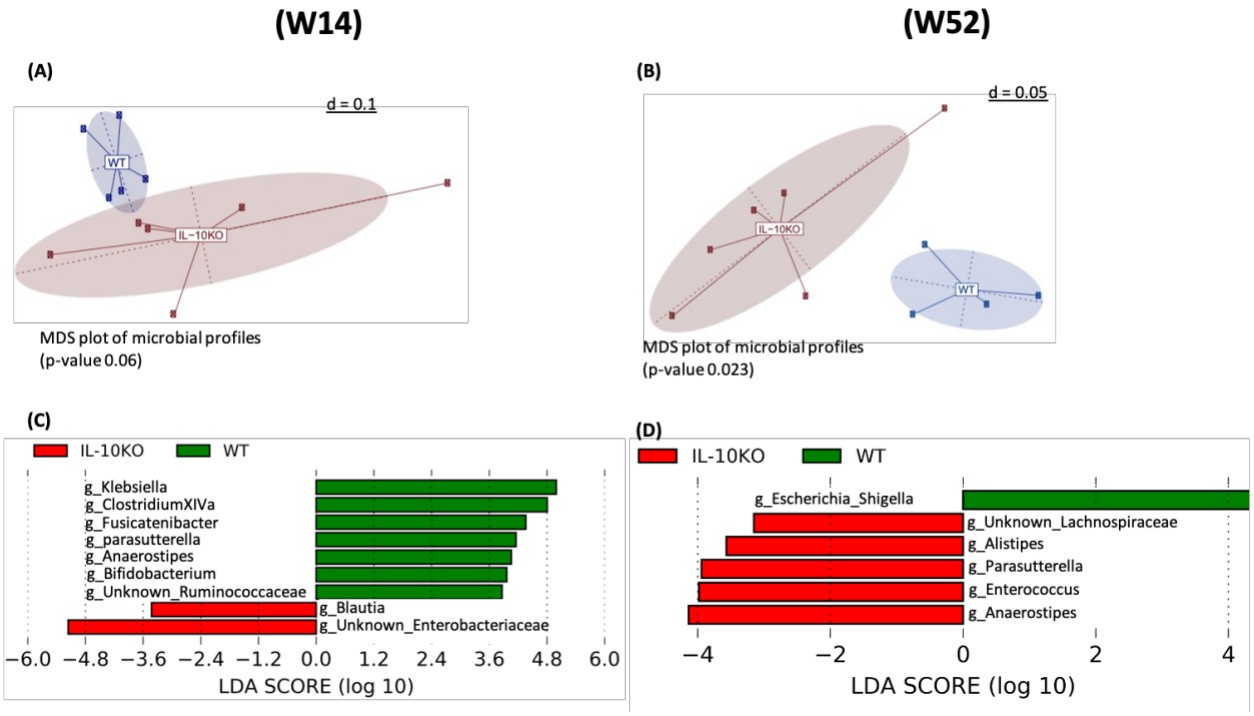

Figure 37 Microbial profiles characterization of mice colonized by CD patient-2 gut microbiota at two time points (W14&W52)
*MDS plots show the microbial profiles of the WT and Il10$^{-/-}$ mice colonized by CD patient-2 microbiota obtained at W14 (**A**) and W52 (**B**). Relative abundance comparison of bacterial genera between Il10$^{-/-}$ and WT mice using LEfSe analysis at W14 (**C**) and W52 (**D**).*

4.4.2.2 Increased percentage of IgA coated bacteria in Il10$^{-/-}$ of mice colonized by CD patient-2 derived microbiota

Semi-quantification analysis of gut microbiota bounded to IgA revealed a significant increase in the overall percentage of the IgA-bound bacterial community in the inflamed *Il10$^{-/-}$* mice compared to their WT counterparts, reaching 90% and 70% for W14 and W52, respectively (**Figure 38**).

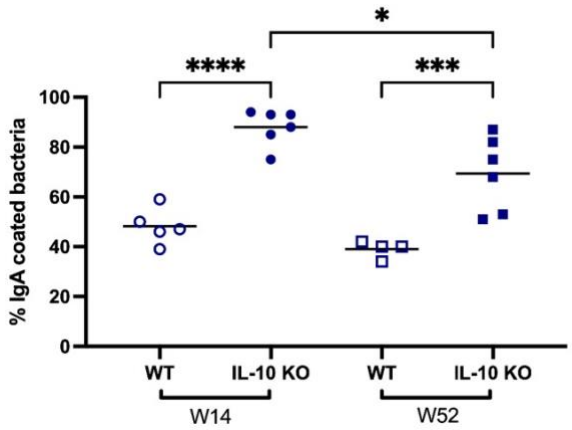

Figure 38 Percentage of IgA-bound bacteria in the gnotobiotic mice colonized by patient CD-2 gut microbiota (W14 & W52)
*One-way ANOVA followed by Bonferroni posthoc comparisons test was used. *, p≤0.05, **, p≤0.01, ***, p≤ 0.001, ****, p≤0.0001.*

4.4.3 Correlation analysis of gut microbiota composition and host phenotypes

Correlation analyses between gut microbial taxa abundance, inflammation, and the IgA-coated bacteria were performed on the gnotobiotic mice (four experiments). The correlation analysis revealed several bacteria such as *Escherichia coli* and *Clostridium XVII* to be positively correlated with the inflammatory score, and other taxa such as *Bacteroidetes*, *Blautia*, and *Parasutterella* were correlated negatively with the pathological scoring in the colon and cecum (**Figure 40**). Interestingly, the association of some of the protective taxa was correlated with higher alpha diversity measures (richness and Shannon effective), and some inflammatory-associated taxa correlated negatively with the alpha diversity measures (**Figure 40**). There was an association between the increased abundance of some bacterial taxa such as *Enterococcus, unknown Enterobacteriaceae, and Morganella* and the increased percentage of IgA-coated bacteria in these experiments (**Figure 40**). There was a negative association between the increased abundance of specific taxa such as *Akkermansia* and *Bacteroidetes* with the decreased percentage of IgA-coated bacteria. These data suggest a selective role of the secreted immunoglobulins in controlling the gut microbiota composition.

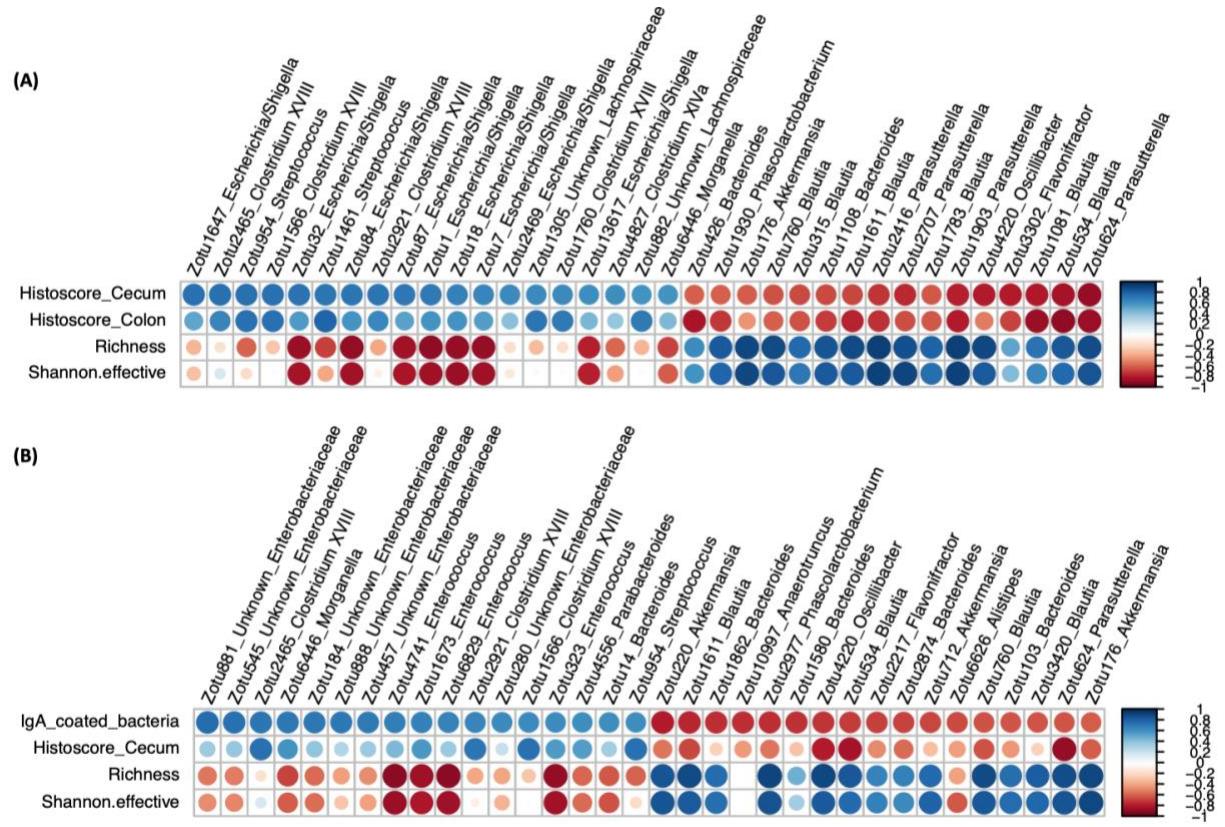

Figure 40 Correlation analysis of gut microbiota components with inflammation scores and the IgA-bound bacteria
*Correlation analysis of the bacterial taxa and the histopathological scores of the gnotobiotic mice, which were colonized with microbiota obtained from CD patient-1 and CD patient-2 (**A**). Correlation analysis of the bacterial taxa and the percentage of the IgA-bound bacteria of the gnotobiotic mice, which were colonized with microbiota obtained from CD patient-1 & CD patient-2 (**B**).*

4.5 Characterization of gut microbial transfer efficiency in the gnotobiotic mouse model

The gut-microbiota colonization efficiency was assessed to address the validity of the gnotobiotic models from ecological and biological perspectives. Transferring the gut microbiota from CD patient-1 and CD patient-2 for both time points (W14 and W52) revealed 33-56% colonization efficiency (**Figure 41A**). Colonization transfer efficiency was calculated by dividing the number of shared bacterial taxa (zOTUs) between the donor samples and its recipient WT mice by the total bacteria (zOTUs) found in the donor samples. In addition, there was a reduction of alpha diversity measures (richness and Shannon effective), especially for CD patient-1 experiments, in the recipients' WT mice when compared to the donor samples (**Figure 41C & Figure 41D**). The comparison of microbial profiles of the donor samples and their recipient mice was calculated using the generalized Unifrac distance. The generalized Unifrac distance (dissimilarity) between donors and recipients ranged from 48%-64% in all four experiments (**Figure 41B**).

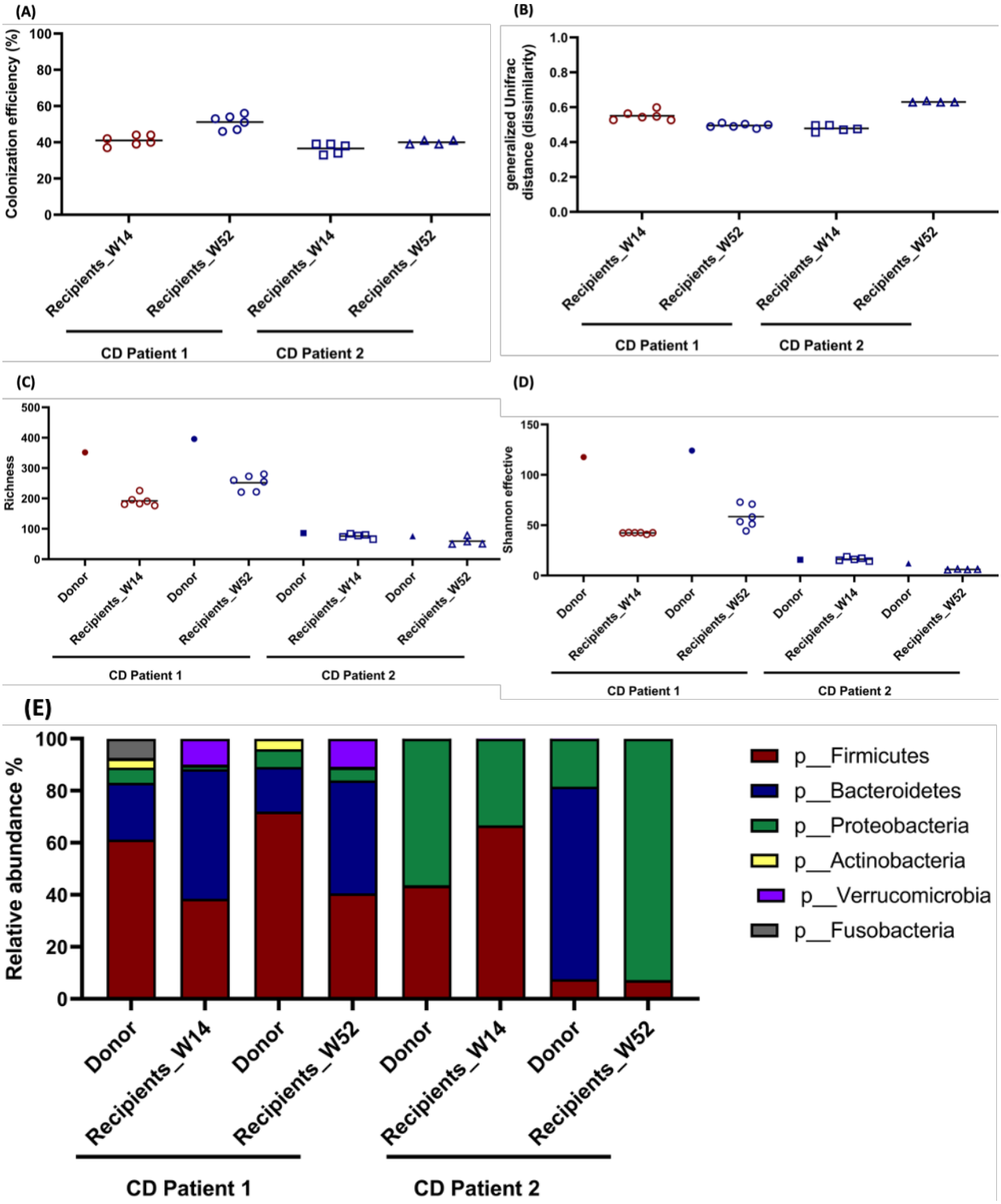

Figure 41 Assessment of gut microbial transfer efficiency in the gnotobiotic mouse model colonized by IBD donor microbiota
*Colonization efficiency (%) in the gnotobiotic mice that were colonized with microbiota obtained from CD patient-1 and CD patient-2 was computed by dividing the number of shared zOTUs between the donor sample and its recipient WT mice by the total zOTUs number of the donor (**A**). The generalized Unifrac distance between each donor sample and its recipient WT mice as a beta-diversity measure between donors and recipients (**B**). Alpha diversity measures, richness (**C**), and Shannon effective (**D**) for donors and its recipient mice. The relative abundance of microbial taxa on the phylum level between the donor samples and their recipient mice (**E**).*

Interestingly, specific taxa did not colonize the mice or, it was at a very low detection level, such as Actinobacteria, Fusobacteria, and *Prevotella* (Bacteroidetes) (**Figure 41E** & **Figure S6**). In addition, there was a shift in the Firmicutes to Bacteroidetes ratio between the donor of CD patient-1 and its recipient WT mice (W14 and W52), where recipient mice showed a higher Firmicutes to Bacteroidetes ratio opposing their donor counterparts (**Figure 41E**). Remarkably, gnotobiotic mice select a specific repertoire of microbial taxa to grow regardless of the human donor microbial abundance status (**Figure 42**), suggesting a vital role of host species in determining gut microbiota composition. Heatmaps demonstrate the details of the relative abundance of all genera of donors and their recipient WT mice in the four gnotobiotic experiments (**Figure S3, S4, S5 & S6**). It shows that specific taxa with a very low abundance in the donor samples bloom in the mice gut and vice versa (**Figure S3, S4, S5 & S6**).

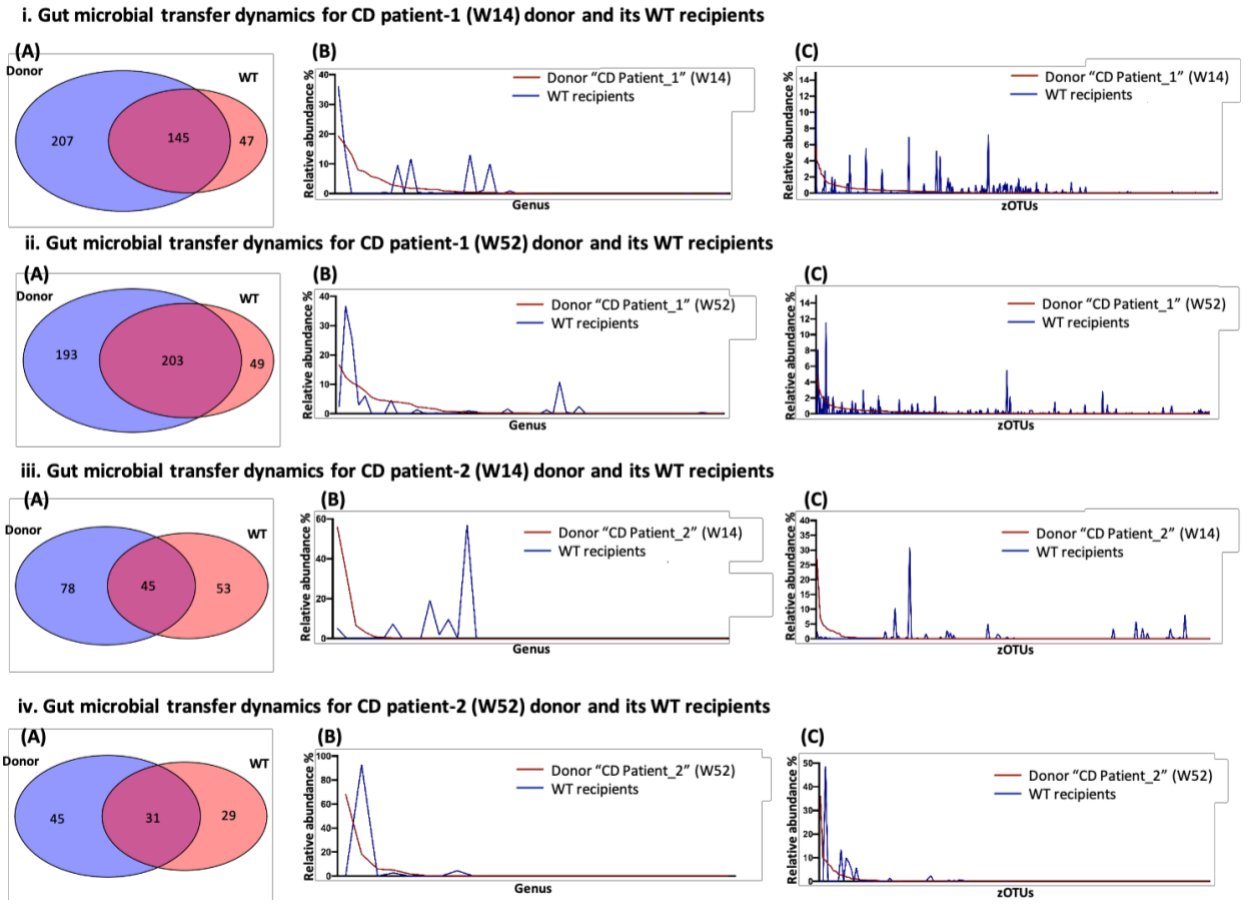

Figure 42 Gut microbial transfer dynamics in the gnotobiotic mouse model inoculated with the gut microbiota of CD patients
*Microbial transfer dynamics of the human-derived gut microbiota colonization (2 CD patients) for the four gnotobiotic experiments (**i, ii, iii, iv**). Numbers of zOTUs that are shared between each donor sample and its WT recipients and the unique ones (**A**). The relative abundance, on the genus level, between each donor sample and its recipient WT mice (**B**). The relative abundance, on the zOTU level, between each donor sample and its recipient WT mice (**C**).*

5 Discussion

In the present work, we studied the stool and mucosa-associated gut microbial profiles of IBD patients and their fecal metabolomic signatures in a longitudinal prospective study (biotherapy cohort). Moreover, we analyzed the fecal gut microbial profiles of two geographically-distinct IBD cohorts (biotherapy cohort and ulcerative colitis lifestyle intervention cohort). Further, we compared two bioinformatics methods for downstream analysis of 16S rRNA data of the gut microbiota composition of the biotherapy cohort. We also investigated the functional relevance of gut microbiota through an IBD gnotobiotic mouse model using CD patients-derived gut microbiota. In addition, we assessed the transfer efficiency of the gut microbiota obtained from human donors in the gnotobiotic mouse model.

5.1 Gut microbial signatures and metabolomic profiles in IBD patients

Our results showed strong intra-personal stool and mucosa-associated gut microbial signatures for IBD patients of the biotherapy cohort for one year, independent of the disease state and the biotherapy medications. Our findings are in line with the reported stable intra-individual gut microbial profiles overtime in healthy individuals and IBD patients (Faith et al., 2013; Galazzo et al., 2019; Lloyd-Price et al., 2019; Mehta et al., 2018; Metwaly et al., 2020; Ohman et al., 2021; Schloissnig et al., 2013). Our results highlighted a significant difference in the microbial profiles between CD and UC patients on the luminal and mucosal levels assessed by alpha and beta diversity analyses. CD patients showed higher levels of *Escherichia coli* and *Ruminococcus.* In contrast, UC patients displayed a higher abundance of *Bifidobacterium*, *Roseburia*, and *Faecalibacterium* in the mucosal and fecal microbial communities. Although the well-documented gut microbial profile difference in the luminal or mucosal levels between IBD patients and healthy individuals (Conte et al., 2006; Hall et al., 2017; Lewis et al., 2015; Ott et al., 2004; Scanlan et al., 2006), there are only a few studies that compared the gut microbial signatures between CD and UC patients. In line with our findings, other studies described distinct microbial profiles between UC and CD patients (Sankarasubramanian et al., 2020; Yilmaz et al., 2019). Similar to our findings, Sankarasubramanian and colleagues described a significant enrichment of *Faecalibacterium* in stool samples from UC patients (Sankarasubramanian et al.,

2020). Interestingly, taxonomical annotation to the genus level of *Clostridium* and *Ruminococcus* was not sufficient to distinguish between CD and UC patients but rather on the species level (Sankarasubramanian et al., 2020), suggesting the need for deep microbial profiling analysis methods, ideally to the strain level, to further dissect disease-associated taxa.

There was no significant difference in alpha diversity of the stool and mucosa-associated gut microbiota between active and inactive IBD patients of the biotherapy cohort. However, LEfSe analysis revealed a higher abundance of *Escherichia coli*, *Klebsiella*, and unknown *Clostridiales* among other taxa in the stool of active IBD patients, suggesting a selective expansion of some bacteria during the disease flare but not the overall microbial community diversity. Our data showed no significant disease-activity associated gut microbial signature in ileal CD patients at the mucosal level, evaluated by alpha and beta diversity measures and LEfSe analysis. However, colonic CD patients with active disease phenotype showed an overall significant difference in the microbial profiles assessed by the beta diversity analysis. Colonic CD patients with active disease had an expansion of *Fusobacterium* and *Bacteroidetes* in the colonic mucosa. Of note, the biotherapy cohort did not have a well-distributed disease activity phenotype, where most of the patients showed active disease during the study duration. The association between gut microbial dysbiosis and disease activity has been reported in several studies with specific microbial differences between active and inactive IBD patients (Andoh et al., 2014; Gevers et al., 2014; Metwaly et al., 2020; Papa et al., 2012). Remarkably, several studies showed that disease activity does not influence gut microbial fluctuations in longitudinal studies (Galazzo et al., 2019; Halfvarson et al., 2017; Ohman et al., 2021), and inter-individual microbial variation in IBD patients was more profound than disease activity variations (Lloyd-Price et al., 2019), highlighting the importance of longitudinal studies in gut microbiota assessment. Ohman and colleagues followed-up the gut microbial profiles of two UC cohorts (newly diagnosed and established diseases) for (36 months and 3-10 months, respectively), and some patients of both cohorts developed flares (Ohman et al., 2021). The results showed high microbial stability for individuals, and it was not affected by disease activity or medications (5-aminosalicylic acid and azathioprine), and gut microbial dissimilarities were higher between patients than within patients (Ohman et al., 2021). Interestingly, most studies, which revealed significant gut microbial differences

between active and inactive IBD disease states, had a cross-sectional experimental design. They compared patients with active disease and patients in remission, neglecting the intra-personal gut microbial signature that can be assessed with longitudinal analysis. Our data showed that mucosa-associated microbial profiles of colonic CD patients were closer to UC patients than CD patients with ileal involvement. Moreover, the mucosa-associated gut microbial profiles revealed significant differences between colonic and ileal CD with *Escherichia coli* and *Vellionella* enrichment in iCD and *Faecalibacterium* and *Roseburia* in cCD patients. Several studies reported significantly different gut microbial community compositions between colonic and ileal CD patients (Imhann et al., 2018; Naftali et al., 2016), and the microbial signature of cCD is more similar to UC patients (Imhann et al., 2018). Ileal CD patients showed higher levels of *Enterobacteriaceae* and *Ruminococcus gnavus* and lower levels of *Roseburia* and *Faecalibacterium Prausnitzii* (Baumgart et al., 2007; Naftali et al., 2016; Sokol et al., 2008; Tyler et al., 2016; Willing et al., 2009; Willing et al., 2010). In a recent study, multi-omics analysis of the gut microbiome and host factors of over 200 IBD patients revealed profound differences between ileal and colonic CD patients, and UC patients had several similarities to colonic CD (Gonzalez et al., 2022). For instance, neutrophil-related proteins were enriched in UC and colonic CD patients compared to CD patients with ileal involvement. Ileal CD patients showed higher levels of *Proteobacteria, Ruminococcus*, and *Blautia*, while cCD patients and UC showed higher levels of *Bacteroides vulgatus* (Gonzalez et al., 2022).

In addition, we compared the fecal gut microbial profiles of IBD patients of the biotherapy and ulcerative colitis lifestyle intervention cohorts. CD patients showed distinct microbial diversity (richness and Shannon effective) compared to UC patients from both cohorts. While we do not have data on the participants' diet and lifestyle, the gut microbial profiles of UC patients in the two cohorts were significantly different, suggesting the role of geographical location, which reflects different diets, lifestyles, and ethnicity, in shaping the gut microbiota composition. Our results are in line with other studies that showed the indispensable effect of geographical location in influencing the gut microbiome in IBD patients (Clooney et al., 2021) and healthy individuals (He et al., 2018). Analyzing microbial profiles (beta diversity) of 120 healthy individuals, 291 CD, and 236 UC patients from Canada and Ireland showed that the geographic location accounted for

most of the microbiota variance out of 25 other environmental factors (Clooney et al., 2021). Thus, geographical location influence on the microbiome proposes a challenge for developing microbiota-based therapeutics and diagnostics applications.

The comparison of different gut microbiota studies must be carefully interpreted for possible technical differences in sampling, sample storage, sample processing, sequencing analysis, and data processing (Abellan-Schneyder et al., 2021; Reitmeier et al., 2021). Several studies reported that different bioinformatic pipelines influence the microbiota composition results (Ducarmon et al., 2020; Sierra et al., 2020). Clustering 16S amplicon sequences based on the sequences' similarities threshold into OTUs and zOTU has been used in microbiome analysis. In brief, an OTU is created by clustering 16S sequencing reads at 97% similarity, and there are three main bioinformatics pipelines used: (MOTHUR (Schloss et al., 2009), QIIME (Caporaso et al., 2010), and USEARCH (Edgar, 2013)). While having the exact 16S biological sequence (100% similarity) is termed a zOTU or an amplicon sequence variant (ASV) or sub-OTUs, and three main bioinformatics pipelines have been developed (DADA2 (Callahan et al., 2016), Deblur (Amir et al., 2017), and UNOISE3 (Edgar, 2016)). Clustering sequences with 100% similarities (zOTUs) offer higher sensitivity and resolution compared to OTU clustering, as an OTU could contain two or more species that have sequence similarities (97%) but varies in biological phenotype. In addition, clustering sequences with 100% similarities can simplify comparing various studies by eliminating the need for re-grouping taxa when different datasets merge. Comparing different clustering algorithms for OTUs (MOTHUR, QIIME, and USEARCH) and exact sequences variants (DADA2, Deblur, and UNOISE3) on a mock community and 2170 fecal samples showed that OTU-level pipelines had lower specificity than the exact sequences variants (zOTUs), and the UNOISE3 showed the best balance between specificity and resolution (Prodan et al., 2020). We investigated the influence of clustering methods (OTUs (Edgar, 2013) and zOTUs (Edgar, 2016)) on the overall microbial community profiles in a subset of the biotherapy cohort. Our results showed similar alpha and beta diversity trends between OTUs and zOTUs analyses, which were also reported in other studies (Abellan-Schneyder et al., 2021; Glassman and Martiny, 2018). However, the zOTUs analysis revealed better resolution at the taxonomic level analysis and avoids making assumptions

about dissimilarities within a taxonomic group, which is considered a weakness of the OTU analysis method.

Although 16S rRNA amplicon sequencing studies have enhanced our knowledge of the gut microbiome's role in health and disease, it has a limited taxonomic resolution (genus-level associations). Enhancing the microbial resolution to the strain level using metagenomic analysis is indispensable to dissecting the influence of microbial strains and disease phenotypes (De Filippis et al., 2019; Hall et al., 2017; Metwaly and Haller, 2019b). Metagenomics analysis does not only delineate better microbial resolution but also gives insights into the microbial genes involved. For instance, metagenomic sequencing was used to study healthy and pediatric CD patients' microbial profiles (Lewis et al., 2015). Pediatric CD patients showed an increase in microbial genes encoding for sulfur relay systems, siderophores biosynthesis, glycerolipid metabolism, galactose metabolism, glutamine/glutamate metabolism, and nitrogen metabolism (Lewis et al., 2015). Interestingly, metagenomic sequencing of the entire genetic content of the stool samples showed that the microbiome of IBD patients correlates with higher levels of human and fungal DNA that could not be analyzed using amplicon sequencing (Lewis et al., 2015). A summary of the associated bacterial species in IBD across several metagenomic studies was reported in further detail (Metwaly et al., 2022b; Schirmer et al., 2019). It showed an increase in Proteobacteria's *E. coli* and a reduction in Actinobacteria and Bacteroidetes species in IBD patients (Schirmer et al., 2019). Firmicutes species showed different abundance trends suggesting strain-specific microbe-host interactions (Schirmer et al., 2019). Functional characterization of the gut microbiome using metatranscriptomic, metaproteomic, and metabolomic is needed for better interpreting the role of gut microbiota in health and disease (Erickson et al., 2012; Heintz-Buschart and Wilmes, 2018). However, only a few studies have explored the functional activity of the gut microbiota. Interestingly, intrapersonal microbial metatranscriptome varied more than metagenome profiles, emphasizing the importance of measuring actual transcriptome for a better understanding of microbiota-related host interactions (Franzosa et al., 2014; Mehta et al., 2018). IBD-related microbial transcriptome showed varied profiles over time, which did not reflect the gut microbial community changes (Schirmer et al., 2018), highlighting the limitations of metagenomics studies. IBD patients revealed significantly different fecal metaproteomic

signatures compared to healthy individuals (Lehmann et al., 2019; Zhang et al., 2018). Furthermore, IBD patients revealed a distinct metabolome profile compared to healthy individuals (De Preter et al., 2015; Franzosa et al., 2019; Jansson et al., 2009; Santoru et al., 2017), but less discriminant between IBD subtypes (Franzosa et al., 2019; Lavelle and Sokol, 2020). Untargeted metabolomics analysis of the biotherapy cohort showed different metabolomic profiles between CD and UC patients characterized by higher levels of bile acids and fatty acids in CD patients, such as lithochol-11-enic acid, hyodeoxycholic acid, and eicosenoic acid, while UC patients had higher levels of medicinal products such as acetaminophen and N-acetyl-5-aminosalicylic acid. Similar to our findings, other studies reported dysregulation of several metabolites such as bile acids (Franzosa et al., 2019; Jacobs et al., 2016; Lloyd-Price et al., 2019), medium-chain and short-chain fatty acids (De Preter et al., 2015; Franzosa et al., 2019; Marchesi et al., 2007), perturbations in sphingolipids metabolism (Franzosa et al., 2019; Kolho et al., 2017), and alterations in amino acids levels (Jacobs et al., 2016; Kolho et al., 2017; Marchesi et al., 2007). Our results showed a significant difference in the metabolomic profiles of UC patients with active and inactive diseases, characterized by an increase in lactosylceramide and platelet-activating factor in active UC patients. Platelet-activating factor has been described as a stool biomarker for IBD patients (Eliakim et al., 1988; Hocke et al., 1999) and lactosylceramides were also reported in inflamed colon tissues of UC patients (Bazarganipour et al., 2019) and proposed as potential biomarkers in pediatric IBD (Filimoniuk et al., 2020). Integrating the fecal microbiome and metabolome data of the biotherapy cohort demonstrated overlapping associations between IBD disease phenotypes. Gut microbiota multi-omics profiling studies is an emerging tool, which is enhancing our knowledge of the molecular changes and cellular responses during health, and disease and enabling the discovery of novel biomarkers (Metwaly and Haller, 2019a). For instance, multi-omics analysis of gut microbiota, metabolites, and host transcriptome showed a correlation between members of the *Roseburia* genus and bile acids and a number of acylcarnitines, suggesting that *Roseburia* is involved in bile acid and carnitine dysregulation in IBD (Lloyd-Price et al., 2019). In a recent multi-omics study, Mills and colleagues integrated serum proteomics and fecal 16S gene amplicon sequencing, shotgun metagenomic sequencing, metaproteomics, metabolomics, and meta-peptidomics from 40 UC patients (Mills et al., 2022). They showed a link

between the overabundance of *Bacteroides vulgatus* proteases with disease severity in UC patients. They validated these findings on a cohort of 210 samples (117 CD, 73 UC, and 20 healthy controls) and in a gnotobiotic mouse model. Colonization of the GF *Il10*$^{-/-}$ mice with microbiota obtained from UC patients, which has a high abundance of *Bacteroides vulgatus* proteases, induced colitis dependent on the protease activity (Mills et al., 2022). Albeit the association between gut microbiota, metabolites, and host pathology in IBD is emerging, the exact relationship between gut microbiota, metabolites, environmental factors, and host physiology is still hampered.

5.2 IBD gnotobiotic models for dissecting the functional role of gut microbial dysbiosis in disease pathogenesis

The gnotobiotic mouse model emerged as a valuable tool to dissect the causal relationship between gut microbiota and disease phenotype. In our work, we colonized germfree *Il10*$^{-/-}$ mice, an IBD mouse model, with microbiota obtained from two IBD patients of the biotherapy cohort collected at two time points (W14 and W52 after therapy initiation) for each patient summing up four experiments. The choice of donors for colonization experiments was dependent on their microbial composition analysis, such as reduced gut microbial diversity and bloom of dysbiotic taxa such as *Escherichia coli*. Disease phenotype in the colonized mice was assessed by the histopathological evaluation and gene expression analysis of pro-inflammatory cytokine in the cecum and colon. Microbial profile analysis of the colonized mice was performed using 16S amplicon sequencing to characterize changes in bacterial community structure. In addition, semi-quantification of the IgA-coated bacteria was done to study the impact of IgA-bound bacteria in disease phenotype in the gnotobiotic *Il10*$^{-/-}$ mouse model.

Interestingly, several studies showed that human-derived microbiota of IBD patients transferred the disease state phenotype in gnotobiotic *Il10*$^{-/-}$ mice (Metwaly et al., 2020; Nagao-Kitamoto et al., 2016), exacerbated the inflammatory phenotype in the chemically-induced colitis mouse model (Du et al., 2015; Natividad et al., 2015), and an adoptive T cell transfer mouse model (Britton et al., 2019). However, our results showed that the transfer of CD patients donors' disease activity phenotype was not fully reproduced (50%) in the *Il10*$^{-/-}$ recipient mice. CD patient-1 showed a successful transfer of disease phenotypes after gut microbial colonization on the

recipient mice in both experiments (W14 and W52). However, CD patient-2 did not recapitulate disease activity in the *Il10*$^{-/-}$ recipient mice for both experiments. Interestingly, inflamed *Il10*$^{-/-}$ mice were enriched in some pathobiont, such as *Escherichia coli* and *Enterococcus*. These data suggest that the disease initiation in this model depends on the colonization of specific taxa that is capable to induce the disease in the absence of IL-10, and it is independent of the donor disease state. However, we have only performed four experiments obtained from two CD donors, and more experiments are needed to confirm these observations. Noteworthy, most of the humanized gnotobiotic experiments were criticized for the small number of donors used that does not capture the high inter-individual variation of the human gut microbiota composition, the lack of healthy donor negative control, lack of rigor in statistical analysis "pseudo-replication", no complete reporting on the description of the dysbiosis in donors and recipients mice, and the absence of the colonization efficiency details of donors and recipients (Walter et al., 2020). The unsuccessful transfer of disease activity phenotype of the donor to its recipient mice could be argued to the species differences between the donor and recipients, or the complex components in the FMT, which does not only contain bacteria. From a microbiological perspective, a substantial proportion of human taxa fails to colonize mice gut (Wos-Oxley et al., 2012; Zhang et al., 2017), and the colonized bacteria did not fully recapitulate their abundance levels compared to the donor gut microbiota (Metwaly et al., 2020; Staley et al., 2017). Remarkably, studies of microbial pathogenicity such as *Salmonella enterica serovar Typhi*, *Campylobacter jejuni*, *Shigella species*, *Treponema pallidum*, *Vibrio cholera*, *Clostridium difficile*, and *Helicobacter pylori*, well-established disease-causing bacteria in humans, have shown the challenges of efficient colonization and causing human-similar disease phenotype in conventional mouse models (Walter et al., 2020). Besides, some environmental factors such as lifestyle, diet, human genotype, and the disease phenotype, which caused or influenced the microbial dysbiosis in human donors, are absent in the recipient mice (Arrieta et al., 2016), suggesting a lower probability of replicating the disease-associated alterations. Additionally, the colonized bacterial taxa in recipient hosts may not engage in the same evolutionarily established host-microbe interactions with their native donor (Douglas, 2018). Our analysis of the colonization efficiency of the transferred gut microbial taxa of donors to the recipients' mice was 33-56% on the zOTUs level. However, other studies

revealed 50-90% colonization efficiency at the genus level (Turnbaugh et al., 2009). The lower colonization efficiency from human donors to the recipient mice can also be attributed to technical reasons during sample handling, such as delay in adding glycerol to the stool samples and inappropriate storage conditions, including cold chain. Aside from the bacterial component in FMT, it also contains viruses and fungi that were reported to show community alteration in IBD patients (Lam et al., 2019; Sokol et al., 2017; Zuo et al., 2019). In sum, using human-derived microbiota in gnotobiotic models is a promising technology to decipher several disease pathogenicity, however stringent experimental design is required (a large number of donors including healthy human donors, concrete analysis of microbial dysbiosis in human and recipient animals, assessing the microbial transfer efficiency and robust statistical analysis) and careful interpretation of the results is of paramount importance, considering the different ecological, biological and environmental dissimilarities between donors and recipients.

Our results showed higher levels of IgA-coated bacteria in *Il10*$^{-/-}$ mice compared to their WT counterparts in all experiments and a higher percentage of IgA-bounded bacteria in mice colonized with microbiota obtained from CD patient-2. Interestingly, the correlation analysis between the gut microbiota abundance and the percentage of IgA-coated bacteria revealed a negative association between the levels of *Bacteroidetes* and *Akkermansia* and lower IgA-bound bacteria. However, there was a positive correlation between the higher abundance of unknown *Enterobacteriaceae*, *Enterococcus*, and *Morganella* and a higher level of IgA-coated bacteria. Although correlation analysis does not infer causation, it shed some light on potential associations of immune-specific host factors to distinct bacterial communities. IBD patients showed higher IgA-coated *Escherichia coli* (Viladomiu et al., 2017) using the IgA-seq technology. IgA-seq technology combines flow cytometry for the IgA-positive community with high-throughput sequencing technology of the microbial community. More recently, IgA-seq was used to study the IgA-bound bacteria in a large IBD cohort, and it revealed associations with disease and treatment (Shapiro et al., 2021). They reported forty-three bacterial taxa that showed significantly higher IgA-bound bacteria in IBD patients than the control group (Shapiro et al., 2021). In brief, the analysis of IgA-coated gut microbiota has the potential to reveal important insights into host-microbe interactions with a potential application to be used as biomarkers for IBD patients.

6 Conclusion and perspectives

In summary, we characterized the longitudinal gut microbial and metabolomic changes over one year for IBD patients undergoing biological therapy. In addition, functional validation of the role of gut microbiota in inducing disease phenotype was assessed in an IBD gnotobiotic mouse model. Our data showed strong intra-individual gut microbial signatures throughout the study duration. Gut microbial composition was significantly different between CD and UC patients. Interestingly, mucosa-associated microbiota showed a significant difference between CD with ileal and colonic involvement. Although the overall gut microbial profiles— evaluated by the alpha and beta diversity measures— did not separate IBD patients based on their disease activity, there was an expansion of selective pathobionts in IBD patients with active disease. Untargeted metabolomics analysis revealed a significant difference in the metabolomic profile of CD and UC patients as well as between active and inactive UC patients. Colonization of the germfree *Il10*$^{-/-}$ mice with gut microbiota obtained from CD patients did not fully replicate the disease activity phenotype of the donors. Nevertheless, expansion of some pathobiont, such as *Escherichia coli* and *Enterococcus,* was observed in the inflamed *Il10*$^{-/-}$ mice. This could be explained by the lower colonization efficiency of the transferred gut microbial components of human donors to recipients' mice.

As IBD is a multifactorial disease, future cohort studies should focus on longitudinal studies and adopt a multi-disciplinary approach connecting host genetics, immune phenotype, epithelial cell status, and deep gut microbial functional assessment. This approach would enhance a better stratification of different IBD phenotypes and embrace a personalized medicine approach. Although the vast gained knowledge of the gut microbial compositional dysbiosis in IBD patients, future studies should focus on dissecting the role of gut microbial functions in IBD pathogenesis. It could be achieved by conducting multi-omics analyses to detect metabolic, proteomic, and transcriptional alterations in IBD patients. Moreover, performing longitudinal studies, ideally cohorts with early-onset IBD, is required in future studies to disentangle the microbe-host interactions at the individual level and isolate and culture bacteria to study the causal effect of microbiota in disease pathogenesis. Finally, findings from the gut microbiota-related differences

in IBD patients have an enormous potential to be implemented in clinical applications in diagnostics and IBD treatment.

Addendum

Supplementary figures

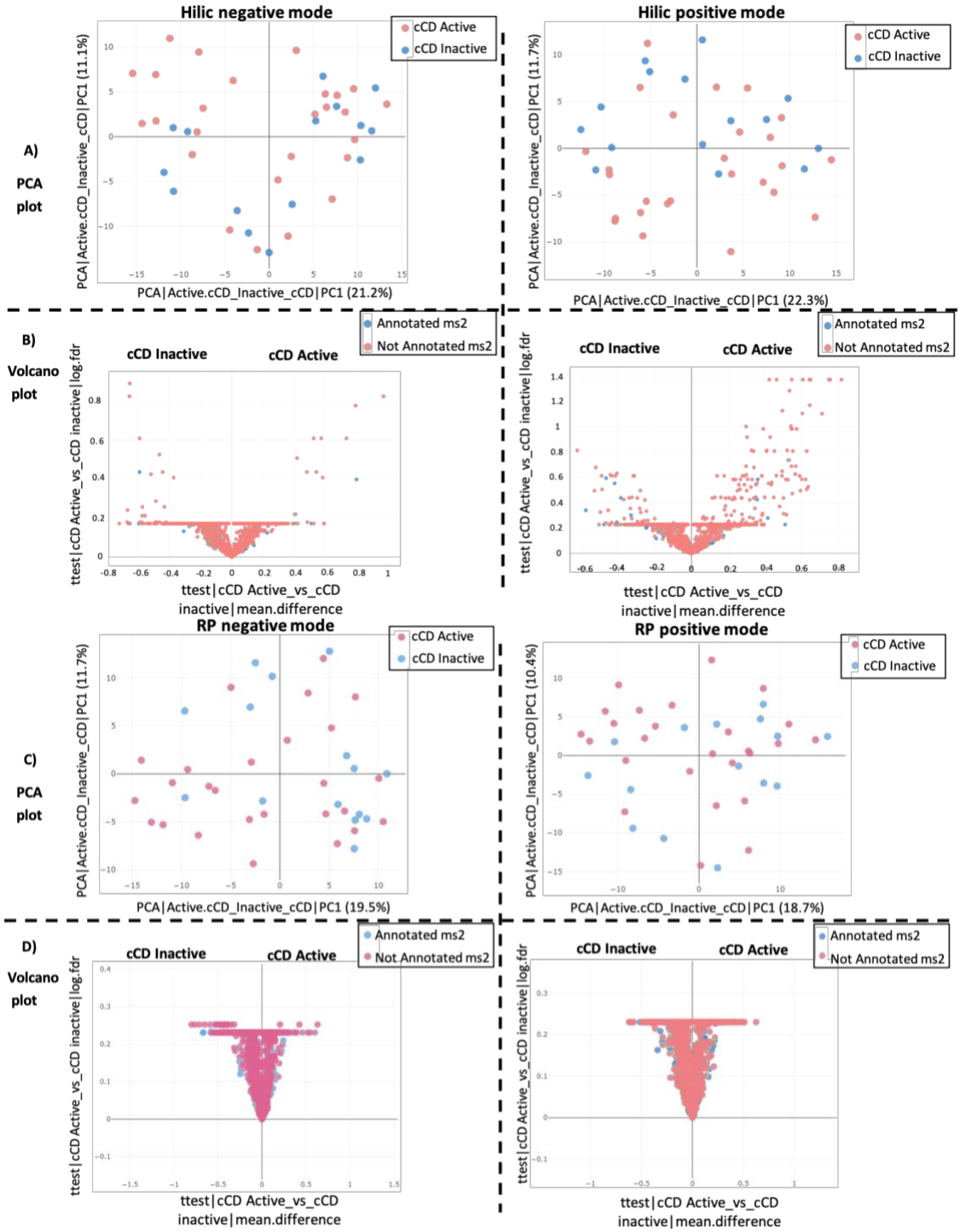

S1 Metabolomic profiles of active and inactive cCD patients

*Principal component analysis (PCA) shows the variation between active and inactive cCD patients in the four measurement modes (**A:** Hilic negative & Hilic positive **& C:** RP negative & RP positive). Volcano plots highlight the key differentiating metabolites between active and inactive cCD patients in the four different measurements (**B:** Hilic negative & Hilic positive **& D:** RP negative & RP positive).*

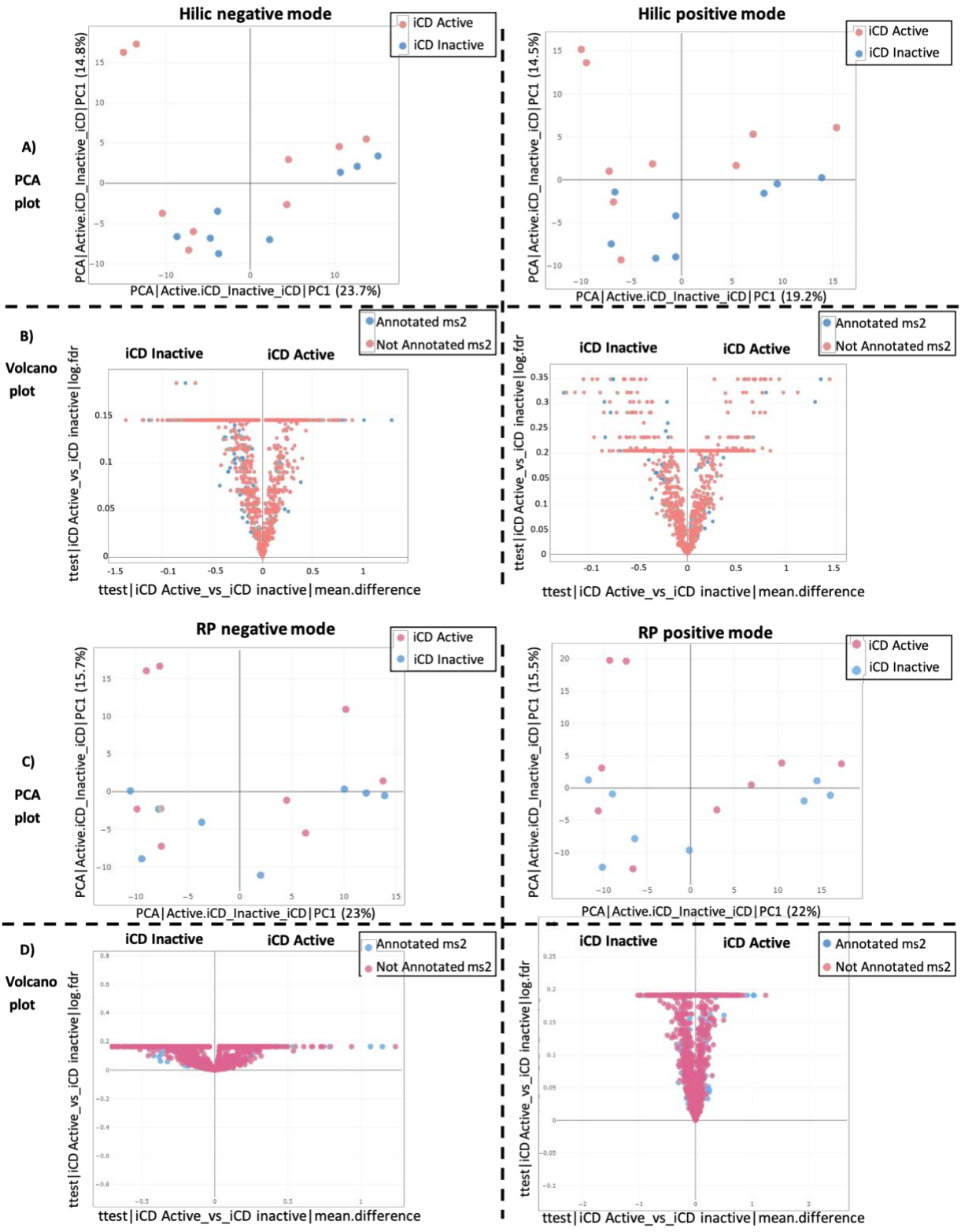

S2 Metabolomic profiles of active and inactive iCD patients

*Principal component analysis (PCA) shows the variation between active and inactive iCD patients in the four measurement modes (**A**). Volcano plots highlighting the key differentiating metabolites between active and inactive iCD patients in the four different measurements (**B**).*

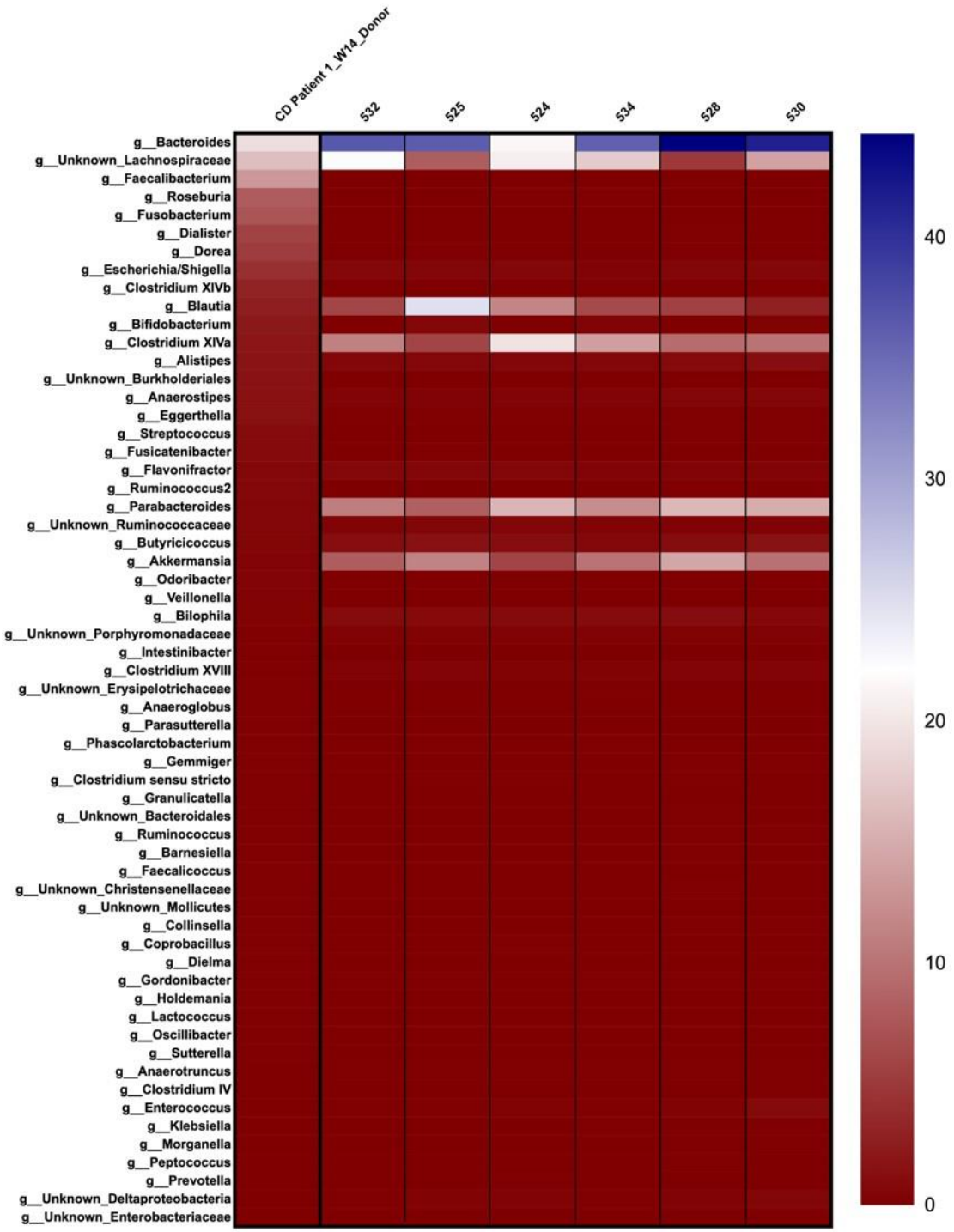

S3 Heatmap shows the relative abundance of all genera in CD patient-1 donor (W14) and the GF recipient WT mice

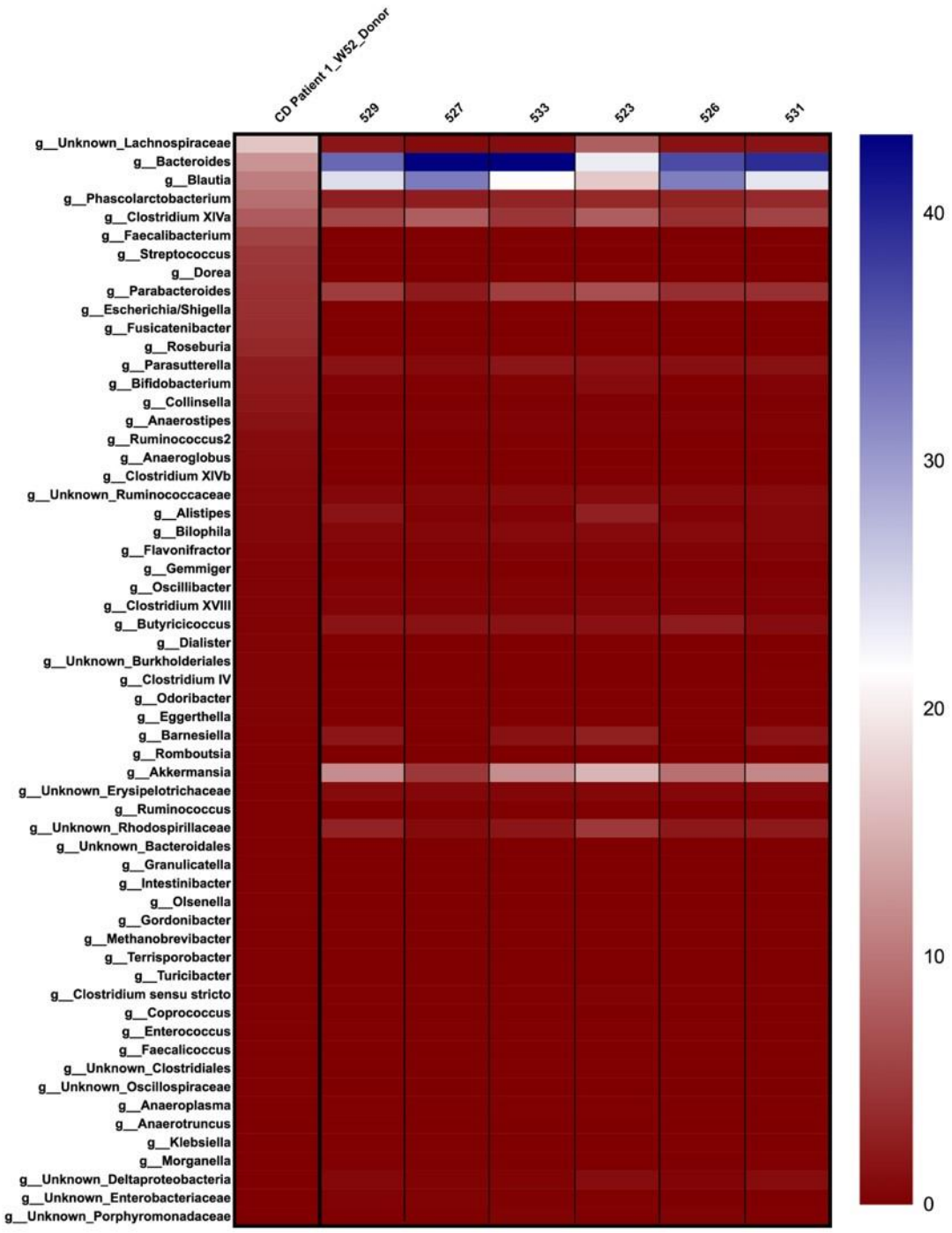

S4 Heatmap shows the relative abundance of all genera in CD patient-1 donor (W52) and the GF recipient WT mice

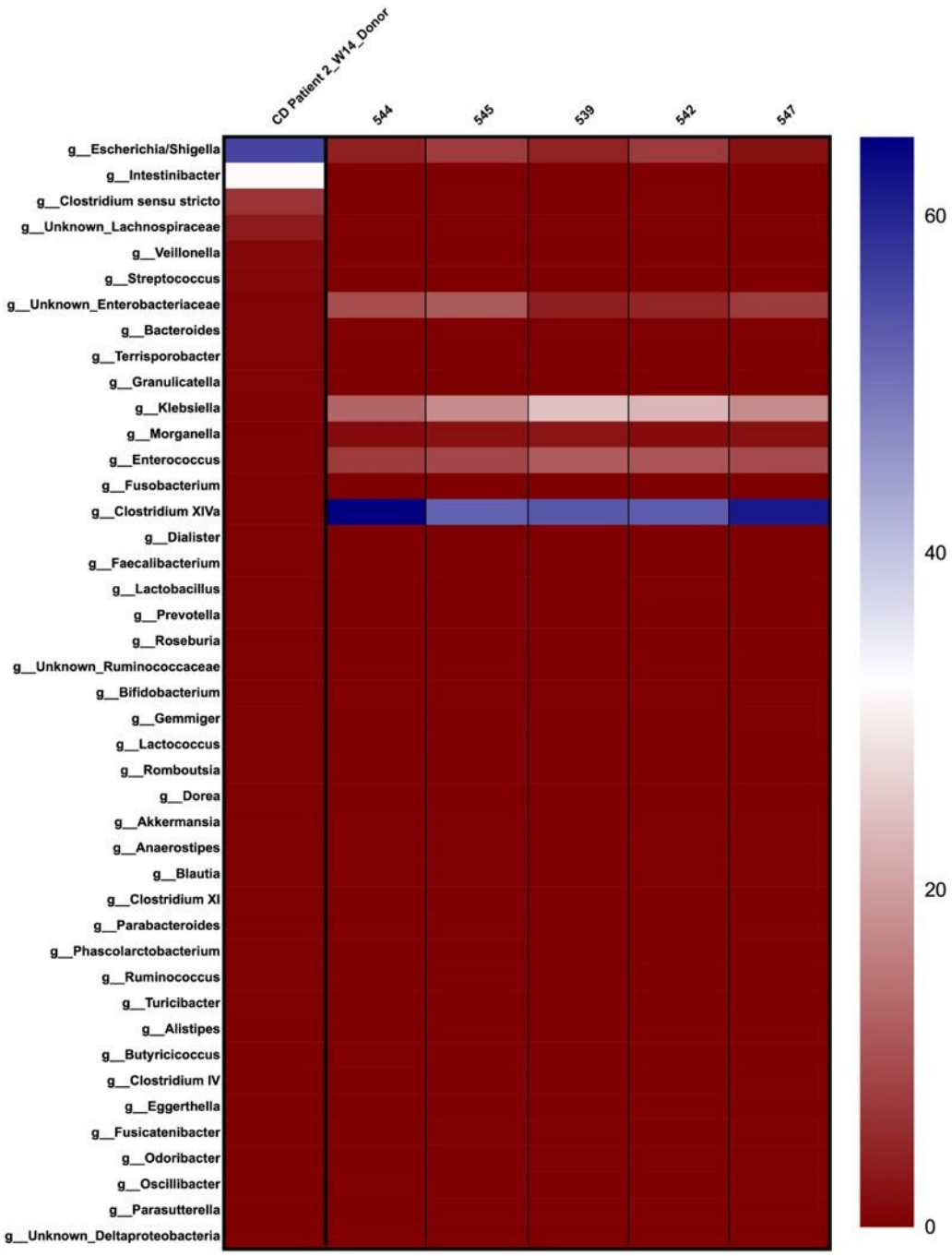

S5 Heatmap shows the relative abundance of all genera in CD patient-2 donor (W14) and the GF recipient WT mice

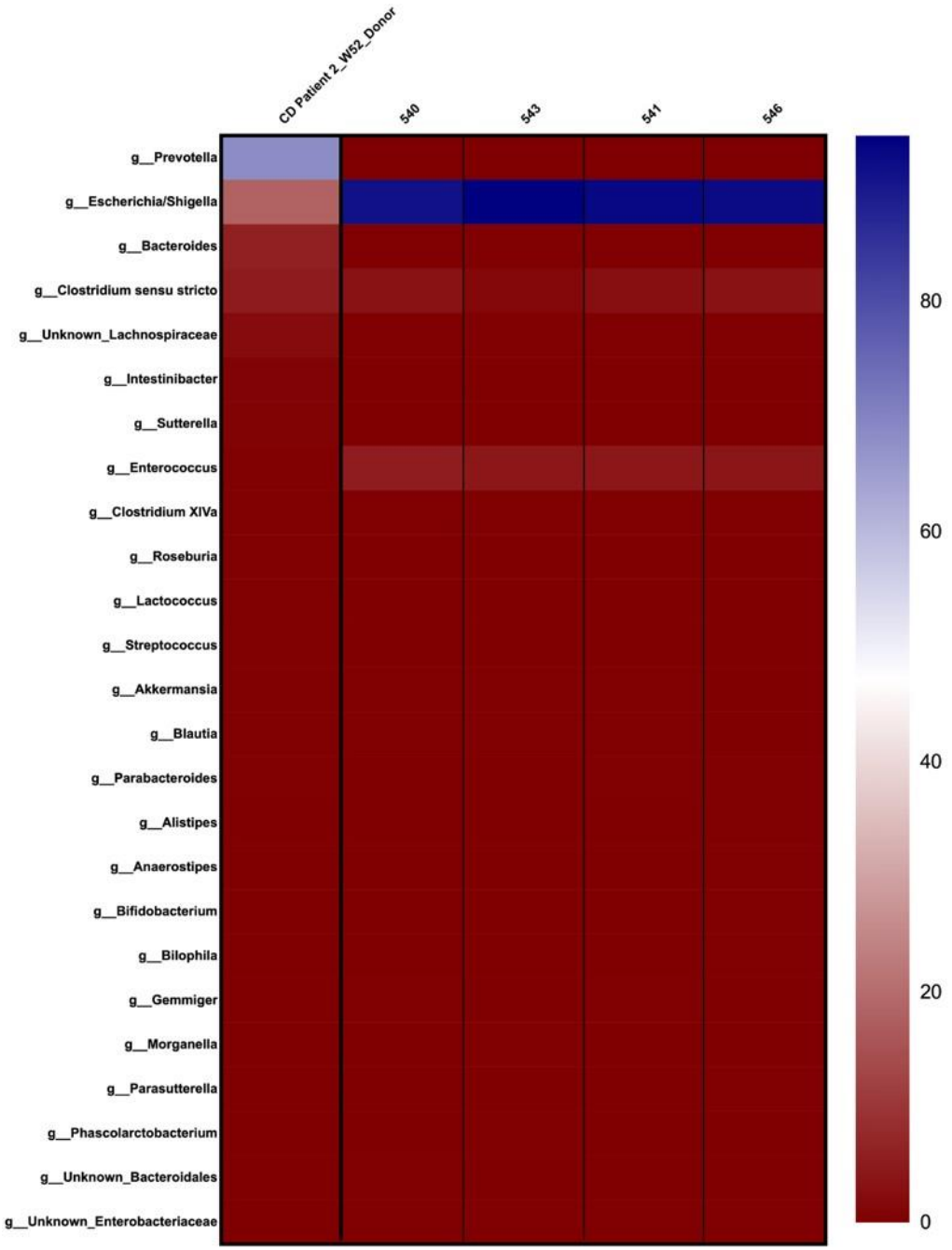

S6 Heatmap shows the relative abundance of all genera in CD patient-2 donor (W52) and the GF recipient WT mice

Supplementary tables

Table S1 Stool sample distribution for the different IBD phenotypes of the biotherapy cohort during various time points and disease activity

	CD (n = 67)*	UC (n = 65)*	pouchitis (n =10)*
W0_Active disease	27	24	3
W0_Inactive disease	0	0	0
W14_Active disease	12	14	2
W14_Inactive disease	10	10	1
W14_missing data for disease activity	3	1	1
W52_Active disease	3	4	3
W52_Inactive disease	12	12	0
W52_ missing data for disease activity	0	0	0

*The total number of collected samples for all timepoints (W0, W14, and W52)

Table S2 Mucosa-associated sample distribution for the different IBD phenotypes of the biotherapy cohort during various time points and the endoscopic disease activity status

	CD (n = 82)*	UC (n = 72)*	pouchitis (n =13)*
W0_Active disease	32	26	5
W0_Inactive disease	0	0	0
W14_Active disease	13	24	5
W14_Inactive disease	11	1	0
W14_missing data for disease activity	0	1	0
W52_Active disease	12	14	3
W52_Inactive disease	13	5	0
W52_ missing data for disease activity	1	1	0

*The total number of collected samples for all timepoints (W0, W14, and W52)

Table S3 The differentiated metabolites of CD and UC patients in the four measurement modes

Annotated metabolites	Mean difference	Log FDR	Disease phenotype	Mode	Detected at MS2	Standard match	Notes
MLS001332469-01!D-Sphingosine123-78-4;C18_Sphingosine;STD_OI	0.5	2.8	CD	Hilic positive	yes		
MLS001332469-01!D-Sphingosine123-78-4;C18_Sphingosine;Elaidi	0.4	3.5			yes		
STD_D,L-Glutamine;Ureidoisobutyric acid;D-Glutamine	-0.3	2.1	UC		not perfect match	RT does not match	
STD_Me-Stearate;Nonadecanoic acid;Pristanic acid	-0.3	1.7			yes	yes, but RT in Database missing	
N-Heptanoylglycine;3-(2-amino-2-oxoethyl)-5-methyl-hexanoic	-0.6	2.4			no match		
4-Acetyl-2(3H)-benzoxazolone;5-hydroxy-1H-indole-3-carboxyli	-1.2	7.2			yes, but no perfect match		

N-acetyl-5-aminosalicylic acid;Salicyluric acid;Dopaquinone	-1.5	7.0			yes		
Glyceraldehyde;L-Lactic acid;Hydroxypropionic acid	0.6	3.5	CD	Hilic negat ive	yes	no	
(Z)-3-Hydroxyoctadec-7-enoic acid (NMR);FA 18:1+1O;FA 18:1+1	0.6	3.1			yes	no	fatty acids
hyodeoxycholic acid;ursodeoxycholic acid;deoxycholic acid	0.6	3.2			yes, but only one fragment		bile acids
FA 18:1+3O;9,12,13-TriHOME;9,10,13-TriHOME	0.5	2.5			yes	no	fatty acids
Methyl acetate;STD_Propionic acid ;Lactaldehyde	0.5	3.2			yes	no	
3-Methoxytyrosine;Methyldopa;3-O-Methyl-a-methyldopa	0.5	2.0			no, Datenbank hit		
3-hydroxyhexadecanoic acid;3-Hydroxyhexadecanoic acid (NMR)	0.5	2.9			yes, only one fragment		fatty acids
11-Eicosenoic acid;11Z-Eicosenoic acid;Ethyl oleate	0.4	2.1			yes, only one fragment		fatty acids
NCGC00384883-01!(2S,3R,4S,5S,6R)-2-[(2R,3R,4S,5S,6R)-4,5-dih	0.4	1.7			not perfect match		
Cysteinyl-Hydroxyproline;Hydroxyprolyl-Cysteine;2-Amino-3-me	0.4	1.8			no		
Nervonic acid;Nervonic acid;(E)-2-Tetracosenoic acid	0.4	1.8			yes, only one fragment		fatty acids
LITHOCHOL-11-ENIC ACID;NCGC00380376-01_C22H40O3_1-Naphthalen	0.3	2.3			yes, only one fragment		bile acids
STD_Taurin	0.3	2.2			yes, but no RT match		
2-Benzothiazolesulfonic acid	-0.3	1.6	UC		yes	no	
Escitalopram;Citalopram;Citalopram	-0.4	1.8			no		
3-Hydroxypyridine;2-Hydroxypyridine;1H-Pyrrole-2-carboxaldeh	-0.6	4.2			yes, only one fragment		
Nicotinic acid;Picolinic acid;2-Hydroxy-4-imino-2,5-cyclohex	-0.8	6.9			yes, only one fragment		
Hydroquinone;Pyrocatechol;(E,E)-2,4-Hexadienedial	-0.8	6.7			yes, but more possibilities		
Salicylamide;Trigonelline;2-Aminobenzoic acid	-0.8	5.4			yes, but not perfect		
Gentisic acid;Protocatechuic acid;2-Pyrocatechuic acid	-0.9	4.9			yes, but more possibilities		
Mevalonic Acid Lactone;4-Acetylbutyrate;p-Hydroxyphenylaceti	-1.0	9.6			yes, but more possibilities		
DIBOA;2-Methyl-3-hydroxy-5-formylpyridine-4-carboxylate;2,4-	-1.1	5.0			yes, but more possibilities		
Dehydrovariabilin;Fenofibric acid;5,7-Dimethoxyisoflavone	-1.2	6.9			yes, but not clear		
4-Aminophenol;2-Acetylpyrrole;1-Methyl-2-pyrrolecarboxaldehy	-1.4	6.9			yes, but not perfect		
3-Hydroxyanthranilic acid;3-Aminosalicylic acid;Aminosalicyl	-1.5	7.3			yes		
Acetaminophen;2-Phenylglycine;Dopamine quinone	-1.6	7.4			yes		
N-acetyl-5-aminosalicylic acid;Salicyluric acid;Dopaquinone	-1.7	6.9			yes		
Sphinganine;Dihydrosphingosine;Linoleoyl ethanolamide	0.4	1.5	CD	RP positi ve	yes		
Hypaconitine;Hypaconitine;Hematoporphyrin IX	0.4	1.5			not a good match		
C18_Sphingosine;MLS001332469-01!D-Sphingosine123-78-4;Elaidi	0.3	1.7			yes, but not perfect		
MG(0:0/16:1(9Z)/0:0);MG(16:1(9Z)/0:0/0:0);Avocadene 1-acetat	0.3	1.7			not a good match		
Karakoline;MLS002153956-01!Karakoline39089-30-0;Karakoline	-0.4	1.8	UC		yes, but not perfect		
MG(0:0/16:1(9Z)/0:0);MG(16:1(9Z)/0:0/0:0);Avocadene 1-acetat	-0.4	1.6			not a good match		
Arbutin;Echothiophate;Arbutin	-0.4	1.6			yes, olny one fragment		
Pesticide7_Fenpropimorph_C20H33NO_Morpholine, 4-[3-[4-(1,1-d	-0.4	2.2			only one fragment --Oleamide?		
Pipecolic acid;L-Pipecolic acid;N4-Acetylaminobutanal	-0.5	1.7			no gut match		
DIBOA;L-2-Amino-4-methylenepentanedioic acid;L-trans-alpha-A	-0.6	5.8			yes	no	
Mesalazine;Aminosalicylic Acid;3-Hydroxyanthranilic acid	-1.2	3.8			yes	yes, but RT does not match	
2-Benzoxazolol	-1.3	6.5			yes	no	
4-Acetyl-2(3H)-benzoxazolone;5-hydroxy-1H-indole-3-carboxyli	-1.5	9.3			not a good match		

STD_Palmitoleic acid ;Palmitelaidic acid;Palmitoleic acid	0.3	1.5	**CD**	**RP negative**	y	y	
N-Methyltyrosine;L-beta-Homotyrosine;L-beta-homotyrosine-HCl	0.3	2.7			y, but not nice spectra	no	Medication
1,7-Dimethyluric acid;1,9-Dimethyluric acid;1,3-Dimethyluric	-0.6	3.2	**UC**		y	not in database	Caffeine marker
DIBOA;2-Methyl-3-hydroxy-5-formylpyridine-4-carboxylate;2,4-	-0.8	4.2			y, but weak annotation	no	whole grain biomarker
Acetaminophen;2-Phenylglycine;Dopamine quinone	-1.5	8.2			y	not in database	Painkiller Treatment?
N-acetyl-5-aminosalicylic acid;Salicyluric acid;Dopaquinone	-1.5	8.2			y	not in database	Mesalazine Drug used in IBD
3-Hydroxyanthranilic acid;Mesalazine;3-Aminosalicylic acid	-1.6	6.2			y	not in database	0

Table S4 The differentiated metabolites of active and inactive UC patients in the four measurement modes

Annotated metabolites	Mean difference	Log FDR	Disease activity phenotype	Mode	Detected at MS2	Standard match	Notes
2-acetyl-1-alkyl-sn-glycero-3-phosphocholine;PAF (Platelet A	0.9	3.5	**Active_UC**	**Hilic positive**	yes		Platelet-activating factor
LysoPhosphatidylcholine_16_0;LPC 16:0;Docosa-4,7,10,13,16-pe	0.7	1.9			yes		
LPC 18:2;LysoPC(18:2(9Z,12Z));2-linoleoyl-sn-glycero-3-phosp	0.6	2.8			yes, but not pferfect		
Lactosylceramide (d18:1/16:0);C16 Lactosyl Ceramide (d18:1/1	0.5	3.2			yes		lactosylceramide
SphingomyelinSM_d18_0_18_1_9Z;SphingomyelinSM_d18_0_18_1_9Z;	0.4	2.3			yes, but not perfect		
STD_Lithocholenic acid;STD_Dehydrolithocholic acid;NCGC00380	-0.5	2.3	**Inactive_UC**		yes	yes, but based on RT it can be Lithocholenic acid or Dehydrolithocholic acid	
STD_5β-Cholic acid-3α-ol-7-one (7-KLCA);STD_5β-Cholic acid-3	-0.6	1.8			yes	yes, bile acids, but more possibilities	
STD_Chenodeoxycholic acid;STD_Deoxycholic acid;STD_Isodeoxyc	-0.8	3.3			yes	yes, bile acids, but more possibilities	
STD_5β-Cholic acid-3α-ol-7-one (7-KLCA);STD_5β-Cholic acid-3	-0.9	3.5			yes	yes, bile acids, but more possibilities	
STD_Lactic acid;Glyceraldehyde;Glyceraldehyde	0.7	1.9	**Active_UC**	**Hilic negative**	yes	yes	
STD_Isolithocholic acid;STD_Allolithocholic acid;STD_Lithoch	-1.0	2.8	**Inactive_UC**				
Arachidonic acid;STD_Oleic acid;Cis-8,11,14,17-Eicosatetraen	0.7	2.0	**UC_Active**	**RP negative**	yes		
Mammeigin;osajin;NCGC00385004-01!5-hydroxy-8,8-dimethyl-6-(2	0.4	1.5			yes, but no hit		
hyodeoxycholic acid;ursodeoxycholic acid;deoxycholic acid	-0.5	2.1	**UC_Inactive**		bile acid		
5-Hydroxyindoleacetic acid;(2-oxo-2,3-dihydro-1H-indol-3-yl)	-0.7	1.8			yes	no	IAA, ICA ??

lithocholic acid;Lithocholic acid;Allolithocholic acid	-0.9	2.6			bile acids		
ursodeoxycholic acid;chenodeoxycholic acid;deoxycholic acid	-0.7	1.6	**UC_inactive**	**RP positive**	yes	but more possiblities, based on RT STD_Chenodeoxycholic acid best match	
ursodeoxycholic acid;Chenodeoxycholic acid;Deoxycholic acid	-0.7	1.6			yes	but more possiblities, based on RT STD_Chenodeoxycholic acid best match	
CUDA* (internal standard);Melophlin B/C/L/N/O	-0.5	1.6			not a good match		
Tetracosapentaenoic acid (24:5n-6);Tetracosapentaenoic acid	-0.9	2.0			not a good match		

Table S5 The key differentiating metabolites of the supervised multi-omics analysis that separated the response-to-therapy of IBD patients from baseline samples

ID	annotated_ms1	annotated_ms2
hilicPos_ID766	1,6-Dimethoxypyrene;Hydroxyprolyl-Methionine;Methionyl-Hydro	NA
hilicPos_ID802	NA	NA
hilicPos_ID869	NA	NA
hilicPos_ID899	monolinolein;MG(0:0/18:2(9Z,12Z)/0:0);MG(18:2(9Z,12Z)/0:0/0:	+
hilicPos_ID1491	NCGC00160302-01!BELLADONNINE;NCGC00160302-01!BELLADONNINE;NC	NA
hilicNeg_ID797	Polyoxyethylene 40 monostearate;2(R)-hydroxyicosanoic acid;1	NA
hilicNeg_ID922	lithocholic acid;Lithocholic acid;Allolithocholic acid	+
hilicNeg_ID1093	NA	NA
hilicNeg_ID1729	PC(15:0/16:1(9Z));PC(16:1(9Z)/15:0);PE(14:0/20:1(11Z))	NA
hilicNeg_ID1875	1,2-Di-O-palmitoyl-3-O-(6-sulfoquinovopyranosyl)glycerol	NA
rpPos_ID109	Hydrogen phosphate;Acetic acid;Glycolaldehyde	NA
rpPos_ID187	NA	NA
rpPos_ID838	3-Methylcyclopentadecanone;(Â±)-2-Dodecylcyclobutanone;Hexade	NA
rpPos_ID1000	Palmitic acid;Trimethyltridecanoic acid;Isopalmitic acid	NA
rpPos_ID1537	NA	NA
rpPos_ID1731	NCGC00186665-03!2,3-dihydroxypropyl hexadecanoate;NCGC001866	+
rpPos_ID1950	MG(0:0/16:0/0:0);MG(16:0/0:0/0:0);MG(i-16:0/0:0/0:0)	NA
rpPos_ID1971	Isopropamide;Leukotriene B4;5(S)-Hydroperoxyeicosatetraenoic	NA
rpPos_ID2466	Pentadecanoylcarnitine;12-Ketodeoxycholic acid;7-Hydroxy-3-o	NA
rpPos_ID3631	NCGC00380672-01!2-[3-(6-acetyloxy-2-hydroxy-6-methyl-3-oxohe	NA
rpNeg_ID480	Pesticide3_Fluometuron_C10H11F3N2O_Urea, N,N-dimethyl-N'-[3-	NA

rpNeg_ID1412	MMV020321;Trehalose-6-Phosphate;7-chloro-2-(3,4-dimethoxyphe	+

Table S6 The main differentiating metabolites of the supervised multi-omics analysis for all IBD patients' samples based on their disease activity

ID	annotated_ms1	annotated_ms2
hilicPos_ID1870	PA(15:0/22:1(13Z));PA(22:1(13Z)/15:0);PC(16:0/16:0)	NA
hilicPos_ID1871	PC(15:0/16:1(9Z));PC(16:1(9Z)/15:0);PE(14:0/20:1(11Z))	NA
hilicPos_ID1878	PC(16:0/P-18:1(11Z));PC(16:0/P-18:1(9Z));PC(16:1(9Z)/P-18:0)	NA
hilicPos_ID1881	PE(18:1(11Z)/P-18:1(11Z));PE(18:1(11Z)/P-18:1(9Z));PE(18:1(9	NA
hilicPos_ID1883	DG(11D3/11D5/0:0);DG(11D5/11D3/0:0);DG(11D5/9D5/0:0)	NA
hilicPos_ID1888	PC(15:0/P-18:1(11Z));PC(15:0/P-18:1(9Z));PE(18:0/P-18:1(11Z)	NA
hilicPos_ID1912	PC(14:0/20:1(11Z));PC(14:1(9Z)/20:0);PC(16:0/18:1(11Z))	NA
hilicPos_ID1919	PC(15:0/18:2(9Z,12Z));PC(18:2(9Z,12Z)/15:0);PE(14:0/22:2(13Z	NA
hilicPos_ID1924	PA(15:0/24:1(15Z));PA(24:1(15Z)/15:0);PC(14:0/20:0)	NA
hilicPos_ID1936	PC(o-16:0/18:0);Phosphatidylcholine alkyl 18;PC(18:1(11Z)/P-	NA
hilicPos_ID1939	PC(18:0/P-18:1(11Z));PC(18:0/P-18:1(9Z));PC(18:1(11Z)/P-18:0	NA
hilicPos_ID1942	PE(20:1(11Z)/P-18:1(11Z));PE(20:1(11Z)/P-18:1(9Z));PE(20:2(1	NA
hilicPos_ID1944	DG(11D3/13D5/0:0);DG(11D5/11D5/0:0);DG(11M5/13M5/0:0)	NA
hilicPos_ID1976	PC(14:0/22:1(13Z));PC(14:1(9Z)/22:0);PC(16:0/20:1(11Z))	NA
hilicPos_ID1980	PC(15:0/20:2(11Z,14Z));PC(20:2(11Z,14Z)/15:0);PE(14:1(9Z)/24	NA
hilicPos_ID1983	NA	NA
hilicPos_ID1997	TG(16:1(9Z)/14:0/16:1(9Z));TG(14:0/14:0/18:2(9Z,12Z));TG(14:	NA
hilicPos_ID2000	PC(o-16:0/20:0);PC(o-18:0/18:0);PC(20:1(11Z)/P-18:1(11Z))	NA
hilicPos_ID2003	PC(20:0/P-18:1(11Z));PC(20:0/P-18:1(9Z));PC(20:1(11Z)/P-18:0	NA
hilicPos_ID2028	PE(24:1(15Z)/P-18:1(11Z));PE(24:1(15Z)/P-18:1(9Z));PE(P-18:1	NA
hilicPos_ID2035	SM(d18:1/24:1(15Z));Sphingomyelin d18	NA
hilicPos_ID2040	TG(14:0/14:0/20:5(5Z,8Z,11Z,14Z,17Z));TG(14:0/14:1(9Z)/20:4(	NA
hilicPos_ID2058	PC(o-16:0/22:0);PC(o-18:0/20:0);PC(22:1(13Z)/P-18:1(11Z))	NA
hilicPos_ID2071	PG(18:0/22:4(7Z,10Z,13Z,16Z));PS(16:1(9Z)/24:1(15Z));PS(18:0	NA
hilicPos_ID2078	NA	NA
hilicPos_ID2092	Lactosylceramide (d18:1/16:0);C16 Lactosyl Ceramide (d18:1/1	+
hilicNeg_ID1990	Galabiosylceramide (d18:1/16:0);Lactosylceramide (d18:1/16:0	NA
hilicNeg_ID1991	NA	NA
hilicNeg_ID1993	3-O-Sulfogalactosylceramide (d18:1/22:0)	NA
hilicNeg_ID1995	All trans decaprenyl diphosphate	NA
hilicNeg_ID2075	Galabiosylceramide (d18:1/24:1(15Z));Lactosylceramide (d18:1	NA

Table S7 The key differentiating metabolites of the supervised multi-omics analysis for all IBD patients' samples based on their disease phenotype

ID	annotated_ms1	annotated_ms2
hilicPos_ID328	4-Acetyl-2(3H)-benzoxazolone;5-hydroxy-1H-indole-3-carboxyli	+

hilicPos_ID405	N-acetyl-5-aminosalicylic acid;Salicyluric acid;Dopaquinone	+
hilicPos_ID825	Clitocine	NA
hilicPos_ID1072	Benzomalvin B_120255;Benzomalvin B_120255;NCGC00384901-01_C2	NA
hilicNeg_ID91	NA	NA
hilicNeg_ID93	4-Aminophenol;2-Acetylpyrrole;1-Methyl-2-pyrrolecarboxaldehy	+
hilicNeg_ID120	Niacinamide;2-Acetylpyrazine	NA
hilicNeg_ID173	Salicylamide;Trigonelline;2-Aminobenzoic acid	+
hilicNeg_ID223	Acetaminophen;2-Phenylglycine;Dopamine quinone	+
hilicNeg_ID230	Mevalonic Acid Lactone;4-Acetylbutyrate;p-Hydroxyphenylaceti	+
hilicNeg_ID232	3-Hydroxyanthranilic acid;3-Aminosalicylic acid;Aminosalicyl	+
hilicNeg_ID236	Gentisic acid;Protocatechuic acid;2-Pyrocatechuic acid	+
hilicNeg_ID392	N-acetyl-5-aminosalicylic acid;Salicyluric acid;Dopaquinone	+
hilicNeg_ID399	N-(4-hydroxyphenyl)ethoxycarbothioamide	NA
hilicNeg_ID430	Hydroxyphenylacetylglycine;3-Carbamoyl-2-phenylpropionic aci	NA
hilicNeg_ID773	3,5,6,7-tetrahydroxy-2-(4-hydroxy-3-methoxyphenyl)-8aH-chrom	NA
rpPos_ID232	2-Benzoxazolol	+
rpPos_ID323	Mesalazine;Aminosalicylic Acid;3-Hydroxyanthranilic acid	+
rpPos_ID326	1-(2-Thienyl)-1-butanone;1-(5-Methyl-2-thienyl)-1-propanone;	NA
rpPos_ID449	4-Hydroxynonenal;2,4-Nonanedione;2-Nonenoic acid	NA
rpPos_ID559	NA	NA
rpNeg_ID42	4-Aminophenol;2-Acetylpyrrole;1-Methyl-2-pyrrolecarboxaldehy	NA
rpNeg_ID144	Acetaminophen;2-Phenylglycine;Dopamine quinone	+
rpNeg_ID160	3-Hydroxyanthranilic acid;Mesalazine;3-Aminosalicylic acid	+
rpNeg_ID306	N-acetyl-5-aminosalicylic acid;Salicyluric acid;Dopaquinone	+
rpNeg_ID382	Hydroxyphenylacetylglycine;3-Carbamoyl-2-phenylpropionic aci	NA
rpNeg_ID392	N-Methylcalystegine B2;N-lactoyl-Valine;1-hydroxyhexanoylgly	NA
rpNeg_ID1521	Bendroflumethiazide;4-Mercaptobutyl glucosinolate;3-Methylth	NA

List of figures

List of supplementary Figures

List of tables

Abbreviations

AMP	Antimicrobial peptides
ASCA	Anti-*Saccharomyces cerevisiae* antibodies
ASF	Altered Schaedler's flora
ASV	Amplicon sequence variant
ATP	Adenosine triphosphate
AUC	Area under the curve
C	Celsius (unit of temperature)
cCD	Colonic Crohn’s disease
CD	Crohn’s disease
CDEIS	Crohn's Disease Endoscopic Index of Severity
cDNA	Complementary DNA
CFU	Colony forming unity
ChgA	Chromogranin A
CRP	C-reactive protein
DAMPs	Damage-associated molecular patterns
DCs	Dendritic cells
DIABLO	Data Integration Analysis for Biomarker discovery using Latent variable approaches for Omics studies
DNA	Deoxyribonucleic acid
EEC	Enteroendocrine cells
EEN	Exclusive enteral nutrition
ER	Endoplasmic reticulum
FDR	False discovery rate
FimH	Fimbrial adhesion protein
FMT	Fecal microbial transplantation
GC	Goblet cell
GF	Germfree
GIT	Gastrointestinal tract
GWAS	Genome wide association studies
HBI	Harvey-Bradshaw Index
H&E	Hematoxylin and Eosin
HFD	High-fat diet
HILIC	Hydrophilic interaction liquid chromatography
HLA	Human leukocyte antigen
HPLC	High-performance liquid chromatography
HSCs	Hematopoietic stem cells
IAP	Intestinal alkaline phosphatase
IBD	Inflammatory Bowel Disease
IBS	Irritable bowel syndrome
iCD	Ileal Crohn’s disease
IDA	Information dependent acquisition
IECs	Intestinal epithelial cells

IFNɣ	Interferon-gamma
IgA-seq	Immunoglobulin A coated bacteria coupled with 16S rRNA-based analysis
IL	Interleukin
ILCs	Innate lymphoid cells
ISCs	Intestinal stem cells
JAK	Janus kinases
KO	Knockout “of a gene of interest”
LDA	Linear discriminant analysis
LEfSe	Linear discriminant analysis effect size
LPS	Lipopolysaccharides
MAMPs	Microbial-associated molecular patterns
M cells	Microfold cells
MDS	Multidimensional scaling
MHC	Major histocompatibility complex
MMLV	Moloney murine leukemia virus
MOFA	Multi-omics factor analysis
MNV	Murine norovirus
MS	Mass spectrometry
MSCs	Mesenchymal stem cells
m/z	Mass-charge-ratio
NEC	Necrotizing enterocolitis
NGS	Next-generation sequencing
NLR	NOD-like receptor
NMR	Nuclear magnetic resonance
NOD	Nucleotide-binding oligomerization domain
OD_{600}	Optical density of a sample measured at a wavelength of 600nm
Oligo-MM	Oligo-Mouse-Microbiota
OmpC	Outer membrane porin C
OTU	Operational taxonomic unit
PBS	Phosphate buffered saline
PC	Paneth cell
PCA	Principal Component Analysis
PCR	Polymerase Chain Reaction
PERMANOVA	permutational multivariate analysis of variances
pH	Potential of hydrogen
PICRUSt	Phylogenetic Investigation of Communities by Reconstruction of Unobserved States tool
PLS-DA	Partial Least-Squares Discriminant Analysis
Poc	Pouchitis
PRRs	Pattern recognition receptors
Q-TOF	Quadrupole Time-of-Flight Mass Spectrometry
RLRs	RIG-I-like receptors
ROC	Receiver operating curve
RP	Reverse phase

Rpm	Round per minute
rRNA	Ribosomal ribonucleic acid
RT	Retention time
SCFA	Short-chain fatty acids
SED	Semisynthetic experimental diet
SFB	Segmented filamentous bacteria
sIgA	Secretory IgA
SIHUMI	Simplified human microbiota consortium
SNP	Single-nucleotide polymorphism
SPF	Specific pathogen free
STAR	Structured Transparent Accessible Reproducible
TFF3	produce trefoil factor 3
Th	T helper cell
TJ	Tight junctions
TLR	Toll-like receptor
TNFSF15	Tumor necrosis factor superfamily-15
TNF	Tumor necrosis factor
T_{reg}	Regulatory T cell
TRUC	T-bet$^{-/-}$ RAG2$^{-/-}$
UC	Ulcerative Colitis
UCEIS	Ulcerative Colitis Endoscopic Index of Severity
UHPLC	Ultra high-performance liquid chromatography
UPR	Unfolded protein response
W	Week
WCA	Wilkins-Chalgren Anaerobe
WT	Wild type
ZO-1	Zonula occludens-1
zOTUs	Zero-radius operational taxonomic unit

References

Abdulla, M., Al Saeed, M., Fardan, R.H., Alalwan, H.F., Ali Almosawi, Z.S., Almahroos, A.F., Al Qamish, J., 2017. Inflammatory bowel disease in Bahrain: single-center experience. Clin Exp Gastroenterol 10, 133-145.

Abegunde, A.T., Muhammad, B.H., Bhatti, O., Ali, T., 2016. Environmental risk factors for inflammatory bowel diseases: Evidence based literature review. World J Gastroenterol 22, 6296-6317.

Abellan-Schneyder, I., Matchado, M.S., Reitmeier, S., Sommer, A., Sewald, Z., Baumbach, J., List, M., Neuhaus, K., 2021. Primer, Pipelines, Parameters: Issues in 16S rRNA Gene Sequencing. mSphere 6.

Adolph, T.E., Tomczak, M.F., Niederreiter, L., Ko, H.J., Bock, J., Martinez-Naves, E., Glickman, J.N., Tschurtschenthaler, M., Hartwig, J., Hosomi, S., Flak, M.B., Cusick, J.L., Kohno, K., Iwawaki, T., Billmann-Born, S., Raine, T., Bharti, R., Lucius, R., Kweon, M.N., Marciniak, S.J., Choi, A., Hagen, S.J., Schreiber, S., Rosenstiel, P., Kaser, A., Blumberg, R.S., 2013. Paneth cells as a site of origin for intestinal inflammation. Nature 503, 272-276.

Ahmed, M., Metwaly, A., Haller, D., 2021. Modeling microbe-host interaction in the pathogenesis of Crohn's disease. Int J Med Microbiol 311, 151489.

Al-Mofarreh, M.A., Al-Mofleh, I.A., 2013. Emerging inflammatory bowel disease in saudi outpatients: a report of 693 cases. Saudi J Gastroenterol 19, 16-22.

Alghamdi, A., Gerasimidis, K., Blackburn, G., Akinci, D., Edwards, C., Russell, R.K., Watson, D.G., 2018. Untargeted Metabolomics of Extracts from Faecal Samples Demonstrates Distinct Differences between Paediatric Crohn's Disease Patients and Healthy Controls but No Significant Changes Resulting from Exclusive Enteral Nutrition Treatment. Metabolites 8.

Almeida, A., Nayfach, S., Boland, M., Strozzi, F., Beracochea, M., Shi, Z.J., Pollard, K.S., Sakharova, E., Parks, D.H., Hugenholtz, P., Segata, N., Kyrpides, N.C., Finn, R.D., 2020. A unified catalog of 204,938 reference genomes from the human gut microbiome. Nat Biotechnol.

Amir, A., McDonald, D., Navas-Molina, J.A., Kopylova, E., Morton, J.T., Zech Xu, Z., Kightley, E.P., Thompson, L.R., Hyde, E.R., Gonzalez, A., Knight, R., 2017. Deblur Rapidly Resolves Single-Nucleotide Community Sequence Patterns. mSystems 2.

Ananthakrishnan, A.N., 2015. Epidemiology and risk factors for IBD. Nat Rev Gastroenterol Hepatol 12, 205-217.

Ananthakrishnan, A.N., Luo, C., Yajnik, V., Khalili, H., Garber, J.J., Stevens, B.W., Cleland, T., Xavier, R.J., 2017. Gut Microbiome Function Predicts Response to Anti-integrin Biologic Therapy in Inflammatory Bowel Diseases. Cell Host Microbe 21, 603-610 e603.

Andoh, A., Kobayashi, T., Kuzuoka, H., Tsujikawa, T., Suzuki, Y., Hirai, F., Matsui, T., Nakamura, S., Matsumoto, T., Fujiyama, Y., 2014. Characterization of gut microbiota profiles by disease activity in patients with Crohn's disease using data mining analysis of terminal restriction fragment length polymorphisms. Biomed Rep 2, 370-373.

Annunziato, F., Cosmi, L., Santarlasci, V., Maggi, L., Liotta, F., Mazzinghi, B., Parente, E., Fili, L., Ferri, S., Frosali, F., Giudici, F., Romagnani, P., Parronchi, P., Tonelli, F., Maggi, E., Romagnani, S., 2007. Phenotypic and functional features of human Th17 cells. J Exp Med 204, 1849-1861.

Argelaguet, R., Arnol, D., Bredikhin, D., Deloro, Y., Velten, B., Marioni, J.C., Stegle, O., 2020. MOFA+: a statistical framework for comprehensive integration of multi-modal single-cell data. Genome Biol 21, 111.

Argelaguet, R., Velten, B., Arnol, D., Dietrich, S., Zenz, T., Marioni, J.C., Buettner, F., Huber, W., Stegle, O., 2018. Multi-Omics Factor Analysis-a framework for unsupervised integration of multi-omics data sets. Mol Syst Biol 14, e8124.

Arrieta, M.C., Walter, J., Finlay, B.B., 2016. Human Microbiota-Associated Mice: A Model with Challenges. Cell Host Microbe 19, 575-578.

Aschard, H., Laville, V., Tchetgen, E.T., Knights, D., Imhann, F., Seksik, P., Zaitlen, N., Silverberg, M.S., Cosnes, J., Weersma, R.K., Xavier, R., Beaugerie, L., Skurnik, D., Sokol, H., 2019. Genetic effects on the commensal microbiota in inflammatory bowel disease patients. PLoS Genet 15, e1008018.

Assimakopoulos, S.F., Papageorgiou, I., Charonis, A., 2011. Enterocytes' tight junctions: From molecules to diseases. World J Gastrointest Pathophysiol 2, 123-137.

Atarashi, K., Suda, W., Luo, C., Kawaguchi, T., Motoo, I., Narushima, S., Kiguchi, Y., Yasuma, K., Watanabe, E., Tanoue, T., Thaiss, C.A., Sato, M., Toyooka, K., Said, H.S., Yamagami, H., Rice, S.A., Gevers, D., Johnson, R.C., Segre, J.A., Chen, K., Kolls, J.K., Elinav, E., Morita, H., Xavier, R.J., Hattori, M., Honda, K., 2017. Ectopic colonization of oral bacteria in the intestine drives TH1 cell induction and inflammation. Science 358, 359-365.

Atarashi, K., Tanoue, T., Ando, M., Kamada, N., Nagano, Y., Narushima, S., Suda, W., Imaoka, A., Setoyama, H., Nagamori, T., Ishikawa, E., Shima, T., Hara, T., Kado, S., Jinnohara, T., Ohno, H., Kondo, T., Toyooka, K., Watanabe, E., Yokoyama, S., Tokoro, S., Mori, H., Noguchi, Y., Morita, H., Ivanov, II, Sugiyama, T., Nunez, G., Camp, J.G., Hattori, M., Umesaki, Y., Honda, K., 2015. Th17 Cell Induction by Adhesion of Microbes to Intestinal Epithelial Cells. Cell 163, 367-380.

Atarashi, K., Tanoue, T., Oshima, K., Suda, W., Nagano, Y., Nishikawa, H., Fukuda, S., Saito, T., Narushima, S., Hase, K., Kim, S., Fritz, J.V., Wilmes, P., Ueha, S., Matsushima, K., Ohno, H., Olle, B., Sakaguchi, S., Taniguchi, T., Morita, H., Hattori, M., Honda, K., 2013. Treg induction by a rationally selected mixture of Clostridia strains from the human microbiota. Nature 500, 232-236.

Atarashi, K., Tanoue, T., Shima, T., Imaoka, A., Kuwahara, T., Momose, Y., Cheng, G., Yamasaki, S., Saito, T., Ohba, Y., Taniguchi, T., Takeda, K., Hori, S., Ivanov, II, Umesaki, Y., Itoh, K., Honda, K., 2011. Induction of colonic regulatory T cells by indigenous Clostridium species. Science 331, 337-341.

Axelrad, J.E., Lichtiger, S., Yajnik, V., 2016. Inflammatory bowel disease and cancer: The role of inflammation, immunosuppression, and cancer treatment. World J Gastroenterol 22, 4794-4801.

Bach, J.F., 2018. The hygiene hypothesis in autoimmunity: the role of pathogens and commensals. Nat Rev Immunol 18, 105-120.

Balish, E., Warner, T., 2002. Enterococcus faecalis induces inflammatory bowel disease in interleukin-10 knockout mice. Am J Pathol 160, 2253-2257.

Bamias, G., Arseneau, K.O., Cominelli, F., 2017. Mouse models of inflammatory bowel disease for investigating mucosal immunity in the intestine. Curr Opin Gastroenterol 33, 411-416.

Barker, N., 2014. Adult intestinal stem cells: critical drivers of epithelial homeostasis and regeneration. Nat Rev Mol Cell Biol 15, 19-33.

Basic, M., Keubler, L.M., Buettner, M., Achard, M., Breves, G., Schroder, B., Smoczek, A., Jorns, A., Wedekind, D., Zschemisch, N.H., Gunther, C., Neumann, D., Lienenklaus, S., Weiss, S., Hornef, M.W., Mahler, M., Bleich, A., 2014. Norovirus triggered microbiota-driven mucosal inflammation in interleukin 10-deficient mice. Inflamm Bowel Dis 20, 431-443.

Basson, A.R., Gomez-Nguyen, A., Menghini, P., Butto, L.F., Di Martino, L., Aladyshkina, N., Osme, A., LaSalla, A., Fischer, D., Ezeji, J.C., Erkkila, H.L., Brennan, C.J., Lam, M., Rodriguez-Palacios, A., Cominelli, F., 2020. Human Gut Microbiome Transplantation in Ileitis Prone Mice: A Tool for the Functional Characterization of the Microbiota in Inflammatory Bowel Disease Patients. Inflamm Bowel Dis 26, 347-359.

Baumgart, D.C., Sandborn, W.J., 2012. Crohn's disease. Lancet 380, 1590-1605.

Baumgart, M., Dogan, B., Rishniw, M., Weitzman, G., Bosworth, B., Yantiss, R., Orsi, R.H., Wiedmann, M., McDonough, P., Kim, S.G., Berg, D., Schukken, Y., Scherl, E., Simpson, K.W., 2007. Culture independent analysis of ileal mucosa reveals a selective increase in invasive Escherichia coli of novel phylogeny relative to depletion of Clostridiales in Crohn's disease involving the ileum. ISME J 1, 403-418.

Bazarganipour, S., Hausmann, J., Oertel, S., El-Hindi, K., Brachtendorf, S., Blumenstein, I., Kubesch, A., Sprinzl, K., Birod, K., Hahnefeld, L., Trautmann, S., Thomas, D., Herrmann, E., Geisslinger, G., Schiffmann, S., Grosch, S., 2019. The Lipid Status in Patients with Ulcerative Colitis: Sphingolipids are Disease-Dependent Regulated. J Clin Med 8.

Benchimol, E.I., Mack, D.R., Guttmann, A., Nguyen, G.C., To, T., Mojaverian, N., Quach, P., Manuel, D.G., 2015. Inflammatory bowel disease in immigrants to Canada and their children: a population-based cohort study. Am J Gastroenterol 110, 553-563.

Bengtson, M.B., Solberg, C., Aamodt, G., Jahnsen, J., Moum, B., Sauar, J., Vatn, M.H., Ibsen Study, G., 2009a. Clustering in time of familial IBD separates ulcerative colitis from Crohn's disease. Inflamm Bowel Dis 15, 1867-1874.

Bengtson, M.B., Solberg, C., Aamodt, G., Sauar, J., Jahnsen, J., Moum, B., Lygren, I., Vatn, M.H., group, I.s., 2009b. Familial aggregation in Crohn's disease and ulcerative colitis in a Norwegian population-based cohort followed for ten years. J Crohns Colitis 3, 92-99.

Berg, D.J., Davidson, N., Kuhn, R., Muller, W., Menon, S., Holland, G., Thompson-Snipes, L., Leach, M.W., Rennick, D., 1996. Enterocolitis and colon cancer in interleukin-10-deficient mice are associated with aberrant cytokine production and CD4(+) TH1-like responses. J Clin Invest 98, 1010-1020.

Berg, G., Rybakova, D., Fischer, D., Cernava, T., Verges, M.C., Charles, T., Chen, X., Cocolin, L., Eversole, K., Corral, G.H., Kazou, M., Kinkel, L., Lange, L., Lima, N., Loy, A., Macklin, J.A., Maguin, E., Mauchline, T., McClure, R., Mitter, B., Ryan, M., Sarand, I., Smidt, H., Schelkle, B., Roume, H., Kiran, G.S., Selvin, J., Souza, R.S.C., van Overbeek, L., Singh, B.K., Wagner, M., Walsh, A., Sessitsch, A., Schloter, M., 2020. Microbiome definition re-visited: old concepts and new challenges. Microbiome 8, 103.

Bernink, J.H., Peters, C.P., Munneke, M., te Velde, A.A., Meijer, S.L., Weijer, K., Hreggvidsdottir, H.S., Heinsbroek, S.E., Legrand, N., Buskens, C.J., Bemelman, W.A., Mjosberg, J.M., Spits, H., 2013. Human type 1 innate lymphoid cells accumulate in inflamed mucosal tissues. Nat Immunol 14, 221-229.

Berry, D., Ben Mahfoudh, K., Wagner, M., Loy, A., 2011. Barcoded primers used in multiplex amplicon pyrosequencing bias amplification. Appl Environ Microbiol 77, 7846-7849.

Bjerrum, J.T., Wang, Y., Hao, F., Coskun, M., Ludwig, C., Gunther, U., Nielsen, O.H., 2015. Metabonomics of human fecal extracts characterize ulcerative colitis, Crohn's disease and healthy individuals. Metabolomics 11, 122-133.

Bolsega, S., Basic, M., Smoczek, A., Buettner, M., Eberl, C., Ahrens, D., Odum, K.A., Stecher, B., Bleich, A., 2019. Composition of the Intestinal Microbiota Determines the Outcome of Virus-Triggered Colitis in Mice. Front Immunol 10, 1708.

Boyapati, R.K., Rossi, A.G., Satsangi, J., Ho, G.T., 2016. Gut mucosal DAMPs in IBD: from mechanisms to therapeutic implications. Mucosal Immunol 9, 567-582.

Brand, S., Beigel, F., Olszak, T., Zitzmann, K., Eichhorst, S.T., Otte, J.M., Diepolder, H., Marquardt, A., Jagla, W., Popp, A., Leclair, S., Herrmann, K., Seiderer, J., Ochsenkuhn, T., Goke, B., Auernhammer, C.J., Dambacher, J., 2006. IL-22 is increased in active Crohn's disease and promotes proinflammatory gene expression and intestinal epithelial cell migration. Am J Physiol Gastrointest Liver Physiol 290, G827-838.

Brant, S.R., Okou, D.T., Simpson, C.L., Cutler, D.J., Haritunians, T., Bradfield, J.P., Chopra, P., Prince, J., Begum, F., Kumar, A., Huang, C., Venkateswaran, S., Datta, L.W., Wei, Z., Thomas, K., Herrinton, L.J., Klapproth, J.A., Quiros, A.J., Seminerio, J., Liu, Z., Alexander, J.S., Baldassano, R.N., Dudley-Brown, S., Cross, R.K., Dassopoulos, T., Denson, L.A., Dhere, T.A., Dryden, G.W., Hanson, J.S., Hou, J.K., Hussain, S.Z., Hyams, J.S., Isaacs, K.L., Kader, H., Kappelman, M.D., Katz, J., Kellermayer, R., Kirschner, B.S., Kuemmerle, J.F., Kwon, J.H., Lazarev, M., Li, E., Mack, D., Mannon, P., Moulton, D.E., Newberry, R.D., Osuntokun, B.O., Patel, A.S., Saeed, S.A., Targan, S.R., Valentine, J.F., Wang, M.H., Zonca, M., Rioux, J.D., Duerr, R.H., Silverberg, M.S., Cho, J.H., Hakonarson, H., Zwick, M.E., McGovern, D.P., Kugathasan, S., 2017. Genome-Wide Association Study Identifies African-Specific Susceptibility Loci in African Americans With Inflammatory Bowel Disease. Gastroenterology 152, 206-217 e202.

Britton, G.J., Contijoch, E.J., Mogno, I., Vennaro, O.H., Llewellyn, S.R., Ng, R., Li, Z., Mortha, A., Merad, M., Das, A., Gevers, D., McGovern, D.P.B., Singh, N., Braun, J., Jacobs, J.P., Clemente, J.C., Grinspan, A., Sands, B.E., Colombel, J.F., Dubinsky, M.C., Faith, J.J., 2019. Microbiotas from Humans with Inflammatory Bowel Disease Alter the Balance of Gut Th17 and RORgammat(+) Regulatory T Cells and Exacerbate Colitis in Mice. Immunity 50, 212-224 e214.

Brugiroux, S., Beutler, M., Pfann, C., Garzetti, D., Ruscheweyh, H.J., Ring, D., Diehl, M., Herp, S., Lotscher, Y., Hussain, S., Bunk, B., Pukall, R., Huson, D.H., Munch, P.C., McHardy, A.C., McCoy, K.D., Macpherson, A.J., Loy, A., Clavel, T., Berry, D., Stecher, B., 2016. Genome-guided design of a defined mouse microbiota that confers colonization resistance against Salmonella enterica serovar Typhimurium. Nat Microbiol 2, 16215.

Bunker, J.J., Flynn, T.M., Koval, J.C., Shaw, D.G., Meisel, M., McDonald, B.D., Ishizuka, I.E., Dent, A.L., Wilson, P.C., Jabri, B., Antonopoulos, D.A., Bendelac, A., 2015. Innate and Adaptive Humoral Responses Coat Distinct Commensal Bacteria with Immunoglobulin A. Immunity 43, 541-553.

Burgueno, J.F., Abreu, M.T., 2020. Epithelial Toll-like receptors and their role in gut homeostasis and disease. Nat Rev Gastroenterol Hepatol 17, 263-278.

Bushman, F.D., Conrad, M., Ren, Y., Zhao, C., Gu, C., Petucci, C., Kim, M.S., Abbas, A., Downes, K.J., Devas, N., Mattei, L.M., Breton, J., Kelsen, J., Marakos, S., Galgano, A., Kachelries, K., Erlichman, J., Hart, J.L., Moraskie, M., Kim, D., Zhang, H., Hofstaedter, C.E., Wu, G.D., Lewis, J.D., Zackular, J.P., Li, H., Bittinger, K., Baldassano, R., 2020. Multi-omic Analysis of the Interaction between

Clostridioides difficile Infection and Pediatric Inflammatory Bowel Disease. Cell Host Microbe 28, 422-433 e427.

Callahan, B.J., McMurdie, P.J., Rosen, M.J., Han, A.W., Johnson, A.J., Holmes, S.P., 2016. DADA2: High-resolution sample inference from Illumina amplicon data. Nat Methods 13, 581-583.

Caporaso, J.G., Kuczynski, J., Stombaugh, J., Bittinger, K., Bushman, F.D., Costello, E.K., Fierer, N., Pena, A.G., Goodrich, J.K., Gordon, J.I., Huttley, G.A., Kelley, S.T., Knights, D., Koenig, J.E., Ley, R.E., Lozupone, C.A., McDonald, D., Muegge, B.D., Pirrung, M., Reeder, J., Sevinsky, J.R., Turnbaugh, P.J., Walters, W.A., Widmann, J., Yatsunenko, T., Zaneveld, J., Knight, R., 2010. QIIME allows analysis of high-throughput community sequencing data. Nat Methods 7, 335-336.

Cassinotti, A., Passamonti, F., Segato, S., 2021. Cell Therapy in Inflammatory Bowel Disease. Pharmacol Res 163, 105247.

Chassaing, B., Ley, R.E., Gewirtz, A.T., 2014. Intestinal epithelial cell toll-like receptor 5 regulates the intestinal microbiota to prevent low-grade inflammation and metabolic syndrome in mice. Gastroenterology 147, 1363-1377 e1317.

Cheema, A., Adeloye, D., Sidhu, S., Sridhar, D., Chan, K.Y., 2014. Urbanization and prevalence of type 2 diabetes in Southern Asia: A systematic analysis. J Glob Health 4, 010404.

Chen, P., Zhou, G., Lin, J., Li, L., Zeng, Z., Chen, M., Zhang, S., 2020. Serum Biomarkers for Inflammatory Bowel Disease. Front Med (Lausanne) 7, 123.

Choung, R.S., Princen, F., Stockfisch, T.P., Torres, J., Maue, A.C., Porter, C.K., Leon, F., De Vroey, B., Singh, S., Riddle, M.S., Murray, J.A., Colombel, J.F., Team, P.S., 2016. Serologic microbial associated markers can predict Crohn's disease behaviour years before disease diagnosis. Aliment Pharmacol Ther 43, 1300-1310.

Claesson, M.J., Cusack, S., O'Sullivan, O., Greene-Diniz, R., de Weerd, H., Flannery, E., Marchesi, J.R., Falush, D., Dinan, T., Fitzgerald, G., Stanton, C., van Sinderen, D., O'Connor, M., Harnedy, N., O'Connor, K., Henry, C., O'Mahony, D., Fitzgerald, A.P., Shanahan, F., Twomey, C., Hill, C., Ross, R.P., O'Toole, P.W., 2011. Composition, variability, and temporal stability of the intestinal microbiota of the elderly. Proc Natl Acad Sci U S A 108 Suppl 1, 4586-4591.

Cleynen, I., Boucher, G., Jostins, L., Schumm, L.P., Zeissig, S., Ahmad, T., Andersen, V., Andrews, J.M., Annese, V., Brand, S., Brant, S.R., Cho, J.H., Daly, M.J., Dubinsky, M., Duerr, R.H., Ferguson, L.R., Franke, A., Gearry, R.B., Goyette, P., Hakonarson, H., Halfvarson, J., Hov, J.R., Huang, H., Kennedy, N.A., Kupcinskas, L., Lawrance, I.C., Lee, J.C., Satsangi, J., Schreiber, S., Theatre, E., van der Meulen-de Jong, A.E., Weersma, R.K., Wilson, D.C., International Inflammatory Bowel Disease Genetics, C., Parkes, M., Vermeire, S., Rioux, J.D., Mansfield, J., Silverberg, M.S., Radford-Smith, G., McGovern, D.P., Barrett, J.C., Lees, C.W., 2016. Inherited determinants of Crohn's disease and ulcerative colitis phenotypes: a genetic association study. Lancet 387, 156-167.

Cleynen, I., Gonzalez, J.R., Figueroa, C., Franke, A., McGovern, D., Bortlik, M., Crusius, B.J., Vecchi, M., Artieda, M., Szczypiorska, M., Bethge, J., Arteta, D., Ayala, E., Danese, S., van Hogezand, R.A., Panes, J., Pena, S.A., Lukas, M., Jewell, D.P., Schreiber, S., Vermeire, S., Sans, M., 2013. Genetic factors conferring an increased susceptibility to develop Crohn's disease also influence disease phenotype: results from the IBDchip European Project. Gut 62, 1556-1565.

Clooney, A.G., Eckenberger, J., Laserna-Mendieta, E., Sexton, K.A., Bernstein, M.T., Vagianos, K., Sargent, M., Ryan, F.J., Moran, C., Sheehan, D., Sleator, R.D., Targownik, L.E., Bernstein, C.N., Shanahan, F., Claesson, M.J., 2021. Ranking microbiome variance in inflammatory bowel disease: a large longitudinal intercontinental study. Gut 70, 499-510.

Collaborators, G.B.D.I.B.D., 2020. The global, regional, and national burden of inflammatory bowel disease in 195 countries and territories, 1990-2017: a systematic analysis for the Global Burden of Disease Study 2017. Lancet Gastroenterol Hepatol 5, 17-30.

Colombel, J.F., Sandborn, W.J., Reinisch, W., Mantzaris, G.J., Kornbluth, A., Rachmilewitz, D., Lichtiger, S., D'Haens, G., Diamond, R.H., Broussard, D.L., Tang, K.L., van der Woude, C.J., Rutgeerts, P., Group, S.S., 2010. Infliximab, azathioprine, or combination therapy for Crohn's disease. N Engl J Med 362, 1383-1395.

Cominelli, F., Arseneau, K.O., Rodriguez-Palacios, A., Pizarro, T.T., 2017. Uncovering Pathogenic Mechanisms of Inflammatory Bowel Disease Using Mouse Models of Crohn's Disease-Like Ileitis: What is the Right Model? Cell Mol Gastroenterol Hepatol 4, 19-32.

Conte, M.P., Schippa, S., Zamboni, I., Penta, M., Chiarini, F., Seganti, L., Osborn, J., Falconieri, P., Borrelli, O., Cucchiara, S., 2006. Gut-associated bacterial microbiota in paediatric patients with inflammatory bowel disease. Gut 55, 1760-1767.

Costello, S.P., Hughes, P.A., Waters, O., Bryant, R.V., Vincent, A.D., Blatchford, P., Katsikeros, R., Makanyanga, J., Campaniello, M.A., Mavrangelos, C., Rosewarne, C.P., Bickley, C., Peters, C., Schoeman, M.N., Conlon, M.A., Roberts-Thomson, I.C., Andrews, J.M., 2019. Effect of Fecal Microbiota Transplantation on 8-Week Remission in Patients With Ulcerative Colitis: A Randomized Clinical Trial. JAMA 321, 156-164.

Couturier-Maillard, A., Secher, T., Rehman, A., Normand, S., De Arcangelis, A., Haesler, R., Huot, L., Grandjean, T., Bressenot, A., Delanoye-Crespin, A., Gaillot, O., Schreiber, S., Lemoine, Y., Ryffel, B., Hot, D., Nunez, G., Chen, G., Rosenstiel, P., Chamaillard, M., 2013. NOD2-mediated dysbiosis predisposes mice to transmissible colitis and colorectal cancer. J Clin Invest 123, 700-711.

Cui, B., Feng, Q., Wang, H., Wang, M., Peng, Z., Li, P., Huang, G., Liu, Z., Wu, P., Fan, Z., Ji, G., Wang, X., Wu, K., Fan, D., Zhang, F., 2015. Fecal microbiota transplantation through mid-gut for refractory Crohn's disease: safety, feasibility, and efficacy trial results. J Gastroenterol Hepatol 30, 51-58.

Cupi, M.L., Sarra, M., Marafini, I., Monteleone, I., Franze, E., Ortenzi, A., Colantoni, A., Sica, G., Sileri, P., Rosado, M.M., Carsetti, R., MacDonald, T.T., Pallone, F., Monteleone, G., 2014. Plasma cells in the mucosa of patients with inflammatory bowel disease produce granzyme B and possess cytotoxic activities. J Immunol 192, 6083-6091.

D'Haens, G.R., Geboes, K., Peeters, M., Baert, F., Penninckx, F., Rutgeerts, P., 1998. Early lesions of recurrent Crohn's disease caused by infusion of intestinal contents in excluded ileum. Gastroenterology 114, 262-267.

Darfeuille-Michaud, A., Boudeau, J., Bulois, P., Neut, C., Glasser, A.L., Barnich, N., Bringer, M.A., Swidsinski, A., Beaugerie, L., Colombel, J.F., 2004. High prevalence of adherent-invasive Escherichia coli associated with ileal mucosa in Crohn's disease. Gastroenterology 127, 412-421.

Das, P., Marcisauskas, S., Ji, B., Nielsen, J., 2019. Metagenomic analysis of bile salt biotransformation in the human gut microbiome. BMC Genomics 20, 517.

Day, A.S., Lopez, R.N., 2015. Exclusive enteral nutrition in children with Crohn's disease. World J Gastroenterol 21, 6809-6816.

De Filippis, F., Pasolli, E., Tett, A., Tarallo, S., Naccarati, A., De Angelis, M., Neviani, E., Cocolin, L., Gobbetti, M., Segata, N., Ercolini, D., 2019. Distinct Genetic and Functional Traits of Human Intestinal Prevotella copri Strains Are Associated with Different Habitual Diets. Cell Host Microbe 25, 444-453 e443.

de Lange, K.M., Moutsianas, L., Lee, J.C., Lamb, C.A., Luo, Y., Kennedy, N.A., Jostins, L., Rice, D.L., Gutierrez-Achury, J., Ji, S.G., Heap, G., Nimmo, E.R., Edwards, C., Henderson, P., Mowat, C., Sanderson, J., Satsangi, J., Simmons, A., Wilson, D.C., Tremelling, M., Hart, A., Mathew, C.G., Newman, W.G., Parkes, M., Lees, C.W., Uhlig, H., Hawkey, C., Prescott, N.J., Ahmad, T., Mansfield, J.C., Anderson, C.A., Barrett, J.C., 2017. Genome-wide association study implicates immune activation of multiple integrin genes in inflammatory bowel disease. Nat Genet 49, 256-261.

De Preter, V., Machiels, K., Joossens, M., Arijs, I., Matthys, C., Vermeire, S., Rutgeerts, P., Verbeke, K., 2015. Faecal metabolite profiling identifies medium-chain fatty acids as discriminating compounds in IBD. Gut 64, 447-458.

de Souza, H.S., Fiocchi, C., 2016. Immunopathogenesis of IBD: current state of the art. Nat Rev Gastroenterol Hepatol 13, 13-27.

Dethlefsen, L., Relman, D.A., 2011. Incomplete recovery and individualized responses of the human distal gut microbiota to repeated antibiotic perturbation. Proc Natl Acad Sci U S A 108 Suppl 1, 4554-4561.

Diederen, K., Li, J.V., Donachie, G.E., de Meij, T.G., de Waart, D.R., Hakvoort, T.B.M., Kindermann, A., Wagner, J., Auyeung, V., Te Velde, A.A., Heinsbroek, S.E.M., Benninga, M.A., Kinross, J., Walker,

A.W., de Jonge, W.J., Seppen, J., 2020. Exclusive enteral nutrition mediates gut microbial and metabolic changes that are associated with remission in children with Crohn's disease. Sci Rep 10, 18879.

Dietrich, A., Matchado, M.S., Zwiebel, M., Olke, B., Lauber, M., Lagkouvardos, I., Baumbach, J., Haller, D., Brandl, B., Skurk, T., Hauner, H., Reitmeier, S., List, M., 2022. Namco: a microbiome explorer. Microb Genom 8.

Dignass, A., Van Assche, G., Lindsay, J.O., Lemann, M., Soderholm, J., Colombel, J.F., Danese, S., D'Hoore, A., Gassull, M., Gomollon, F., Hommes, D.W., Michetti, P., O'Morain, C., Oresland, T., Windsor, A., Stange, E.F., Travis, S.P., European, C.s., Colitis, O., 2010. The second European evidence-based Consensus on the diagnosis and management of Crohn's disease: Current management. J Crohns Colitis 4, 28-62.

Douglas, A.E., 2018. Which experimental systems should we use for human microbiome science? PLoS Biol 16, e2005245.

Douglas, G.M., Maffei, V.J., Zaneveld, J.R., Yurgel, S.N., Brown, J.R., Taylor, C.M., Huttenhower, C., Langille, M.G.I., 2020. PICRUSt2 for prediction of metagenome functions. Nat Biotechnol 38, 685-688.

Du, Z., Hudcovic, T., Mrazek, J., Kozakova, H., Srutkova, D., Schwarzer, M., Tlaskalova-Hogenova, H., Kostovcik, M., Kverka, M., 2015. Development of gut inflammation in mice colonized with mucosa-associated bacteria from patients with ulcerative colitis. Gut Pathog 7, 32.

Ducarmon, Q.R., Hornung, B.V.H., Geelen, A.R., Kuijper, E.J., Zwittink, R.D., 2020. Toward Standards in Clinical Microbiota Studies: Comparison of Three DNA Extraction Methods and Two Bioinformatic Pipelines. mSystems 5.

Dulai, P.S., Singh, S., Vande Casteele, N., Boland, B.S., Rivera-Nieves, J., Ernst, P.B., Eckmann, L., Barrett, K.E., Chang, J.T., Sandborn, W.J., 2019. Should We Divide Crohn's Disease Into Ileum-Dominant and Isolated Colonic Diseases? Clin Gastroenterol Hepatol 17, 2634-2643.

Eastaff-Leung, N., Mabarrack, N., Barbour, A., Cummins, A., Barry, S., 2010. Foxp3+ regulatory T cells, Th17 effector cells, and cytokine environment in inflammatory bowel disease. J Clin Immunol 30, 80-89.

Edgar, R.C., 2013. UPARSE: highly accurate OTU sequences from microbial amplicon reads. Nat Methods 10, 996-998.

Edgar, R.C., 2016. UNOISE2: improved error-correction for Illumina 16S and ITS amplicon sequencing. bioRxiv, 081257.

Edgar, R.C., Haas, B.J., Clemente, J.C., Quince, C., Knight, R., 2011. UCHIME improves sensitivity and speed of chimera detection. Bioinformatics 27, 2194-2200.

Eliakim, R., Karmeli, F., Razin, E., Rachmilewitz, D., 1988. Role of platelet-activating factor in ulcerative colitis. Enhanced production during active disease and inhibition by sulfasalazine and prednisolone. Gastroenterology 95, 1167-1172.

Erickson, A.R., Cantarel, B.L., Lamendella, R., Darzi, Y., Mongodin, E.F., Pan, C., Shah, M., Halfvarson, J., Tysk, C., Henrissat, B., Raes, J., Verberkmoes, N.C., Fraser, C.M., Hettich, R.L., Jansson, J.K., 2012. Integrated metagenomics/metaproteomics reveals human host-microbiota signatures of Crohn's disease. PLoS One 7, e49138.

Eun, C.S., Mishima, Y., Wohlgemuth, S., Liu, B., Bower, M., Carroll, I.M., Sartor, R.B., 2014. Induction of bacterial antigen-specific colitis by a simplified human microbiota consortium in gnotobiotic interleukin-10-/- mice. Infect Immun 82, 2239-2246.

Fadlallah, J., Sterlin, D., Fieschi, C., Parizot, C., Dorgham, K., El Kafsi, H., Autaa, G., Ghillani-Dalbin, P., Juste, C., Lepage, P., Malphettes, M., Galicier, L., Boutboul, D., Clement, K., Andre, S., Marquet, F., Tresallet, C., Mathian, A., Miyara, M., Oksenhendler, E., Amoura, Z., Yssel, H., Larsen, M., Gorochov, G., 2019. Synergistic convergence of microbiota-specific systemic IgG and secretory IgA. J Allergy Clin Immunol 143, 1575-1585 e1574.

Faith, J.J., Guruge, J.L., Charbonneau, M., Subramanian, S., Seedorf, H., Goodman, A.L., Clemente, J.C., Knight, R., Heath, A.C., Leibel, R.L., Rosenbaum, M., Gordon, J.I., 2013. The long-term stability of the human gut microbiota. Science 341, 1237439.

Faith, J.J., Rey, F.E., O'Donnell, D., Karlsson, M., McNulty, N.P., Kallstrom, G., Goodman, A.L., Gordon, J.I., 2010. Creating and characterizing communities of human gut microbes in gnotobiotic mice. ISME J 4, 1094-1098.

Falony, G., Joossens, M., Vieira-Silva, S., Wang, J., Darzi, Y., Faust, K., Kurilshikov, A., Bonder, M.J., Valles-Colomer, M., Vandeputte, D., Tito, R.Y., Chaffron, S., Rymenans, L., Verspecht, C., De Sutter, L., Lima-Mendez, G., D'Hoe, K., Jonckheere, K., Homola, D., Garcia, R., Tigchelaar, E.F., Eeckhaudt, L., Fu, J., Henckaerts, L., Zhernakova, A., Wijmenga, C., Raes, J., 2016. Population-level analysis of gut microbiome variation. Science 352, 560-564.

Feagan, B.G., Rutgeerts, P., Sands, B.E., Hanauer, S., Colombel, J.F., Sandborn, W.J., Van Assche, G., Axler, J., Kim, H.J., Danese, S., Fox, I., Milch, C., Sankoh, S., Wyant, T., Xu, J., Parikh, A., Group, G.S., 2013. Vedolizumab as induction and maintenance therapy for ulcerative colitis. N Engl J Med 369, 699-710.

Feagan, B.G., Sandborn, W.J., Gasink, C., Jacobstein, D., Lang, Y., Friedman, J.R., Blank, M.A., Johanns, J., Gao, L.L., Miao, Y., Adedokun, O.J., Sands, B.E., Hanauer, S.B., Vermeire, S., Targan, S., Ghosh, S., de Villiers, W.J., Colombel, J.F., Tulassay, Z., Seidler, U., Salzberg, B.A., Desreumaux, P.,

Lee, S.D., Loftus, E.V., Jr., Dieleman, L.A., Katz, S., Rutgeerts, P., Group, U.-I.-U.S., 2016. Ustekinumab as Induction and Maintenance Therapy for Crohn's Disease. N Engl J Med 375, 1946-1960.

Ferrante, M., Henckaerts, L., Joossens, M., Pierik, M., Joossens, S., Dotan, N., Norman, G.L., Altstock, R.T., Van Steen, K., Rutgeerts, P., Van Assche, G., Vermeire, S., 2007. New serological markers in inflammatory bowel disease are associated with complicated disease behaviour. Gut 56, 1394-1403.

Filimoniuk, A., Blachnio-Zabielska, A., Imierska, M., Lebensztejn, D.M., Daniluk, U., 2020. Sphingolipid Analysis Indicate Lactosylceramide as a Potential Biomarker of Inflammatory Bowel Disease in Children. Biomolecules 10.

Finotti, A., Gasparello, J., Lampronti, I., Cosenza, L.C., Maconi, G., Matarese, V., Gentili, V., Di Luca, D., Gambari, R., Caselli, M., 2017. PCR detection of segmented filamentous bacteria in the terminal ileum of patients with ulcerative colitis. BMJ Open Gastroenterol 4, e000172.

Flint, H.J., Duncan, S.H., Louis, P., 2017. The impact of nutrition on intestinal bacterial communities. Curr Opin Microbiol 38, 59-65.

Forbes, G.M., Sturm, M.J., Leong, R.W., Sparrow, M.P., Segarajasingam, D., Cummins, A.G., Phillips, M., Herrmann, R.P., 2014. A phase 2 study of allogeneic mesenchymal stromal cells for luminal Crohn's disease refractory to biologic therapy. Clin Gastroenterol Hepatol 12, 64-71.

Frank, D.N., St Amand, A.L., Feldman, R.A., Boedeker, E.C., Harpaz, N., Pace, N.R., 2007. Molecular-phylogenetic characterization of microbial community imbalances in human inflammatory bowel diseases. Proc Natl Acad Sci U S A 104, 13780-13785.

Franzosa, E.A., Morgan, X.C., Segata, N., Waldron, L., Reyes, J., Earl, A.M., Giannoukos, G., Boylan, M.R., Ciulla, D., Gevers, D., Izard, J., Garrett, W.S., Chan, A.T., Huttenhower, C., 2014. Relating the metatranscriptome and metagenome of the human gut. Proc Natl Acad Sci U S A 111, E2329-2338.

Franzosa, E.A., Sirota-Madi, A., Avila-Pacheco, J., Fornelos, N., Haiser, H.J., Reinker, S., Vatanen, T., Hall, A.B., Mallick, H., McIver, L.J., Sauk, J.S., Wilson, R.G., Stevens, B.W., Scott, J.M., Pierce, K., Deik, A.A., Bullock, K., Imhann, F., Porter, J.A., Zhernakova, A., Fu, J., Weersma, R.K., Wijmenga, C., Clish, C.B., Vlamakis, H., Huttenhower, C., Xavier, R.J., 2019. Gut microbiome structure and metabolic activity in inflammatory bowel disease. Nat Microbiol 4, 293-305.

Fujimura, K.E., Lynch, S.V., 2015. Microbiota in allergy and asthma and the emerging relationship with the gut microbiome. Cell Host Microbe 17, 592-602.

Furusawa, Y., Obata, Y., Fukuda, S., Endo, T.A., Nakato, G., Takahashi, D., Nakanishi, Y., Uetake, C., Kato, K., Kato, T., Takahashi, M., Fukuda, N.N., Murakami, S., Miyauchi, E., Hino, S., Atarashi, K.,

Onawa, S., Fujimura, Y., Lockett, T., Clarke, J.M., Topping, D.L., Tomita, M., Hori, S., Ohara, O., Morita, T., Koseki, H., Kikuchi, J., Honda, K., Hase, K., Ohno, H., 2013. Commensal microbe-derived butyrate induces the differentiation of colonic regulatory T cells. Nature 504, 446-450.

Galazzo, G., Tedjo, D.I., Wintjens, D.S.J., Savelkoul, P.H.M., Masclee, A.A.M., Bodelier, A.G.L., Pierik, M.J., Jonkers, D., Penders, J., 2019. Faecal Microbiota Dynamics and their Relation to Disease Course in Crohn's Disease. J Crohns Colitis 13, 1273-1282.

Gasparini, R.G., Sassaki, L.Y., Saad-Hossne, R., 2018. Inflammatory bowel disease epidemiology in Sao Paulo State, Brazil. Clin Exp Gastroenterol 11, 423-429.

Gensollen, T., Iyer, S.S., Kasper, D.L., Blumberg, R.S., 2016. How colonization by microbiota in early life shapes the immune system. Science 352, 539-544.

Geremia, A., Arancibia-Carcamo, C.V., Fleming, M.P., Rust, N., Singh, B., Mortensen, N.J., Travis, S.P., Powrie, F., 2011. IL-23-responsive innate lymphoid cells are increased in inflammatory bowel disease. J Exp Med 208, 1127-1133.

Gerlach, K., Hwang, Y., Nikolaev, A., Atreya, R., Dornhoff, H., Steiner, S., Lehr, H.A., Wirtz, S., Vieth, M., Waisman, A., Rosenbauer, F., McKenzie, A.N., Weigmann, B., Neurath, M.F., 2014. TH9 cells that express the transcription factor PU.1 drive T cell-mediated colitis via IL-9 receptor signaling in intestinal epithelial cells. Nat Immunol 15, 676-686.

Gersemann, M., Becker, S., Kubler, I., Koslowski, M., Wang, G., Herrlinger, K.R., Griger, J., Fritz, P., Fellermann, K., Schwab, M., Wehkamp, J., Stange, E.F., 2009. Differences in goblet cell differentiation between Crohn's disease and ulcerative colitis. Differentiation 77, 84-94.

Gevers, D., Kugathasan, S., Denson, L.A., Vazquez-Baeza, Y., Van Treuren, W., Ren, B., Schwager, E., Knights, D., Song, S.J., Yassour, M., Morgan, X.C., Kostic, A.D., Luo, C., Gonzalez, A., McDonald, D., Haberman, Y., Walters, T., Baker, S., Rosh, J., Stephens, M., Heyman, M., Markowitz, J., Baldassano, R., Griffiths, A., Sylvester, F., Mack, D., Kim, S., Crandall, W., Hyams, J., Huttenhower, C., Knight, R., Xavier, R.J., 2014. The treatment-naive microbiome in new-onset Crohn's disease. Cell Host Microbe 15, 382-392.

Glassman, S.I., Martiny, J.B.H., 2018. Broadscale Ecological Patterns Are Robust to Use of Exact Sequence Variants versus Operational Taxonomic Units. mSphere 3.

Glocker, E.O., Kotlarz, D., Boztug, K., Gertz, E.M., Schaffer, A.A., Noyan, F., Perro, M., Diestelhorst, J., Allroth, A., Murugan, D., Hatscher, N., Pfeifer, D., Sykora, K.W., Sauer, M., Kreipe, H., Lacher, M., Nustede, R., Woellner, C., Baumann, U., Salzer, U., Koletzko, S., Shah, N., Segal, A.W., Sauerbrey, A., Buderus, S., Snapper, S.B., Grimbacher, B., Klein, C., 2009. Inflammatory bowel disease and mutations affecting the interleukin-10 receptor. N Engl J Med 361, 2033-2045.

Gonzalez, C.G., Mills, R.H., Zhu, Q., Sauceda, C., Knight, R., Dulai, P.S., Gonzalez, D.J., 2022. Location-specific signatures of Crohn's disease at a multi-omics scale. Microbiome 10, 133.

Goodrich, J.K., Davenport, E.R., Beaumont, M., Jackson, M.A., Knight, R., Ober, C., Spector, T.D., Bell, J.T., Clark, A.G., Ley, R.E., 2016. Genetic Determinants of the Gut Microbiome in UK Twins. Cell Host Microbe 19, 731-743.

Gopalakrishnan, S., Zeissig, Y., Strigli, A., Basic, M., Hartwig, J., Wang, J., Muders, M., Barreton, G., Baines, J.F., Bleich, A., Hampe, J., Zeissig, S., 2019. DOP12 Mutations in the X-linked inhibitor of apoptosis protein promote susceptibility to microbiota-induced intestinal inflammation. Journal of Crohn's and Colitis 13, S033-S034.

Goyette, P., Boucher, G., Mallon, D., Ellinghaus, E., Jostins, L., Huang, H., Ripke, S., Gusareva, E.S., Annese, V., Hauser, S.L., Oksenberg, J.R., Thomsen, I., Leslie, S., International Inflammatory Bowel Disease Genetics, C., Australia, New Zealand, I., Belgium, I.B.D.G.C., Italian Group for, I.B.D.G.C., Consortium, N.I.B.D.G., United Kingdom, I., Wellcome Trust Case Control, C., Quebec, I.B.D.G.C., Daly, M.J., Van Steen, K., Duerr, R.H., Barrett, J.C., McGovern, D.P., Schumm, L.P., Traherne, J.A., Carrington, M.N., Kosmoliaptsis, V., Karlsen, T.H., Franke, A., Rioux, J.D., 2015. High-density mapping of the MHC identifies a shared role for HLA-DRB1*01:03 in inflammatory bowel diseases and heterozygous advantage in ulcerative colitis. Nat Genet 47, 172-179.

Graham, D.B., Xavier, R.J., 2020. Pathway paradigms revealed from the genetics of inflammatory bowel disease. Nature 578, 527-539.

Grover, Z., Muir, R., Lewindon, P., 2014. Exclusive enteral nutrition induces early clinical, mucosal and transmural remission in paediatric Crohn's disease. J Gastroenterol 49, 638-645.

Gunther, C., Martini, E., Wittkopf, N., Amann, K., Weigmann, B., Neumann, H., Waldner, M.J., Hedrick, S.M., Tenzer, S., Neurath, M.F., Becker, C., 2011. Caspase-8 regulates TNF-alpha-induced epithelial necroptosis and terminal ileitis. Nature 477, 335-339.

Haberman, Y., Schirmer, M., Dexheimer, P.J., Karns, R., Braun, T., Kim, M.O., Walters, T.D., Baldassano, R.N., Noe, J.D., Rosh, J., Markowitz, J., Crandall, W.V., Mack, D.R., Griffiths, A.M., Heyman, M.B., Baker, S.S., Kellermayer, R., Moulton, D., Patel, A.S., Gulati, A.S., Steiner, S.J., LeLeiko, N., Otley, A., Oliva-Hemker, M., Ziring, D., Kirschner, B.S., Keljo, D.J., Guthery, S.L., Cohen, S.A., Snapper, S., Evans, J., Dubinsky, M., Aronow, B., Hyams, J.S., Kugathasan, S., Huttenhower, C., Xavier, R.J., Denson, L.A., 2019. Age-of-diagnosis dependent ileal immune intensification and reduced alpha-defensin in older versus younger pediatric Crohn Disease patients despite already established dysbiosis. Mucosal Immunol 12, 491-502.

Halfvarson, J., 2011. Genetics in twins with Crohn's disease: less pronounced than previously believed? Inflamm Bowel Dis 17, 6-12.

Halfvarson, J., Brislawn, C.J., Lamendella, R., Vazquez-Baeza, Y., Walters, W.A., Bramer, L.M., D'Amato, M., Bonfiglio, F., McDonald, D., Gonzalez, A., McClure, E.E., Dunklebarger, M.F., Knight, R., Jansson, J.K., 2017. Dynamics of the human gut microbiome in inflammatory bowel disease. Nat Microbiol 2, 17004.

Hall, A.B., Yassour, M., Sauk, J., Garner, A., Jiang, X., Arthur, T., Lagoudas, G.K., Vatanen, T., Fornelos, N., Wilson, R., Bertha, M., Cohen, M., Garber, J., Khalili, H., Gevers, D., Ananthakrishnan, A.N., Kugathasan, S., Lander, E.S., Blainey, P., Vlamakis, H., Xavier, R.J., Huttenhower, C., 2017. A novel Ruminococcus gnavus clade enriched in inflammatory bowel disease patients. Genome Med 9, 103.

Hansson, G.C., Johansson, M.E., 2010. The inner of the two Muc2 mucin-dependent mucus layers in colon is devoid of bacteria. Gut Microbes 1, 51-54.

Harbord, M., Eliakim, R., Bettenworth, D., Karmiris, K., Katsanos, K., Kopylov, U., Kucharzik, T., Molnar, T., Raine, T., Sebastian, S., de Sousa, H.T., Dignass, A., Carbonnel, F., European, C.s., Colitis, O., 2017. Third European Evidence-based Consensus on Diagnosis and Management of Ulcerative Colitis. Part 2: Current Management. J Crohns Colitis 11, 769-784.

Hart, A.L., Al-Hassi, H.O., Rigby, R.J., Bell, S.J., Emmanuel, A.V., Knight, S.C., Kamm, M.A., Stagg, A.J., 2005. Characteristics of intestinal dendritic cells in inflammatory bowel diseases. Gastroenterology 129, 50-65.

Harvey, R.F., Bradshaw, J.M., 1980. A simple index of Crohn's-disease activity. Lancet 1, 514.

He, Y., Wu, W., Zheng, H.M., Li, P., McDonald, D., Sheng, H.F., Chen, M.X., Chen, Z.H., Ji, G.Y., Zheng, Z.D., Mujagond, P., Chen, X.J., Rong, Z.H., Chen, P., Lyu, L.Y., Wang, X., Wu, C.B., Yu, N., Xu, Y.J., Yin, J., Raes, J., Knight, R., Ma, W.J., Zhou, H.W., 2018. Regional variation limits applications of healthy gut microbiome reference ranges and disease models. Nat Med 24, 1532-1535.

Heintz-Buschart, A., Wilmes, P., 2018. Human Gut Microbiome: Function Matters. Trends Microbiol 26, 563-574.

Heller, F., Florian, P., Bojarski, C., Richter, J., Christ, M., Hillenbrand, B., Mankertz, J., Gitter, A.H., Burgel, N., Fromm, M., Zeitz, M., Fuss, I., Strober, W., Schulzke, J.D., 2005. Interleukin-13 is the key effector Th2 cytokine in ulcerative colitis that affects epithelial tight junctions, apoptosis, and cell restitution. Gastroenterology 129, 550-564.

Henriksen, M., Jahnsen, J., Lygren, I., Stray, N., Sauar, J., Vatn, M.H., Moum, B., Group, I.S., 2008. C-reactive protein: a predictive factor and marker of inflammation in inflammatory bowel disease. Results from a prospective population-based study. Gut 57, 1518-1523.

Hildner, K., Waldschmitt, N., Haller, D., 2018. Microbiome and Diseases: Inflammatory Bowel Diseases, The Gut Microbiome in Health and Disease. Springer, pp. 151-174.

Hocke, M., Richter, L., Bosseckert, H., Eitner, K., 1999. Platelet activating factor in stool from patients with ulcerative colitis and Crohn's disease. Hepatogastroenterology 46, 2333-2337.

Hormannsperger, G., Schaubeck, M., Haller, D., 2015. Intestinal Microbiota in Animal Models of Inflammatory Diseases. ILAR J 56, 179-191.

Huang, H., Fang, M., Jostins, L., Umicevic Mirkov, M., Boucher, G., Anderson, C.A., Andersen, V., Cleynen, I., Cortes, A., Crins, F., D'Amato, M., Deffontaine, V., Dmitrieva, J., Docampo, E., Elansary, M., Farh, K.K., Franke, A., Gori, A.S., Goyette, P., Halfvarson, J., Haritunians, T., Knight, J., Lawrance, I.C., Lees, C.W., Louis, E., Mariman, R., Meuwissen, T., Mni, M., Momozawa, Y., Parkes, M., Spain, S.L., Theatre, E., Trynka, G., Satsangi, J., van Sommeren, S., Vermeire, S., Xavier, R.J., International Inflammatory Bowel Disease Genetics, C., Weersma, R.K., Duerr, R.H., Mathew, C.G., Rioux, J.D., McGovern, D.P.B., Cho, J.H., Georges, M., Daly, M.J., Barrett, J.C., 2017. Fine-mapping inflammatory bowel disease loci to single-variant resolution. Nature 547, 173-178.

Human Microbiome Project, C., 2012. Structure, function and diversity of the healthy human microbiome. Nature 486, 207-214.

Imhann, F., Vich Vila, A., Bonder, M.J., Fu, J., Gevers, D., Visschedijk, M.C., Spekhorst, L.M., Alberts, R., Franke, L., van Dullemen, H.M., Ter Steege, R.W.F., Huttenhower, C., Dijkstra, G., Xavier, R.J., Festen, E.A.M., Wijmenga, C., Zhernakova, A., Weersma, R.K., 2018. Interplay of host genetics and gut microbiota underlying the onset and clinical presentation of inflammatory bowel disease. Gut 67, 108-119.

Ivanov, II, Atarashi, K., Manel, N., Brodie, E.L., Shima, T., Karaoz, U., Wei, D., Goldfarb, K.C., Santee, C.A., Lynch, S.V., Tanoue, T., Imaoka, A., Itoh, K., Takeda, K., Umesaki, Y., Honda, K., Littman, D.R., 2009. Induction of intestinal Th17 cells by segmented filamentous bacteria. Cell 139, 485-498.

Jackson, D.N., Panopoulos, M., Neumann, W.L., Turner, K., Cantarel, B.L., Thompson-Snipes, L., Dassopoulos, T., Feagins, L.A., Souza, R.F., Mills, J.C., Blumberg, R.S., Venuprasad, K., Thompson, W.E., Theiss, A.L., 2020. Mitochondrial dysfunction during loss of prohibitin 1 triggers Paneth cell defects and ileitis. Gut.

Jacobs, J.P., Goudarzi, M., Singh, N., Tong, M., McHardy, I.H., Ruegger, P., Asadourian, M., Moon, B.H., Ayson, A., Borneman, J., McGovern, D.P., Fornace, A.J., Jr., Braun, J., Dubinsky, M., 2016. A Disease-Associated Microbial and Metabolomics State in Relatives of Pediatric Inflammatory Bowel Disease Patients. Cell Mol Gastroenterol Hepatol 2, 750-766.

Jakobsson, H.E., Jernberg, C., Andersson, A.F., Sjolund-Karlsson, M., Jansson, J.K., Engstrand, L., 2010. Short-term antibiotic treatment has differing long-term impacts on the human throat and gut microbiome. PLoS One 5, e9836.

Jansson, J., Willing, B., Lucio, M., Fekete, A., Dicksved, J., Halfvarson, J., Tysk, C., Schmitt-Kopplin, P., 2009. Metabolomics reveals metabolic biomarkers of Crohn's disease. PLoS One 4, e6386.

Jardine, S., Dhingani, N., Muise, A.M., 2019. TTC7A: Steward of Intestinal Health. Cell Mol Gastroenterol Hepatol 7, 555-570.

Jochum, L., Stecher, B., 2020. Label or Concept - What Is a Pathobiont? Trends Microbiol 28, 789-792.

Johansson, M.E., Larsson, J.M., Hansson, G.C., 2011. The two mucus layers of colon are organized by the MUC2 mucin, whereas the outer layer is a legislator of host-microbial interactions. Proc Natl Acad Sci U S A 108 Suppl 1, 4659-4665.

Jostins, L., Ripke, S., Weersma, R.K., Duerr, R.H., McGovern, D.P., Hui, K.Y., Lee, J.C., Schumm, L.P., Sharma, Y., Anderson, C.A., Essers, J., Mitrovic, M., Ning, K., Cleynen, I., Theatre, E., Spain, S.L., Raychaudhuri, S., Goyette, P., Wei, Z., Abraham, C., Achkar, J.P., Ahmad, T., Amininejad, L., Ananthakrishnan, A.N., Andersen, V., Andrews, J.M., Baidoo, L., Balschun, T., Bampton, P.A., Bitton, A., Boucher, G., Brand, S., Buning, C., Cohain, A., Cichon, S., D'Amato, M., De Jong, D., Devaney, K.L., Dubinsky, M., Edwards, C., Ellinghaus, D., Ferguson, L.R., Franchimont, D., Fransen, K., Gearry, R., Georges, M., Gieger, C., Glas, J., Haritunians, T., Hart, A., Hawkey, C., Hedl, M., Hu, X., Karlsen, T.H., Kupcinskas, L., Kugathasan, S., Latiano, A., Laukens, D., Lawrance, I.C., Lees, C.W., Louis, E., Mahy, G., Mansfield, J., Morgan, A.R., Mowat, C., Newman, W., Palmieri, O., Ponsioen, C.Y., Potocnik, U., Prescott, N.J., Regueiro, M., Rotter, J.I., Russell, R.K., Sanderson, J.D., Sans, M., Satsangi, J., Schreiber, S., Simms, L.A., Sventoraityte, J., Targan, S.R., Taylor, K.D., Tremelling, M., Verspaget, H.W., De Vos, M., Wijmenga, C., Wilson, D.C., Winkelmann, J., Xavier, R.J., Zeissig, S., Zhang, B., Zhang, C.K., Zhao, H., International, I.B.D.G.C., Silverberg, M.S., Annese, V., Hakonarson, H., Brant, S.R., Radford-Smith, G., Mathew, C.G., Rioux, J.D., Schadt, E.E., Daly, M.J., Franke, A., Parkes, M., Vermeire, S., Barrett, J.C., Cho, J.H., 2012. Host-microbe interactions have shaped the genetic architecture of inflammatory bowel disease. Nature 491, 119-124.

Kabbert, J., Benckert, J., Rollenske, T., Hitch, T.C.A., Clavel, T., Cerovic, V., Wardemann, H., Pabst, O., 2020. High microbiota reactivity of adult human intestinal IgA requires somatic mutations. J Exp Med 217.

Kamada, N., Hisamatsu, T., Okamoto, S., Chinen, H., Kobayashi, T., Sato, T., Sakuraba, A., Kitazume, M.T., Sugita, A., Koganei, K., Akagawa, K.S., Hibi, T., 2008. Unique CD14 intestinal macrophages contribute to the pathogenesis of Crohn disease via IL-23/IFN-gamma axis. J Clin Invest 118, 2269-2280.

Kaplan, G.G., 2015. The global burden of IBD: from 2015 to 2025. Nat Rev Gastroenterol Hepatol 12, 720-727.

Kaplan, G.G., Ng, S.C., 2016. Globalisation of inflammatory bowel disease: perspectives from the evolution of inflammatory bowel disease in the UK and China. Lancet Gastroenterol Hepatol 1, 307-316.

Kaser, A., Lee, A.H., Franke, A., Glickman, J.N., Zeissig, S., Tilg, H., Nieuwenhuis, E.E., Higgins, D.E., Schreiber, S., Glimcher, L.H., Blumberg, R.S., 2008. XBP1 links ER stress to intestinal inflammation and confers genetic risk for human inflammatory bowel disease. Cell 134, 743-756.

Kau, A.L., Planer, J.D., Liu, J., Rao, S., Yatsunenko, T., Trehan, I., Manary, M.J., Liu, T.C., Stappenbeck, T.S., Maleta, K.M., Ashorn, P., Dewey, K.G., Houpt, E.R., Hsieh, C.S., Gordon, J.I., 2015. Functional characterization of IgA-targeted bacterial taxa from undernourished Malawian children that produce diet-dependent enteropathy. Sci Transl Med 7, 276ra224.

Keubler, L.M., Buettner, M., Hager, C., Bleich, A., 2015. A Multihit Model: Colitis Lessons from the Interleukin-10-deficient Mouse. Inflamm Bowel Dis 21, 1967-1975.

Khaloian, S., Rath, E., Hammoudi, N., Gleisinger, E., Blutke, A., Giesbertz, P., Berger, E., Metwaly, A., Waldschmitt, N., Allez, M., Haller, D., 2020. Mitochondrial impairment drives intestinal stem cell transition into dysfunctional Paneth cells predicting Crohn's disease recurrence. Gut.

Kiesslich, R., Duckworth, C.A., Moussata, D., Gloeckner, A., Lim, L.G., Goetz, M., Pritchard, D.M., Galle, P.R., Neurath, M.F., Watson, A.J., 2012. Local barrier dysfunction identified by confocal laser endomicroscopy predicts relapse in inflammatory bowel disease. Gut 61, 1146-1153.

Kim, S.C., Tonkonogy, S.L., Albright, C.A., Tsang, J., Balish, E.J., Braun, J., Huycke, M.M., Sartor, R.B., 2005. Variable phenotypes of enterocolitis in interleukin 10-deficient mice monoassociated with two different commensal bacteria. Gastroenterology 128, 891-906.

Kim, S.C., Tonkonogy, S.L., Karrasch, T., Jobin, C., Sartor, R.B., 2007. Dual-association of gnotobiotic IL-10-/- mice with 2 nonpathogenic commensal bacteria induces aggressive pancolitis. Inflamm Bowel Dis 13, 1457-1466.

Klindworth, A., Pruesse, E., Schweer, T., Peplies, J., Quast, C., Horn, M., Glockner, F.O., 2013. Evaluation of general 16S ribosomal RNA gene PCR primers for classical and next-generation sequencing-based diversity studies. Nucleic Acids Res 41, e1.

Knights, D., Lassen, K.G., Xavier, R.J., 2013. Advances in inflammatory bowel disease pathogenesis: linking host genetics and the microbiome. Gut 62, 1505-1510.

Knights, D., Silverberg, M.S., Weersma, R.K., Gevers, D., Dijkstra, G., Huang, H., Tyler, A.D., van Sommeren, S., Imhann, F., Stempak, J.M., Huang, H., Vangay, P., Al-Ghalith, G.A., Russell, C., Sauk, J., Knight, J., Daly, M.J., Huttenhower, C., Xavier, R.J., 2014. Complex host genetics influence the microbiome in inflammatory bowel disease. Genome Med 6, 107.

Koch, S., Kucharzik, T., Heidemann, J., Nusrat, A., Luegering, A., 2010. Investigating the role of proinflammatory CD16+ monocytes in the pathogenesis of inflammatory bowel disease. Clin Exp Immunol 161, 332-341.

Koeth, R.A., Wang, Z., Levison, B.S., Buffa, J.A., Org, E., Sheehy, B.T., Britt, E.B., Fu, X., Wu, Y., Li, L., Smith, J.D., DiDonato, J.A., Chen, J., Li, H., Wu, G.D., Lewis, J.D., Warrier, M., Brown, J.M., Krauss, R.M., Tang, W.H., Bushman, F.D., Lusis, A.J., Hazen, S.L., 2013. Intestinal microbiota metabolism of L-carnitine, a nutrient in red meat, promotes atherosclerosis. Nat Med 19, 576-585.

Kolho, K.L., Korpela, K., Jaakkola, T., Pichai, M.V., Zoetendal, E.G., Salonen, A., de Vos, W.M., 2015. Fecal Microbiota in Pediatric Inflammatory Bowel Disease and Its Relation to Inflammation. Am J Gastroenterol 110, 921-930.

Kolho, K.L., Pessia, A., Jaakkola, T., de Vos, W.M., Velagapudi, V., 2017. Faecal and Serum Metabolomics in Paediatric Inflammatory Bowel Disease. J Crohns Colitis 11, 321-334.

Kontoyiannis, D., Pasparakis, M., Pizarro, T.T., Cominelli, F., Kollias, G., 1999. Impaired on/off regulation of TNF biosynthesis in mice lacking TNF AU-rich elements: implications for joint and gut-associated immunopathologies. Immunity 10, 387-398.

Kostic, A.D., Gevers, D., Siljander, H., Vatanen, T., Hyotylainen, T., Hamalainen, A.M., Peet, A., Tillmann, V., Poho, P., Mattila, I., Lahdesmaki, H., Franzosa, E.A., Vaarala, O., de Goffau, M., Harmsen, H., Ilonen, J., Virtanen, S.M., Clish, C.B., Oresic, M., Huttenhower, C., Knip, M., Group, D.S., Xavier, R.J., 2015. The dynamics of the human infant gut microbiome in development and in progression toward type 1 diabetes. Cell Host Microbe 17, 260-273.

Kronman, M.P., Zaoutis, T.E., Haynes, K., Feng, R., Coffin, S.E., 2012. Antibiotic exposure and IBD development among children: a population-based cohort study. Pediatrics 130, e794-803.

Kurilshikov, A., Medina-Gomez, C., Bacigalupe, R., Radjabzadeh, D., Wang, J., Demirkan, A., Le Roy, C.I., Raygoza Garay, J.A., Finnicum, C.T., Liu, X., Zhernakova, D.V., Bonder, M.J., Hansen, T.H., Frost, F., Ruhlemann, M.C., Turpin, W., Moon, J.Y., Kim, H.N., Lull, K., Barkan, E., Shah, S.A., Fornage, M., Szopinska-Tokov, J., Wallen, Z.D., Borisevich, D., Agreus, L., Andreasson, A., Bang, C., Bedrani, L., Bell, J.T., Bisgaard, H., Boehnke, M., Boomsma, D.I., Burk, R.D., Claringbould, A., Croitoru, K., Davies, G.E., van Duijn, C.M., Duijts, L., Falony, G., Fu, J., van der Graaf, A., Hansen, T., Homuth, G., Hughes, D.A., Ijzerman, R.G., Jackson, M.A., Jaddoe, V.W.V., Joossens, M., Jorgensen, T., Keszthelyi, D., Knight, R., Laakso, M., Laudes, M., Launer, L.J., Lieb, W., Lusis, A.J., Masclee, A.A.M., Moll, H.A., Mujagic, Z., Qibin, Q., Rothschild, D., Shin, H., Sorensen, S.J., Steves, C.J., Thorsen, J., Timpson, N.J., Tito, R.Y., Vieira-Silva, S., Volker, U., Volzke, H., Vosa, U., Wade, K.H., Walter, S., Watanabe, K., Weiss, S., Weiss, F.U., Weissbrod, O., Westra, H.J., Willemsen, G., Payami, H., Jonkers, D., Arias Vasquez, A., de Geus, E.J.C., Meyer, K.A., Stokholm, J., Segal, E., Org, E., Wijmenga, C., Kim, H.L., Kaplan, R.C., Spector, T.D., Uitterlinden, A.G., Rivadeneira, F., Franke, A., Lerch, M.M., Franke, L., Sanna, S., D'Amato, M., Pedersen, O., Paterson, A.D., Kraaij, R., Raes, J., Zhernakova, A., 2021. Large-scale association analyses identify host factors influencing human gut microbiome composition. Nat Genet 53, 156-165.

Lagier, J.C., Dubourg, G., Million, M., Cadoret, F., Bilen, M., Fenollar, F., Levasseur, A., Rolain, J.M., Fournier, P.E., Raoult, D., 2018. Culturing the human microbiota and culturomics. Nat Rev Microbiol 16, 540-550.

Lagkouvardos, I., Fischer, S., Kumar, N., Clavel, T., 2017. Rhea: a transparent and modular R pipeline for microbial profiling based on 16S rRNA gene amplicons. PeerJ 5, e2836.

Lagkouvardos, I., Joseph, D., Kapfhammer, M., Giritli, S., Horn, M., Haller, D., Clavel, T., 2016. IMNGS: A comprehensive open resource of processed 16S rRNA microbial profiles for ecology and diversity studies. Sci Rep 6, 33721.

Lakatos, L., Kiss, L.S., David, G., Pandur, T., Erdelyi, Z., Mester, G., Balogh, M., Szipocs, I., Molnar, C., Komaromi, E., Lakatos, P.L., 2011. Incidence, disease phenotype at diagnosis, and early disease course in inflammatory bowel diseases in Western Hungary, 2002-2006. Inflamm Bowel Dis 17, 2558-2565.

Lam, S., Zuo, T., Ho, M., Chan, F.K.L., Chan, P.K.S., Ng, S.C., 2019. Review article: fungal alterations in inflammatory bowel diseases. Aliment Pharmacol Ther 50, 1159-1171.

Lamas, B., Richard, M.L., Leducq, V., Pham, H.P., Michel, M.L., Da Costa, G., Bridonneau, C., Jegou, S., Hoffmann, T.W., Natividad, J.M., Brot, L., Taleb, S., Couturier-Maillard, A., Nion-Larmurier, I., Merabtene, F., Seksik, P., Bourrier, A., Cosnes, J., Ryffel, B., Beaugerie, L., Launay, J.M., Langella, P., Xavier, R.J., Sokol, H., 2016. CARD9 impacts colitis by altering gut microbiota metabolism of tryptophan into aryl hydrocarbon receptor ligands. Nat Med 22, 598-605.

Langhorst, J., Schols, M., Cinar, Z., Eilert, R., Kofink, K., Paul, A., Zempel, C., Elsenbruch, S., Lauche, R., Ahmed, M., Haller, D., Cramer, H., Dobos, G., Koch, A.K., 2020. Comprehensive Lifestyle-Modification in Patients with Ulcerative Colitis-A Randomized Controlled Trial. J Clin Med 9.

Lapaquette, P., Glasser, A.L., Huett, A., Xavier, R.J., Darfeuille-Michaud, A., 2010. Crohn's disease-associated adherent-invasive E. coli are selectively favoured by impaired autophagy to replicate intracellularly. Cell Microbiol 12, 99-113.

Larsen, N., Vogensen, F.K., van den Berg, F.W., Nielsen, D.S., Andreasen, A.S., Pedersen, B.K., Al-Soud, W.A., Sorensen, S.J., Hansen, L.H., Jakobsen, M., 2010. Gut microbiota in human adults with type 2 diabetes differs from non-diabetic adults. PLoS One 5, e9085.

Lavelle, A., Lennon, G., O'Sullivan, O., Docherty, N., Balfe, A., Maguire, A., Mulcahy, H.E., Doherty, G., O'Donoghue, D., Hyland, J., Ross, R.P., Coffey, J.C., Sheahan, K., Cotter, P.D., Shanahan, F., Winter, D.C., O'Connell, P.R., 2015. Spatial variation of the colonic microbiota in patients with ulcerative colitis and control volunteers. Gut 64, 1553-1561.

Lavelle, A., Sokol, H., 2020. Gut microbiota-derived metabolites as key actors in inflammatory bowel disease. Nat Rev Gastroenterol Hepatol 17, 223-237.

Lawley, T.D., Clare, S., Walker, A.W., Stares, M.D., Connor, T.R., Raisen, C., Goulding, D., Rad, R., Schreiber, F., Brandt, C., Deakin, L.J., Pickard, D.J., Duncan, S.H., Flint, H.J., Clark, T.G., Parkhill, J., Dougan, G., 2012. Targeted restoration of the intestinal microbiota with a simple, defined bacteriotherapy resolves relapsing Clostridium difficile disease in mice. PLoS Pathog 8, e1002995.

Lecuyer, E., Rakotobe, S., Lengline-Garnier, H., Lebreton, C., Picard, M., Juste, C., Fritzen, R., Eberl, G., McCoy, K.D., Macpherson, A.J., Reynaud, C.A., Cerf-Bensussan, N., Gaboriau-Routhiau, V., 2014. Segmented filamentous bacterium uses secondary and tertiary lymphoid tissues to induce gut IgA and specific T helper 17 cell responses. Immunity 40, 608-620.

Lee, M., Chang, E.B., 2021. Inflammatory Bowel Diseases (IBD) and the Microbiome-Searching the Crime Scene for Clues. Gastroenterology 160, 524-537.

Lehmann, T., Schallert, K., Vilchez-Vargas, R., Benndorf, D., Puttker, S., Sydor, S., Schulz, C., Bechmann, L., Canbay, A., Heidrich, B., Reichl, U., Link, A., Heyer, R., 2019. Metaproteomics of fecal samples of Crohn's disease and Ulcerative Colitis. J Proteomics 201, 93-103.

Lengfelder, I., Sava, I.G., Hansen, J.J., Kleigrewe, K., Herzog, J., Neuhaus, K., Hofmann, T., Sartor, R.B., Haller, D., 2019. Complex Bacterial Consortia Reprogram the Colitogenic Activity of Enterococcus faecalis in a Gnotobiotic Mouse Model of Chronic, Immune-Mediated Colitis. Front Immunol 10, 1420.

Lewis, J.D., Chen, E.Z., Baldassano, R.N., Otley, A.R., Griffiths, A.M., Lee, D., Bittinger, K., Bailey, A., Friedman, E.S., Hoffmann, C., Albenberg, L., Sinha, R., Compher, C., Gilroy, E., Nessel, L., Grant, A., Chehoud, C., Li, H., Wu, G.D., Bushman, F.D., 2015. Inflammation, Antibiotics, and Diet as Environmental Stressors of the Gut Microbiome in Pediatric Crohn's Disease. Cell Host Microbe 18, 489-500.

Li, Q., Lee, C.H., Peters, L.A., Mastropaolo, L.A., Thoeni, C., Elkadri, A., Schwerd, T., Zhu, J., Zhang, B., Zhao, Y., Hao, K., Dinarzo, A., Hoffman, G., Kidd, B.A., Murchie, R., Al Adham, Z., Guo, C., Kotlarz, D., Cutz, E., Walters, T.D., Shouval, D.S., Curran, M., Dobrin, R., Brodmerkel, C., Snapper, S.B., Klein, C., Brumell, J.H., Hu, M., Nanan, R., Snanter-Nanan, B., Wong, M., Le Deist, F., Haddad, E., Roifman, C.M., Deslandres, C., Griffiths, A.M., Gaskin, K.J., Uhlig, H.H., Schadt, E.E., Muise, A.M., 2016. Variants in TRIM22 That Affect NOD2 Signaling Are Associated With Very-Early-Onset Inflammatory Bowel Disease. Gastroenterology 150, 1196-1207.

Lindsay, J.O., Allez, M., Clark, M., Labopin, M., Ricart, E., Rogler, G., Rovira, M., Satsangi, J., Farge, D., Hawkey, C.J., group, A.t., European Society for, B., Marrow Transplantation Autoimmune Disease Working, P., European, C.s., Colitis, O., 2017. Autologous stem-cell transplantation in treatment-refractory Crohn's disease: an analysis of pooled data from the ASTIC trial. Lancet Gastroenterol Hepatol 2, 399-406.

Liu, J.Z., van Sommeren, S., Huang, H., Ng, S.C., Alberts, R., Takahashi, A., Ripke, S., Lee, J.C., Jostins, L., Shah, T., Abedian, S., Cheon, J.H., Cho, J., Dayani, N.E., Franke, L., Fuyuno, Y., Hart, A.,

Juyal, R.C., Juyal, G., Kim, W.H., Morris, A.P., Poustchi, H., Newman, W.G., Midha, V., Orchard, T.R., Vahedi, H., Sood, A., Sung, J.Y., Malekzadeh, R., Westra, H.J., Yamazaki, K., Yang, S.K., International Multiple Sclerosis Genetics, C., International, I.B.D.G.C., Barrett, J.C., Alizadeh, B.Z., Parkes, M., Bk, T., Daly, M.J., Kubo, M., Anderson, C.A., Weersma, R.K., 2015. Association analyses identify 38 susceptibility loci for inflammatory bowel disease and highlight shared genetic risk across populations. Nat Genet 47, 979-986.

Liu, T.C., Gurram, B., Baldridge, M.T., Head, R., Lam, V., Luo, C., Cao, Y., Simpson, P., Hayward, M., Holtz, M.L., Bousounis, P., Noe, J., Lerner, D., Cabrera, J., Biank, V., Stephens, M., Huttenhower, C., McGovern, D.P., Xavier, R.J., Stappenbeck, T.S., Salzman, N.H., 2016. Paneth cell defects in Crohn's disease patients promote dysbiosis. JCI Insight 1, e86907.

Livak, K.J., Schmittgen, T.D., 2001. Analysis of relative gene expression data using real-time quantitative PCR and the 2(-Delta Delta C(T)) Method. Methods 25, 402-408.

Lloyd-Price, J., Arze, C., Ananthakrishnan, A.N., Schirmer, M., Avila-Pacheco, J., Poon, T.W., Andrews, E., Ajami, N.J., Bonham, K.S., Brislawn, C.J., Casero, D., Courtney, H., Gonzalez, A., Graeber, T.G., Hall, A.B., Lake, K., Landers, C.J., Mallick, H., Plichta, D.R., Prasad, M., Rahnavard, G., Sauk, J., Shungin, D., Vazquez-Baeza, Y., White, R.A., 3rd, Investigators, I., Braun, J., Denson, L.A., Jansson, J.K., Knight, R., Kugathasan, S., McGovern, D.P.B., Petrosino, J.F., Stappenbeck, T.S., Winter, H.S., Clish, C.B., Franzosa, E.A., Vlamakis, H., Xavier, R.J., Huttenhower, C., 2019. Multi-omics of the gut microbial ecosystem in inflammatory bowel diseases. Nature 569, 655-662.

Lozupone, C.A., Stombaugh, J.I., Gordon, J.I., Jansson, J.K., Knight, R., 2012. Diversity, stability and resilience of the human gut microbiota. Nature 489, 220-230.

Lu, P., Sodhi, C.P., Yamaguchi, Y., Jia, H., Prindle, T., Jr., Fulton, W.B., Vikram, A., Bibby, K.J., Morowitz, M.J., Hackam, D.J., 2018. Intestinal epithelial Toll-like receptor 4 prevents metabolic syndrome by regulating interactions between microbes and intestinal epithelial cells in mice. Mucosal Immunol 11, 727-740.

Mabbott, N.A., Donaldson, D.S., Ohno, H., Williams, I.R., Mahajan, A., 2013. Microfold (M) cells: important immunosurveillance posts in the intestinal epithelium. Mucosal Immunol 6, 666-677.

Maloy, K.J., Powrie, F., 2011. Intestinal homeostasis and its breakdown in inflammatory bowel disease. Nature 474, 298-306.

Marchesi, J.R., Holmes, E., Khan, F., Kochhar, S., Scanlan, P., Shanahan, F., Wilson, I.D., Wang, Y., 2007. Rapid and noninvasive metabonomic characterization of inflammatory bowel disease. J Proteome Res 6, 546-551.

Mariat, D., Firmesse, O., Levenez, F., Guimaraes, V., Sokol, H., Dore, J., Corthier, G., Furet, J.P., 2009. The Firmicutes/Bacteroidetes ratio of the human microbiota changes with age. BMC Microbiol 9, 123.

Mary, J.Y., Modigliani, R., 1989. Development and validation of an endoscopic index of the severity for Crohn's disease: a prospective multicentre study. Groupe d'Etudes Therapeutiques des Affections Inflammatoires du Tube Digestif (GETAID). Gut 30, 983-989.

McDole, J.R., Wheeler, L.W., McDonald, K.G., Wang, B., Konjufca, V., Knoop, K.A., Newberry, R.D., Miller, M.J., 2012. Goblet cells deliver luminal antigen to CD103+ dendritic cells in the small intestine. Nature 483, 345-349.

Mehta, R.S., Abu-Ali, G.S., Drew, D.A., Lloyd-Price, J., Subramanian, A., Lochhead, P., Joshi, A.D., Ivey, K.L., Khalili, H., Brown, G.T., DuLong, C., Song, M., Nguyen, L.H., Mallick, H., Rimm, E.B., Izard, J., Huttenhower, C., Chan, A.T., 2018. Stability of the human faecal microbiome in a cohort of adult men. Nat Microbiol 3, 347-355.

Metwaly, A., Dunkel, A., Waldschmitt, N., Raj, A.C.D., Lagkouvardos, I., Corraliza, A.M., Mayorgas, A., Martinez-Medina, M., Reiter, S., Schloter, M., Hofmann, T., Allez, M., Panes, J., Salas, A., Haller, D., 2020. Integrated microbiota and metabolite profiles link Crohn's disease to sulfur metabolism. Nat Commun 11, 4322.

Metwaly, A., Haller, D., 2019a. Multi-omics in IBD biomarker discovery: the missing links. Nat Rev Gastroenterol Hepatol 16, 587-588.

Metwaly, A., Haller, D., 2019b. Strain-Level Diversity in the Gut: The P. copri Case. Cell Host Microbe 25, 349-350.

Metwaly, A., Jovic, J., Waldschmitt, N., Khaloian, S., Heimes, H., Haecker, D., Hammoudi, N., Le Bourhis, L., Mayorgas, A., Siebert, K., 2022a. Diet prevents the expansion of segmented filamentous bacteria and ileo-colonic inflammation in a model of Crohn's disease. bioRxiv.

Metwaly, A., Reitmeier, S., Haller, D., 2022b. Microbiome risk profiles as biomarkers for inflammatory and metabolic disorders. Nat Rev Gastroenterol Hepatol 19, 383-397.

Middel, P., Raddatz, D., Gunawan, B., Haller, F., Radzun, H.J., 2006. Increased number of mature dendritic cells in Crohn's disease: evidence for a chemokine mediated retention mechanism. Gut 55, 220-227.

Mills, R.H., Dulai, P.S., Vazquez-Baeza, Y., Sauceda, C., Daniel, N., Gerner, R.R., Batachari, L.E., Malfavon, M., Zhu, Q., Weldon, K., Humphrey, G., Carrillo-Terrazas, M., Goldasich, L.D., Bryant, M., Raffatellu, M., Quinn, R.A., Gewirtz, A.T., Chassaing, B., Chu, H., Sandborn, W.J., Dorrestein, P.C., Knight, R., Gonzalez, D.J., 2022. Multi-omics analyses of the ulcerative colitis gut microbiome link Bacteroides vulgatus proteases with disease severity. Nat Microbiol 7, 262-276.

Mizoguchi, A., Takeuchi, T., Himuro, H., Okada, T., Mizoguchi, E., 2016. Genetically engineered mouse models for studying inflammatory bowel disease. J Pathol 238, 205-219.

Mizoguchi, E., Low, D., Ezaki, Y., Okada, T., 2020. Recent updates on the basic mechanisms and pathogenesis of inflammatory bowel diseases in experimental animal models. Intest Res 18, 151-167.

Moayyedi, P., Surette, M.G., Kim, P.T., Libertucci, J., Wolfe, M., Onischi, C., Armstrong, D., Marshall, J.K., Kassam, Z., Reinisch, W., Lee, C.H., 2015. Fecal Microbiota Transplantation Induces Remission in Patients With Active Ulcerative Colitis in a Randomized Controlled Trial. Gastroenterology 149, 102-109 e106.

Moller, F.T., Andersen, V., Wohlfahrt, J., Jess, T., 2015. Familial risk of inflammatory bowel disease: a population-based cohort study 1977-2011. Am J Gastroenterol 110, 564-571.

Moran, J.P., Walter, J., Tannock, G.W., Tonkonogy, S.L., Sartor, R.B., 2009. Bifidobacterium animalis causes extensive duodenitis and mild colonic inflammation in monoassociated interleukin-10-deficient mice. Inflamm Bowel Dis 15, 1022-1031.

Morgan, X.C., Tickle, T.L., Sokol, H., Gevers, D., Devaney, K.L., Ward, D.V., Reyes, J.A., Shah, S.A., LeLeiko, N., Snapper, S.B., Bousvaros, A., Korzenik, J., Sands, B.E., Xavier, R.J., Huttenhower, C., 2012. Dysfunction of the intestinal microbiome in inflammatory bowel disease and treatment. Genome Biol 13, R79.

Morgulis, A., Coulouris, G., Raytselis, Y., Madden, T.L., Agarwala, R., Schaffer, A.A., 2008. Database indexing for production MegaBLAST searches. Bioinformatics 24, 1757-1764.

Muegge, B.D., Kuczynski, J., Knights, D., Clemente, J.C., Gonzalez, A., Fontana, L., Henrissat, B., Knight, R., Gordon, J.I., 2011. Diet drives convergence in gut microbiome functions across mammalian phylogeny and within humans. Science 332, 970-974.

Naftali, T., Reshef, L., Kovacs, A., Porat, R., Amir, I., Konikoff, F.M., Gophna, U., 2016. Distinct Microbiotas are Associated with Ileum-Restricted and Colon-Involving Crohn's Disease. Inflamm Bowel Dis 22, 293-302.

Nagao-Kitamoto, H., Shreiner, A.B., Gillilland, M.G., 3rd, Kitamoto, S., Ishii, C., Hirayama, A., Kuffa, P., El-Zaatari, M., Grasberger, H., Seekatz, A.M., Higgins, P.D., Young, V.B., Fukuda, S., Kao, J.Y., Kamada, N., 2016. Functional Characterization of Inflammatory Bowel Disease-Associated Gut Dysbiosis in Gnotobiotic Mice. Cell Mol Gastroenterol Hepatol 2, 468-481.

Nale, J.Y., Redgwell, T.A., Millard, A., Clokie, M.R.J., 2018. Efficacy of an Optimised Bacteriophage Cocktail to Clear Clostridium difficile in a Batch Fermentation Model. Antibiotics (Basel) 7.

Natividad, J.M., Pinto-Sanchez, M.I., Galipeau, H.J., Jury, J., Jordana, M., Reinisch, W., Collins, S.M., Bercik, P., Surette, M.G., Allen-Vercoe, E., Verdu, E.F., 2015. Ecobiotherapy Rich in Firmicutes Decreases Susceptibility to Colitis in a Humanized Gnotobiotic Mouse Model. Inflamm Bowel Dis 21, 1883-1893.

Neurath, M.F., 2019. Targeting immune cell circuits and trafficking in inflammatory bowel disease. Nat Immunol 20, 970-979.

Ng, S.C., Leung, W.K., Shi, H.Y., Li, M.K., Leung, C.M., Ng, C.K., Lo, F.H., Hui, Y.T., Tsang, S.W., Chan, Y.K., Loo, C.K., Chan, K.H., Hui, A.J., Chow, W.H., Harbord, M., Ching, J.Y., Lee, M., Chan, V., Tang, W., Hung, I.F., Ho, J., Lao, W.C., Wong, M.T., Sze, S.F., Shan, E.H., Lam, B.C., Tong, R.W., Mak, L.Y., Wong, S.H., Wu, J.C., Chan, F.K., Sung, J.J., 2016. Epidemiology of Inflammatory Bowel Disease from 1981 to 2014: Results from a Territory-Wide Population-Based Registry in Hong Kong. Inflamm Bowel Dis 22, 1954-1960.

Ng, S.C., Shi, H.Y., Hamidi, N., Underwood, F.E., Tang, W., Benchimol, E.I., Panaccione, R., Ghosh, S., Wu, J.C.Y., Chan, F.K.L., Sung, J.J.Y., Kaplan, G.G., 2018. Worldwide incidence and prevalence of inflammatory bowel disease in the 21st century: a systematic review of population-based studies. Lancet 390, 2769-2778.

Ng, S.C., Tang, W., Ching, J.Y., Wong, M., Chow, C.M., Hui, A.J., Wong, T.C., Leung, V.K., Tsang, S.W., Yu, H.H., Li, M.F., Ng, K.K., Kamm, M.A., Studd, C., Bell, S., Leong, R., de Silva, H.J., Kasturiratne, A., Mufeena, M.N.F., Ling, K.L., Ooi, C.J., Tan, P.S., Ong, D., Goh, K.L., Hilmi, I., Pisespongsa, P., Manatsathit, S., Rerknimitr, R., Aniwan, S., Wang, Y.F., Ouyang, Q., Zeng, Z., Zhu, Z., Chen, M.H., Hu, P.J., Wu, K., Wang, X., Simadibrata, M., Abdullah, M., Wu, J.C., Sung, J.J.Y., Chan, F.K.L., Asia-Pacific, C.s., Colitis Epidemiologic Study Study, G., 2013. Incidence and phenotype of inflammatory bowel disease based on results from the Asia-pacific Crohn's and colitis epidemiology study. Gastroenterology 145, 158-165 e152.

Nikolaus, S., Schulte, B., Al-Massad, N., Thieme, F., Schulte, D.M., Bethge, J., Rehman, A., Tran, F., Aden, K., Hasler, R., Moll, N., Schutze, G., Schwarz, M.J., Waetzig, G.H., Rosenstiel, P., Krawczak, M., Szymczak, S., Schreiber, S., 2017. Increased Tryptophan Metabolism Is Associated With Activity of Inflammatory Bowel Diseases. Gastroenterology 153, 1504-1516 e1502.

Nitzan, O., Elias, M., Peretz, A., Saliba, W., 2016. Role of antibiotics for treatment of inflammatory bowel disease. World J Gastroenterol 22, 1078-1087.

Noor, N.M., Verstockt, B., Parkes, M., Lee, J.C., 2020. Personalised medicine in Crohn's disease. Lancet Gastroenterol Hepatol 5, 80-92.

Ohman, L., Lasson, A., Strombeck, A., Isaksson, S., Hesselmar, M., Simren, M., Strid, H., Magnusson, M.K., 2021. Fecal microbiota dynamics during disease activity and remission in newly diagnosed and established ulcerative colitis. Sci Rep 11, 8641.

Orcutt, R., Gianni, F., Judge, R., 1987. Development of an “altered Schaedler flora” for NCI gnotobiotic rodents. Microecol Ther 17.

Ordas, I., Eckmann, L., Talamini, M., Baumgart, D.C., Sandborn, W.J., 2012. Ulcerative colitis. Lancet 380, 1606-1619.

Ott, S.J., Musfeldt, M., Wenderoth, D.F., Hampe, J., Brant, O., Folsch, U.R., Timmis, K.N., Schreiber, S., 2004. Reduction in diversity of the colonic mucosa associated bacterial microflora in patients with active inflammatory bowel disease. Gut 53, 685-693.

Pabst, O., Slack, E., 2020. IgA and the intestinal microbiota: the importance of being specific. Mucosal Immunol 13, 12-21.

Pagnini, C., Pizarro, T.T., Cominelli, F., 2019. Novel Pharmacological Therapy in Inflammatory Bowel Diseases: Beyond Anti-Tumor Necrosis Factor. Front Pharmacol 10, 671.

Paine, E.R., 2014. Colonoscopic evaluation in ulcerative colitis. Gastroenterol Rep (Oxf) 2, 161-168.

Palm, N.W., de Zoete, M.R., Cullen, T.W., Barry, N.A., Stefanowski, J., Hao, L., Degnan, P.H., Hu, J., Peter, I., Zhang, W., Ruggiero, E., Cho, J.H., Goodman, A.L., Flavell, R.A., 2014. Immunoglobulin A coating identifies colitogenic bacteria in inflammatory bowel disease. Cell 158, 1000-1010.

Panes, J., Garcia-Olmo, D., Van Assche, G., Colombel, J.F., Reinisch, W., Baumgart, D.C., Dignass, A., Nachury, M., Ferrante, M., Kazemi-Shirazi, L., Grimaud, J.C., de la Portilla, F., Goldin, E., Richard, M.P., Diez, M.C., Tagarro, I., Leselbaum, A., Danese, S., Collaborators, A.C.S.G., 2018. Long-term Efficacy and Safety of Stem Cell Therapy (Cx601) for Complex Perianal Fistulas in Patients With Crohn's Disease. Gastroenterology 154, 1334-1342 e1334.

Papa, E., Docktor, M., Smillie, C., Weber, S., Preheim, S.P., Gevers, D., Giannoukos, G., Ciulla, D., Tabbaa, D., Ingram, J., Schauer, D.B., Ward, D.V., Korzenik, J.R., Xavier, R.J., Bousvaros, A., Alm, E.J., 2012. Non-invasive mapping of the gastrointestinal microbiota identifies children with inflammatory bowel disease. PLoS One 7, e39242.

Papp, K.A., Langley, R.G., Lebwohl, M., Krueger, G.G., Szapary, P., Yeilding, N., Guzzo, C., Hsu, M.C., Wang, Y., Li, S., Dooley, L.T., Reich, K., investigators, P.s., 2008. Efficacy and safety of ustekinumab, a human interleukin-12/23 monoclonal antibody, in patients with psoriasis: 52-week results from a randomised, double-blind, placebo-controlled trial (PHOENIX 2). Lancet 371, 1675-1684.

Paramsothy, S., Kamm, M.A., Kaakoush, N.O., Walsh, A.J., van den Bogaerde, J., Samuel, D., Leong, R.W.L., Connor, S., Ng, W., Paramsothy, R., Xuan, W., Lin, E., Mitchell, H.M., Borody, T.J., 2017a. Multidonor intensive faecal microbiota transplantation for active ulcerative colitis: a randomised placebo-controlled trial. Lancet 389, 1218-1228.

Paramsothy, S., Paramsothy, R., Rubin, D.T., Kamm, M.A., Kaakoush, N.O., Mitchell, H.M., Castano-Rodriguez, N., 2017b. Faecal Microbiota Transplantation for Inflammatory Bowel Disease: A Systematic Review and Meta-analysis. J Crohns Colitis 11, 1180-1199.

Pascal, V., Pozuelo, M., Borruel, N., Casellas, F., Campos, D., Santiago, A., Martinez, X., Varela, E., Sarrabayrouse, G., Machiels, K., Vermeire, S., Sokol, H., Guarner, F., Manichanh, C., 2017. A microbial signature for Crohn's disease. Gut 66, 813-822.

Pedersen, N., Duricova, D., Elkjaer, M., Gamborg, M., Munkholm, P., Jess, T., 2010. Risk of extra-intestinal cancer in inflammatory bowel disease: meta-analysis of population-based cohort studies. Am J Gastroenterol 105, 1480-1487.

Peery, A.F., Crockett, S.D., Murphy, C.C., Lund, J.L., Dellon, E.S., Williams, J.L., Jensen, E.T., Shaheen, N.J., Barritt, A.S., Lieber, S.R., Kochar, B., Barnes, E.L., Fan, Y.C., Pate, V., Galanko, J., Baron, T.H., Sandler, R.S., 2019. Burden and Cost of Gastrointestinal, Liver, and Pancreatic Diseases in the United States: Update 2018. Gastroenterology 156, 254-272 e211.

Peloquin, J.M., Goel, G., Villablanca, E.J., Xavier, R.J., 2016. Mechanisms of Pediatric Inflammatory Bowel Disease. Annu Rev Immunol 34, 31-64.

Perminow, G., Beisner, J., Koslowski, M., Lyckander, L.G., Stange, E., Vatn, M.H., Wehkamp, J., 2010. Defective paneth cell-mediated host defense in pediatric ileal Crohn's disease. Am J Gastroenterol 105, 452-459.

Petersen, C., Round, J.L., 2014. Defining dysbiosis and its influence on host immunity and disease. Cell Microbiol 16, 1024-1033.

Peterson, L.W., Artis, D., 2014. Intestinal epithelial cells: regulators of barrier function and immune homeostasis. Nat Rev Immunol 14, 141-153.

Plichta, D.R., Graham, D.B., Subramanian, S., Xavier, R.J., 2019. Therapeutic Opportunities in Inflammatory Bowel Disease: Mechanistic Dissection of Host-Microbiome Relationships. Cell 178, 1041-1056.

Png, C.W., Linden, S.K., Gilshenan, K.S., Zoetendal, E.G., McSweeney, C.S., Sly, L.I., McGuckin, M.A., Florin, T.H., 2010. Mucolytic bacteria with increased prevalence in IBD mucosa augment in vitro utilization of mucin by other bacteria. Am J Gastroenterol 105, 2420-2428.

Portela, F., Magro, F., Lago, P., Cotter, J., Cremers, I., de Deus, J., Vieira, A., Lopes, H., Caldeira, P., Barros, L., Reis, J., Carvalho, L., Goncalves, R., Campos, M.J., Ministro, P., Duarte, M.A., Amil, J., Rodrigues, S., Azevedo, L., Costa-Pereira, A., 2010. Ulcerative colitis in a Southern European country: a national perspective. Inflamm Bowel Dis 16, 822-829.

Prodan, A., Tremaroli, V., Brolin, H., Zwinderman, A.H., Nieuwdorp, M., Levin, E., 2020. Comparing bioinformatic pipelines for microbial 16S rRNA amplicon sequencing. PLoS One 15, e0227434.

Qin, J., Li, Y., Cai, Z., Li, S., Zhu, J., Zhang, F., Liang, S., Zhang, W., Guan, Y., Shen, D., Peng, Y., Zhang, D., Jie, Z., Wu, W., Qin, Y., Xue, W., Li, J., Han, L., Lu, D., Wu, P., Dai, Y., Sun, X., Li, Z., Tang, A., Zhong,

S., Li, X., Chen, W., Xu, R., Wang, M., Feng, Q., Gong, M., Yu, J., Zhang, Y., Zhang, M., Hansen, T., Sanchez, G., Raes, J., Falony, G., Okuda, S., Almeida, M., LeChatelier, E., Renault, P., Pons, N., Batto, J.M., Zhang, Z., Chen, H., Yang, R., Zheng, W., Li, S., Yang, H., Wang, J., Ehrlich, S.D., Nielsen, R., Pedersen, O., Kristiansen, K., Wang, J., 2012. A metagenome-wide association study of gut microbiota in type 2 diabetes. Nature 490, 55-60.

Qiu, Y., Chen, B., Li, Y., Xiong, S., Zhang, S., He, Y., Zeng, Z., Ben-Horin, S., Chen, M., Mao, R., 2019. Risk factors and long-term outcome of disease extent progression in Asian patients with ulcerative colitis: a retrospective cohort study. BMC Gastroenterol 19, 7.

Qiu, Y., Li, M.Y., Feng, T., Feng, R., Mao, R., Chen, B.L., He, Y., Zeng, Z.R., Zhang, S.H., Chen, M.H., 2017. Systematic review with meta-analysis: the efficacy and safety of stem cell therapy for Crohn's disease. Stem Cell Res Ther 8, 136.

Quast, C., Pruesse, E., Yilmaz, P., Gerken, J., Schweer, T., Yarza, P., Peplies, J., Glockner, F.O., 2013. The SILVA ribosomal RNA gene database project: improved data processing and web-based tools. Nucleic Acids Res 41, D590-596.

Quraishi, M.N., Widlak, M., Bhala, N., Moore, D., Price, M., Sharma, N., Iqbal, T.H., 2017. Systematic review with meta-analysis: the efficacy of faecal microbiota transplantation for the treatment of recurrent and refractory Clostridium difficile infection. Aliment Pharmacol Ther 46, 479-493.

Rakoff-Nahoum, S., Hao, L., Medzhitov, R., 2006. Role of toll-like receptors in spontaneous commensal-dependent colitis. Immunity 25, 319-329.

Rehman, A., Rausch, P., Wang, J., Skieceviciene, J., Kiudelis, G., Bhagalia, K., Amarapurkar, D., Kupcinskas, L., Schreiber, S., Rosenstiel, P., Baines, J.F., Ott, S., 2016. Geographical patterns of the standing and active human gut microbiome in health and IBD. Gut 65, 238-248.

Reitmeier, S., Hitch, T.C.A., Treichel, N., Fikas, N., Hausmann, B., Ramer-Tait, A.E., Neuhaus, K., Berry, D., Haller, D., Lagkouvardos, I., Clavel, T., 2021. Handling of spurious sequences affects the outcome of high-throughput 16S rRNA gene amplicon profiling. ISME Communications 1, 31.

Reitmeier, S., Kiessling, S., Clavel, T., List, M., Almeida, E.L., Ghosh, T.S., Neuhaus, K., Grallert, H., Linseisen, J., Skurk, T., Brandl, B., Breuninger, T.A., Troll, M., Rathmann, W., Linkohr, B., Hauner, H., Laudes, M., Franke, A., Le Roy, C.I., Bell, J.T., Spector, T., Baumbach, J., O'Toole, P.W., Peters, A., Haller, D., 2020a. Arrhythmic Gut Microbiome Signatures Predict Risk of Type 2 Diabetes. Cell Host Microbe.

Reitmeier, S., Kiessling, S., Neuhaus, K., Haller, D., 2020b. Comparing Circadian Rhythmicity in the Human Gut Microbiome. STAR Protoc 1, 100148.

Renz, H., von Mutius, E., Brandtzaeg, P., Cookson, W.O., Autenrieth, I.B., Haller, D., 2011. Gene-environment interactions in chronic inflammatory disease. Nat Immunol 12, 273-277.

Rescigno, M., Urbano, M., Valzasina, B., Francolini, M., Rotta, G., Bonasio, R., Granucci, F., Kraehenbuhl, J.P., Ricciardi-Castagnoli, P., 2001. Dendritic cells express tight junction proteins and penetrate gut epithelial monolayers to sample bacteria. Nat Immunol 2, 361-367.

Ridaura, V.K., Faith, J.J., Rey, F.E., Cheng, J., Duncan, A.E., Kau, A.L., Griffin, N.W., Lombard, V., Henrissat, B., Bain, J.R., Muehlbauer, M.J., Ilkayeva, O., Semenkovich, C.F., Funai, K., Hayashi, D.K., Lyle, B.J., Martini, M.C., Ursell, L.K., Clemente, J.C., Van Treuren, W., Walters, W.A., Knight, R., Newgard, C.B., Heath, A.C., Gordon, J.I., 2013. Gut microbiota from twins discordant for obesity modulate metabolism in mice. Science 341, 1241214.

Rivas, M.A., Avila, B.E., Koskela, J., Huang, H., Stevens, C., Pirinen, M., Haritunians, T., Neale, B.M., Kurki, M., Ganna, A., Graham, D., Glaser, B., Peter, I., Atzmon, G., Barzilai, N., Levine, A.P., Schiff, E., Pontikos, N., Weisburd, B., Lek, M., Karczewski, K.J., Bloom, J., Minikel, E.V., Petersen, B.S., Beaugerie, L., Seksik, P., Cosnes, J., Schreiber, S., Bokemeyer, B., Bethge, J., International, I.B.D.G.C., Consortium, N.I.G., Consortium, T.D.G., Heap, G., Ahmad, T., Plagnol, V., Segal, A.W., Targan, S., Turner, D., Saavalainen, P., Farkkila, M., Kontula, K., Palotie, A., Brant, S.R., Duerr, R.H., Silverberg, M.S., Rioux, J.D., Weersma, R.K., Franke, A., Jostins, L., Anderson, C.A., Barrett, J.C., MacArthur, D.G., Jalas, C., Sokol, H., Xavier, R.J., Pulver, A., Cho, J.H., McGovern, D.P.B., Daly, M.J., 2018. Insights into the genetic epidemiology of Crohn's and rare diseases in the Ashkenazi Jewish population. PLoS Genet 14, e1007329.

Roda, G., Jharap, B., Neeraj, N., Colombel, J.F., 2016. Loss of Response to Anti-TNFs: Definition, Epidemiology, and Management. Clin Transl Gastroenterol 7, e135.

Rogala, A.R., Oka, A., Sartor, R.B., 2020. Strategies to Dissect Host-Microbial Immune Interactions That Determine Mucosal Homeostasis vs. Intestinal Inflammation in Gnotobiotic Mice. Front Immunol 11, 214.

Rogler, G., Singh, A., Kavanaugh, A., Rubin, D.T., 2021. Extraintestinal Manifestations of Inflammatory Bowel Disease: Current Concepts, Treatment, and Implications for Disease Management. Gastroenterology 161, 1118-1132.

Rohart, F., Gautier, B., Singh, A., Le Cao, K.A., 2017. mixOmics: An R package for 'omics feature selection and multiple data integration. PLoS Comput Biol 13, e1005752.

Rook, G.A., 2012. Hygiene hypothesis and autoimmune diseases. Clin Rev Allergy Immunol 42, 5-15.

Rossen, N.G., Fuentes, S., van der Spek, M.J., Tijssen, J.G., Hartman, J.H., Duflou, A., Lowenberg, M., van den Brink, G.R., Mathus-Vliegen, E.M., de Vos, W.M., Zoetendal, E.G., D'Haens, G.R.,

Ponsioen, C.Y., 2015. Findings From a Randomized Controlled Trial of Fecal Transplantation for Patients With Ulcerative Colitis. Gastroenterology 149, 110-118 e114.

Rothschild, D., Weissbrod, O., Barkan, E., Kurilshikov, A., Korem, T., Zeevi, D., Costea, P.I., Godneva, A., Kalka, I.N., Bar, N., Shilo, S., Lador, D., Vila, A.V., Zmora, N., Pevsner-Fischer, M., Israeli, D., Kosower, N., Malka, G., Wolf, B.C., Avnit-Sagi, T., Lotan-Pompan, M., Weinberger, A., Halpern, Z., Carmi, S., Fu, J., Wijmenga, C., Zhernakova, A., Elinav, E., Segal, E., 2018. Environment dominates over host genetics in shaping human gut microbiota. Nature 555, 210-215.

Round, J.L., Mazmanian, S.K., 2010. Inducible Foxp3+ regulatory T-cell development by a commensal bacterium of the intestinal microbiota. Proc Natl Acad Sci U S A 107, 12204-12209.

Ruemmele, F.M., Veres, G., Kolho, K.L., Griffiths, A., Levine, A., Escher, J.C., Amil Dias, J., Barabino, A., Braegger, C.P., Bronsky, J., Buderus, S., Martin-de-Carpi, J., De Ridder, L., Fagerberg, U.L., Hugot, J.P., Kierkus, J., Kolacek, S., Koletzko, S., Lionetti, P., Miele, E., Navas Lopez, V.M., Paerregaard, A., Russell, R.K., Serban, D.E., Shaoul, R., Van Rheenen, P., Veereman, G., Weiss, B., Wilson, D., Dignass, A., Eliakim, A., Winter, H., Turner, D., European, C.s., Colitis, O., European Society of Pediatric Gastroenterology, H., Nutrition, 2014. Consensus guidelines of ECCO/ESPGHAN on the medical management of pediatric Crohn's disease. J Crohns Colitis 8, 1179-1207.

Rutgeerts, P., Goboes, K., Peeters, M., Hiele, M., Penninckx, F., Aerts, R., Kerremans, R., Vantrappen, G., 1991. Effect of faecal stream diversion on recurrence of Crohn's disease in the neoterminal ileum. Lancet 338, 771-774.

Rutgeerts, P., Sandborn, W.J., Feagan, B.G., Reinisch, W., Olson, A., Johanns, J., Travers, S., Rachmilewitz, D., Hanauer, S.B., Lichtenstein, G.R., de Villiers, W.J., Present, D., Sands, B.E., Colombel, J.F., 2005. Infliximab for induction and maintenance therapy for ulcerative colitis. N Engl J Med 353, 2462-2476.

Sadaghian Sadabad, M., Regeling, A., de Goffau, M.C., Blokzijl, T., Weersma, R.K., Penders, J., Faber, K.N., Harmsen, H.J., Dijkstra, G., 2015. The ATG16L1-T300A allele impairs clearance of pathosymbionts in the inflamed ileal mucosa of Crohn's disease patients. Gut 64, 1546-1552.

Sandborn, W.J., Feagan, B.G., Rutgeerts, P., Hanauer, S., Colombel, J.F., Sands, B.E., Lukas, M., Fedorak, R.N., Lee, S., Bressler, B., Fox, I., Rosario, M., Sankoh, S., Xu, J., Stephens, K., Milch, C., Parikh, A., Group, G.S., 2013. Vedolizumab as induction and maintenance therapy for Crohn's disease. N Engl J Med 369, 711-721.

Sandborn, W.J., Gasink, C., Gao, L.L., Blank, M.A., Johanns, J., Guzzo, C., Sands, B.E., Hanauer, S.B., Targan, S., Rutgeerts, P., Ghosh, S., de Villiers, W.J., Panaccione, R., Greenberg, G., Schreiber, S., Lichtiger, S., Feagan, B.G., Group, C.S., 2012. Ustekinumab induction and maintenance therapy in refractory Crohn's disease. N Engl J Med 367, 1519-1528.

Sands, B.E., Sandborn, W.J., Panaccione, R., O'Brien, C.D., Zhang, H., Johanns, J., Adedokun, O.J., Li, K., Peyrin-Biroulet, L., Van Assche, G., Danese, S., Targan, S., Abreu, M.T., Hisamatsu, T., Szapary, P., Marano, C., Group, U.S., 2019. Ustekinumab as Induction and Maintenance Therapy for Ulcerative Colitis. N Engl J Med 381, 1201-1214.

Sankarasubramanian, J., Ahmad, R., Avuthu, N., Singh, A.B., Guda, C., 2020. Gut Microbiota and Metabolic Specificity in Ulcerative Colitis and Crohn's Disease. Front Med (Lausanne) 7, 606298.

Santoru, M.L., Piras, C., Murgia, A., Palmas, V., Camboni, T., Liggi, S., Ibba, I., Lai, M.A., Orru, S., Blois, S., Loizedda, A.L., Griffin, J.L., Usai, P., Caboni, P., Atzori, L., Manzin, A., 2017. Cross sectional evaluation of the gut-microbiome metabolome axis in an Italian cohort of IBD patients. Sci Rep 7, 9523.

Sartor, R.B., Wu, G.D., 2017. Roles for Intestinal Bacteria, Viruses, and Fungi in Pathogenesis of Inflammatory Bowel Diseases and Therapeutic Approaches. Gastroenterology 152, 327-339 e324.

Scanlan, P.D., Shanahan, F., O'Mahony, C., Marchesi, J.R., 2006. Culture-independent analyses of temporal variation of the dominant fecal microbiota and targeted bacterial subgroups in Crohn's disease. J Clin Microbiol 44, 3980-3988.

Schaedler, R.W., Dubs, R., Costello, R., 1965. Association of Germfree Mice with Bacteria Isolated from Normal Mice. J Exp Med 122, 77-82.

Schaubeck, M., Clavel, T., Calasan, J., Lagkouvardos, I., Haange, S.B., Jehmlich, N., Basic, M., Dupont, A., Hornef, M., von Bergen, M., Bleich, A., Haller, D., 2016. Dysbiotic gut microbiota causes transmissible Crohn's disease-like ileitis independent of failure in antimicrobial defence. Gut 65, 225-237.

Scher, J.U., Sczesnak, A., Longman, R.S., Segata, N., Ubeda, C., Bielski, C., Rostron, T., Cerundolo, V., Pamer, E.G., Abramson, S.B., Huttenhower, C., Littman, D.R., 2013. Expansion of intestinal Prevotella copri correlates with enhanced susceptibility to arthritis. Elife 2, e01202.

Schirmer, M., Franzosa, E.A., Lloyd-Price, J., McIver, L.J., Schwager, R., Poon, T.W., Ananthakrishnan, A.N., Andrews, E., Barron, G., Lake, K., Prasad, M., Sauk, J., Stevens, B., Wilson, R.G., Braun, J., Denson, L.A., Kugathasan, S., McGovern, D.P.B., Vlamakis, H., Xavier, R.J., Huttenhower, C., 2018. Dynamics of metatranscription in the inflammatory bowel disease gut microbiome. Nat Microbiol 3, 337-346.

Schirmer, M., Garner, A., Vlamakis, H., Xavier, R.J., 2019. Microbial genes and pathways in inflammatory bowel disease. Nat Rev Microbiol 17, 497-511.

Schloissnig, S., Arumugam, M., Sunagawa, S., Mitreva, M., Tap, J., Zhu, A., Waller, A., Mende, D.R., Kultima, J.R., Martin, J., Kota, K., Sunyaev, S.R., Weinstock, G.M., Bork, P., 2013. Genomic variation landscape of the human gut microbiome. Nature 493, 45-50.

Schloss, P.D., Westcott, S.L., Ryabin, T., Hall, J.R., Hartmann, M., Hollister, E.B., Lesniewski, R.A., Oakley, B.B., Parks, D.H., Robinson, C.J., Sahl, J.W., Stres, B., Thallinger, G.G., Van Horn, D.J., Weber, C.F., 2009. Introducing mothur: open-source, platform-independent, community-supported software for describing and comparing microbial communities. Appl Environ Microbiol 75, 7537-7541.

Schmitz, J.M., Tonkonogy, S.L., Dogan, B., Leblond, A., Whitehead, K.J., Kim, S.C., Simpson, K.W., Sartor, R.B., 2019. Murine Adherent and Invasive E. coli Induces Chronic Inflammation and Immune Responses in the Small and Large Intestines of Monoassociated IL-10-/- Mice Independent of Long Polar Fimbriae Adhesin A. Inflamm Bowel Dis 25, 875-885.

Schrimpe-Rutledge, A.C., Codreanu, S.G., Sherrod, S.D., McLean, J.A., 2016. Untargeted Metabolomics Strategies-Challenges and Emerging Directions. J Am Soc Mass Spectrom 27, 1897-1905.

Schwerd, T., Frivolt, K., Clavel, T., Lagkouvardos, I., Katona, G., Mayr, D., Uhlig, H.H., Haller, D., Koletzko, S., Bufler, P., 2016. Exclusive enteral nutrition in active pediatric Crohn disease: Effects on intestinal microbiota and immune regulation. J Allergy Clin Immunol 138, 592-596.

Segata, N., Haake, S.K., Mannon, P., Lemon, K.P., Waldron, L., Gevers, D., Huttenhower, C., Izard, J., 2012. Composition of the adult digestive tract bacterial microbiome based on seven mouth surfaces, tonsils, throat and stool samples. Genome Biol 13, R42.

Segata, N., Izard, J., Waldron, L., Gevers, D., Miropolsky, L., Garrett, W.S., Huttenhower, C., 2011. Metagenomic biomarker discovery and explanation. Genome Biol 12, R60.

Sender, R., Fuchs, S., Milo, R., 2016. Revised Estimates for the Number of Human and Bacteria Cells in the Body. PLoS Biol 14, e1002533.

Shapiro, J.M., de Zoete, M.R., Palm, N.W., Laenen, Y., Bright, R., Mallette, M., Bu, K., Bielecka, A.A., Xu, F., Hurtado-Lorenzo, A., Shah, S.A., Cho, J.H., LeLeiko, N.S., Sands, B.E., Flavell, R.A., Clemente, J.C., 2021. Immunoglobulin A Targets a Unique Subset of the Microbiota in Inflammatory Bowel Disease. Cell Host Microbe 29, 83-93 e83.

Shaw, K.A., Bertha, M., Hofmekler, T., Chopra, P., Vatanen, T., Srivatsa, A., Prince, J., Kumar, A., Sauer, C., Zwick, M.E., Satten, G.A., Kostic, A.D., Mulle, J.G., Xavier, R.J., Kugathasan, S., 2016. Dysbiosis, inflammation, and response to treatment: a longitudinal study of pediatric subjects with newly diagnosed inflammatory bowel disease. Genome Med 8, 75.

Sierra, M.A., Li, Q., Pushalkar, S., Paul, B., Sandoval, T.A., Kamer, A.R., Corby, P., Guo, Y., Ruff, R.R., Alekseyenko, A.V., Li, X., Saxena, D., 2020. The Influences of Bioinformatics Tools and Reference Databases in Analyzing the Human Oral Microbial Community. Genes (Basel) 11.

Silverberg, M.S., Satsangi, J., Ahmad, T., Arnott, I.D., Bernstein, C.N., Brant, S.R., Caprilli, R., Colombel, J.F., Gasche, C., Geboes, K., Jewell, D.P., Karban, A., Loftus, E.V., Jr., Pena, A.S., Riddell, R.H., Sachar, D.B., Schreiber, S., Steinhart, A.H., Targan, S.R., Vermeire, S., Warren, B.F., 2005. Toward an integrated clinical, molecular and serological classification of inflammatory bowel disease: report of a Working Party of the 2005 Montreal World Congress of Gastroenterology. Can J Gastroenterol 19 Suppl A, 5A-36A.

Singh, A., Shannon, C.P., Gautier, B., Rohart, F., Vacher, M., Tebbutt, S.J., Le Cao, K.A., 2019. DIABLO: an integrative approach for identifying key molecular drivers from multi-omics assays. Bioinformatics 35, 3055-3062.

Sivignon, A., Bouckaert, J., Bernard, J., Gouin, S.G., Barnich, N., 2017. The potential of FimH as a novel therapeutic target for the treatment of Crohn's disease. Expert Opin Ther Targets 21, 837-847.

Smith, C.A., Want, E.J., O'Maille, G., Abagyan, R., Siuzdak, G., 2006. XCMS: processing mass spectrometry data for metabolite profiling using nonlinear peak alignment, matching, and identification. Anal Chem 78, 779-787.

Sokol, H., Landman, C., Seksik, P., Berard, L., Montil, M., Nion-Larmurier, I., Bourrier, A., Le Gall, G., Lalande, V., De Rougemont, A., Kirchgesner, J., Daguenel, A., Cachanado, M., Rousseau, A., Drouet, E., Rosenzwajg, M., Hagege, H., Dray, X., Klatzman, D., Marteau, P., Saint-Antoine, I.B.D.N., Beaugerie, L., Simon, T., 2020. Fecal microbiota transplantation to maintain remission in Crohn's disease: a pilot randomized controlled study. Microbiome 8, 12.

Sokol, H., Leducq, V., Aschard, H., Pham, H.P., Jegou, S., Landman, C., Cohen, D., Liguori, G., Bourrier, A., Nion-Larmurier, I., Cosnes, J., Seksik, P., Langella, P., Skurnik, D., Richard, M.L., Beaugerie, L., 2017. Fungal microbiota dysbiosis in IBD. Gut 66, 1039-1048.

Sokol, H., Pigneur, B., Watterlot, L., Lakhdari, O., Bermudez-Humaran, L.G., Gratadoux, J.J., Blugeon, S., Bridonneau, C., Furet, J.P., Corthier, G., Grangette, C., Vasquez, N., Pochart, P., Trugnan, G., Thomas, G., Blottiere, H.M., Dore, J., Marteau, P., Seksik, P., Langella, P., 2008. Faecalibacterium prausnitzii is an anti-inflammatory commensal bacterium identified by gut microbiota analysis of Crohn disease patients. Proc Natl Acad Sci U S A 105, 16731-16736.

Sommer, F., Backhed, F., 2013. The gut microbiota--masters of host development and physiology. Nat Rev Microbiol 11, 227-238.

Spehlmann, M.E., Begun, A.Z., Burghardt, J., Lepage, P., Raedler, A., Schreiber, S., 2008. Epidemiology of inflammatory bowel disease in a German twin cohort: results of a nationwide study. Inflamm Bowel Dis 14, 968-976.

Staley, C., Kaiser, T., Beura, L.K., Hamilton, M.J., Weingarden, A.R., Bobr, A., Kang, J., Masopust, D., Sadowsky, M.J., Khoruts, A., 2017. Stable engraftment of human microbiota into mice with a single oral gavage following antibiotic conditioning. Microbiome 5, 87.

Steck, N., Hoffmann, M., Sava, I.G., Kim, S.C., Hahne, H., Tonkonogy, S.L., Mair, K., Krueger, D., Pruteanu, M., Shanahan, F., Vogelmann, R., Schemann, M., Kuster, B., Sartor, R.B., Haller, D., 2011. Enterococcus faecalis metalloprotease compromises epithelial barrier and contributes to intestinal inflammation. Gastroenterology 141, 959-971.

Strachan, D.P., 1989. Hay fever, hygiene, and household size. BMJ 299, 1259-1260.

Strachan, D.P., 2000. Family size, infection and atopy: the first decade of the "hygiene hypothesis". Thorax 55 Suppl 1, S2-10.

Strati, F., Cavalieri, D., Albanese, D., De Felice, C., Donati, C., Hayek, J., Jousson, O., Leoncini, S., Renzi, D., Calabro, A., De Filippo, C., 2017. New evidences on the altered gut microbiota in autism spectrum disorders. Microbiome 5, 24.

Strauss, J., Kaplan, G.G., Beck, P.L., Rioux, K., Panaccione, R., Devinney, R., Lynch, T., Allen-Vercoe, E., 2011. Invasive potential of gut mucosa-derived Fusobacterium nucleatum positively correlates with IBD status of the host. Inflamm Bowel Dis 17, 1971-1978.

Subramanian, B., Gao, S., Lercher, M.J., Hu, S., Chen, W.H., 2019. Evolview v3: a webserver for visualization, annotation, and management of phylogenetic trees. Nucleic Acids Res 47, W270-W275.

Suskind, D.L., Brittnacher, M.J., Wahbeh, G., Shaffer, M.L., Hayden, H.S., Qin, X., Singh, N., Damman, C.J., Hager, K.R., Nielson, H., Miller, S.I., 2015. Fecal microbial transplant effect on clinical outcomes and fecal microbiome in active Crohn's disease. Inflamm Bowel Dis 21, 556-563.

Swidsinski, A., Ladhoff, A., Pernthaler, A., Swidsinski, S., Loening-Baucke, V., Ortner, M., Weber, J., Hoffmann, U., Schreiber, S., Dietel, M., Lochs, H., 2002. Mucosal flora in inflammatory bowel disease. Gastroenterology 122, 44-54.

Swidsinski, A., Weber, J., Loening-Baucke, V., Hale, L.P., Lochs, H., 2005. Spatial organization and composition of the mucosal flora in patients with inflammatory bowel disease. J Clin Microbiol 43, 3380-3389.

Swinburn, B.A., Sacks, G., Hall, K.D., McPherson, K., Finegood, D.T., Moodie, M.L., Gortmaker, S.L., 2011. The global obesity pandemic: shaped by global drivers and local environments. Lancet 378, 804-814.

Tanoue, T., Morita, S., Plichta, D.R., Skelly, A.N., Suda, W., Sugiura, Y., Narushima, S., Vlamakis, H., Motoo, I., Sugita, K., Shiota, A., Takeshita, K., Yasuma-Mitobe, K., Riethmacher, D., Kaisho, T.,

Norman, J.M., Mucida, D., Suematsu, M., Yaguchi, T., Bucci, V., Inoue, T., Kawakami, Y., Olle, B., Roberts, B., Hattori, M., Xavier, R.J., Atarashi, K., Honda, K., 2019. A defined commensal consortium elicits CD8 T cells and anti-cancer immunity. Nature 565, 600-605.

Targan, S.R., Landers, C.J., Yang, H., Lodes, M.J., Cong, Y., Papadakis, K.A., Vasiliauskas, E., Elson, C.O., Hershberg, R.M., 2005. Antibodies to CBir1 flagellin define a unique response that is associated independently with complicated Crohn's disease. Gastroenterology 128, 2020-2028.

Thachil, E., Hugot, J.P., Arbeille, B., Paris, R., Grodet, A., Peuchmaur, M., Codogno, P., Barreau, F., Ogier-Denis, E., Berrebi, D., Viala, J., 2012. Abnormal activation of autophagy-induced crinophagy in Paneth cells from patients with Crohn's disease. Gastroenterology 142, 1097-1099 e1094.

Thia, K.T., Sandborn, W.J., Harmsen, W.S., Zinsmeister, A.R., Loftus, E.V., Jr., 2010. Risk factors associated with progression to intestinal complications of Crohn's disease in a population-based cohort. Gastroenterology 139, 1147-1155.

Torok, H.P., Glas, J., Endres, I., Tonenchi, L., Teshome, M.Y., Wetzke, M., Klein, W., Lohse, P., Ochsenkuhn, T., Folwaczny, M., Goke, B., Folwaczny, C., Muller-Myhsok, B., Brand, S., 2009. Epistasis between Toll-like receptor-9 polymorphisms and variants in NOD2 and IL23R modulates susceptibility to Crohn's disease. Am J Gastroenterol 104, 1723-1733.

Torres, J., Mehandru, S., Colombel, J.F., Peyrin-Biroulet, L., 2017. Crohn's disease. Lancet 389, 1741-1755.

Travis, S.P., Schnell, D., Krzeski, P., Abreu, M.T., Altman, D.G., Colombel, J.F., Feagan, B.G., Hanauer, S.B., Lichtenstein, G.R., Marteau, P.R., Reinisch, W., Sands, B.E., Yacyshyn, B.R., Schnell, P., Bernhardt, C.A., Mary, J.Y., Sandborn, W.J., 2013. Reliability and initial validation of the ulcerative colitis endoscopic index of severity. Gastroenterology 145, 987-995.

Tremlett, H., Fadrosh, D.W., Faruqi, A.A., Zhu, F., Hart, J., Roalstad, S., Graves, J., Lynch, S., Waubant, E., Centers, U.S.N.o.P.M., 2016. Gut microbiota in early pediatric multiple sclerosis: a case-control study. Eur J Neurol 23, 1308-1321.

Tsugawa, H., Cajka, T., Kind, T., Ma, Y., Higgins, B., Ikeda, K., Kanazawa, M., VanderGheynst, J., Fiehn, O., Arita, M., 2015. MS-DIAL: data-independent MS/MS deconvolution for comprehensive metabolome analysis. Nat Methods 12, 523-526.

Turnbaugh, P.J., Quince, C., Faith, J.J., McHardy, A.C., Yatsunenko, T., Niazi, F., Affourtit, J., Egholm, M., Henrissat, B., Knight, R., Gordon, J.I., 2010. Organismal, genetic, and transcriptional variation in the deeply sequenced gut microbiomes of identical twins. Proc Natl Acad Sci U S A 107, 7503-7508.

Turnbaugh, P.J., Ridaura, V.K., Faith, J.J., Rey, F.E., Knight, R., Gordon, J.I., 2009. The effect of diet on the human gut microbiome: a metagenomic analysis in humanized gnotobiotic mice. Sci Transl Med 1, 6ra14.

Turpin, W., Espin-Garcia, O., Xu, W., Silverberg, M.S., Kevans, D., Smith, M.I., Guttman, D.S., Griffiths, A., Panaccione, R., Otley, A., Xu, L., Shestopaloff, K., Moreno-Hagelsieb, G., Consortium, G.E.M.P.R., Paterson, A.D., Croitoru, K., 2016. Association of host genome with intestinal microbial composition in a large healthy cohort. Nat Genet 48, 1413-1417.

Tursi, A., Brandimarte, G., Papa, A., Giglio, A., Elisei, W., Giorgetti, G.M., Forti, G., Morini, S., Hassan, C., Pistoia, M.A., Modeo, M.E., Rodino, S., D'Amico, T., Sebkova, L., Sacca, N., Di Giulio, E., Luzza, F., Imeneo, M., Larussa, T., Di Rosa, S., Annese, V., Danese, S., Gasbarrini, A., 2010. Treatment of relapsing mild-to-moderate ulcerative colitis with the probiotic VSL#3 as adjunctive to a standard pharmaceutical treatment: a double-blind, randomized, placebo-controlled study. Am J Gastroenterol 105, 2218-2227.

Tyler, A.D., Kirsch, R., Milgrom, R., Stempak, J.M., Kabakchiev, B., Silverberg, M.S., 2016. Microbiome Heterogeneity Characterizing Intestinal Tissue and Inflammatory Bowel Disease Phenotype. Inflamm Bowel Dis 22, 807-816.

Umiker, B., Lee, H.H., Cope, J., Ajami, N.J., Laine, J.P., Fregeau, C., Ferguson, H., Alves, S.E., Sciammetta, N., Kleinschek, M., Salmon, M., 2019. The NLRP3 inflammasome mediates DSS-induced intestinal inflammation in Nod2 knockout mice. Innate Immun 25, 132-143.

Ungaro, R., Mehandru, S., Allen, P.B., Peyrin-Biroulet, L., Colombel, J.F., 2017. Ulcerative colitis. Lancet 389, 1756-1770.

Uo, M., Hisamatsu, T., Miyoshi, J., Kaito, D., Yoneno, K., Kitazume, M.T., Mori, M., Sugita, A., Koganei, K., Matsuoka, K., Kanai, T., Hibi, T., 2013. Mucosal CXCR4+ IgG plasma cells contribute to the pathogenesis of human ulcerative colitis through FcgammaR-mediated CD14 macrophage activation. Gut 62, 1734-1744.

Ursell, L.K., Haiser, H.J., Van Treuren, W., Garg, N., Reddivari, L., Vanamala, J., Dorrestein, P.C., Turnbaugh, P.J., Knight, R., 2014. The intestinal metabolome: an intersection between microbiota and host. Gastroenterology 146, 1470-1476.

van der Flier, L.G., Clevers, H., 2009. Stem cells, self-renewal, and differentiation in the intestinal epithelium. Annu Rev Physiol 71, 241-260.

van der Post, S., Jabbar, K.S., Birchenough, G., Arike, L., Akhtar, N., Sjovall, H., Johansson, M.E.V., Hansson, G.C., 2019. Structural weakening of the colonic mucus barrier is an early event in ulcerative colitis pathogenesis. Gut 68, 2142-2151.

van Nood, E., Vrieze, A., Nieuwdorp, M., Fuentes, S., Zoetendal, E.G., de Vos, W.M., Visser, C.E., Kuijper, E.J., Bartelsman, J.F., Tijssen, J.G., Speelman, P., Dijkgraaf, M.G., Keller, J.J., 2013. Duodenal infusion of donor feces for recurrent Clostridium difficile. N Engl J Med 368, 407-415.

Vandenbroucke, K., de Haard, H., Beirnaert, E., Dreier, T., Lauwereys, M., Huyck, L., Van Huysse, J., Demetter, P., Steidler, L., Remaut, E., Cuvelier, C., Rottiers, P., 2010. Orally administered L. lactis secreting an anti-TNF Nanobody demonstrate efficacy in chronic colitis. Mucosal Immunol 3, 49-56.

Vandeputte, D., Falony, G., Vieira-Silva, S., Tito, R.Y., Joossens, M., Raes, J., 2016. Stool consistency is strongly associated with gut microbiota richness and composition, enterotypes and bacterial growth rates. Gut 65, 57-62.

Vaughn, B.P., Vatanen, T., Allegretti, J.R., Bai, A., Xavier, R.J., Korzenik, J., Gevers, D., Ting, A., Robson, S.C., Moss, A.C., 2016. Increased Intestinal Microbial Diversity Following Fecal Microbiota Transplant for Active Crohn's Disease. Inflamm Bowel Dis 22, 2182-2190.

Vavricka, S.R., Brun, L., Ballabeni, P., Pittet, V., Prinz Vavricka, B.M., Zeitz, J., Rogler, G., Schoepfer, A.M., 2011. Frequency and risk factors for extraintestinal manifestations in the Swiss inflammatory bowel disease cohort. Am J Gastroenterol 106, 110-119.

Vavricka, S.R., Rogler, G., Gantenbein, C., Spoerri, M., Prinz Vavricka, M., Navarini, A.A., French, L.E., Safroneeva, E., Fournier, N., Straumann, A., Froehlich, F., Fried, M., Michetti, P., Seibold, F., Lakatos, P.L., Peyrin-Biroulet, L., Schoepfer, A.M., 2015. Chronological Order of Appearance of Extraintestinal Manifestations Relative to the Time of IBD Diagnosis in the Swiss Inflammatory Bowel Disease Cohort. Inflamm Bowel Dis 21, 1794-1800.

Ventham, N.T., Kennedy, N.A., Nimmo, E.R., Satsangi, J., 2013. Beyond gene discovery in inflammatory bowel disease: the emerging role of epigenetics. Gastroenterology 145, 293-308.

Verstockt, B., Sudahakar, P., Creyns, B., Verstockt, S., Cremer, J., Wollants, W.-J., Organe, S., Korcsmaros, T., Madgwick, M., Van Assche, G., Breynaert, C., Vermeire, S., Ferrante, M., 2019. DOP70 An integrated multi-omics biomarker predicting endoscopic response in ustekinumab treated patients with Crohn's disease. Journal of Crohn's and Colitis 13, S072-S073.

Vich Vila, A., Imhann, F., Collij, V., Jankipersadsing, S.A., Gurry, T., Mujagic, Z., Kurilshikov, A., Bonder, M.J., Jiang, X., Tigchelaar, E.F., Dekens, J., Peters, V., Voskuil, M.D., Visschedijk, M.C., van Dullemen, H.M., Keszthelyi, D., Swertz, M.A., Franke, L., Alberts, R., Festen, E.A.M., Dijkstra, G., Masclee, A.A.M., Hofker, M.H., Xavier, R.J., Alm, E.J., Fu, J., Wijmenga, C., Jonkers, D., Zhernakova, A., Weersma, R.K., 2018. Gut microbiota composition and functional changes in inflammatory bowel disease and irritable bowel syndrome. Sci Transl Med 10.

Viladomiu, M., Kivolowitz, C., Abdulhamid, A., Dogan, B., Victorio, D., Castellanos, J.G., Woo, V., Teng, F., Tran, N.L., Sczesnak, A., Chai, C., Kim, M., Diehl, G.E., Ajami, N.J., Petrosino, J.F., Zhou,

X.K., Schwartzman, S., Mandl, L.A., Abramowitz, M., Jacob, V., Bosworth, B., Steinlauf, A., Scherl, E.J., Wu, H.J., Simpson, K.W., Longman, R.S., 2017. IgA-coated E. coli enriched in Crohn's disease spondyloarthritis promote TH17-dependent inflammation. Sci Transl Med 9.

Vlantis, K., Wullaert, A., Polykratis, A., Kondylis, V., Dannappel, M., Schwarzer, R., Welz, P., Corona, T., Walczak, H., Weih, F., Klein, U., Kelliher, M., Pasparakis, M., 2016. NEMO Prevents RIP Kinase 1-Mediated Epithelial Cell Death and Chronic Intestinal Inflammation by NF-kappaB-Dependent and -Independent Functions. Immunity 44, 553-567.

Walter, J., Armet, A.M., Finlay, B.B., Shanahan, F., 2020. Establishing or Exaggerating Causality for the Gut Microbiome: Lessons from Human Microbiota-Associated Rodents. Cell 180, 221-232.

Wang, J., Thingholm, L.B., Skieceviciene, J., Rausch, P., Kummen, M., Hov, J.R., Degenhardt, F., Heinsen, F.A., Ruhlemann, M.C., Szymczak, S., Holm, K., Esko, T., Sun, J., Pricop-Jeckstadt, M., Al-Dury, S., Bohov, P., Bethune, J., Sommer, F., Ellinghaus, D., Berge, R.K., Hubenthal, M., Koch, M., Schwarz, K., Rimbach, G., Hubbe, P., Pan, W.H., Sheibani-Tezerji, R., Hasler, R., Rosenstiel, P., D'Amato, M., Cloppenborg-Schmidt, K., Kunzel, S., Laudes, M., Marschall, H.U., Lieb, W., Nothlings, U., Karlsen, T.H., Baines, J.F., Franke, A., 2016. Genome-wide association analysis identifies variation in vitamin D receptor and other host factors influencing the gut microbiota. Nat Genet 48, 1396-1406.

Wang, Q., Garrity, G.M., Tiedje, J.M., Cole, J.R., 2007. Naive Bayesian classifier for rapid assignment of rRNA sequences into the new bacterial taxonomy. Appl Environ Microbiol 73, 5261-5267.

Wang, Y., Gao, X., Zhang, X., Xiao, F., Hu, H., Li, X., Dong, F., Sun, M., Xiao, Y., Ge, T., Li, D., Yu, G., Liu, Z., Zhang, T., 2021. Microbial and metabolic features associated with outcome of infliximab therapy in pediatric Crohn's disease. Gut Microbes 13, 1-18.

Wang, Y., Yin, Y., Chen, X., Zhao, Y., Wu, Y., Li, Y., Wang, X., Chen, H., Xiang, C., 2019. Induction of Intestinal Th17 Cells by Flagellins From Segmented Filamentous Bacteria. Front Immunol 10, 2750.

Wang, Y.R., Loftus, E.V., Jr., Cangemi, J.R., Picco, M.F., 2013. Racial/Ethnic and regional differences in the prevalence of inflammatory bowel disease in the United States. Digestion 88, 20-25.

Wehkamp, J., Salzman, N.H., Porter, E., Nuding, S., Weichenthal, M., Petras, R.E., Shen, B., Schaeffeler, E., Schwab, M., Linzmeier, R., Feathers, R.W., Chu, H., Lima, H., Jr., Fellermann, K., Ganz, T., Stange, E.F., Bevins, C.L., 2005. Reduced Paneth cell alpha-defensins in ileal Crohn's disease. Proc Natl Acad Sci U S A 102, 18129-18134.

Weinstock, G.M., 2012. Genomic approaches to studying the human microbiota. Nature 489, 250-256.

Welz, P.S., Wullaert, A., Vlantis, K., Kondylis, V., Fernandez-Majada, V., Ermolaeva, M., Kirsch, P., Sterner-Kock, A., van Loo, G., Pasparakis, M., 2011. FADD prevents RIP3-mediated epithelial cell necrosis and chronic intestinal inflammation. Nature 477, 330-334.

Willing, B., Halfvarson, J., Dicksved, J., Rosenquist, M., Jarnerot, G., Engstrand, L., Tysk, C., Jansson, J.K., 2009. Twin studies reveal specific imbalances in the mucosa-associated microbiota of patients with ileal Crohn's disease. Inflamm Bowel Dis 15, 653-660.

Willing, B.P., Dicksved, J., Halfvarson, J., Andersson, A.F., Lucio, M., Zheng, Z., Jarnerot, G., Tysk, C., Jansson, J.K., Engstrand, L., 2010. A pyrosequencing study in twins shows that gastrointestinal microbial profiles vary with inflammatory bowel disease phenotypes. Gastroenterology 139, 1844-1854 e1841.

Windsor, J.W., Kaplan, G.G., 2019. Evolving Epidemiology of IBD. Curr Gastroenterol Rep 21, 40.

Wishart, D.S., Feunang, Y.D., Marcu, A., Guo, A.C., Liang, K., Vazquez-Fresno, R., Sajed, T., Johnson, D., Li, C., Karu, N., Sayeeda, Z., Lo, E., Assempour, N., Berjanskii, M., Singhal, S., Arndt, D., Liang, Y., Badran, H., Grant, J., Serra-Cayuela, A., Liu, Y., Mandal, R., Neveu, V., Pon, A., Knox, C., Wilson, M., Manach, C., Scalbert, A., 2018. HMDB 4.0: the human metabolome database for 2018. Nucleic Acids Res 46, D608-D617.

Wohlgemuth, S., Bower, M., Gulati, A., Sartor, B.R., 2011. Simplified human microbiota - a humanized gnotobiotic rodent model to study complex microbe-host interactions in ileal Crohn's disease: P-213. Inflammatory Bowel Diseases 17, S75-S75.

Wos-Oxley, M., Bleich, A., Oxley, A.P., Kahl, S., Janus, L.M., Smoczek, A., Nahrstedt, H., Pils, M.C., Taudien, S., Platzer, M., Hedrich, H.J., Medina, E., Pieper, D.H., 2012. Comparative evaluation of establishing a human gut microbial community within rodent models. Gut Microbes 3, 234-249.

Wu, G.D., Chen, J., Hoffmann, C., Bittinger, K., Chen, Y.Y., Keilbaugh, S.A., Bewtra, M., Knights, D., Walters, W.A., Knight, R., Sinha, R., Gilroy, E., Gupta, K., Baldassano, R., Nessel, L., Li, H., Bushman, F.D., Lewis, J.D., 2011. Linking long-term dietary patterns with gut microbial enterotypes. Science 334, 105-108.

Yang, Z.H., Liu, F., Zhu, X.R., Suo, F.Y., Jia, Z.J., Yao, S.K., 2021. Altered profiles of fecal bile acids correlate with gut microbiota and inflammatory responses in patients with ulcerative colitis. World J Gastroenterol 27, 3609-3629.

Yasuda, K., Oh, K., Ren, B., Tickle, T.L., Franzosa, E.A., Wachtman, L.M., Miller, A.D., Westmoreland, S.V., Mansfield, K.G., Vallender, E.J., Miller, G.M., Rowlett, J.K., Gevers, D., Huttenhower, C., Morgan, X.C., 2015. Biogeography of the intestinal mucosal and lumenal microbiome in the rhesus macaque. Cell Host Microbe 17, 385-391.

Yen, D., Cheung, J., Scheerens, H., Poulet, F., McClanahan, T., McKenzie, B., Kleinschek, M.A., Owyang, A., Mattson, J., Blumenschein, W., Murphy, E., Sathe, M., Cua, D.J., Kastelein, R.A., Rennick, D., 2006. IL-23 is essential for T cell-mediated colitis and promotes inflammation via IL-17 and IL-6. J Clin Invest 116, 1310-1316.

Yilmaz, B., Juillerat, P., Oyas, O., Ramon, C., Bravo, F.D., Franc, Y., Fournier, N., Michetti, P., Mueller, C., Geuking, M., Pittet, V.E.H., Maillard, M.H., Rogler, G., Swiss, I.B.D.C.I., Wiest, R., Stelling, J., Macpherson, A.J., 2019. Microbial network disturbances in relapsing refractory Crohn's disease. Nat Med 25, 323-336.

Yoon, S.H., Ha, S.M., Kwon, S., Lim, J., Kim, Y., Seo, H., Chun, J., 2017. Introducing EzBioCloud: a taxonomically united database of 16S rRNA gene sequences and whole-genome assemblies. Int J Syst Evol Microbiol 67, 1613-1617.

Zeissig, S., Burgel, N., Gunzel, D., Richter, J., Mankertz, J., Wahnschaffe, U., Kroesen, A.J., Zeitz, M., Fromm, M., Schulzke, J.D., 2007. Changes in expression and distribution of claudin 2, 5 and 8 lead to discontinuous tight junctions and barrier dysfunction in active Crohn's disease. Gut 56, 61-72.

Zeissig, Y., Petersen, B.S., Milutinovic, S., Bosse, E., Mayr, G., Peuker, K., Hartwig, J., Keller, A., Kohl, M., Laass, M.W., Billmann-Born, S., Brandau, H., Feller, A.C., Rocken, C., Schrappe, M., Rosenstiel, P., Reed, J.C., Schreiber, S., Franke, A., Zeissig, S., 2015. XIAP variants in male Crohn's disease. Gut 64, 66-76.

Zhang, A., Sun, H., Wang, P., Han, Y., Wang, X., 2012a. Modern analytical techniques in metabolomics analysis. Analyst 137, 293-300.

Zhang, L., Bahl, M.I., Roager, H.M., Fonvig, C.E., Hellgren, L.I., Frandsen, H.L., Pedersen, O., Holm, J.C., Hansen, T., Licht, T.R., 2017. Environmental spread of microbes impacts the development of metabolic phenotypes in mice transplanted with microbial communities from humans. ISME J 11, 676-690.

Zhang, T., DeSimone, R.A., Jiao, X., Rohlf, F.J., Zhu, W., Gong, Q.Q., Hunt, S.R., Dassopoulos, T., Newberry, R.D., Sodergren, E., Weinstock, G., Robertson, C.E., Frank, D.N., Li, E., 2012b. Host genes related to paneth cells and xenobiotic metabolism are associated with shifts in human ileum-associated microbial composition. PLoS One 7, e30044.

Zhang, X., Deeke, S.A., Ning, Z., Starr, A.E., Butcher, J., Li, J., Mayne, J., Cheng, K., Liao, B., Li, L., Singleton, R., Mack, D., Stintzi, A., Figeys, D., 2018. Metaproteomics reveals associations between microbiome and intestinal extracellular vesicle proteins in pediatric inflammatory bowel disease. Nat Commun 9, 2873.

Zhou, G.X., Liu, Z.J., 2017. Potential roles of neutrophils in regulating intestinal mucosal inflammation of inflammatory bowel disease. J Dig Dis 18, 495-503.

Zuo, T., Lu, X.J., Zhang, Y., Cheung, C.P., Lam, S., Zhang, F., Tang, W., Ching, J.Y.L., Zhao, R., Chan, P.K.S., Sung, J.J.Y., Yu, J., Chan, F.K.L., Cao, Q., Sheng, J.Q., Ng, S.C., 2019. Gut mucosal virome alterations in ulcerative colitis. Gut 68, 1169-1179.

Acknowledgments

Throughout my Ph.D., I have received a great deal of support and assistance. I would first like to thank Prof. Dirk Haller for his support and guidance during my Ph.D. journey from the start till the end. A special thanks to all members of the examination committee for critically reviewing my dissertation.

I would like to deeply acknowledge my colleagues that without their support, it may have taken me a decade to finish my PhD. I would like to thank Amira Metwaly, Ilias Lagkouvardos, Nadine Waldschmitt, Baraa Altaha, Adam Sorbie, Gabriele Hörmannsperger, Nico Gebhardt, Sigrd Kisling, Silvia Pitariu, Ingrid Schmöller, David Wylensek, Thomas Clavel, Jelena Calasan, Hongsup Yoon, Isabella Lengfelder, Elena Lobner, Valentina Schüppel, Sevana Khaloian, Sarah Just, Klaus Neuhaus, Sandra Bierwirth, Brita Sturm, Yunhui Niu, Marjolein Heddes, Patricia Richter, Malwine Solecki, Caroline Ziegler, Simone Daxauer, Stephanie Ewald, Melanie Klein, Alexander Wolf, Deborah Püngel, Marlene Geiger, Katharina Pracht, Felicitas Firlus, Eva Rath, Hélène Omer, Senja Beck, Franziska Giehren, Isabel Abellan-Schneyder, Silke Kiessling, Miriam Ecker, Janine Kövilein, Nina Heppner, Elisabeth Gleisinger, Sabine Schwamberger, Sandra Reitmeier, and Olivia Coleman. I would like to thank Dr. med. Tobias Schwerd and his team, Prof. Dr. med. Jost Langhorst and his team, Prof. Dr. Mathias Heikenwälder and his team, Dr. Karin Kleigrewe and the Bayerisches Zentrum für Biomolekulare Massenspektrometrie team and Dr. Josch Konstantin Pauling and his team. I would like to thank Nikolai Köhler, Chen Meng, Elena Kotsiliti, Valentina Leone, Klara Frivolt, Anna Koch, Kerstin Kofink, Ronja Eilert, and Anna Brückner.

In addition, I would like to deeply thank my family and friends, who provided stimulating discussions as well as happy distractions to rest my mind outside of my research. I would like to especially thank my parents, my brother, my sisters, Elsa, Matthias, Johannes, Mahmoud, Mona, Theresa, Caro, my aunts & uncles, Basti, Osama, Hardy, Martin, Kevin, Philip, Chuks, Osama, Salah, Ziad, Fares, and Yousef.

Publications and presentations

List of scientific Publications:

- Metwaly, A., Jovic, J., Waldschmitt, N., Khaloian, S., Heimes, H., Haecker, D., **Ahmed M.,** Hammoudi, N., Le Bourhis, L., Mayorgas, A., Siebert, K., Basic M., Schwerd T., Allez M., Panes J., Salas A., Bleich A., Zeissig S., Schnupf P., Cominelli F., Haller D., 2022. Diet prevents the expansion of segmented filamentous bacteria and ileo-colonic inflammation in a model of Crohn's disease. (Submitted manuscript)
- **Ahmed M**, Metwaly A, Hammoudi N, Meng C, Köhler N, Le Bourhis L, Pauling J, Kleigrewe K, Allez M, Haller D. P540 Longitudinal Dynamics of Gut Microbiome and Metabolome After Biological Therapy in Inflammatory Bowel Diseases. Journal of Crohn's and Colitis. 2022 Jan;16(Supplement_1): i488-9.
- Metwaly A, Calasan J, Waldschmitt N, Khaloian S, Häcker D, **Ahmed M**, Butto LF, Hammoudi N, Le Bourhis L, Mayorgas A, Siebert K. P059 Diet controls segmented filamentous bacteria in driving Crohn's disease-like inflammation in TNFdeltaARE mice. Journal of Crohn's and Colitis. 2022 Jan;16(Supplement_1): i168-i168.
- **Ahmed M***, Metwaly M*, Haller D. Modeling microbe-host interaction in the pathogenesis of Crohn's disease. International Journal of Medical Microbiology 311.3 (2021): 151489.
- Langhorst J, Schöls M, Cinar Z, Eilert R, Kofink K, Paul A, Zempel C, Elsenbruch S, Lauche R, **Ahmed M**, Haller D. Comprehensive Lifestyle-Modification in Patients with Ulcerative Colitis–A Randomized Controlled Trial. Journal of Clinical Medicine. 2020 Oct;9(10):3087.
- Brückner A, Werkstetter KJ, Frivolt K, Shokry E, **Ahmed M**, Metwaly A, Marques JG, Uhl O, Krohn K, Hajji M, Otte S. Partial enteral nutrition has no benefit on bone health but improves growth in paediatric patients with quiescent or mild Crohn's disease. Clinical Nutrition. 2020 Dec 1;39(12):3786-96.

Poster Presentations

UEG Week 2021

- **M. Ahmed,** A. Metwaly, N. Hammoudi, C. Meng, N. Köhler, L. Le Bourhis, J.K. Pauling, K.Kleigrewe, M. Allez, D. Haller. Longitudinal Dynamics of Gut Microbiome and Metabolome After Biological Therapy in Inflammatory Bowel Diseases

11th Seeon Conference and Science Camp "From sequencing to function" (Seeon, Germany, 2018)

- **M. Ahmed**, A. Brückner, K. Frivolt, S. Liptay, K. Krohn, M. Hajji, S. Otte, K. Werkstetter, T. Schwerd, D. Haller, S. Koletzko. The impact of partial enteral nutrition on gut microbiota composition in paediatric crohn's disease patients'
- J. Calasan, N. Waldschmitt, **M. Ahmed**, M. Basic, A. Bleich, D. Haller. Role of segmented filamentous bacteria in Crohn's disease-like ileitis

UEG Week 2017

- Rath E, Waldschmitt N, **Ahmed M**, Khaloian S, Schaubeck M, Hörmannsperger G, Planchais J, Sokol H, Haller D. GLP-1 expressing enteroendocrine cell numbers are reduced at the site of active disease in various mouse models of intestinal inflammation